Lecture Notes in Networks and Systems 3

Mirsad Hadžikadić
Samir Avdaković *Editors*

Advanced Technologies, Systems, and Applications

Springer

Lecture Notes in Networks and Systems

Volume 3

Series editor

Janusz Kacprzyk, Polish Academy of Sciences, Warsaw, Poland
e-mail: kacprzyk@ibspan.waw.pl

The series "Lecture Notes in Networks and Systems" publishes the latest developments in Networks and Systems—quickly, informally and with high quality. Original research reported in proceedings and post-proceedings represents the core of LNNS.

Volumes published in LNNS embrace all aspects and subfields of, as well as new challenges in, Networks and Systems.

The series contains proceedings and edited volumes in systems and networks, spanning the areas of Cyber-Physical Systems, Autonomous Systems, Sensor Networks, Control Systems, Energy Systems, Automotive Systems, Biological Systems, Vehicular Networking and Connected Vehicles, Aerospace Systems, Automation, Manufacturing, Smart Grids, Nonlinear Systems, Power Systems, Robotics, Social Systems, Economic Systems and other. Of particular value to both the contributors and the readership are the short publication timeframe and the world-wide distribution and exposure which enable both a wide and rapid dissemination of research output.

The series covers the theory, applications, and perspectives on the state of the art and future developments relevant to systems and networks, decision making, control, complex processes and related areas, as embedded in the fields of interdisciplinary and applied sciences, engineering, computer science, physics, economics, social, and life sciences, as well as the paradigms and methodologies behind them.

Mirsad Hadžikadić · Samir Avdaković
Editors

Advanced Technologies, Systems, and Applications

Springer

Editors
Mirsad Hadžikadić
Department of Software and Information Systems
Complex Systems Institute
Charlotte, NC
USA

Samir Avdaković
Faculty of Electrical Engineering
University of Sarajevo
Sarajevo
Bosnia and Herzegovina

ISSN 2367-3370 ISSN 2367-3389 (electronic)
Lecture Notes in Networks and Systems
ISBN 978-3-319-47294-2 ISBN 978-3-319-47295-9 (eBook)
DOI 10.1007/978-3-319-47295-9

Library of Congress Control Number: 2016954521

Printed on acid-free paper

This Springer imprint is published by Springer Nature
The registered company is Springer International Publishing AG
The registered company address is: Gewerbestrasse 11, 6330 Cham, Switzerland

Contents

Contributors

Robert Abbott University of North Carolina at Charlotte, Charlotte, NC, USA

Alma Ademović-Tahirović JP Elektroprivreda BiH d.d. Sarajevo, Sarajevo, Bosnia and Herzegovina

Jasmina Agačević Pritt Electical Utility Company, sarajevo, Bosnia and Herzegovina

Sanjin Albinovic Department of Roads and Transportation, Faculty of Civil Engineering, University of Sarajevo, Sarajevo, Bosnia and Herzegovina

Samir Avdaković Faculty of Electrical Engineering, University of Sarajevo, Sarajevo, Bosnia and Herzegovina

Sena Bajraktarević University Sarajevo School of Science and Technology, Sarajevo, Bosnia and Herzegovina

Zijad Bajramović Independent System Operator in B & H, Sarajevo, Bosnia and Herzegovina; Pritt Electical Utility Company, Sarajevo, Bosnia and Herzegovina

Admir Bašić Sarajevo, Bosnia and Herzegovina

Emil Brajković Faculty of Science and Education, University of Mostar, Mostar, Bosnia and Herzegovina

Adnan Čaršimamović Independent System Operator in B & H, Sarajevo, Bosnia and Herzegovina

Dragan Ćućilo Institute for Standardization of BiH, Istočno Sarajevo, Bosnia and Herzegovina

Sabina Dacić-Lepara JP Elektroprivreda BiH, Sarajevo, Bosnia and Herzegovina

Nedis Dautbašić Faculty of Electrical Engineering, University of Sarajevo, Sarajevo, Bosnia and Herzegovina

Maja Muftić Dedović Faculty of Electrical Engineering, University of Sarajevo, Sarajevo, Bosnia and Herzegovina

Slobodan Djukanović Faculty of Electrical Engineering, University of Montenegro, Podgorica, Montenegro

Vlatko Doleček Academy of Sciences and Arts, Sarajevo, Bosnia and Herzegovina

Una Drakulić University of Bihać, Bihać, Bosnia and Herzegovina

Boško Drinovac University of Sarajeve, Sarajeve, Bosnia and Herzegovina; Public Company Roads of Federation of Bosnia and Herzegovina, Sarajevo, Bosnia and Herzegovina

Ejub Dzaferovic University of Sarajevo, Sarajevo, Bosnia and Herzegovina

Hajrudin Dzafo University of Sarajevo, Sarajevo, Bosnia and Herzegovina

Enisa Džananović JP Elektroprivreda BiH, Sarajevo, Bosnia and Herzegovina

Suada Dzebo Department of Roads and Transportation, Faculty of Civil Engineering, University of Sarajevo, Sarajevo, Bosnia and Herzegovina

Mirsad Hadžikadić University of North Carolina at Charlotte, Charlotte, NC, USA; Complex Systems Institute, UNC Charlotte, Charlotte, USA

Jasna Hivziefendic International Burch University, Sarajevo, Bosnia and Herzegovina

Mujo Hodzic BH Telecom d.d, Sarajevo, Bosnia and Herzegovina

Migdat I. Hodžić International University of Sarajevo, Sarajevo, Bosnia and Herzegovina

Alija Jusić Pritt Electical Utility Company, sarajevo, Bosnia and Herzegovina

Isak Karabegović University of Bihać, Bihać, Bosnia and Herzegovina

Vladimir A. Katić Faculty of Technical Sciences, University of Novi Sad, Novi Sad, Serbia

Anes Kazagić EPC Elektroprivreda BiH d.d. Sarajevo, Sarajevo, Bosnia and Herzegovina

Adna Kolaković University Sarajevo School of Science and Technology, Sarajevo, Bosnia and Herzegovina

Marko Koljancic INOVA Informaticki Inzenjering, d.o.o, Banja Luka, Bosnia and Herzegovina

Sead Kreso Faculty of Electrical Engineering, University of Sarajevo, Sarajevo, Bosnia and Herzegovina

Deni Memic Sarajevo School of Science and Technology, Sarajevo, Bosnia and Herzegovina

Ajla Merzić JP Elektroprivreda BiH d.d. Sarajevo, Sarajevo, Bosnia and Herzegovina

Nikolina Mijic INOVA Informaticki Inzenjering, d.o.o, Banja Luka, Bosnia and Herzegovina

Indira Muhić International University of Sarajevo, Sarajevo, Bosnia and Herzegovina

Aljo Mujčić Faculty of Electrical Engineering Tuzla, University of Tuzla, Tuzla, Bosnia and Herzegovina

Edin Mujčić University of Bihać, Bihać, Bosnia and Herzegovina

Adnan Mujezinović Faculty of Electrical Engineering, University of Sarajevo, Sarajevo, Bosnia and Herzegovina

Saša Mujović Faculty of Electrical Engineering, University of Montenegro, Podgorica, Montenegro

Mustafa Musić JP Elektroprivreda BiH d.d. Sarajevo, Sarajevo, Bosnia and Herzegovina

Tarik Namas International University of Sarajevo, Sarajevo, Bosnia and Herzegovina

Mirza Pozder Department of Roads and Transportation, Faculty of Civil Engineering, University of Sarajevo, Sarajevo, Bosnia and Herzegovina

Belma Ramić-Brkić University Sarajevo School of Science and Technology, Sarajevo, Bosnia and Herzegovina

Elma Redzić JP Elektroprivreda BiH d.d. Sarajevo, Sarajevo, Bosnia and Herzegovina

Ammar Saric Department of Roads and Transportation, Faculty of Civil Engineering, University of Sarajevo, Sarajevo, Bosnia and Herzegovina

Mirza Saric JP EP BiH—d.d. Sarajevo, Sarajevo, Bosnia and Herzegovina

Maksim Sestic INOVA Informaticki Inzenjering, d.o.o, Banja Luka, Bosnia and Herzegovina

Selma Skaljic-Memic Centralna Banka Bosne i Hercegovine, Sarajevo, Bosnia and Herzegovina

Merisa Škrgić University of Bihać, Bihać, Bosnia and Herzegovina

Izet Smajević Sarajevo, Bosnia and Herzegovina

Mirjana Šućur Institute for Standardization of BiH, Istočno Sarajevo, Bosnia and Herzegovina

Irfan Turković Pritt Electical Utility Company, Sarajevo, Bosnia and Herzegovina

Daniel Vasić Faculty of Science and Education, University of Mostar, Mostar, Bosnia and Herzegovina

Meludin Veledar Independent System Operator in B & H, Sarajevo, Bosnia and Herzegovina

Tomislav Volarić Faculty of Science and Education, University of Mostar, Mostar, Bosnia and Herzegovina

Salko Zahirović University of Sarajevo, Sarajevo, Bosnia and Herzegovina

Smail Zubčević University of Sarajevo, Sarajevo, Bosnia and Herzegovina

The Case for Interdisciplinary and Cross-Disciplinary Exploration

This volume is both interesting and important because it spans a wide range of technical disciplines and technologies, including complex systems, biomedical engineering, electrical engineering, energy, telecommunications, mechanical engineering, civil engineering, and computer science. The papers included in this volume were presented at the International Symposium on Innovative and Interdisciplinary Applications of Advanced Technologies (IAT), held in Neum, Bosnia and Herzegovina on June 26 and 27, 2016. Symposia like IAT are rare. It is customary these days to organize conferences that are focused on an increasingly narrow set of questions within a specific subdiscipline. Such conferences are clearly needed. However, there is value in taking an opposite approach, the one in which a diverse set of researchers, developers, and practitioners is brought to the same place to exchange ideas and accomplishments. Such events often result in new insights, ideas, and solutions. Conversations take unexpected turns. Unexpected analogies emerge. Best practices are critically evaluated. New collaborations arise. Horizons get expanded.

The volume begins with a chapter on complex systems and biomedical engineering. The first paper offers an example of systems thinking, embodied in an agent-based simulation of predator–prey life situations. The following paper addresses the issue of analysis of electroencephalogram on children with epilepsy. The next paper of this chapter describes a technical system in which the authors discover target digital signatures of objects tracked by devices such as high-resolution radars and synthetic aperture radars. The final paper offers an analysis of a wireless network of low energy sensors.

The second chapter is devoted to power systems. It is the largest chapter of the volume, reflecting the current interest in energy, efficient management of power systems, and smart grids. The papers in this chapter reflect a wide range of topics: impact of personal computers on the grid, energy efficient public lighting, analysis and optimization of load profiles, standardization efforts, design and implementation of the transmission lines, utilization of solar and wind energy, power

transformer modeling, automatic compensation in the distribution grid, management of the power distribution network reconstruction, software for grounding system design, challenges in designing a power system, and the relationship between the GDP and electricity consumption.

The third chapter is focused on mechanical and civil engineering systems. The first paper discusses the issue of biomass and thermal power plants efficiency. The next paper provides a numerical simulation of air-water flow over Coanda-effect screen structure. The third paper explains the use of concrete for the construction of roads and railways superstructure. The last paper in the chapter offers a case study of CAD-GIS integration.

The last chapter is dedicated to computer science-related papers. The papers' topics range from profitability determinants of the banking sector and closed-loop temperature control to advertising LED systems and adaptive tools for teaching programming using conceptual maps.

Overall, the whole volume is devoted to various aspects and types of systems. Systems thinking is crucial for successfully building and understanding man-made, natural, and social systems. We hope that this volume will be the first volume in a series of publications dedicated to systems design, implementation, and evaluation.

Mirsad Hadžikadić
Samir Avdaković

Complex Adaptive Systems, Systems Thinking, and Agent-Based Modeling

Robert Abbott and Mirsad Hadžikadić

Abstract Systems thinking and complex adaptive systems theories share a number of components, namely emergence, self-organization, and hierarchies of interacting systems. We seek to integrate these schools of thought and discuss the similarities and differences of these two models, to introduce systems dynamics and agent-based modeling as methods for modeling complex systems, and how causal-loop diagrams can be used as a means to clarify the complex interactions among components (agents). We then apply a mixture of these different but similar techniques to a fly ecosystem modeling problem to demonstrate their effectiveness.

1 Complex Adaptive Systems

Complex adaptive systems (CAS) are all around us. Common examples given are ecosystems, financial markets, the brain, ant colonies, economies, and many other examples where large numbers of constituents independently interact on a local level that yield some unanticipated nonlinear outcome at scale. Despite the ubiquity of these systems, it is generally conceded that there is no one standard definition of CAS. For our purpose, we shall define a CAS as:

> a system composed of a large number of independent simple components that locally interact in an independent and nonlinear fashion, exhibit self-organization through interactions that are neither completely random nor completely regular and are not influenced by some central or global mechanism, and yield emergent behavior at large scales that is not predictable from observation of the behavior of the components [1, 2].

The smallest component elements of a CAS are commonly referred to as *agents* [3]. Agents are the smallest unit of organization in the system capable of producing

R. Abbott (✉) · M. Hadžikadić
University of North Carolina at Charlotte, Charlotte, NC, USA
e-mail: rabbott5@uncc.edu

M. Hadžikadić
e-mail: mirsad@uncc.edu

M. Hadžikadić and S. Avdaković (eds.), *Advanced Technologies, Systems, and Applications*, Lecture Notes in Networks and Systems 3,
DOI 10.1007/978-3-319-47295-9_1

a given response for a specific stimulus. This stimulus/response behavior of an agent is governed by a few very simple rules. In CAS, we see local interactions of groups of agents, both homogenous and heterogeneous, in a variety of different configurations. In small quantities these interactions can be anticipated, as there are usually a limited set of interactions that each agent can perform. These random local interactions generally yield outcomes approximate to the sum of the potential of each interaction; in some cases, however, as we see larger combinations of agents in varying proportions acting in different ways, we see complex and potentially novel behaviors from these combinations of agents that yield significantly greater outcomes than we would expect. When agents combine in such a way as to produce these emergent behaviors, we refer to this as aggregation and to the specific collection of agents required to produce the effects as *aggregate agents* [3]. These aggregate agents group together with other aggregate agents to form increasingly larger CAS with richer sets of emergent behaviors and interactions.

2 Systems Thinking

Another mechanism used to describe complex systems is *systems thinking* [4]. In systems thinking, we look at the combination of interdependent component systems that make up the whole and study how the state of the global system changes as a result of the interactions of the component systems [5]. This concept is referred to as a *system of systems* [6]. How a system component reacts to information from its environment, as well as the range of interaction options available to the component, identifies the type of behavior exhibited by the component. These behaviors are generally classified as either *goal-seeking* or *purposeful* [6]. With goal-seeking behaviors, a component system is capable of producing a single fixed response using a range of methods in a single environment; these are sometimes referred to as *responsive* [6] or *uni-minded* [5] systems. Purposeful behaviors, alternately, are exhibited by a component system that is capable of producing multiple varied responses to multiple stimuli under many different conditions. Systems that operate with purposeful behaviors produce a much greater variety of potential outcomes and, therefore, provide the greatest potential for novel emergent behaviors. These systems are sometimes referred to as *multi-minded systems* [5]. Four concepts are necessary to describe a purposeful system: a hierarchy of systems; processes of communication among the systems; the stimulus/response combinations that can be activated to produce change among component systems; and definable emergent properties that arise from the interdependent systems [4].

Analytical approaches to system modeling work well with goal-seeking systems, since it is possible to deconstruct these systems into their component parts, study the function of those parts, and then attempt to explain the behavior of the aggregate system in terms of those interactions [5]. In many cases, these interactions can be described using systems of equations and a mathematical model of the system produced. For purposeful systems, however, it is either impractical to capture all of

the possible stimulus-response cases to produce an exhaustive system of equations or the sheer quantity of these equations produces an intractable or unsolvable system. Because of the vast number and variety of combinations of interactions among agents in these systems, many times it is either impossible or impractical to use analytical methods to determine systems of equations capable of exhaustively describing the dynamics of these systems.

3 Agent-Based Modeling

Returning to our definition in 1.1, a CAS is a system composed of a large number of agents that interact with each other in a nontrivial manner and yield emergent behaviors. Each of these agents operate using a set of simple rules as their *internal model* of the global system and produce outcomes using simple rules that are part of this model [3, 7, 8]. Internal model refers to the mechanisms used by an agent to issue a response to a given stimulus and to "learn" new rules through interaction with its surroundings. An *agent-based model* (ABM) is a representation of the constituent agents that make up a system along with a mechanism to allow agents to interact through information exchange with the environment as well as other agents. These agents operate according to rules that attempt to approximately replicate the properties and behaviors of the actual components in the real world.

ABMs are computational models that enable us to understand how different combinations of large numbers of agents produce global outcomes through their discrete local interactions. The outcomes of these models are sensitive to initial conditions and may produce different outcomes according to the inherent randomness of nature that they attempt to reproduce. Mathematical or statistical analysis may be used to verify output of ABMs to determine how accurately they represent the corresponding real-world system; it is very difficult in many cases, however, generate mathematical models to represent the same varied nonlinear emergent outcomes possible as these systems are NP-Hard or NP-Complete [9, 10]. Because of this feature of complex systems, ABMs are one of a handful of tools useful for exploring the emergent behavior of such systems.

4 Systems Dynamics

Just as ABM is a modeling method couched in the language of CAS, systems dynamics (SD) is a modeling method traditionally applied to problems in the social sciences and similar disciplines. Similar to ABMs, SD models are solved computationally through iteration over time. SD models differ from ABMs, however, in that the interactions among components of the system are defined in terms of state variables which are controlled through systems of difference equations. This requires a much more mathematically-rigorous definition of a complex system than

is required by ABM; however, the resulting model can be directly-analyzed using mathematical methods, unlike the output of ABMs that requires additional statistical analyses after the fact [8].

Since SD models are described in terms of systems of difference equations, such descriptions do not always provide an intuitive guide to the interactions of system components. To remedy this, a mechanism known as *causal loop diagramming* (CLD) was developed to provide a visual description of system components and their interactions. A good discussion of CLDs is found in [11]. A CLD provides a mechanism to illustrate the interaction among the state variables (i.e., systems) through the use of positive and negative feedback loops. While this method does not necessarily capture the relative magnitude of information flows among the various components, it does make it very easy to understand which relationships are responsible for system expansion (*reinforcing loops*) and which relationships help to keep the system in control (*balancing loops*). We believe that CLDs can also be a good mechanism to describe the interactions among agents in an ABM.

5 Application

An example case that we shall use for this study is the interactions among fly populations, climate, and the environment and how they can lead to large-scale fly infestations. We shall begin by describing the general problem in terms of fly biology and environmental interactions. Next, we will present a systems thinking approach to the problem describing it as a systems of systems. Then we present our implementation of the ABM used to represent the CAS. Finally, we provide a discussion of our work.

The biology of common species of flies documents the relationships between temperature and humidity and fly development and reproduction. Using this information, we have been able to develop and validate an ABM that generates outcomes compatible with historical data over a five-year period. We have also sought to extend the composition of these systems with other systems such as dumpster placement, sanitation methods and schedules, insect control programs, and the effects of customer interactions with the environment can be modeled as a purposeful system of systems.

In Fig. 1, we model the individual systems and their interactions using a CLD. In our model, we are primarily concerned with the density of our local fly population, as this is the leading indicator of whether a fly infestation of the adjoining facility will reach a problematic level. In an unregulated environment, populations are affected by two means: reproduction and migration [12]. As food availability increases, population density increases as flies from surrounding communities immigrate into the local community. As population density increases, the chance of mating increases accordingly, which leads to increased egg-laying activity. If egg laying increases and the ambient air temperature is within an acceptable range, egg

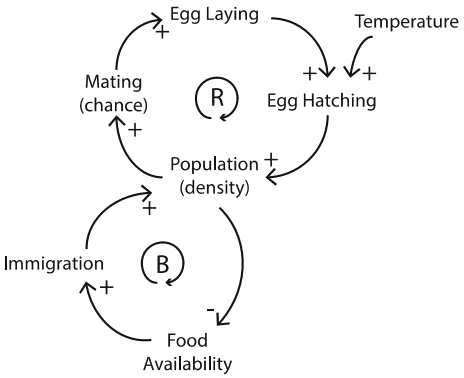

Fig. 1 Causal loop model of a fly ecosystem (Abbott, R. and Bacaksizlar, N.)

hatching increases proportionally, leading to additional increases in population density.

This allows us to expose the exchange of information among the individual systems and the corresponding interdependencies and increased complexity that emerges from these exchanges. This diagram allows us to explain the known relationships among system components; however, it does not allow us to identify novel behaviors that may emerge over time as the system scales along various dimensions.

In an attempt to model the complex system that represents this ecosystem, we created an ABM that emulates the interaction of the most common fly species with their environment to determine conditions under which fly populations will emerge to a significant enough level to threaten a business establishment and what configurations and barriers are most effective at mitigating this health risk. This model was constructed using NetLogo, a powerful tool for developing ABMs [13]. We also included seven years of climate data [14] for the area to drive the behavior of the agents, and we used data [15] derived from the inspection system of a local pest control management company to assist in validating the outcomes produced by the model.

Using information on the biology of common flies [12], we produced a model agent using a small number of rules. These rules governed the migration and life cycle behaviors of the individual fly agents as they interacted with their environment. For each iteration of the model, we began with different random initial conditions for the number of fly agents at various stages of their life cycle. We also varied the placement of food to simulate the placement of waste receptacles (e.g., trash cans, dumpsters, etc.) as well as incidental food-bearing waste dropped around the facility, such as next to cars in the parking lot as well as along high-traffic foot routes.

When running our base model, we learned some interesting behaviors about the randomness of a fly bloom occurring. With no external controls on the population (e.g., pest control and sanitization protocols or non-natural food sources), even with a thorough seeding of random insect populations, it is not likely that a long-lived fly

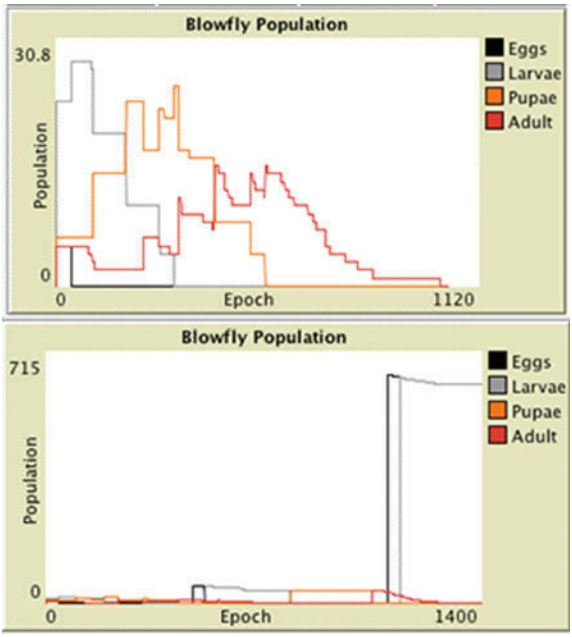

Fig. 2 The *top graph* indicates a model run that did not yield a continuing generation, while the *bottom graph* indicates a continuing generation

plague will occur, as represented by the top graph in Fig. 2. In most iterations of the model, the local fly population will leave the area in favor of other more food-rich environments. With just the right combination of flies at the proper life-cycle stage and placement of food sources, a continuing generation can be produced by the population, as shown in the bottom graph in Fig. 2.

A single continuing generation, however, is not enough to indicate that a fly population will infest adjoining facilities. As seen in the bottom graph of Fig. 2, a continuing generation has only produced on the order of 700 eggs, total. Problems encountered at the degree necessary to produce infestations typically are the result of multiple generations of offspring, which can be produced within two weeks during warmer seasons [12]. From our model results, once a third generation of offspring are produced in an area with a continuing food source, the fly population will continue to grow unless active steps are taken to remove the food or to kill the population. A successful third-generation fly bloom is shown in Fig. 3.

When comparing the CLD and the output of the ABM, it is easy to recognize the strengths and limitations of each method. In CLD nomenclature, it is possible to clearly document the interactions between an agent and its environment, as both reinforcing and balancing forces [11]. The CLD, however, does not make it easy to measure the degree of these interactions or to identify emergent behavior such as explosive nonlinear growth that can occur under certain conditions. ABMs, in contrast, are able to surface these emergent behaviors as they are run under differing initial conditions; however, they do not provide a means for directly identifying the

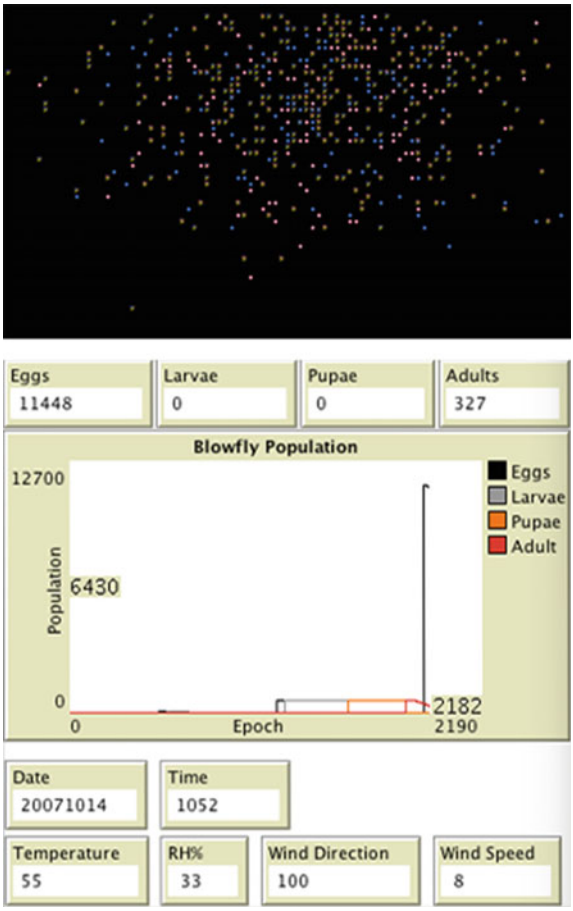

Fig. 3 A successful multi-generation fly colony achieved during epoch 1911 of our model

specific interactions that lead to such emergent behavior. These interactions usually identified during detailed analysis of model results.

We have described two different schools of thought, systems thinking and complex adaptive systems, both of which seek to describe the complexity of systems in terms of interacting components that share information and are capable of evolving or displaying novel behaviors through interaction. We have also described two different but similar modeling methods, systems dynamics and agent-based modeling, both used to simulate complex systems so that we can better understand and predict outcomes of complex systems. We have also described causal-loop diagrams, a method of illustrating the interactions among system components and how those interactions affect the overall organization of the system. We then applied some of these methods to the description of a biological system to demonstrate how the different systems can be effectively integrated to explore complex systems.

6 Summary

Systems thinking is an important way of approaching complex phenomena today. Complex Adaptive Systems and Agent-Based Modeling proved to be a potent combination of paradigms to address simulation and modeling of practical issues that challenge the society of today. In this paper we demonstrated the utility of combining Systems thinking and ABM on the example of pest control and management. Future work will focus on turning this type of thinking into a general-purpose tool for simulation and modeling.

References

1. Mitchell M (2009) Complexity: a guided tour. Oxford University Press, New York
2. Bar-Yam Y (1997) Dynamics of complex systems, vol 213. Addison-Wesley, Reading
3. Holland JH (1995) Hidden order: how adaptation builds complexity. Addison-Wesley, Reading
4. Checkland P (2012) Four conditions for serious systems thinking and action. Syst Res Behav Sci 29:465–469
5. Gharajedaghi J (2011) Systems thinking: managing chaos and complexity: a platform for designing business architecture. Elsevier, London
6. Ackoff RL (1971) Towards a system of systems concepts. Manage Sci 17:661–671
7. Holland JH (2012) Signals and boundaries: building blocks for complex adaptive systems. MIT Press, Cambridge
8. Sayama H (2015) Introduction to the modeling and analysis of complex systems. Open SUNY Textbooks, Milne Library
9. Chapman WL, Rozenblit J, Bahill AT (2001) System design is an NP-complete problem. Syst Eng 4:222–229
10. Cheeseman P, Kanefsky B, Taylor WM (1991) Where the really hard problems are. In: IJCAI, pp 331–337
11. Sterman JD (2001) System dynamics modeling: tools for learning in a complex world. Calif Manage Rev 43:8–25
12. Smith EH, Whitman RC (2007) NPMA field guide to structural pests. In: NPMA
13. Wilensky U (1999) NetLogo (and NetLogo user manual). In: Center for Connected Learning and Computer-Based Modeling, Northwestern University. http://ccl/northwestern.edu/netlogo
14. N. N. C. f. E. Information (2008–2015) Quality controlled local climatological data (QCLCD). http://www.ncdc.noaa.gov/data-access/land-based-station-data/land-based-datasets/quality-controlled-local-climatological-data-qclcd
15. Abbott RL (2015) Pest population data extracted from inspection management system (Unpublished raw data)

The Role of Service Robots and Robotic Systems in the Treatment of Patients in Medical Institutions

Isak Karabegović and Vlatko Doleček

Abstract The development of new technologies has contributed to the development of robot technology. Information technologies and sensor technologies gave the largest contribution to the development of robot technology. Parallel with their development, the development of robot technology took place. The development of service robotics comes along with the development of industrial robotics. Over 300 of service robots for non-production applications have designed as result of development of information technologies as well as the advancement in sensor and servo-drive technology. Service robots are designed to perform professional job tasks as well as for service used in areas of everyday life. One of the fields for service robots application is medicine. Medicine can be categorized as a scientific, research, human discipline—and thus, application of service robots in medicine represents a scientific contribution, due to a huge application of different robotic devices for various purposes, different technological achievements in various fields of medicine. These robotic devices are used to replace missing limbs, perform complex surgical procedures, serve patients in hospital rooms, perform laboratory tests, diagnose diseases, and help in rehabilitation after stroke. This paper will review the presence of service robots in medicine, as well as the application in various areas of medicine such as: surgery, orthopaedics, rehabilitation, distance treatment, serving patients, etc. We have conducted a comparative analysis of the service robots application in medicine with the service robots application in military industry, after which conclusions have been drawn.

I. Karabegović (✉)
University of Bihać, Bihać, Bosnia and Herzegovina
e-mail: isak1910@hotmail.com

V. Doleček
Academy of Sciences and Arts, Sarajevo, Bosnia and Herzegovina
e-mail: vldolecek@gmail.com

M. Hadžikadić and S. Avdaković (eds.), *Advanced Technologies, Systems, and Applications*, Lecture Notes in Networks and Systems 3,
DOI 10.1007/978-3-319-47295-9_2

1 Introduction

Robotics technology is engaged in the development and implementation of industrial robots, as well as service robots. Robotic technology is a multidisciplinary scientific discipline that combines much of systemic knowledge such as mechanical engineering, electrical engineering, information technology, industrial engineering, ergonomics and marketing. Because of its great importance in the post-industrial society, it also enters the domains of medicine, economic, sociology, philosophy and art. Robotics technology is very attractive, challenging and imaginative discipline. Robotics as a science has a task, i.e. a noble objective—for example, to replace a man in performing tiresome, monotonous or dangerous and health-endangering jobs. Service robots are increasingly becoming the subject of research and a very important area of science so that the 21st century will be marked as the century of development of service robots. Service robots are an excellent "System Engineering" research example because it includes a lot of scientific research, namely in the area of mechanical engineering, electrical engineering, electronics, computer science, social science, and more. People in the 21st century want to lead a healthy lifestyle and are concerned because they do not want to get a job with 3Ds (Dirty, Dangerous and Demeaning), nor a position where task performance is monotonous and tedious. Due to aforementioned reasons, service robots that perform these jobs instead of people are the main focus of research nowadays. Many countries in the world are faced with the aging of population, for instance, the population in Japan which needs help and care. Service robotics is among the most promising technologies when it comes to solution to this problem concerning the elderly. Service robots, in some cases, may replace home care (a caregiver) so as to take care of the elderly. In addition, service robots help maintain an increased level of dignity in the course of receiving assistance, such as the cases of using toilet. The user may request service from a service robot without inconvenience. For this reason, it is possible to receive a better service from the intelligent service robot than of a human caregiver. As service robots perform their tasks in the same environment as humans, service robots should have the abilities people have. The service robots should be able to recognize faces, gestures, signs, objects, speech and atmosphere. Successful realization of set tasks results in bypassing obstacles without collision and destruction in the shortest possible time and distance. They should communicate with people on the basis of emotion. During the 1980s and early 1990s, advances in new technologies, sensor technologies, computers and servo-drive led to the development of hundreds of different types of service robots for non-production applications. After a relatively long period of trials and disappointments, robots have finally come out of stores to find their way into our homes, offices, museums and other public spaces, in the form of a self-governing air purifiers, lawn mowers, vacuum cleaners, window washers, toys, surgical operators, etc. Service robots are designed to perform professional tasks in civil engineering, maintenance, inspection, agriculture, medicine, as well as other fields of application in everyday life: at home, at work, in public environment, etc.

[1–13, 14]. These are robots that take over and successfully execute ever more challenging tasks. Robots will sooner or later change our daily lives, such as: assistants, servants, helpers, friends, assistant to surgeons in medical operations, intervention in hazardous environments of any search or rescue, in agriculture and forestry, cleaning, digging, dangerous transportation, construction, and demolition. Service robots are becoming ever more important for scientific research as well as industry because they are and will be used in new areas of industrial branches. Robots and artificial intelligence today live with each other, but it is also difficult to imagine a robot of today which is not some type of artificial intelligence. With robots, androids and fusion of all three life forms—as with artificial intelligence too—there is a question what if they get out of control. According to one of the robot/AI experts, Hans Moravec, robots will become as smart as a man by 2040, and we are sure it will be even smarter than many of the inhabitants. Unlike pessimistic and paranoid predictions, Moravec is not worried. He believes our robots and artificial intelligence will actually extend the life of man and improve the quality of life in general. It is difficult for laymen to assess which of the scientists are right; the truth is some of the possibilities and theories are alarming, but we realized that even by reading some of the great works of science fiction. As it seems, evolution will do its part—it has led a man nearly to the degree that it can build an intelligent being like himself! The whole thing is now far advanced and probably impossible to control. We could maybe just try to turn it in our favour. As we noticed preparing the paper about artificial intelligence, the only real danger is the man, who perhaps (is) used his time to destroy nature, waging war and sowing hatred. On the other hand, some of the science fiction works have shown that the coexistence of artificial intelligence/robots/androids and humans is possible, but only under the condition that a man progresses together with these creatures. In any case, the century we live in has already brought a good deal of scientific excitement and those who do not perceive this outcome positively are actually rare. We live in a time that will undoubtedly be remembered for many things in the distant future, and it would be a shame if we are not aware of it now. A major break-through in robotics is that robots and humans work closely together, as servants or helpers in everyday life. Robotics is a relatively young technical branch, but it al-ready has a rich tradition. It turned out that robots, just like people, passed generation cycles. Each new generation of robots received the more advanced features than the previous one, which is primarily related to the actual degree of intelligence, supporting computing power, enhanced dynamic indicators, and more advanced control algorithms. With a rapid computerization of all forms of business and a vast expansion of the Internet, it is expected there will be a large gap in the 21st century between those who are technologically advanced and those who have lost their connection with modern times. Most people are not even aware of the extent to which robots are already represented within their lives. Their cars and computers are almost certainly partially assembled with the help of a robot. The price of robots is declining steadily and they are coming into ever wider use. It is only a matter of time before robots become available to the population of today's high school students, just as it happened with computers and cell phones. The chapter will be

dedicated to researchers in medicine, students, and engineers, who want to restore and expand their knowledge with modern and innovative service robots applications in medicine. We hope the ideas and concepts presented in the chapter will be useful to many who deal with these issues, as well as that they will contribute to solving numerous problems and improving service robots application in all segments of society as a whole. Our aim will be to offer readers as much useful information as possible and attract their interest in service robots application.

2 Application of the Service Robots in the World

UNECE (*United National Economic Commission for Europe*) and IFR (*International Federation of Robotics*) created and adopted classification of robots where service robots are divided into two groups:

1. professional service robots,
2. personal/home service robots,

and detailed description of the use is given in [2]. Annual supply and overall application of service robots in the world according to their application is presented, based on the statistical data given in the literature [2–5].

Based on Fig. 1, we see that service robots application for professional services has a growing trend, so that about 5000 units of service robots were supplied in 2005, with a growing trend year after year, and thus it reached application value of about 24,000 units of service robots in 2014. We conclude that the increase takes place by linear progression. This trend of service robots application is due to the development of new technologies, primarily information and sensor technologies that are the wind at the back of robotic technologies. We analyze Fig. 1 (right chart) and see that annual supply of service robots for household and personal use from 2005 to 2014 has a growing trend. A total of 871,822 units of robots were applied in 2005 and 4,915,500 units of service robots in 2014, which means that the trend of application increased by 5.6 times in ten years. In 2009, the use of service robots

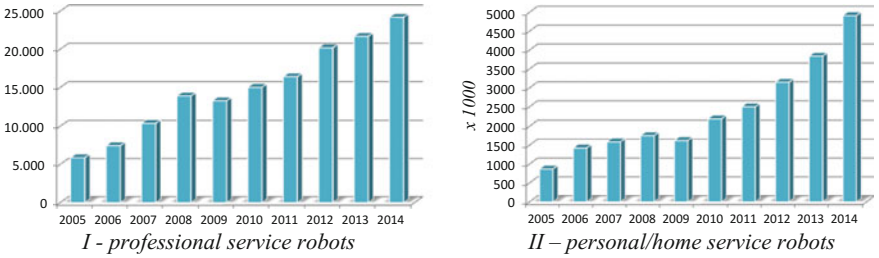

Fig. 1 Annual supply of service robots for professional services, as well as household and personal use from 2005 to 2014 [2–5, 15, 16]

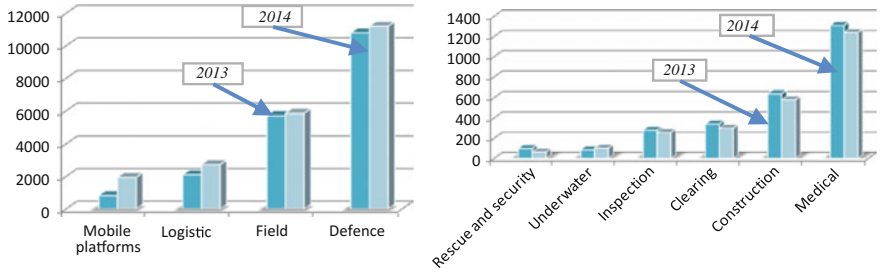

Fig. 2 Annual supply of service robots for professional services in 2013 and 2014 [2–4]

somewhat decreased, so that 1,624,803 units of robots have been applied—which is a reflection of the global economic and industrial crisis. In order to get the complete picture of the application of service robots for professional services – which is the topic of this paper, we will analyze the application of these robots in the last two years.

Figure 2 shows the total annual supply of service robots for professional use in logistics, agriculture, defence, mobile platforms, rescue and safety, underwater use, inspections, cleaning, construction and medicine in 2013 and 2014. Based on the first figure, we can conclude that more service robots have been applied for mobile platforms, logistics, agriculture and defence, in 2014 then in 2013. The first place is occupied by service robots for defence because about 11,000 units of robots have been applied in 2013 and 2014 In the past years, they have the trend of always taking the first place when it comes to professional robots. If we also analyse the application of service robots in medicine, we conclude that they occupy the fifth place in 2013 and 2014, which results from the fact that about 1225 units of robots were applied in 2013 and 2014. This trend is irrational if viewed from the standpoint of protection and assistance to the man as a human being. For this reason, we will conduct the analysis of the application of service robots in medicine and defence in the last ten years.

The application of service robots in medicine and defence for the period from 2005 to 2014 is shown in Fig. 3. If we perform an analysis of service robots

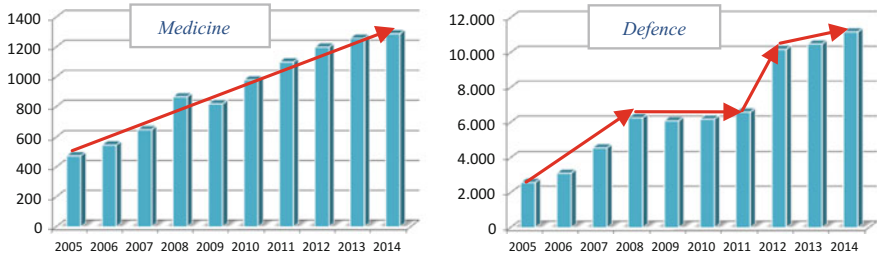

Fig. 3 Total annual application of service robots in medicine and defence from 2005 to 2014 [2–5, 15, 16]

application at the annual level in the medical field, we see that there is a growing trend. It can be said that it is a linear progression so that 476 units of robots were applied in 2005, and 1290 units of robots were applied in 2014. Based on Fig. 3, we conclude that there has been an increase almost every year. However, the application of service robots for defence purposes is somewhat different: it can be concluded that the application has been increasing each year in the period from 2005 to 2008, so that 3355 units of robots were applied in 2005 and 5029 units of robots were applied in 2008. It can be said that it is almost a linear progression in the application of service robots in this period. Based on Fig. 3, it can be concluded that there was a constant application of about 6000 units of robots at an annual level from 2008 to 2011. When it comes to the period 2012–2014, there was a linear increase in application from 8796 units to 11,256 units of the robot in 2014.

Comparing the periods of service robots application in defence, we see that the trend is different in different periods, which can be related to the security situation in the world at that time. When we analyse the number of service robots applications in medicine and defence, we obtain shocking information: the service robots application in defence is 10 times higher than the application in medicine, which is not a common sense. It would be logical to have more service robots used, not in the defence, but in medicine—in order to help people because health is the matter of concern. However, the use of service robots is dictated by the market, and thus the situation is just the way it is.

To see what the application of service robots will be in the future, we presented a projection of the application of service robots for entertainment and household for the period 2015–2018. in Fig. 4 [2]. It can be concluded that there will be an expansion of service robots application in the future. It is expected that about 28 million service robots will be used in households in 2018. A growing trend in service robots application is expected in all areas of application, for professional use as well as entertainment and household.

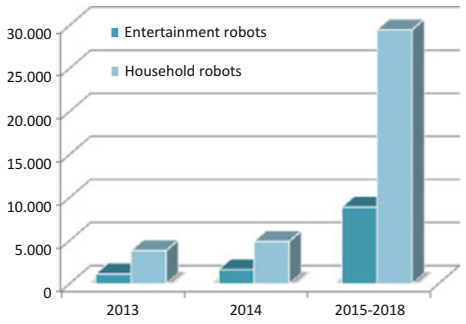

Fig. 4 The projection of service robots application for entertainment and in household from 2015 to 2018 [1, 2]

3 Service Robots in Medicine

Medicine is an interesting field for service robots application. Service robots are applied in medicine for the following purposes: neurosurgery, orthopaedics, endoscopy, surgery, spot radiation, colonoscopy, serving patients, performing delicate surgical procedures, delivering neurorehabilitation therapy to patients who have experienced stroke, teaching children with learning disabilities, enabling visits to patients and guiding, i.e. monitoring operating procedures remotely (*telesurgery*). These also include helping patients during rehabilitation that they must undergo after the stroke, helping in cases of fractures and other damages, as well as performing a growing number of other similar tasks related to patients' recovery [1–4, 17]. The development of information technologies, new materials and robotic technology gives the opportunity to overcome the problems that could not be solved previously, as well as to enhance orthopaedics and help patients to recover quickly and return to the normal state in which they were before the injury. Nowadays, service robots have an important place in medicine:

- these robots provided numerous benefits to clinical practice,
- facilitate medical processes by providing precise control of instruments,
- the application of diagnostic equipment and tools for diagnosis and therapy,
- an increase safety and overall quality of a surgery,
- better care for patients, education and staff training performed through simulation, and
- promotion of the use of information in diagnosis and therapy.

The goal is to develop service robots that meet real needs in the areas of social assistance, as well as in nursing people, the area that demands high-level technology. The application of such next-generation robots will be promoted in areas where robots have more physical contact with people, provided that man safety is secured. For this reason, the idea is aimed to design robots that support rehabilitation exercises and specific movements that a person cannot perform alone, as well as robots that assist a man in performing certain tasks. Service robots application in medicine for 2014 was 1290 units, which is only 5.32 % of the total application of service robots for professional use in 2014. Different areas of application are shown in percentage in Fig. 5.

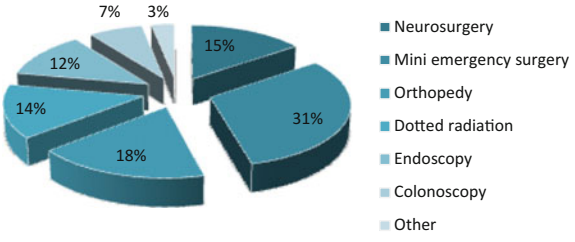

Fig. 5 Percentage of service robots application in medicine by areas for 2014 [1, 2]

Based on Fig. 5, we conclude that service robots in medicine are mainly used for small interventions in surgery (31 % in 2014). Orthopedics is the second place with 18 %—which can be explained by service robots application in handling solid entities, such as bones (because these are not flexible like tissue), and in rehabilitation, which is an integral part of orthopedics. Neurosurgery is the third place (15 % in 2014). The fourth place in service robots application is occupied by spot radiation (14 %). The rest of the statistics is as follows: endoscopy 12 %, colonoscopy 7 %, all other activities of service robots application in medicine 3 %. Service robots in medicine have found application in diagnostics, therapy, surgery, and patients care. They enable paramedics to determine the anatomic location of catheter placement (regardless of the location at the body to which it is going to be set), to diagnose patients and perform surgical procedures. Robotic diagnostic apparatus may be placed at a certain distance from a human body, directly on a patient's body, or in a patient's body. Service robots make the job easier for a surgeon because they ensure precision and accuracy, which leads to great enhancement. They are used for the following purposes: to assist, hold, place and direct instruments; for telesurgery potentials; for navigation, positioning, and application in surgical procedures. A three-dimensional tumour scanning is performed prior to treatment using the CT scanner, based on which the dose and the density of radiation are calculated. The apparatus for radiation is placed on a robotic arm so that it is possible to perform radiation of different strength and density for various positions according to the pre-determined plan. Service robots are characterized by a programmed dose of radiation from the proper position, except that it does not damage adjacent tissue. Let us name a few of the robotic systems helping patients' fast recovery and movement. AutoAmbulator, developed by Health South Corporation (USA), consists of two robot arms that help patients to stand and distribute their body weight on demand. The interface for patient's legs is secured using bands at the thigh and ankle. ReWalk is a wearable, motorized quasi robotic system, manufactured by Argo, which is working on the design of medical equipment (Israel). The user walks using crutches; movement is controlled depending on the patient's motion through subtle changes in center of gravity and upper body. HAL (The Hybrid Assistive Limb) is a series of robots designed by Professor Sankai at the University of Tsukuba (Japan) and has been launched by the Cyberdyne company (Japan). The exoskeleton has been developed to increase patient's existing power by a factor between 2 and 10. Socially useful robotics focuses on helping people through social rather than physical interaction.

It has the aim to improve the quality of life for the general population of users: the elderly, people with physical disabilities as well as people with cognitive and social impairment. We will show some applications of service robots usage in medicine Fig. 6.

Robotic systems *DA VINCI, ZEUS, AESOP* and *Neuro Arm* and other newly designed automated systems are used in surgery. The robotic systems are sophisticated and designed to expand surgeons' capabilities and enable complex surgeries using a minimally invasive approach. DA VINCI surgical system (Fig. 7) is a minimally invasive surgical system consisting of these components: *InSite Vision*

Fig. 6 Examples of service robots for application in medicine for spot radiation, surgical procedures, and skeleton to help patients who have mobility issues [1, 15–18]

System, *Surgical Arm Cart* (that have two or three interactive robotic arms) and EndoWrist instruments, as well as *Surgeon Console*. Using this device, a surgeon sits comfortably in the control panel and performs a surgery on the basis of a presented high-quality 3D image. This system performs advanced surgical techniques; a surgery is performed through a small incision of only one to two centimetres, and a surgeon can use a wide range of laparoscopic instruments. Certain instruments have seven degrees of freedom of movement, allowing them to emulate the skill of a wrist. Each instrument has a specific application, which allows them to perform operations such as cutting, sewing, and tissue manipulation. Devices for visualization provide high-quality 3D image of the operating area. This device ensures the transfer of refined and optimized real-time image of instruments in surgery to the surgeon in the management console. Improved visualization allows the increase of image to several times, which enables a greater precision for a surgeon when performing a procedure; the conventional methods are far surpassed when it comes to precision.

ZEUS robotic surgical system (designed by company Computer Motion, year 1995, shown in Fig. 8) was approved for use in 2002, to be applied in general and laparoscopic surgery (minimally invasive surgery within the abdominal cavity) with a patient and a surgeon in the same room. Zeus is a surgical robot which consists of three robotic arms placed at a table, where one of them holds an AESOP (*Automated Endoscopic System for Optimal Positioning*), which provides a view of the interior of the operating field, while the other two arms hold surgical

Fig. 7 DA VINCI robotic surgical system [1, 19]

Fig. 8 Elements and the principle of managing ZEUS robotic surgical system [1, 18, 20–30]

instruments. Robotic arms are controlled by a surgeon, who sits at the control console a few feet away from a patient. During surgical operation, surgeon has possibility of visualization on the screen, voice communication and working robot arm is under the complete control of the surgeon. There are more than fifty medical instruments that are designed for Zeus surgical system. These include various scissors, forceps, dissectors, needle holders, stabilizers and scalpels.

This service robot is used for assisting surgeons in surgeries such as a beating heart bypass surgery. Zeus system is designed to provide the following benefits: small incisions in the body, about the diameter of a pencil; significantly reduced pain in patients and trauma in cases of minimally invasive surgery; shorter hospital stay and recovery time in cases with minimally invasive surgery; usable in the approach of beating heart as well as non-beating heart; improved surgical precision and skill; improved visualization in 2D and 3D fields; minimized fatigue of a surgeon due to ergonomic operating environment.

The Computer Motion company, founded in 1989, offered its first product on the market: the robotic system "AESOP", used to hold endoscopic cameras in minimally invasive laparoscopic surgery. FDA (Food and Drug Administration) approved system "AESOP 1000" in December 1993. This system has become the first robotic surgical visually supported device. Foot pedals, although easy to manage for well-trained surgeons, presented a problem for new users because they had to look down at the pedals before they were able to adapt them. AESOP 2000, approved in 1996, used voice control, while AESOP 3000, approved in 1998, added another degree of freedom in hand. A combination of voice recognition technology with devices that hold the camera in the surgery is contained in the AESOP 3000 system in order to control a robotic arm with seven degrees of freedom of motion, providing further flexibility in the desired positioning of the endoscope. In recent years, thousands of surgical procedures have been performed using the AESOP robotic technology. AESOP manipulator is a manipulator designed to hold the endoscopic camera, enabling a surgeon to perform solo operations without the need for human assistants. The surgeon controls the manipulator using voice commands pre-recorded on a voice card inserted inside the controller. There are two reasons for its great application in orthopedic surgery. The first lies in the fact that a technology is well suited for operation on the bones, and the second is that a bone differs from soft tissues because it is less prone to deformation when pressed.

Fig. 9 The display of Computer Motion AESOP system [1]

Robotic surgeries increase the implementation accuracy because the current surgical technique often results in incorrect positioning and balancing in hip replacement. With computer navigation system and surgical robots, precision and accuracy are increased greatly (Fig. 9).

Neuro Arm was designed by Canadian scientists and engineers and performs risky operations at the highest level by operating within MRI magnetic resonance, providing a clear 3-D display of even the smallest nerve. Magnetic resonance imaging (MRI) is the name of the medical device which serves to display layers of the human body. NeuroArm is an MRI, compact, image-guided and computer-assisted robotic system designed for neurosurgery, which performs microsurgical as well as biopsy and stereotaxic surgery. A stereotaxic biopsy is an accurate method of sampling small areas of brain tissue, using image guidance and minimally invasive techniques.

NeuroArm surgical robot presented at Fig. 10 is 914.4 mm high, 609.6 mm wide and adaptable to the necessary height of the operating table. It weighs 226.8 kg and has two arms at whose ends suitable instruments are placed. Microsurgery is a general term for an operation that requires an operating microscope. It is a delicate operation that requires the use of precision instruments and is performed by means of miniature precision instruments, including scalpels, needles and specially designed optical microscopes. Although mostly used in plastic surgery, microsurgical techniques are often used in reconstructive surgery such as general surgery, orthopedic surgery, gynecological surgery, pediatric surgery, etc.

The System incorporates:

- Workstation,
- System control cabinet, and
- Two remote manipulators placed on a mobile base.

The workstation is a link between the surgeon and the NeuroArm surgical system. Figure 11 shows the layout of the workstation where the surgeon sits and

Fig. 10 The appearance of NeuroArm surgical system in the operating room [1, 31]

Fig. 11 The appearance of WorkStation and the manipulator of NeuroArm a surgical system with an MR compatibility [1, 31]

controls the robot, i.e. the robot's manipulators, using the hand-held controllers with a stereoscopic display of the surgical site as one of its components, and performs complex surgical procedures such as microsurgery and stereotaxic surgery. In addition to the aforementioned hand-held controllers, its component parts include video monitors and touch-screen computers. The touch screen enables 3D graphics that can be manipulated in any direction. With the help of a microphone located near the surgical instruments, a surgeon can even hear the robot work. NeuroArm includes two MR (Magnetic Resonance) compatible manipulators with grippers that have seven degrees of freedom of movement and a third hand with two cameras offering 3D stereoscopic display, which connect with microsurgical tools. The surgical microscope offers a stereoscopic view of the brain, which provides depth perception, while MRI magnetic resonance imaging and robotic sensors generate three-dimensional map of the brain. It also contains filters to eliminate an

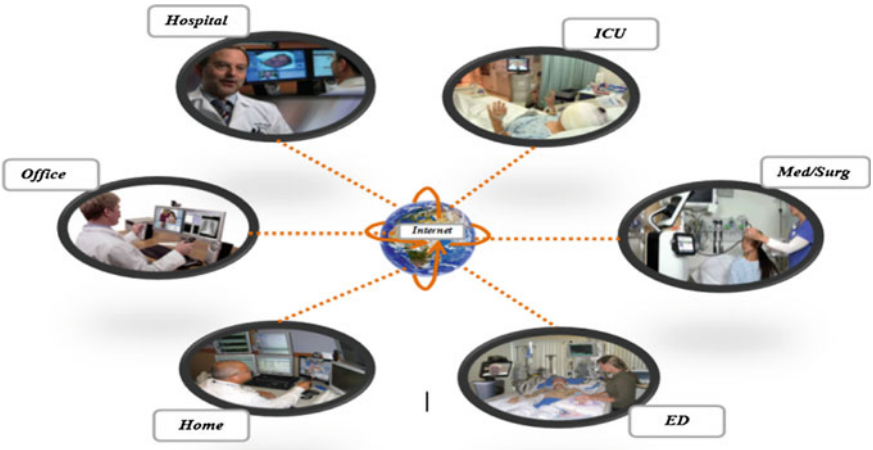

Fig. 12 A "many to many" system structure [1, 32]

unwanted tremor. Grippers are equipped with three-dimensional power sensors, providing a surgeon with a sense of touch while performing the surgery.

Innovation of the robot called Remote Presence-7 (RP 7) has marked the improved and better means of communication at a distance. The robot RP-7 has been produced by a private company InTouch Health located in Santa Barbara, California. The company was established in January 2002. with goal to develops, manufactures and distributes Remote Presence technology. Remote Presence (RP) is the ability to project oneself to another location (without leaving your current location) and the ability to see, hear, and talk as if you were actually there. This robot has a size comparable to the size of a man and allows individuals, as has been said, to project oneself from one location to another in order to be able to see, hear and speak, and thereby remain at the current location. Remote Presence is a new modality of interaction between a doctor and a patient. Wherever access to medical expertise is limited, Remote Presence can effectively extend a doctor's ability to provide care to patients. The system operates on a "many to many" system architecture (Fig. 12), allowing a doctor to connect from an office, hospital or home to the robot located at the intensive care unit or a patient's hospital room, and thus communicate with patients, their families, medical staff, etc. Using this technology, medical expertise can be made available to a patient at any time and at any place.

There are three main components of Remote Presence technology applied to the aforementioned type of a robot:

- RP 7 robot,
- Control Station,
- Connectivity service of RP (Remote Presence) technology.

RP (Remote Presence) Connectivity Service forms the basis of infrastructure, providing reliable connectivity between the robot and the control station. It delivers

continuous monitoring of each robot, allowing direct quality control and maximal time of accuracy. Service, support, license fees and software improvement all together are involved in RP Connectivity Service and are essential components of Remote Presence Robot. The RP 7 robot is a wireless, mobile robot with the applied Remote Presence technology that allows us to "be in two places at the same time." Under the direct control of a doctor, located in the control station, the robot can move without restriction, allowing the doctor to communicate freely with patients or members of the hospital staff.

The technology used by the RP 7 robot:

- Virtually There interactive technology,
- Holonomic Drive System,
- SenseArray 360 System, and
- RP System Core.

Although physical presence of a doctor near a patient cannot and must not be replaced, service robots for use in telemedicine have been developed because certain countries have very old population, a limited number of doctors, especially in rural areas where there are no doctors and where the application of these robots ideal. We refer to RP-7 service robot shown in Fig. 13.

This robot has a size that is comparable to the size of a man and allows an individual, as it has been said, to project oneself from one location to another to be able to see, hear and speak, and thereby remains in one's current location. Examples of service robots application for treatment of patients at a distance are shown in Fig. 13.

Service robots are used in helping the disabled and rehabilitating patients in rehabilitation centres. An example of such service robots is shown in Fig. 14.

Rehabilitation robots help the disabled in activities that they cannot perform on their own, or are involved in therapies for people to improve their physical functions. Areas of rehabilitation robots are general divided into therapy and robot's assistance. In addition, rehabilitation robots include prosthesis (prosthetics), nerve stimulation and devices for monitoring people during daily activities, as shown in Fig. 14.

Fig. 13 The robotic courier system used in medical institutions to serve patients [1, 32]

Fig. 14 Examples of service robots application for rehabilitation and helping the disabled [18, 20–30]

There are the following categories:

- robotic therapy for mobility (walking),
- personal rehabilitation robots,
- robotic therapy of the upper extremities,
- smart prostheses, and
- social service robots for personal care, autism and care of the elderly.

Giving back mobility to a patient is particularly tiresome and hard work for therapists, and this is the primary target for automation. Dozens of mobile robotic systems for training, i.e. rehabilitation is already in use in clinics around the world.

Service robots in medicine can, among other things, help in obtaining or distributing medications, while robots that help patients can assist in raising and positioning of patients who find it difficult to relate to. A Large part of activities related to providing professional medical assistance is logistical. It includes meeting the daily needs of patients (delivery of mail or personal care products, cleaning tasks), as well as supplying patients with medicaments and food. An example of such a system is the TUG system—an autonomous mobile robotic system also known as automated robotic system for delivery. This system automates the delivery and tracking of most hospital equipment and supplies such as medicaments, linen, blood samples, medical records, etc. It helps the circulation of the internal supply chain inventories in the hospital. TUG system requires wireless network access for communication with the base computer, lifts, and elevators at a ground floor, as well as areas where more TUG systems may encounter one another. The system contains a computer with an advanced TUG operating system, which uses its detailed map of a hospital and sophisticated navigation software in order to plan routes, avoid obstacles (it has sensors) and monitor its location constantly. The system may use carts connected in one column for transport, so that it can be used for virtually any application: patients' care, pharmacy, laboratory, primary supply, medical records delivery, etc. (Fig. 15).

Autonomous service robots working as a team (group) in order to complete the delivery of blood samples and courier tasks in hospitals and laboratories are controlled using computers. It is expected the service robots application in the field of human care and social assistance will increase. The strategic goal is to develop

Fig. 15 The robotic courier system used in medical institutions to serve patients [1]

service robots that meet real needs in the areas of social assistance as well as in areas of human care which demand an advanced technology. The application of such next-generation robots will be promoted in areas where robots have more physical contact with people, provided that it guarantees man safety.

4 Conclusion

Robotics technology is very attractive, challenging and imaginative discipline. Robotics as a science has a task, i.e. a noble objective—for example, to replace a man in performing tiresome, monotonous or dangerous and health-endangering jobs. A major breakthrough in robotics is that robots and humans work closely together, as servants or helpers in everyday life. Robotics is a relatively young technical branch, but it already has a rich tradition. It turned out that robots, just like people, passed generation cycles. Each new generation of robots received the more advanced features than the previous one, which is primarily related to the actual degree of intelligence, supporting computing power, enhanced dynamic indicators, and more advanced control algorithms. There are a number of facts that speak in favour of rapid long-term growth in the market for auxiliary robotic systems for the elderly and the disabled. The number of temporarily and permanently disabled persons is increasing, as well as the quota of the elderly in the world. This will increase the need for nursing and care of these people. Given the decline in the next 10–15 years in the number of people from active life who are interested in performing the role of a caregiver, there is a huge potential of demand for auxiliary robotic systems and service robots. For this reason, important scientific institutions working on service robots are developing new prototypes of service robots to assist the elderly and persons in need of rehabilitation.

References

1. Karabegović I (2012) Doleček V., i dr.: Servisni roboti, Tehnički fakultet, Bihać
2. World Robotics 2015 (2015) IFR, United Nations, New York and Geneva
3. World Robotics 2014 (2014) IFR, United Nations, New York and Geneva
4. World Robotics 2012 (2012) IFR, United Nations, New York and Geneva
5. World Robotics 2010 (2010) IFR, United Nations, New York and Geneva
6. Muller RA (2010) Physics and technology for future presidents: an introduction to the essential physics every world leader needs to know hardcover, May 2010
7. Teich AH (2012) Technology and the future
8. von Stackelberg P (2007) Technology & the future: managing change and innovation in the 21st century (Kindle Edition)
9. Bertalan Meskó: The Guide to the Future of Medicine: Technology and The Human Touch Paperback, 2014
10. Friedman DD (2011) Future imperfect: technology and freedom in an uncertain world
11. Karabegović I, Karabegović E, Mijović B, Ujević D (2010) Roboti primjenjeni u medicinskim ustanovama, 3. Međunarodni stručno-znanstveni skup, Zadar, 22–25. rujan, 2010, pp 321–327
12. Karabegović I, Karabegović E, Husak E (2010) Ergonomic integration of service robots with human body,. In: 4th international ergonomics conference, Stubičke Toplice, pp 249–254, June 30 till July 3, 2010, ISBN 978-953-98741-5-3
13. Vlatko D (2015) Future of technology. In: 2nd international conference on new technologies, NT-2015 development and application, pp 1–12, Mostar, 24–25 April 2015, ISSN 2303-5668
14. Karabegović I, Husak E (2010) Robot integration in modelling and simulation of manufacturing process. In: 1st international scientific conference on engineering MAT 2010, pp 37–41, Mostar 18–20. Nov 2010, ISSN 1986-9126
15. Karabegović, Felić M, Đukanović M (2013) Design and application of service robots in assisting patients and rehabilitations of patients. Int J Eng Technol 13(02):11–17
16. Karabegović I, Karabegović E, Husak E (2013) Application of service robots in rehabilitation and support of patients. Medicina 49(2):167–174
17. Doleček V, Karabegović II (2008) Roboti u industriji, Tehnički fakultet, Bihać
18. www.exoskeleton-suit.com; 03 Feb 2016
19. Karabegović I, Karabegović E, Husak E (2012) Application of robotic technology in the textile and clothing industry. In: 5th međunarodno znanastveno-stručno savjetovanje Tekstila znanosti i gospodarstva, 26. Siječanj, 2012, Zagreb, Croation, pp 285–290, ISSN 1847-2877
20. www.worldrobotics.org. 05 Jan 2016
21. http://www.technovely.com. 07 Jan 2016
22. www.eere.energy.gov/industry/mining/pdfs/robot.; 07 Jan 2016
23. www.ad.siemens.de/sinas/index_00.htm; 05 Jan 2016
24. www.robotik.dfki-bremen.de; 12 Jan 2016
25. www.intouchhealth.com; 14 Jan 2016
26. www.apparelyzed.com; 14 Jan 2016
27. www.twendyone.com; 06 Feb 2016
28. www.aist.org; 10 Feb 2016
29. www.vecnc.com; 10 Feb 2016
30. www.soundcloud.com; 12 Feb 2016
31. www.neuroarm.org; 7 July 2016
32. www.allonrobots.com; 7 July 2016
33. Doleček V.,Karabegović I. I dr.: Robotika, Tehnički fakultet, Bihać, 2002

Analysis of Electroencephalogram on Children with Epilepsy Using Global Wavelet Spectrum

Salko Zahirović, Nedis Dautbašić, Maja Muftić Dedović, Smail Zubčević and Samir Avdaković

Abstract The electroencephalography (EEG) is an electrophysiological monitoring method to record electrical activity of the brain and is used as the method of choice for the diagnosis of epilepsy. Nowadays, we can find dozens of EEG signal analysis papers using mathematical approach and with a focus on identification of epilepsy. This paper presents some results relating to the analysis of EEG on children using the Global Wavelet Spectrum (GWS). The signals are analyzed and collected on the UKCS during 2015 and 2016 using GWS. To be able to make comparison, EEG signals are gathered from both patients with and without epilepsy. Using this approach it is possible to clearly differentiate patients with a diagnosis of epilepsy from healthy ones.

1 Introduction

This paper represents further research presented in [1].

Epilepsy is a disease of the brain defined by any of the following conditions [2]:

S. Zahirović · N. Dautbašić · M. Muftić Dedović (✉) · S. Zubčević · S. Avdaković
University of Sarajevo, Sarajevo, Bosnia and Herzegovina
e-mail: mm14843@etf.unsa.ba

S. Zahirović
e-mail: salkozahirovic@gmail.com

N. Dautbašić
e-mail: nd15231@etf.unsa.ba

S. Zubčević
e-mail: smail.zubcevic@gmail.com

S. Avdaković
e-mail: samir.avdakovic@etf.unsa.ba

M. Hadžikadić and S. Avdaković (eds.), *Advanced Technologies, Systems, and Applications*, Lecture Notes in Networks and Systems 3,
DOI 10.1007/978-3-319-47295-9_3

- At least two unprovoked (or reflex) seizures occurring >24 h apart,
- One unprovoked (or reflex) seizure and a probability of further seizures similar to the general recurrence risk (at least 60 %) after two unprovoked seizures, occurring over the next 10 years and
- Diagnosis of an epilepsy syndrome.

EEG is an electrophysiological monitoring method to record electrical activity of the brain. Diagnostic accuracy of a single routine EEG is relatively poor, with a reported sensitivity of 30–50 %. Errors in interpretation—over reading is more harmful than under reading. Experience, practice and doctor‘s subjective perception [3].

EEG has established itself as an important means of identifying and analyzing epileptic seizure activity in humans. In most cases, identification of the epileptic EEG signal is done manually by skilled professionals, who are small in number [4].

2 Materials and Methods

Wavelet Transform (WT) represents one of the most effective mathematical tools for time-frequency analysis of nonstationary signals. It has significant applications in all branches of science.

The wavelet transform (WT) introduces a useful representation of a function in the time-frequency domain [5–7]. Basically, a wavelet is a function $\psi = L^2(R)$ with a zero average:

$$\int_{-\infty}^{\infty} \psi(t)dt = 0. \tag{1}$$

Continuous Wavelet transform (CWT) is applied (using Morlet wavelet function) for analysis of EEG signals. Global Wavelet Spectrum is used for discrimination between healthy and epileptic patients.

A multiresolution is relation between time and frequency resolution. Signal database set consist of 5 patients:

- 2—healthy patients;
- 3—patients with epileptic syndrome—study state.

Additional characteristics of the analyzed data:

- 19 signals-channels of EEG,
- Duration—20 s or 2688 samples and
- Sampling rate Fs = 134.4 Hz which is enough for identification of all components of EEG signals.

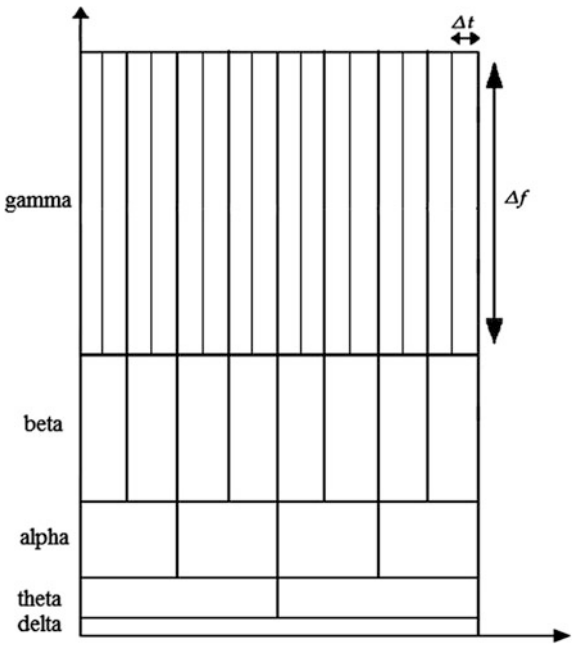

Fig. 1 Spectral density in the wavelet transform domain (time frequency domain)

The coefficients distribution of a WT is presented in the time–frequency domain, shown on Fig. 1 [8].

Wavelet transform is often referred to as mathematical microscope because of its multiresolutional analysis which provides very complex analysis of nonstationary signals such as EEG signals.

First it is sampled very well in time, then very high frequencies are obtained, then frequency band is doubled to get the better frequency resolution and so on (Fig. 1). Basically we have wavelets (short wavelike functions that can be scaled and translated) and similarities between wavelets and signals at different scales are measured using them.

Also in Table 1. are presented five frequency bands and corresponding EEG signal components. Components of EEG signals are gamma, beta, alpha, theta and delta. Of particular importance are alpha (8.40–16.80), theta (4.20–8.40) and delta (0.00–4.20). This is presented in [9–12].

Table 1 Frequency bands and corresponding EEG signal components

Frequency band (Hz)	Components of EEG signals
33.60–67.20	Gamma
16.80–33.60	Beta
8.40–16.80	Alpha
4.20–8.40	Theta
0.00–4.20	Delta

3 Results and Discussion

On Fig. 2 is presented electroencephalogram of one healthy child and on Fig. 3 is presented electroencephalogram of one child with epilepsy in steady state.

The illustrative examples of EEG signal of healthy patient and EEG signal of a patient with an epileptic syndrome—steady state (first channel) are presented in Figs. 4 and 5.

By just looking at Figs. 4 and 5 it can be seen that signals are very similar and it is very difficult to discriminate healthy patient from patient with epilepsy. Signals presented at these two figures are not processed yet. On Figs. 6 and 7 Wavelet Power Spectrum (WPS) and GWS of a healthy child and child with an epileptic syndrome are shown.

On Figs. 6 and 7 are presented signals from Figs. 4 and 5, but with Wavelet transform applied. So left side on both figures represents Wavelet Power Spectrum and right side presents Global Wavelet Spectrum. Those figures represent time-frequency wavelet analysis.

Figure 8 presents GWS of two healthy patients and first epileptic patient:

- first 19 GWS are related to healthy patient,
- second 19 GWS are related to healthy patient and
- third 19 GWS are related to epileptic patient.

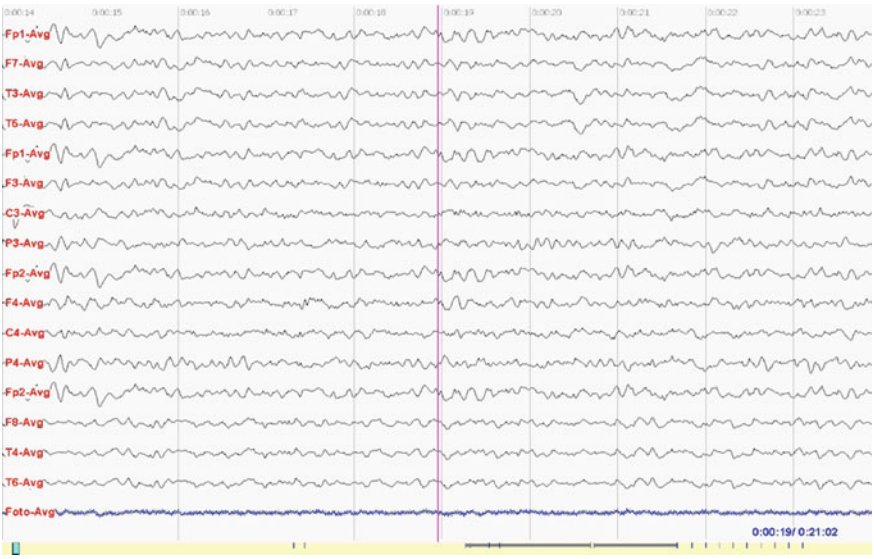

Fig. 2 The electroencephalogram of healthy child

Fig. 3 The electroencephalogram of child with epilepsy in steady state

Fig. 4 EEG signal of healthy patient (first channel)

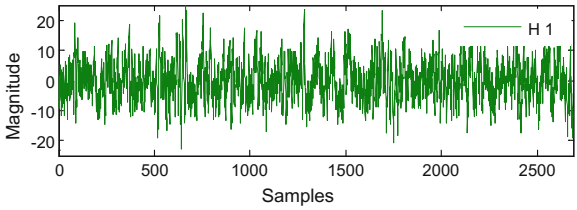

Fig. 5 EEG signal of a patient with an epileptic syndrome—steady state (first channel)

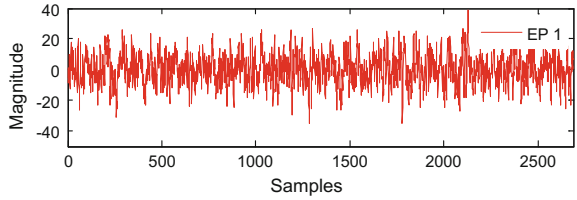

It can be seen that alpha, theta and delta components of EEG signal have much higher values for patient with epilepsy. On the z-axis are presented powers of EEG signals and are much higher for persons with epilepsy. The same situation can be seen on the Figs. 9 and 10.

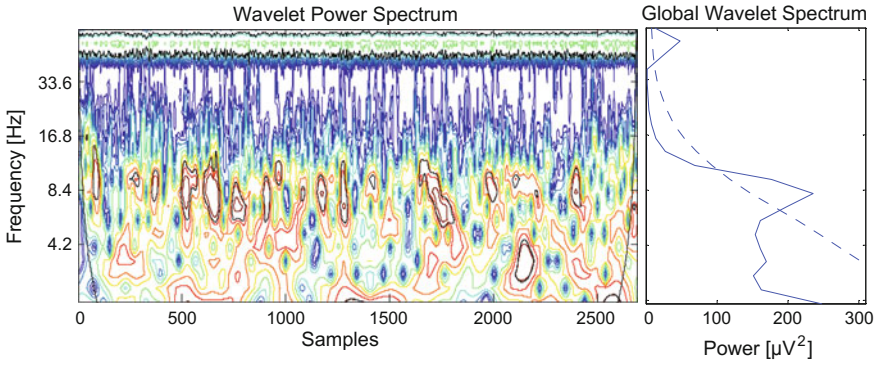

Fig. 6 WPS and GWS of a healthy subject

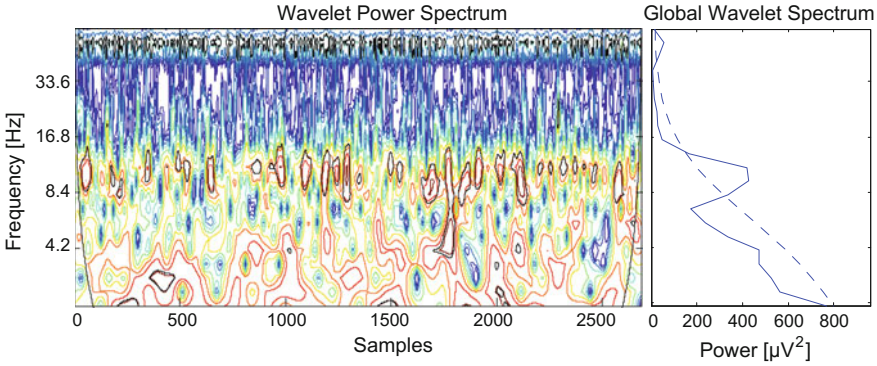

Fig. 7 WPS and GWS of a patient with an epileptic syndrome without seizure

GWS of two healthy patients and second epileptic patient:

- first 19 GWS are related to healthy patient,
- second 19 GWS are related to healthy patient and
- third 19 GWS are related to epileptic patient.

GWS of two healthy patients and third epileptic patient:

- first 19 GWS are related to healthy patient,
- second 19 GWS are related to healthy patient and
- third 19 GWS are related to epileptic patient.

As additional approvals of our methodology statistical features are extracted for the GWS magnitude of one healthy patient signal and one patient with epilepsy. Special frequency bands are alpha, theta and delta and features for those

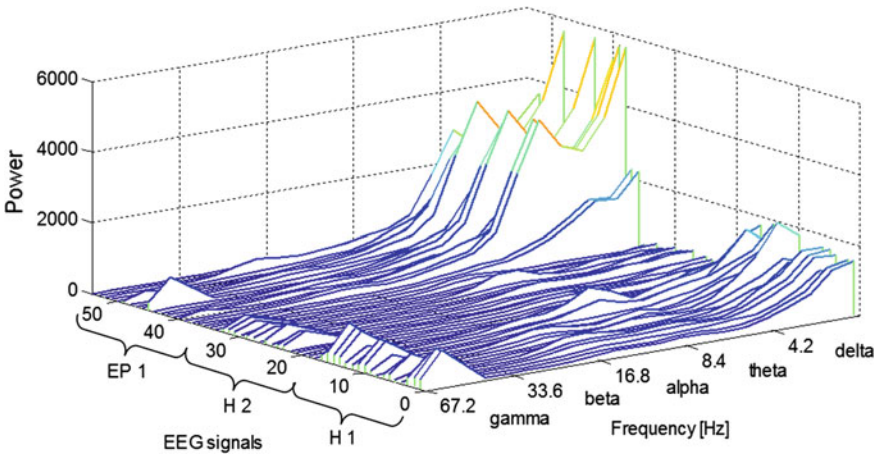

Fig. 8 GWS of two healthy patients and first epileptic patient

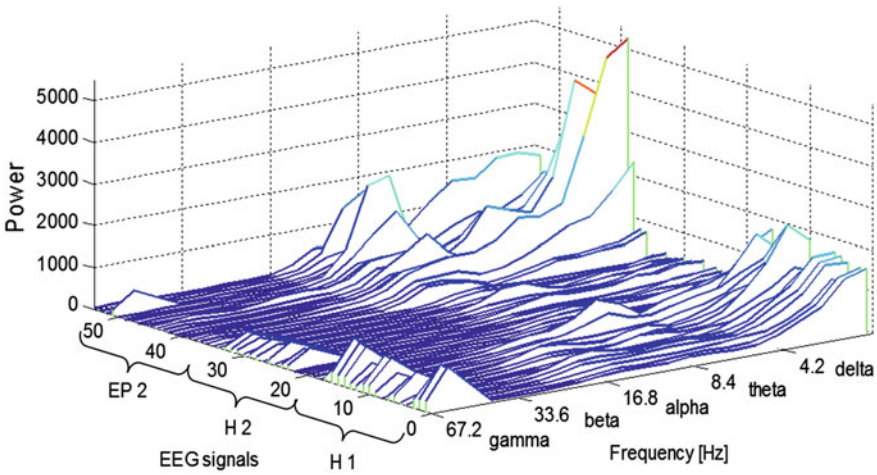

Fig. 9 GWS of two healthy patients and second epileptic patient

components are mean and mode. Mean is the most frequent value while mode is the average value extracted from the signals of healthy patient and patient with epilepsy. From Table 2 it can be seen that values for mean and mode are much lower than values of mean and mode of patient with epilepsy.

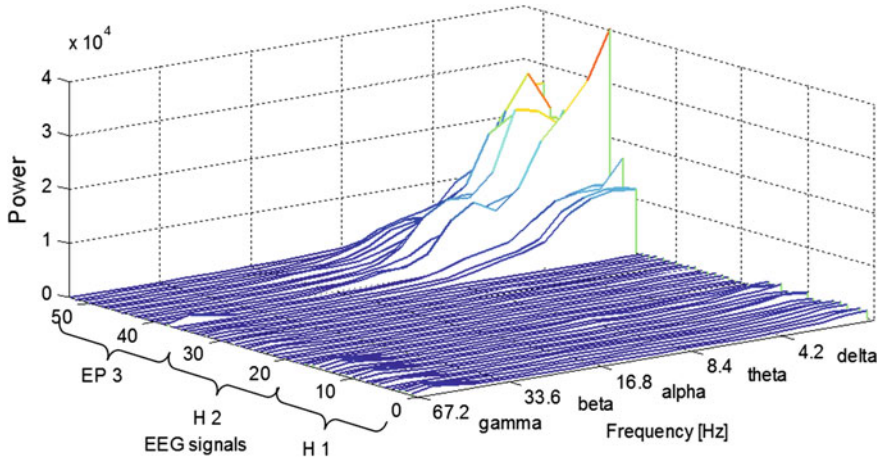

Fig. 10 GWS of two healthy patients and third epileptic patient

Table 2 Statistical features extracted for the GWS magnitude of one healthy patient signal and one epileptic patient

Frequency band (Hz)	Feature	Healthy patient	Epileptic syndrome
0.0–4.2	Mean	235.29	1072.39
	Mode	142.26	225.66
4.2–8.4	Mean	323.89	6028.64
	Mode	188.40	1708.54
8.4–16.8	Mean	1092.90	15914.47
	Mode	540.31	9373.13

4 Conclusion

WT as a mathematical tool has been in use for analysis of the EEG signal for a long time. In this work WT proved to be a successful technique in terms of EEG analysis on children (under 18 years). Visual EEG analysis often does not provide quality conclusions.

The GWS presentation of the EEG signal enables excellent observation of activities within the specific components (delta and theta), and clear distinction between healthy and epileptic children.

5 Further Research

At the department of Neuro Pediatricians of the Pediatric Clinic of the University Clinical Centre in Sarajevo it is planned to collect EEG signals on 100 patients.

Using the same approach (GWS) will be done detailed analysis and will be discussed the possibility of implementing an automatic classifier. Also analysis will be done using DWT on which it is possible to completely isolate each component of the EEG signal. Over the same signals analysis will be done by Hilbert-Huang Transform.

References

1. Zahirovic S, Zubcevic S, Avdakovic S, Dautbasic N, Muftic Dedovic M (2015) Analysis of electroencephalogram report using the wavelet transform. J Neurol Surg A Cent Eur Neurosurg 76:A094
2. Omerhodžić I, Avdaković S, Nuhanović A, Dizdarević K (2010) Energy distribution of EEG signals: EEG signal wavelet-neural network classifier. Int J Biol Life Sci 6:210–216
3. Barkmeier DT, Senador D, Leclercq K, Pai D, Hua J, Boutros NN, Kaminski RM, Loeb JA (2012) Electrical, molecular and behavioral effects of interictal spiking in the rat. Neurobiol Dis 92–101
4. Patnaika LM, Manyamb OK (2008) Epileptic EEG detection using neural networks and post-classification. Elsevier 91:100–109
5. Daubechies I (1992) Ten Lectures on Wavelets. Society for Industrial and Applied Mathematics, Philadelphia
6. He H, Starzyk JA (2006) A self-organizing learning array system for power quality classification based on wavelet transform. IEEE Trans Power Delivery 21(1):286–295
7. Mallat S (1998) A wavelet tour of signal processing. Academic, San Diego, CA
8. Morales C, Ronquillo–Jarillo G, Campos–Enríquez JO (2009) Multi-scale analysis of well–logging data in petrophysical and stratigraphic correlation. Geofisica
9. Avdakovic S, Omerhodzic I, Badnjevic A, Boskovic D (2015) Diagnosis of epilepsy from EEG signals using global wavelet power spectrum. In: 6th European conference of the international federation for medical and biological engineering. Springer International Publishing, pp 481–484
10. Ibrić S, Avdaković S, Omerhodžić I, Suljanović N, Mujčić A (2015) Diagnosis of epilepsy from EEG signals using Hilbert Huang transform. Folia Med Fac Univ Saraeviensis 50(1): 68–73
11. Subasi A, Alkan A, Koklukaya E, Kiymik MK (2007) EEG signal classification using wavelet feature extraction and a mixture of expert model. Expert Syst Appl 32(4):1084–1093
12. Subasi A, Ercelebi E (2005) Classification of EEG signals using neural network and logistic regression, Comput Methods Programs Biomed 87–99

Target Signatures and Pose Estimation

Migdat I. Hodžić and Tarik Namas

Abstract The paper discusses an important class of defense and commercial applications in the context of Ground Target (Object) Identification, Classification, and Tracking. The data base of target digital signatures is assembled and formed for a full spatial circle (360°) analysis from such sources as High Resolution Radar and Synthetic Aperture Radar. These digital signatures are analyzed from which various spatial as well as frequency (wavelet) characteristics of the targets are formed and interpreted, in order to make good estimate of target pose angle. This angle is key for tracking maneuvering targets. Various statistical measures are obtained from digital signatures to assist in pose angle estimation. We also use certain geometrical considerations to determine an initial pose estimate which is the refined using a variety of correlation coefficients. Expected precision of pose estimate is within few degrees, i.e. within few neighboring target signatures. The paper presents several real life ground target signatures as well as several simulated signatures to illustrate our approach.

1 Introduction

Modern developments in the areas of various high resolution radar technologies, made the ground targets reflection signatures much richer and useful features of these targets can be identified. Successful target identification and tracking exploit this feature information to determine target type and its dynamics. In the process of automatic target recognition, the pose angle estimates are obtained as well, provided target data base contains full 360° target signatures in small angle increments. Figure 1 shows typical pose angle (aspect and depression) geometry. The depression angle relates to sensor position and aspect angle is deduced from radar signatures. For ground targets, since their velocity vector is aligned most of the time with the body's longitudinal axis, the pose angles carry kinematic information that

M.I. Hodžić (✉) · T. Namas
International University of Sarajevo, Sarajevo, Bosnia and Herzegovina
e-mail: mhodzic@ius.edu.ba

M. Hadžikadić and S. Avdaković (eds.), *Advanced Technologies, Systems, and Applications*, Lecture Notes in Networks and Systems 3,
DOI 10.1007/978-3-319-47295-9_4

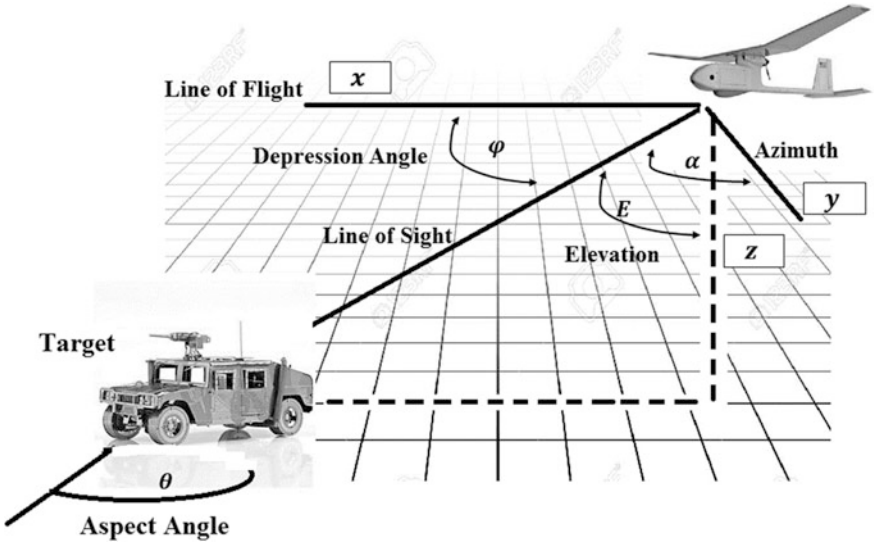

Fig. 1 Target and sensor platform geometry

can be used to improve target tracking particularly during the target maneuvering periods [3–14].

In this paper we continue our previous and continuing work related to new methodology for improved automatic target identification as well as pose estimate, which can in turn improve target tracking and reduce target miss-association probability. In a typical airborne application (USA JSTAR is good example) [15–18], a ground target is detected from a distance, identified and classified using stored target data base, and then tracked after that. In this paper we expand our work reported in [1, 2], where we analyzed certain number of targets in spatial domain in particular. Section 2 in this paper reviews several targets signatures from USA public Moving and Stationary Target Acquisition and Recognition (MSTAR) program database [15–18]. The MSTAR data consists of SAR data in X-band, with 1×1-foot resolution, at 15° depression angle. In addition to these real targets we generate a number of our own synthetic targets as a reference targets to test our pose estimation methodology. In summary, we average radar raw data along X and Y coordinates and test them individually for target identification purposes. Each target has 274 signatures at different pose angles, for a full circle, given in a form of a radar digital bit map. We form corresponding target data base with additional target features useful in aiding in real time target identification, as elaborated in Sect. 3.

In particular, we use target geometry as well as autocorrelation and cross correlation spatial characteristics to draw conclusions about target features which would place it in a certain precise place in the target data base. We analyze all 274 individual target signatures (total of 360°) and form a variety of statistical measures to associate with each signature. Another approach is to use second order statistics such as autocorrelation envelopes with minimum and maximum frequency

information, which can be identified with certain geometric and spatial dimensions of the targets.

We will also explore frequency (wavelet) aspect of the signature data in our future work. Note that in this case the "frequency" is an inverse of spatial rather than time coordinates. Besides standard first and second order statistics we also employ newly introduced statistical notion of Brownian Distance and the corresponding correlation index [19] which both measure independency of two random sequences.

This is very powerful method and we employ it in target signature independence testing, for different targets and poses as well. Overall, the purpose of additional signature statistical analysis is to gain insight into key signature features which discriminate against other targets.

The resulting expanded target data base has original raw radar data, as well as additional target features and statistics (Fig. 4). This stored information is used in a subsequent real time target identification when its signature is compared against the data base in order to correctly identify the target with the lowest possible probability of wrong association. At the same time, we also estimate pose in the process which in turn makes target tracking much easier and more precise. One notable historical ATR application is well known USA Air-force JSTAR platform [16–18] which was deployed in mid and late 1990s, in Bosnia and Herzegovina to enforce Dayton Peace Agreement (Kosovo as well). The platform was used for ATR and large arms collection confirmations. There is a current JSTAR modernization effort under way. Our methodology is applicable to other defense as well as commercial areas, such as traffic control and possible facial recognition also.

2 Target Signature Data Base

Basic target and sensor platform geometry is given in Fig. 1. In [1] we used three signatures for analysis, and they are repeated here as a reference in Fig. 2 (raw continuous data) and Fig. 3 (16 digitized signature values).

In [2] we expanded our spatial analysis to many more targets, digitization was at the level of 32 and 64 data points, and we also defined a synthetic target as a reference in statistical testing. In this paper we employ more precise data to make better target identification and pose estimate along the way. Figure 4 shows various components of our analysis, and Figs. 5, 6 and 7 show three real life target signatures. Data resolution is 1×1 foot, depression angle is 15°. Figure 8 is our own made synthetic target used as a reference in the statistical analysis.

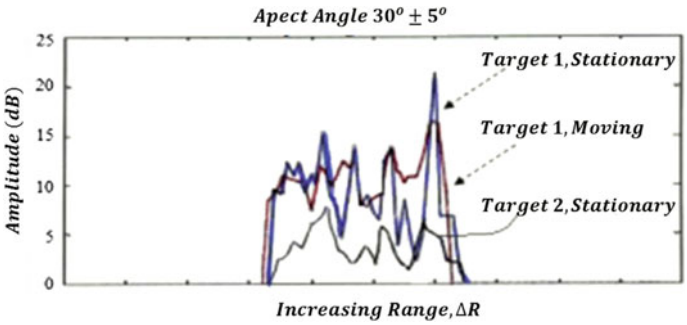

Fig. 2 Continuous SAR range data over ΔR

Fig. 3 Digitized data, stationary target 1

Fig. 4 Target identification and pose estimation

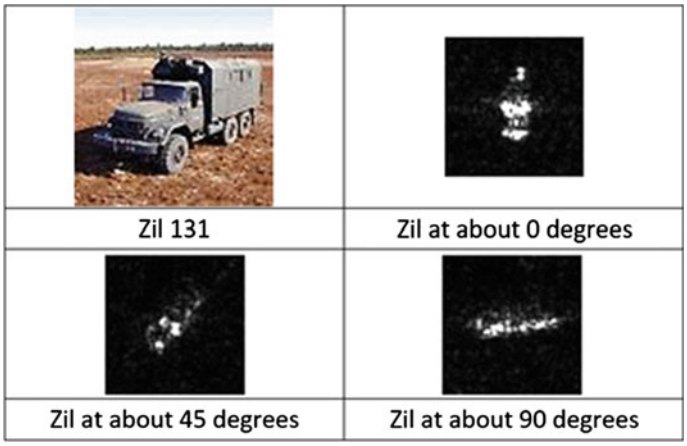

Fig. 5 Zil truck raw SAR images

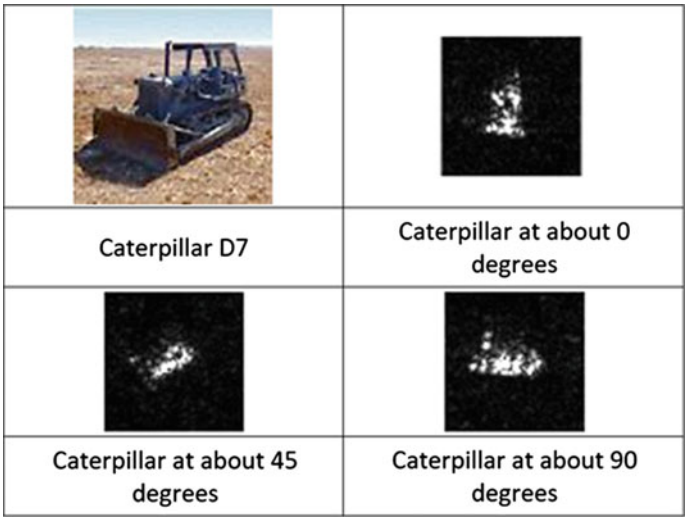

Fig. 6 Caterpillar bulldozer raw SAR images

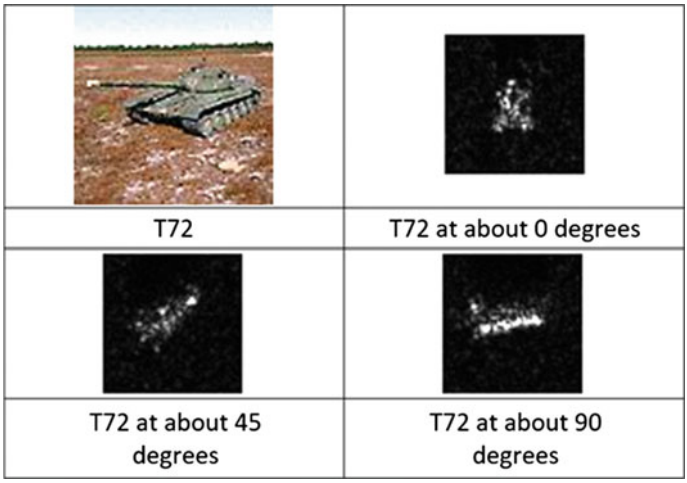

Fig. 7 Tank T72 raw SAR images

3 Target Signatures as Stochastic Processes

There are a total of 274 signatures for 4 quadrants, i.e. for 360°. The three real life targets in Figs. 5, 6, 7 and 8 span a range of different features and sizes. The MSAR data base [15–18], has more targets and our methodology can be applied to any of them, or to a similar target data base. In order to analyze target signatures, let us first

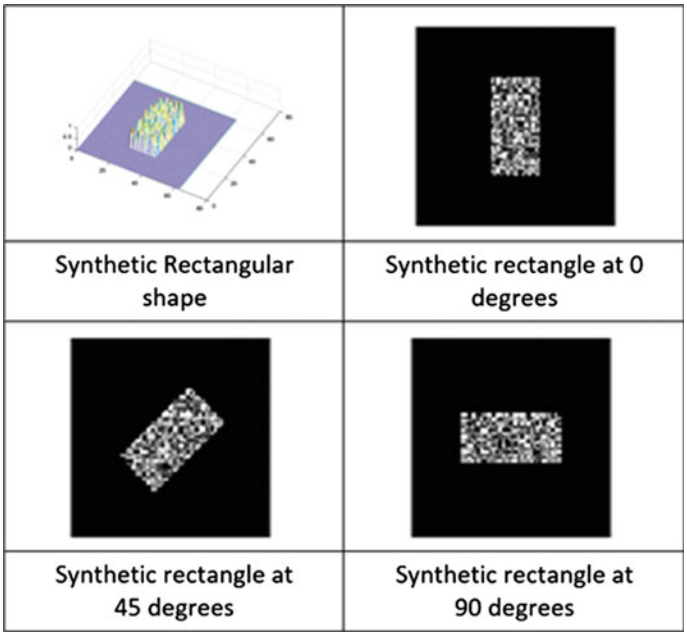

Fig. 8 Rectangular synthetic target with random pixels

define two families of stochastic processes $X(i, j) = X(T_i, \theta_j)$ and $Y(i, j) = Y(T_i, \theta_j)$ as follows:

$$\begin{aligned} X\left(T_i, \theta_j\right) &= \text{Radar X signature, ith target, jth pose} \\ Y\left(T_i, \theta_j\right) &= \text{Radar Y signature, ith target, jth pose} \end{aligned} \tag{1}$$

where i = 1, 2, 3, 4 (1–3 are real targets while 4 is synthetic), j = 1, 2,… 274 (4 quadrants, 360°). Table 1 summarizes all target and pose combinations [5]. The vectors X(i, j) and Y(i, j) are K dimensional, such that X(i, j) = [X1(i, j), X2(i, j), …,Xk(i, j)]T, and similarly for Y, where K is the number of radar signature pixels along X and Y. Figure 3 shows X(i, j) with K = 16. In this paper K = 32 or K = 64 and similarly for Y(i, j). This number is based on two considerations. First, the number of significant signature pixels for all targets is K or less. If less than K, we append required number of zeros to the right of the signature. Second, for future research in wavelet domain, we want this number to be a power of 2. Signature numerical values are means along X and Y, X(i, j) and Y(i, j), of pixels gray values from MSTAR data base. Figure 9 shows Zil truck (Target 3) signatures, where the gray scale levels are translated into digital signatures by averaging the gray level values along the X and Y axis.

In other words, if we take the average of pixels of Fig. 5 when the truck is at zero degrees in both X and Y axis we get Fig. 9. Figure 10 adds variances as well,

Table 1 Target signature template

Pose/target	Pose 1	Pose 2	…	Pose 274	Signature/correlation
Target 1/tank	X(1, 1)/Y (1, 1)	X(1, 2)/Y (1, 2)	…	X(1, 274)/Y (1, 274)	T_1 SAC
Target 2/bulldozer	X(2, 1)/Y (2, 1)	X(2, 2)/Y (2, 2)	…	X(2, 274)/Y (2, 274)	T_2 SAC
Target 3/truck	X(3, 1)/Y (3, 1)	X(3, 2)/Y (3, 2)	…	X(3, 274)/Y (3, 274)	T_3 SAC
Target 4/rectangle	X(4, 1)/Y (4, 1)	X(4, 2)/Y (4, 2)	…	X(4, 274)/Y (4, 274)	T_4 SAC
Statistics	P_1 SS	P_2 SS	…	P_{274} SS	CTC
Pose/target	Pose 1	Pose 2	…	Pose 274	Signature/correlation

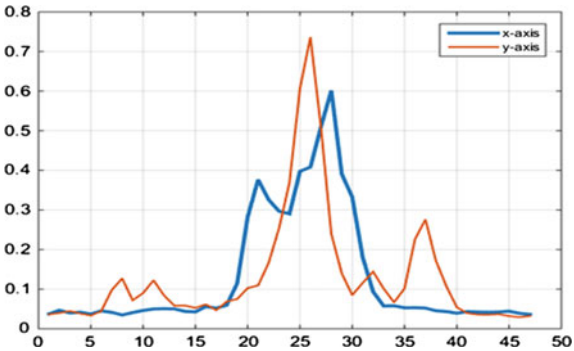

Fig. 9 Raw to X and Y digital target signature

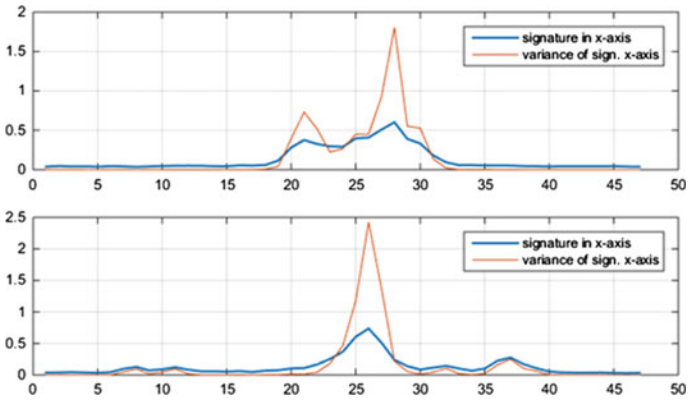

Fig. 10 Target X and Y with corresponding variances

Table 2 Target Pose Estimation Example

X_1 (Width)	8.98 pixels
X_2 (Length)	31.06 pixels
X_3 (Pose)	65.63°
Position No	50

which are useful in target and pose discrimination. Note that the signatures are filtered and very small values to the left and to the right are set to zeros. The last row in Table 1 indicates jth Pose Sample Statistics (P_jSS) for any target, across $X_k(j)$ and $Y_k(j)$, with k = 1, 2,…, K, j = 1, 2,…, 274. We dropped target indicator "i" for simplicity. These statistics are summarized in Table 2 for X(j), with similar table for Y(j), more on this in Sect. 4.

4 Target Geometry Analysis

In this Section we consider simplified target geometry and assume we have a rectangular target. Figure 11 illustrates this idea in (*X, Y*) coordinates using an angled target signature, between 0° and 90°. Note that not every target will be a perfect rectangular shape but this is very good approximation for any symmetric target if we are interested in its maximum (length) and minimum (width) dimensions. From Fig. 12 we easily obtain the following set of three nonlinear algebraic equations which summarize geometric relationships among three key geometric features of the target signature, i.e. width, lengths and pose angle.

These equations need to be solved for X-s given Y-s, when we acquire "real time" target as well as for justification of their use for the known data base targets. In order to calculate Y_1 and Y_2 we need to perform further analysis of the target signatures. Namely, we will need to "clean up" or "pre filter" target signatures by eliminating all zero or near zero amplitudes right before the target signature exhibits significant spatial amplitude, starting from the left side. We can call these signature leading zeroes. Similarly, we will clean the trailing zero on the right side of the signature. Equations 2 can be solved for a "real time" target once acquired by the

Fig. 11 Geometry of ideal rectangular target

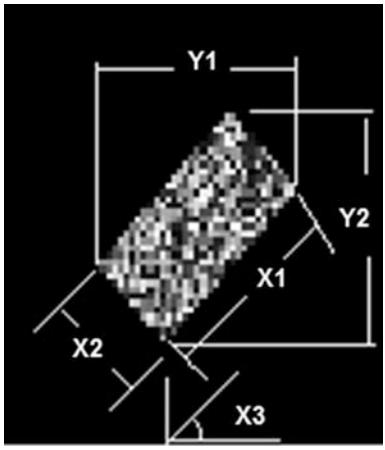

Fig. 12 Synthetic target pose determination

sensor platform. The solutions X_1 and X_2 correspond to the length and width of the rectangular target, and X_3 is corresponding pose angle estimate.

$$\begin{aligned} X_1 \cos(X_3) + X_2 \sin(X_3) &= Y_1 \\ X_1 \sin(X_3) + X_2 \cos(X_3) &= Y_2 \\ X_1 X_2 &= Y_3 \end{aligned} \tag{2}$$

The initial solution is generically presented in 1st quadrant (0° to 90°) but real quadrant is determined in the second step when we calculate 1st order statistics. This will act as an initial estimate of pose and will identify the target type as well. Further use of other statistics will improve the estimate. That is the basic idea in our approach. The following example illustrates the approach. We chose a random synthetic target at 224th position in the synthetic target data base (Fig. 11 for simulated raw pixels, Fig. 13 for averaged X and Y signatures). After solving the equations for X_1, X_2, and X_3 we get the first estimate of the target geometry and pose (Table 2).

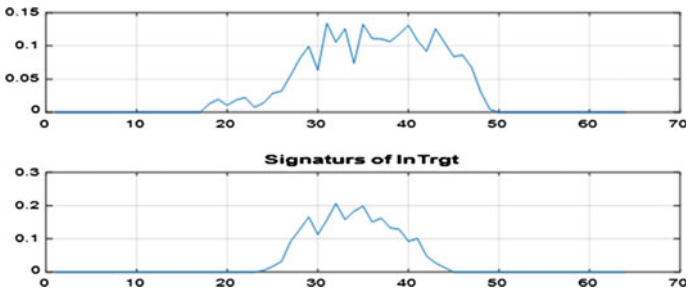

Fig. 13 X and Y signatures for synthetic target

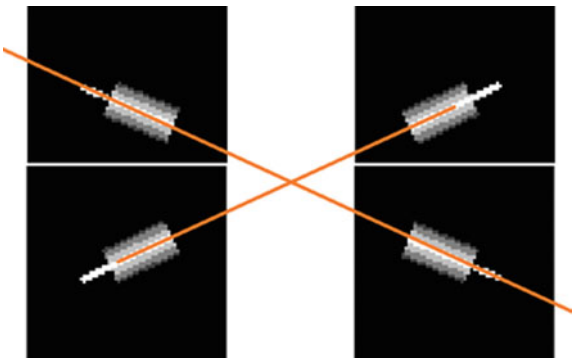

Fig. 14 Geometric symmetricity of target signatures

This information determines the target position at 50 (1st quadrant), out of 274 in the circle. The real quadrant (4 in this case) is determined by analyzing three more signatures shifted 90 degrees from target 50, and situated in quadrants 2, 3 and 4 (Fig. 14). Next we take three synthetic targets from target data base plus a number of additional signatures with poses around signature 50, shift them 90 degrees as well, and compare their signatures with the signatures in Fig. 13. For these comparisons we use several correlation coefficients, namely Pearson, Spearman, Kendal, and also Brownian to identify the target and also right quadrant. Tables 3 and 4 show correlations for X and Y, for these four correlation coefficients, for various poses, and their sum (boldfaced) as an ultimate measure of coincidence between the correlations. The correlations are at the peak with Target 1 and pose 225 (7.6881 vs. 6.7915 and 6.4929), and the target is in 4th quadrant. Hence we missed by one pose position, error of 1 in 274 or 0.365 %, which is an excellent estimate between (i) geometrical and (ii) correlation comparisons. See our papers [1, 2] for more information on correlation coefficients. In general, this still does not mean we found the correct pose, it is an initial estimate only. More statistical tests can be done to find the correct pose.

We check the result (pose 225) by comparing X and Y signature variances. Without going into the details, we obtain the same pose 225 estimate. At this point we can continue with more statistical tests to fine tune the estimate to correct pose 224 or be satisfied with estimate at 225. For the real signatures there may be some additional pose estimation errors hence more tests could be required. See next Sects. 5 and 6.

5 Signature Statistics Across Poses

Table 5 summarizes a list of signature statistics which can be used for further pose estimation refinement. We are currently looking into the importance of all of the individual statistics in order to form their optimal combination, for not all carry useful information. Table 5 is a summary of all the statistics, Figs. 16 and 17 have

their values for Zil truck (Fig. 5) and ideal rectangular (Fig. 8). Table 6 summarizes sample autocorrelations which are relevant for target identification and pose estimation. The autocorrelation measures signature correlation between components in X(i, j), for each target and for every pose individually, for a total of 4 times 274, i.e. 1096 autocorrelations. Likewise, for Y axes. The autocorrelation captures certain

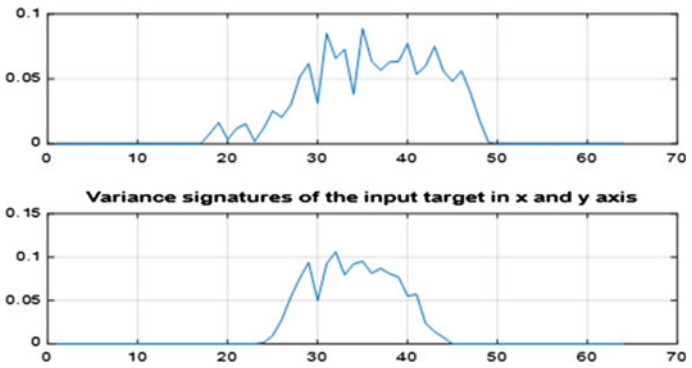

Fig. 15 Target signature variances

Table 3 1st target correlations

223	224	225	226	227
0.9697	0.9712	0.9719	0.9680	0.9724
0.9751	0.9789	0.9795	0.9807	0.9809
0.9762	0.9783	0.9824	0.9799	0.9789
0.9462	0.9808	0.9803	0.9803	0.9645
0.9004	0.9086	0.9213	0.9109	0.9073
0.9001	0.9447	0.9419	0.9415	0.9231
0.9395	0.9416	0.9425	0.9346	0.9444
0.9624	0.9677	0.9682	0.9698	0.9701
7.5696	7.6719	7.6881	7.6657	7.6417

Table 4 2nd and 3rd target correlation

226	227	228	227	228
0.8148	0.8212	0.8152	0.7736	0.7761
0.9415	0.9476	0.9514	0.9227	0.9272
0.8458	0.8496	0.8503	0.7979	0.7981
0.9210	0.9213	0.9213	0.9041	0.9045
0.7391	0.7507	0.7546	0.6953	0.6911
0.8699	0.8694	0.8670	0.8474	0.8494
0.7003	0.7095	0.7013	0.6477	0.6508
0.9144	0.9224	0.9278	0.8892	0.8956
6.7469	6.7915	6.7890	6.4780	6.4929

Table 5 List of target signature statistics

Statistics	Description
X_{max}, k_{max}	Maximum signature and position among k
X_m	Mean signature value $\Sigma_k\ X_k(j)/k$
X_{mead}	Signature median, ordered middle value
X_{var}	Signature variance $\Sigma_k\ [X_k(j) - S_{mean}]^2/k$
X_{stedv}	Signature standard deviation $(S_{var})^{0.5}$
X_{vare}	Signature variance energy $\Sigma_k\ [X_k(j) - S_{mean}]^2$
$X_{max/mean}$	Signature max/mean ratio S_{max}/S_{mean}
X_{varm}, k_{mv}	Max variance and position in K samples
X_{energy}	Signature energy $\Sigma_k\ X_k^2(j)$
X_{skew}	Signature skew adjusted FP
X^1_{skew}	Adjusted FP signature skew
X^1_{skewv}	Adjusted FP signature skew variance

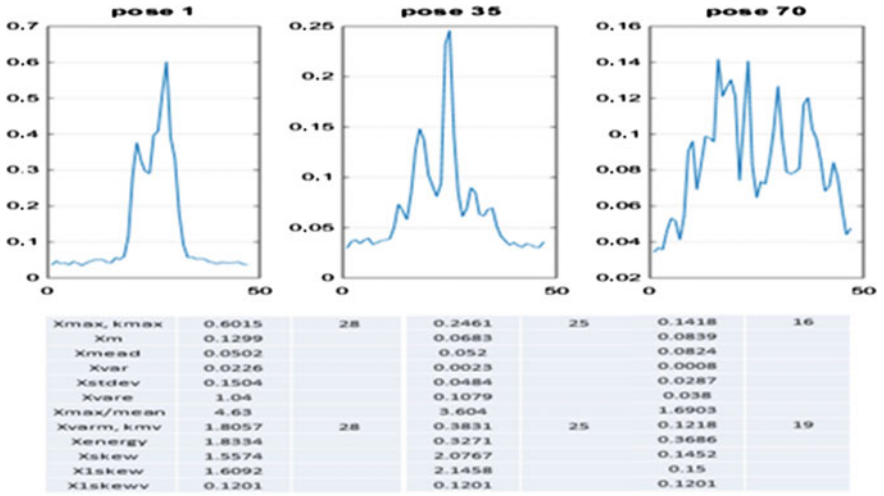

Fig. 16 Zil truck signature statistics across 3 poses

geometrical features of the targets. In particularly the zero crossing Xzcor indicates the relative size of the signature projection onto X. The zero crossing also corresponds to the number of non-zero signature samples (Fig. 15).

We assume that signature has no leading zeros for they would shift autocorrelation zero crossing. As pose angle change we get different zero crossings for different target projection onto X and Y. In Section V we refer to zero crossing man/min ratio, Xz/max/min, which indicates approximate length/width ratio.

Zil truck dimensions can be found on line and compared. Figure 17 shows ideal rectangular target, with length L = 32, and width W = 16 feet, for 1-foot resolution as in MSTAR. Here zero crossings correspond to W, L and 45° X projection, so that we have:

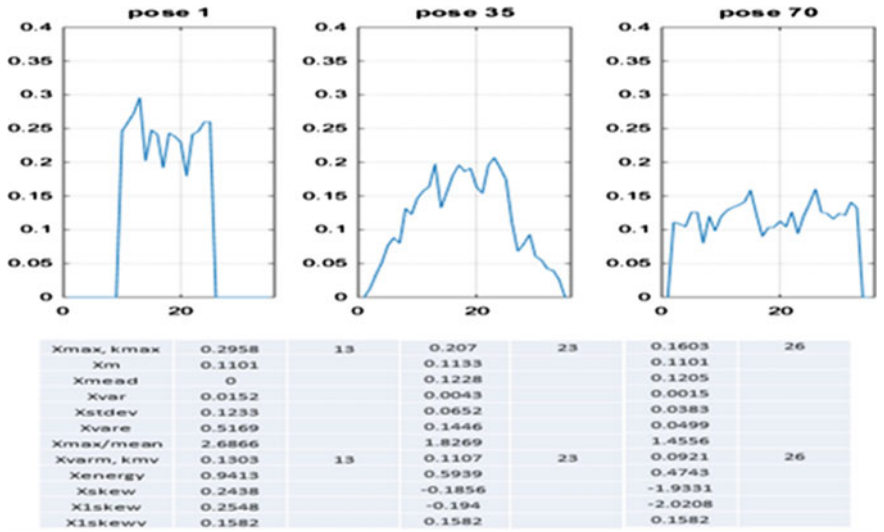

Fig. 17 Synthetic signature statistics across 3 poses

Table 6 Pose j sample autocorrelations (PjSS)

Variable	Description
X_{cor}	Signature autocorrelation function
X_{zcor}	Signature autocorrelation zero crossing
X_{ecor}	Signature autocorrelation error
X_{npix}	Number of pixels along X

$$\text{Xproj} = \text{L}\ \sin(45) + \text{W}\ \cos(45) = 35.6$$

6 Signature Statistics Across One Target

The last column in Table 1 indicates ith Target Signature Auto Correlation (TiSAC) features for each of four targets across every pose, for both X(i, j) and Y(i, j). We first consider two correlation measures, Pearson and Spearman coefficients. Then

Table 7 Auto correlation features (Ti SAC)

Variable	Description
X_p	Pearson coefficient
X_s	Spearman coefficient
X_{psauto}	Pose shifted autocorrelation envelope
X_{zpauto}	Pose shifted autocorrelation zero crossing
$X_{z/max/min}$	Autocorrelation max/min zero crossing

we look into pose shifted autocorrelations. Table 7 has corresponding statistics summary.

We can start with X(1, 1) and correlate it with X(1, 2), then with X(1, 3), etc., and finally with X(1, 274) forming envelope of correlations. This results in a $4 \times 274 = 1096$ correlations. These capture cross statistics for poses and can be used to discriminate poses. Figures 18 and 19 show Pearson and Spearman

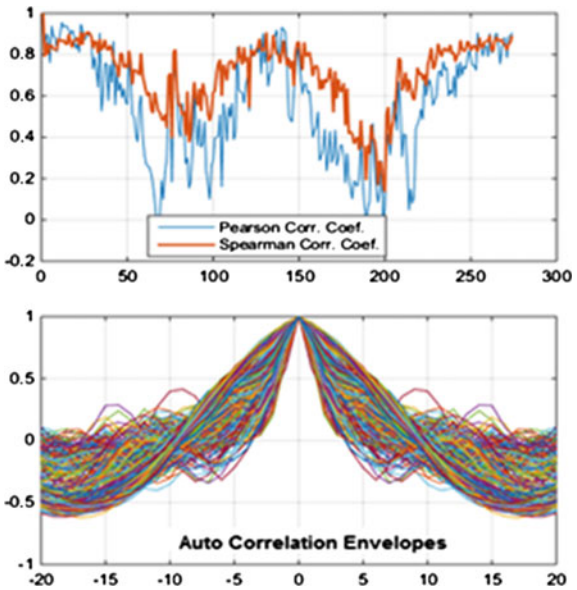

Fig. 18 Zil truck pose shifted correlations

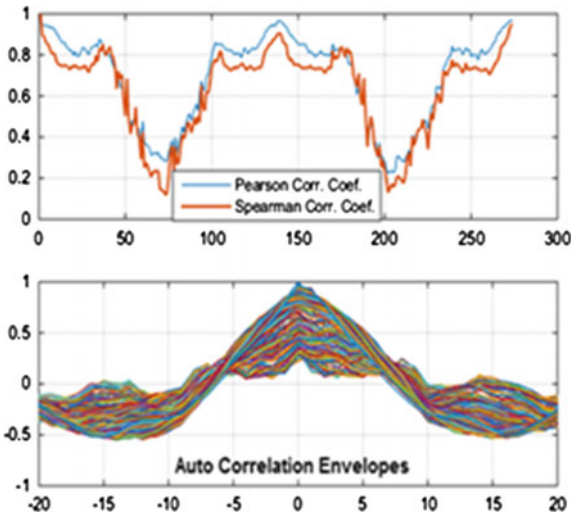

Fig. 19 Ideal rectangular pose shifted correlations

coefficients, as well as correlation envelopes, as a function of the pose for Zil Truck and for our rectangular synthetic target.

7 Statistics Across Different Targets

The final step in our target signature analysis is to look at the cross target statistics and correlations. We will make a practical assumption that the corresponding target signatures form sets of independent stochastic processes, or at least uncorrelated (orthogonal) processes. For example we correlate X(1, j) with X(2, j), then with X (3, j), and with X(4, j), assuming the same pose angle j, against independence or uncorrelated (orthogonal) assumption.

Each of correlations produces an envelope for 274 poses, for total of 4 envelopes. In view of that, we use cross covariance and correlations to test lack of correlation, and also classic Chi-square and newly introduced Brownian Distance Covariance [19], to test for independence among various target signatures. Also, when a "real time" target signature is acquired, it will also be tested against all other four sets of stored target signatures. Table 8 summarizes target cross correlation features, both for X and Y signatures.

Chi-square test is used to test the independency of two sequences [1, 2]. The test returns the value from Chi-squared distribution χ^2 and the degrees of freedom number [20]. Once χ^2 is calculated, a program like Matlab or Excel, returns "the probability P that a value of χ^2 statistic at least as high as the value calculated could happen by chance under the assumption of independence", with an appropriate number of degrees of freedom, df = K − 1.

Finally, we use the newest form of correlation [19], i.e. distance covariance and correlation (Brownian distance covariance and correlation). The key is that zero correlation implies independence, plus the method captures non stationary and nonlinear correlations as well (Figs. 20, 21, 22 and 23).

Table 8 Cross targets correlation features (CTC)

Variable	Description
χ	Cross target Chi-square test
$V_k^2(i, j)$	Cross target Brownian distance covariance
$R_k^2(i, j)$	Cross target Brownian distance correlation
V_k^2	Target Brownian sample distance variance
X_{ccor}	Cross target correlations

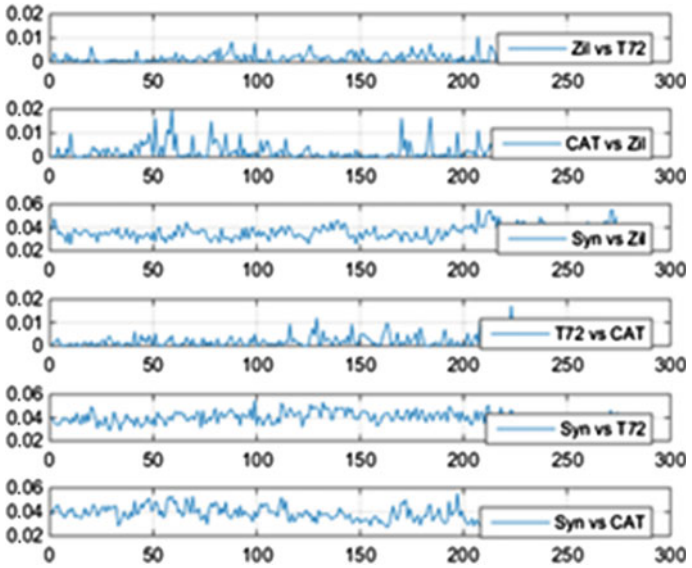

Fig. 20 Cross target Chi-square test

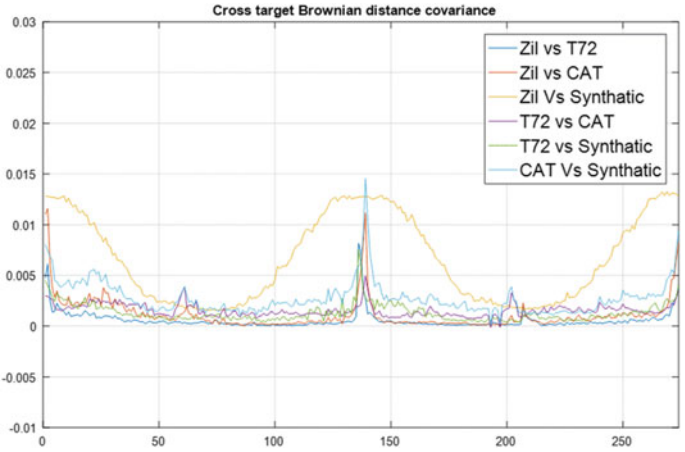

Fig. 21 Cross target Brownian distance covariance

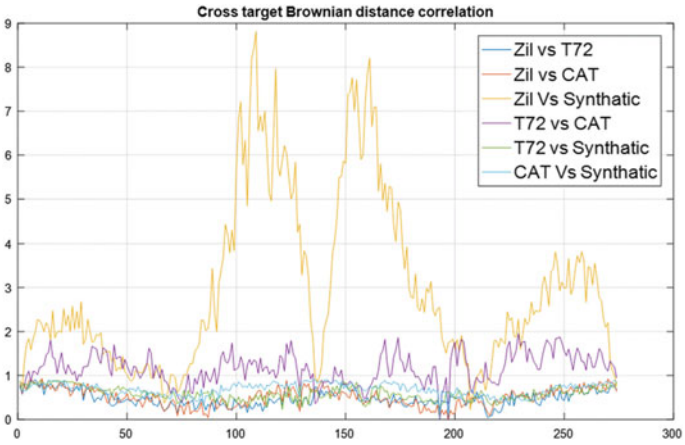

Fig. 22 Cross target Brownian distance correlation

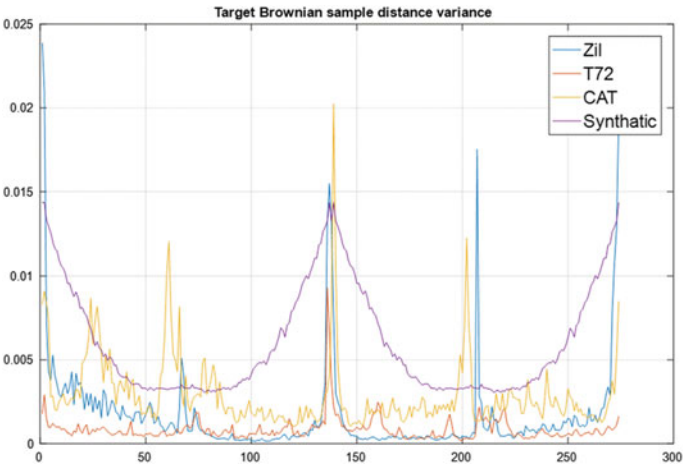

Fig. 23 Target Brownian sample distance variance

8 Conclusion

In this paper we present continuation of our previous work in analysis of digital target signatures and the corresponding problem of pose estimation. Quality pose estimation is a required step in subsequent automatic target tracking operation. The target signatures are obtained from USA MSTAR public data base where varieties of commercial as well as military targets are included, obtained by SAR and HRR radars. The methodology we employ is based on geometrical as well as several statistical correlation measures such as various autocorrelations and

cross-correlations, as well as Brownian and Chi-square statistical tests for sequence independence, which compare stored target data base against real time target. In particular, we start target identification and pose estimation process by (i) using target geometry which reliably determines the target type and 1st quadrant pose estimate, we then follow with (ii) variety of first order statistics to further fine tune the pose, and (iii) more 2nd order statistics for the final pose refinement. In this paper we presented first two items for synthetic targets, and are currently working on the item (iii) and real target signatures. Certain geometrical features of the targets can be identified from the corresponding correlations. In a follow up research we will address all these additional items as well as corresponding frequency based on Haar wavelet analysis, combine it with spatial analysis, and use hypothesis testing when determining real target identification and pose estimate. These inputs will serve as entry data for target tracking.

References

1. Hodzic M, Namas T (2015) Pose estimation methodology for target identification and tracking. In: Proceedings of international conference on systems, control, signal proceesing & informatics. In: INASE SCSI, ECS April 2015
2. Hodzic M, Namas T (2015) Spatial analysis for target signatures. In: IEEE ICAT proceedings, XXV international conference on information, communication and automation technologies, Sarajevo, Oct 2015
3. Kahler B, Blasch E (2008) Robust multi-look HRR ATR investigation through decision—level fusion evaluation. In: Proceedings of 11th international conference on information fusion 2008
4. Kahler B, Querns J (2008) An ATR challenge problem using HRR data. In: Proceedings of SPIE, vol 6970
5. Layne J, Simon D (1999) A multiple model estimator for a tightly coupled HRR automatic target recognition and MTI tracking system. In: SPIE conference on algorithms for synthetic aperture radar imagery
6. Blasch E (1999) Derivation of a belief filter for high range resolution radar simultaneous target tracking and identification. Ph.D. dissertation, Wright State University
7. Blasch E, Yang C (2004) Ten methods to fuse GMTI and HRR measurements for joint tracking and ID. In: Fusion 04
8. Gross D, Oppenheimer M, Kahler B, Keaffaber B, Williams R (2002) Preliminary comparison of HRR signatures of moving and stationary ground vehicles. In: Proceedings of SPIE, vol 4727
9. Williams R, Westerkamp J, Gross D, Palomino A (2000) Automatic target recognition of time critical moving targets using 1D high range resolution (HRR) radar. In: IEEE AES systems magazine
10. Mitchell R, Westerkamp J (1999) Robust statistical feature based aircraft identification. IEEE Trans Aerospace Electron Syst 35(3)
11. Blasch E, Westerkamp J, Layne J, Hong L, Garber FD, Shaw A (2000) Identifying moving HRR signatures with an ATR belief filter. In: SPIE
12. Blasch E, Huang S (2000) Multilevel feature-based fuzzy fusion for target recognition. In: SPIE
13. Snyder W, Ettinger G, Laprise S (2003) Modeling performance and image collection utility for multiple look ATR. In: SPIE

14. Dicander F, Jonsson R (2001) Comparison of some HRR classification algorithms. In: SPIE
15. JSTARS (2001) Joint surveillance and target attack radar system USA, from the website for Defense Industries, Air Force, Dec 2001
16. Joint STARS/JSTARS (2001) Intelligence resource program, FAS Website, Dec 2001
17. Joint STARS in Bosnia, Too much data too little. Intel, Military Intelligence Professional Bulletin, http//fas.org/irp/agency/army/tradoc/usaic/mipb/1996-4/agee.htm
18. MSTAR online databe www.sdms.afrl.af.mil
19. Szekelyi GJ, Rizzo ML (2009) Brownian distance covariance. Ann Appl Stat 3(4)
20. Leon-Garcia A (2008) Probability, statistics, and random processes for electrical engineering, 3rd ed. Pearson Prentice Hall, New York

Simultaneous Operation of Personal Computers and Mathematical Assessment of Their Harmonic Impact on the Grid

Saša Mujović, Slobodan Djukanović and Vladimir A. Katić

Abstract In the smart grids environment, non-linear electronic devices are present to a great extent. Since these devices generate higher harmonics in the current spectrum and require high voltage quality in order to operate properly, the power quality issue becomes very important. This study deals with mathematical modelling of parameters of current and voltage harmonic distortion due to operation of PC cluster. The proposed models are developed using measurements and simulation results. Model parameters are derived in the least squares manner. The models are convenient for practical engineering application.

1 Introduction

Nowadays, in the era of deregulation, integration of distributed generators and great improvements in modern electric power systems (Smart Grids), power quality issues are becoming very important. A wide spread introduction of switching power electronics converters into low power and industrial loads, as well as into renewable energy sources (wind, solar or hydro) generators, has given rise to current and voltage harmonic distortion. Therefore, the need for measuring and continuous monitoring of harmonic distortion becomes more important.

Low power electronics or microelectronics loads, based on the AC/DC power conversion, draw current with distorted or even discontinuous waveform during the AC voltage cycle. Individually, these loads produce small amounts of harmonic current. However, when operating in large numbers, they have the capability of

S. Mujović (✉) · S. Djukanović
Faculty of Electrical Engineering, University of Montenegro, Podgorica, Montenegro
e-mail: sasam@ac.me

S. Djukanović
e-mail: slobdj@ac.me

V.A. Katić
Faculty of Technical Sciences, University of Novi Sad, Novi Sad, Serbia
e-mail: katav@uns.ac.rs

M. Hadžikadić and S. Avdaković (eds.), *Advanced Technologies, Systems, and Applications*, Lecture Notes in Networks and Systems 3,
DOI 10.1007/978-3-319-47295-9_5

high current harmonic emission that overloads neutral conductors and transformers, and cause voltage harmonic distortion, additional losses and reduction of power factor [1]. The use of such devices in customers' installations is expected to increase [2]. Therefore, utility companies are very interested in ensuring that potential harmonic effects do not jeopardize the voltage quality, where harmonic state estimation plays a crucial role [3].

In the class of non-linear loads, personal computers (PCs) represent the most important factor due to two main reasons: (1) switching mode of PC power supply unit (PSU) prompts PC-generated current rich in odd harmonics (Figs. 1 and 2) PC clustering as a common practice. Generally, two types of clusters can be distinguished, one formed in a designed manner, like in computer centres, insurance companies, banks, and stock markets, and the other formed in a random manner, like in residential and collective housing areas, university campuses, and free wireless network access areas [4]. Operation of a PC cluster distorts input current waveform. Distorted current produces harmonic voltage drops on system impedance and results in voltage harmonic at the supply buses. Such a case is shown in Fig. 2, where a group of connected PCs produces harmonic voltage drop on equivalent system impedance (Z_e):

$$Z_e = Z_{net} + Z_L + Z_{Be}, \quad Z_{Be} = \left(\sum_{i=1}^{N} \frac{1}{Z_{Bi}} \right)^{-1}, \tag{1}$$

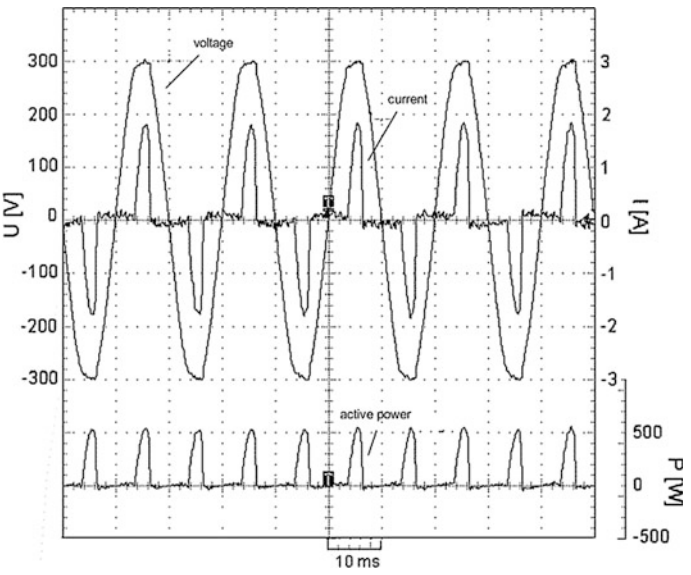

Fig. 1 Input voltage and current wave-shapes (*above*) and instant power consumption (*below*)

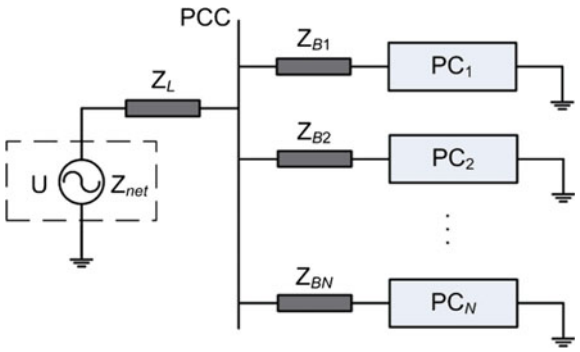

Fig. 2 N PCs connected to common bus

where Z_{net} is the network impedance, Z_L the line impedance, Z_{Bi} the impedance of the i-th branch, Z_{Be} the equivalent branch impedance and N is the number of PCs in cluster.

Harmonic distortion caused by PCs can be expressed using power quality indices which serve as system performance metrics [5]. Information about the influence of PC cluster on voltage quality can be obtained by comparing these indices with standard defined limits (e.g. IEEE 519 [6] and IEC 61000-3-2 standards [7]). The most important indices are the total harmonic distortion of current (THD_I) and the total demand distortion of current (TDD_I), defined as follows:

$$THD_I(\%) = \frac{\sqrt{\sum_{h=2}^{\infty} I_h^2}}{I_1} 100, \quad TDD_I(\%) = \frac{\sqrt{\sum_{h=2}^{\infty} I_h^2}}{I_L} 100, \tag{2}$$

where h is the harmonic order, I_1 and I_h the root mean square (RMS) values of the fundamental and the h-th harmonic, respectively, and I_L the maximum load current, recommended to be the average of the maximum demand for the last 12 months [6].

In power quality analysis, THD_I is more frequently used than TDD_I [8], which is supported by the fact that measuring devices usually record THD_I. In addition, TDD_I is usually calculated based on the THD_I value:

$$TDD_I = \frac{THD_I}{I_L} I_1. \tag{3}$$

The importance of knowing the PC cluster's THD_I has to be stressed for several reasons. Namely, the IEC 61000-3-2 standard considers harmonic generation due to single equipment (single PC), but not due to multiple devices or PC cluster. In PC clusters, harmonics values cannot be obtained simply by summing individual PC harmonics [9]. Tracking and monitoring THD_I may provide valuable information about the PC cluster compatibility, especially when the total cluster input current exceeds 16A and the IEC 61000-3-4 standard should be applied. Also, PC clusters generate a strong 3rd harmonic, which does not cancel out in neutral wire (high value of the 3rd harmonic also means high THD_I value). In that case, neutral wire

overload may reach up to 1.7 times full rated current. This is a special problem with desktop PCs.

Simultaneous use of PCs can negatively affect grid conditions [10]. Namely, the cluster operation results in voltage deviation from sinusoidal shape, i.e., in increasing voltage harmonic:

$$U_h = Z_e I_h = (R_e + jhX_e) I_h, \tag{4}$$

where h is the harmonic order, Re and Xe are active and reactive parts of equivalent system impedance, respectively, and I_h is the RMS value of the h-th harmonic current of PC cluster.

The key index quantifying voltage distortion is total harmonic distortion of voltage THD_U, defined as

$$THD_U(\%) = \sqrt{\frac{\sum_{h=2}^{\infty} U_h^2}{U_1^2}} 100, \tag{5}$$

where U_1 and U_h are the RMS values of the fundamental and the h-th harmonic voltage, respectively.

Knowing the PC cluster's THD_U level is of great importance, since the comparison of the THD_U level with its limits, given in standards [6, 11], may provide insight into potential negative effects of PC cluster operation on voltage quality.

The THD_I and THD_U are undoubtedly the most relevant measures of PCs impact on power quality conditions. Their determination can be carried out in three ways. The first one is to use special instruments, e.g. power quality analysers [12]. Although the most accurate approach, it is often complex since in addition to instruments it requires trained personnel, various permits and repeated measurements in case of any configuration changes.

The second approach is based on the state space model in PC modelling, which requires solving differential equations representing states that the AC/DC converter of PC PSU goes through during the operation cycle. This model has proved to be very complex and time consuming for computer simulation, although some attempts for its simplification can be found in [13].

The third approach, considered in our research, uses mathematical modelling to express the THD_I dependence on the most influential parameters. The development of such model is not easy, but it is the least expensive and the most convenient solution for engineering application.

The aim of this research is to propose comprehensive, yet not mathematically demanding models for the THD_I and THD_U calculation in dependence on the main load side and line side parameters. In that sense, the proposed models has a multi-parameter input and enables the THD_I and THD_U calculation for arbitrary PC cluster size. The validity of the models was confirmed by conducting measurements at two sites and analysing their applicability with different measuring site conditions.

2 Background

In this section, we emphasize all major parameters that affect THD_I and THD_U, which should be included into comprehensive THD_I and THD_U mathematical models. Also, diversity of THD_I and THD_U models and values that can be found in the literature will be discussed.

2.1 THD_I Models in Literature

Considering the theoretical analysis of behaviour of single-phase full-wave rectifier with DC smoothing capacitor, as the main part of the PC PSU, given in [14], several main factors may be distinguished that determine the THD_I value of a PC cluster [8]. They are the PC cluster size N_{PC} (number of switched-on PCs in a cluster), line side parameters (grid stiffness S_{SC}) and load side parameters (capacitance of smoothing capacitor C within the PC PSU).

Apart from these parameters, many other exist (frequency, phase (line) voltage RMS, dependence of active and reactive power on the phase voltage RMS), from both line and load side. Theoretically, these parameters could affect THD_I [8, 15]. However, modern devices and power supply networks meet requirements defined by the EN 50160 standard. In such environments, frequency and phase voltage variations are negligible and therefore these parameters do not have significant impact.

The most significant influence on the THD_I level have N_{PC}, S_{SC}, and C. Individual and combined effects of these parameters have been reported in the literature. However, an overall model, that considers the effects of all major parameters on THD_I, has not been proposed.

Single PC THD_I depends on the PC configuration and operation mode. Therefore, different THD_I values reported in references, namely 100 % [8], 119 % [10], 118–122 % [1], 140 % [16], are result of these influencing factors. When a PC cluster is considered, the THD_I level decreases with the increase of cluster size N_{PC}. Namely, as N_{PC} increases, both the current that a PC cluster draws from the grid, and the voltage distortion increase. At the same time, the current pulse waveform becomes wider and taller, as a consequence of attenuation and diversity [8]. In various publications, the THD_I values differ for the same N_{PC}. For example, with $N_{PC} = 10$, the recorded THD_I values are 58 % [8] and 92 % [10]. The explanation can be found in a strong THD_I dependence on S_{SC}, so different S_{SC} values were considered in these publications. Also, different PC configurations [17], different network parameters, the use of various measuring devices, as well as probable presence of additional (non-PC) loads lead to a wide range of THD_I values reported for a fixed cluster size. A more detailed overview of the THD_I values versus N_{PC} is given in [10].

Due to the overall complexity, only a few studies dealing with the THD_I modelling can be found in the literature. In [18], two mathematical models are proposed as follows:

$$THD_I(\%) = -0.0067I_L + 6.54, \tag{6}$$

$$THD_I(\%) = 11.57e^{-0.003I_L}. \tag{7}$$

Models (6) and (7) are derived for low voltage buses supplying not only PCs, but also other small loads, and therefore are not appropriate for determination of THD_I caused exclusively by a PC cluster.

In [19], the THD_I dependence on N_{PC} is modelled as

$$THD_I(\%) = -0.81N_{PC} + 80.11. \tag{8}$$

Model (8) has been developed using the measurement results and is valid only for $N_{PC} \leq 25$. Nowadays it is a common situation that $N_{PC} > 25$, implying that the results provided by (8) are completely unrealistic (for example, THD_I can take negative values).

A simplified approach in the THD_I modelling is used in [20], where N_{PC} represents a parameter and the impacts of the 11th, 13th, 15th and higher order harmonics are neglected. The model reads

$$THD_I(\%) = \sqrt{(I_3/I_1)^2 + (I_5/I_1)^2 + (I_7/I_1)^2 + (I_9/I_1)^2}, \tag{9}$$

where I_3/I_1, I_5/I_1, I_7/I_1, I_9/I_1 represent the harmonic distortions of the 3rd, 5th, 7th and 9th harmonics, respectively, defined as follows:

$$I_3/I_1 = -0.0099N_{PC}^2 + 0.5596N_{PC} + 49.532, \tag{10}$$

$$I_5/I_1 = -0.9751N_{PC} + 41.443, \tag{11}$$

$$I_7/I_1 = -6.694N_{PC} + 35.367, \tag{12}$$

$$I_9/I_1 = -0.0401N_{PC}^2 + 1.7213N_{PC} + 23.716. \tag{13}$$

The effects of the PSU capacitance on THD_I is analysed in [21]. The proposed model takes into account effects of N_{PC} and C on THD_I. It assumes the value of S_{SC} = 4000 kVA (which is the most common case in 400/230 V distribution networks) and reads

$$THD_I(\%) = \begin{cases} (19 - N_{PC})C' - 0.67N_{PC} + 100, & \text{for } N_{PC} < -70C' + 97 \\ 15C' + 28, & \text{for } N_{PC} \geq -70C' + 97 \end{cases} \tag{14}$$

where C' represents the C value in per unit (p.u.), normalized with 1μF. The model is easy to use and applicable for all PSU types in modern PCs. However, as THD_I depends on S_{SC}, it should be also incorporated in a model.

A significant improvement has been achieved in [10], where, using the curve fitting approach, the analytical THD_I expression was derived depending on N_{PC} and having S_{SC} as a parameter. The model is developed for the C = 235 μF, as the most common value of the PSU capacitance in modern PCs, and is applicable for $N_{PC} \leq 200$:

$$THD_I(\%) = \begin{cases} (0.095S'_{SC} - 1.24)N_{PC} + 2.43S'_{SC} + 91.5, & \text{for } N_{PC} < (9S'_{SC} + 45.5) \\ 3S'_{SC} + 19.2, & \text{for } N_{PC} \geq (9S'_{SC} + 45.5), \end{cases} \quad (15)$$

where S'_{SC} represents the S_{SC} value in p.u., normalized with 1000 kVA. Since (15) takes into account only the impact of the grid stiffness on THD_I, it cannot be considered as a complete solution for the THD_I determination.

A recent contribution in the area has been reported in [15]. It deals with establishing relationships between some parameters (source voltage, impedance, frequency and background voltage distortion) and THD_I for a group of 20 PCs. The paper does not provide a unique THD_I model, but several independent models developed by the curve fitting technique. A downside to these models is that they are derived for a fixed number of connected PCs, i.e. variable N_{PC} is not taken into account. Also, the proposed set of models having only one parameter and neglecting the other ones is not a comprehensive solution.

2.2 THD_U Models in Literature

The voltage distortion is an essential topic in power quality analysis. It is result of harmonic current emission of various non-linear loads, as explained in the Introduction section and operation of power electronics converters, used for integration of renewable energy sources and energy storage devices [22]. Also, advanced application of power electronics in electrical energy transmission and high voltage DC transmission brings additional harmonic distortion in networks [23].

Numerous papers that address voltage distortion caused by nonlinear loads are oriented to the presentation of individual and/or group impact of these loads on voltage supply quality. However, only few papers deal with the THD_U on common buses supplying only PCs [1, 24]. Measurement results of voltage and current distortion given in [1, 24] present a case study which considers the impact of 109 PCs (around 35 PCs per phase). Therefore, these results do not have general validity for various grid characteristics.

The impact of simultaneous operation of 120 PCs (around 40 per phase) on the THD_U level through a simulation model is considered in [24]. Also, the THD_U estimation when more PCs are considered, namely 240 and 800 PCs, is given. The simulations show that the THD_U increases as the PC cluster size increases. However, the proposed model is not complete since it does not take into account all influencing parameters, including the grid stiffness and some internal PC parameters.

To the best of our knowledge, only one paper offers mathematical models for the THD_U calculation [18]. In particular, two models, linear and exponential, are introduced in [18] as follows:

$$THD_U = 0.002I_L + 0.5417, \tag{16}$$

$$THD_U = 0.747e^{0.0014I_L}. \tag{17}$$

Models (16) and (17) enable the THD_U calculation in dependence on the connected load current I_L, given per unit in the above relations. However, the models are derived for low voltage buses supplying not only PCs, but also other small loads (lamps, small motors, heaters). In that sense, these models are not appropriate for determination of the THD_U that is exclusively caused by the operation of a PC cluster, which is the main concern of this study.

Model that considers the impact of PC cluster on THD_U should incorporate dependence on the PC cluster size. In addition, research on the impact of S_{SC} on THD_U reveals that THD_U is strongly affected by S_{SC}, imposing the necessity to include this dependence in model as well. Namely, it is stated in [8] that, for the same N_{PC}, THD_U decreases with the increase of S_{SC}. This statement is supported by measurements carried out at the Computer Centre of the Faculty of Technical Science (CCFTS) in Novi Sad, Serbia, in 2003 and 2010. In 2003, the measurements were conducted at the point of common coupling (PCC) from which a group of 109 PCs is supplied. The maximal recorded THD_U value was THD_U = 4.8 %. In 2010, the PC cluster size was around 170 PCs and the maximal recorded value was THD_U = 5.3 %. Analysing these results, a wrong conclusion can be drawn that connection of additional 61 PCs on the PCC causes negligible increase of THD_U. However, the increase of the grid stiffness on the PCC, which occurred between 2003 and 2010, is the actual cause of such a low THD_U increase.

Aside from N_{PC} and S_{SC}, THD_U depends on several other factors, such as the cable cross-section and the initial THD_U of the phase voltage at no-load state. However, simulations that we have performed revealed that their impact is minor.

3 Measurement and Simulation Results

We have conducted measurements at two different sites, namely at CCFTS and in the building of the NLB Montenegrobanka bank (NLBMB), in Podgorica, Montenegro. Both sites, with completely different line side characteristics, are equipped with considerable number of PCs. The obtained measurements were used for developing of THD_I and THD_U models (results from CCFTS), as well as for assessment of validity and accuracy of the proposed models (results from NLBMB). Also, we have developed a MATLAB Simulink model of CCFTS, which is based on simple presentation of the PC PSU taken from [8].

3.1 Measurements at CCFTS

CCFTS has been chosen for harmonic emission measurements since it represents a good example of harmonic generation out of a large number of grouped PCs. The complete electrical installation is presented in Fig. 3. The measurement lasted for seven days, while measuring samples were taken at intervals of 10 min with reference to IEC 61000-4-7 Standard [25].

The main building of the Faculty of Technical Sciences is supplied from the Main Distribution Panel (MDP), which is powered from the distribution network transformer station (TS) 10/0.4 kV (Fig. 3). CCFTS, which consists of seven major laboratories ("L1"-"L6" and "M"), three smaller laboratories ("H1"-"H3") and an administrative room ("Adm"), is connected to the MDP via three phase five wire cable. Measurement were conducted at the grid (PCC) from which a group of 163 PCs (153 personal PCs and 10 server PCs of total power 28.1 kW), as well as lighting (fluorescent lamps with magnetic ballast) of laboratories "L6" and "M" (total active power of 1.6 kW) are supplied. The largest numbers of PCs are deployed in the "L1" laboratory (31 PCs). In other laboratories, approximately the same number of PCs is connected (14–20). Ten server PCs are continuously in

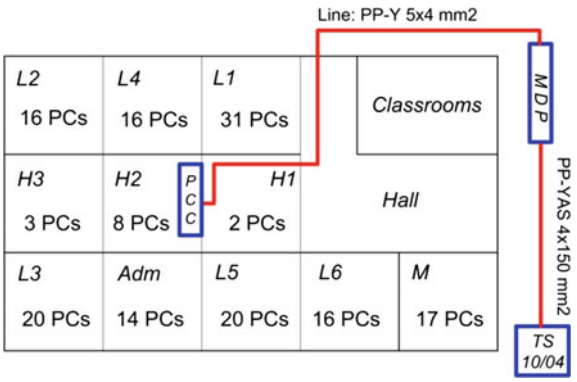

Fig. 3 Disposition of CCFTS laboratories

operation. They are equipped with adequate Uninterruptible Power Supplies (UPS) devices and operating in the administrative room. Rated power of a single PC is 150–200 W and of single server is 450 W. I_{SC} at the grid is 6 kA and the average full load current of CCFTS is I_L = 35.2 A, giving the ratio I_{SC}/I_L = 170.

Related to the CCFTS measurements, the following points should be emphasized:

- calculated value of S_{SC} (ratio of nominal transformer power (VA) and transformer short-circuit voltage (%)), at the point from which the PC cluster in CCFTS is supplied, was 4000 kVA;
- PSU capacitance (C) of all PCs in CCFTS was 235 μF;
- maximal THD_I recorded values (per phases 1, 2 and 3) were 55.8, 61.2 and 61.3 %;
- maximal THD_U recorded values (per phases 1, 2 and 3) were 5.18, 5.26 and 5.3 %.

To determine the THD_I level for different number of connected PCs, a simulation MATLAB/Simulink model of CCFTS has been developed. The model uses individual PC model proposed in [8]. The developed model is presented in Fig. 4.

The model has been tested on 56 PCs of CCFTS connected to the most loaded phase (phase 3). Cables that connect power supply from distribution network to PCs, through local distribution panels, are modelled by an equivalent "π" scheme characterized by parameters $r = 4.6 \times 10^{-3}$ Ω/m, $l = 0.1 \times 10^{-3}$ H/m and $c = 10^{-15}$ F/m. Each block (denoted as *L1 Lab*, *L2 Lab*, …, *M Lab*) represents a

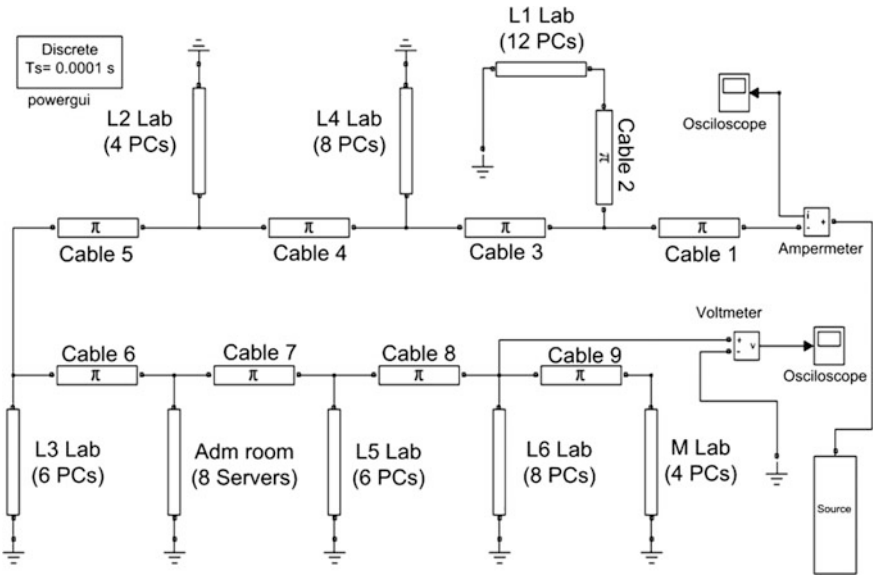

Fig. 4 MATLAB/Simulink model of PCs group (56 PCs)

laboratory of CCFTS. The number of PCs in each block equals the number of PCs connected to the considered phase (phase 3) in the corresponding laboratory. A high level of matching of the obtained current harmonics values of PCs group (56 PCs) with measurements ones is achieved.

It should be mentioned that the initial THD_U values (background harmonic distortion), recorded in the CCFTS (2.25, 2.18 and 2.1 %, per phases 1, 2 and 3, respectively), are taken into account in the simulation model by pre-setting the amplitudes and phase angles of supply voltage harmonics to the values recorded by the measuring devices. In this way, the supply voltage harmonics are not in phase with PC-generated harmonics at the same frequency and the impact of attenuation and diversity is not neglected, thus representing real grid conditions.

3.2 Measurements at NLBMB

Additional measurements were performed at NLBMB. The NLBMB building is equipped with 244 PCs (83, 80, 81 per phases 1, 2, 3, respectively). The measurements were taken in two sites, namely at the feeder in TS 10/04, which supplies the bank building, and at the PCC in the bank building, which supplies all PCs in the bank.

Related to the bank measurements, the following points should be emphasized:

- calculated value of S_{SC} was 5800 kVA;
- 222 PCs have the capacitance of 235 μF, whereas 22 PCs have the capacitance of 500 μF;
- maximal THD_I recorded values (per phases 1, 2 and 3) were 47.9, 52.4 and 49.2 %;
- maximal THD_U recorded values (per phases 1, 2 and 3) were 4.92, 5.01 and 5.04 %;
- in addition to PCs, linear loads (water heaters, fluorescent lamps etc.) of active power 1350 W, were turned on during the measurements.

4 Development of THD_I and THD_U Mathematical Models

This section presents an overview of THD_I and THD_U models derived in [26, 27], respectively. In both models, the model parameters are derived using the least squares (LS) approach.

4.1 THD_I Modelling

The proposed THD_I model is based on mathematical processing of measured and simulation data. As stated in Sect. 2.1, THD_I (due to PC cluster operation) depends on N_{PC}, S_{SC} and C, where N_{PC} and S_{SC} are the dominant ones. To that end, simulations were performed for different ranges of the N_{PC}, S_{SC} and C (N_{PC} = 1–150 PCs per phase, S_{SC} = 3000–6000 kVA and C = 235–500 μF). The obtained THD_I values are presented in Fig. 5.

It should be pointed out that the selected S_{SC} range covers the most commonly found S_{SC} values in modern low-voltage (400/230 V) distribution grids. For example, in CCFTS, S_{SC} = 4000 kVA. In the model, instead of S_{SC}, the p.u. value $S'_{SC} = S_{SC}/S_{SCb}$ ($S_{SCb} = 1$ (kVA) will be used, as shown in Fig. 5.

Also, the selected C range, in particular capacitances 235, 340, 410 and 500 μF, represent actual C values in PSUs of modern PCs. In the model, instead of the original capacitance C, the p.u. value $C' = C/C_b$ (C_b = 1 μF) will be used.

Finally, the observed N_{PC} range of 1–150 PCs per phase suffices for drawing conclusions regarding the THD_I behaviour for an arbitrary number of PCs.

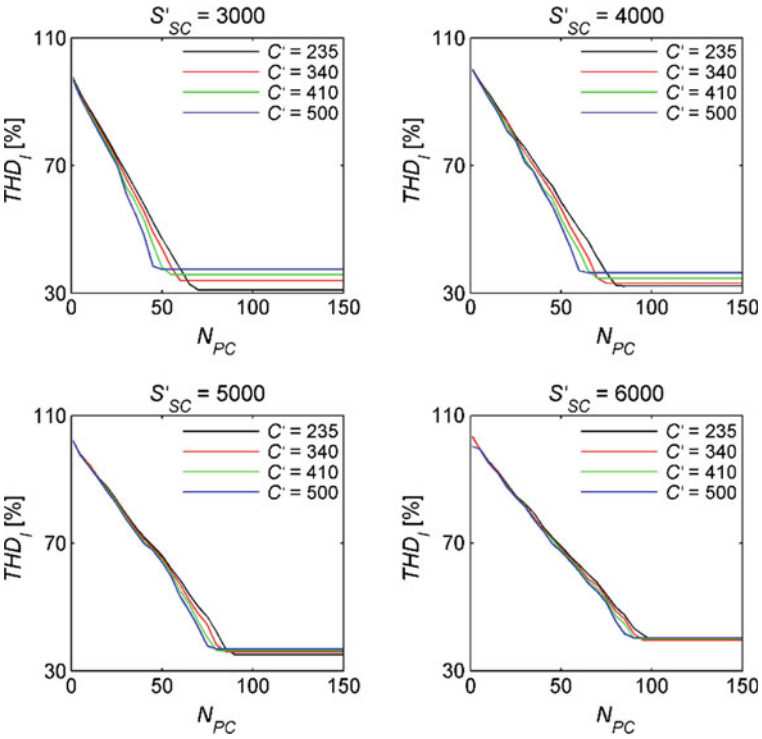

Fig. 5 THD_I versus N_{PC} for different S'_{SC} values. S'_{SC} and C' represent the p.u. values, i.e. $S'_{SC} = S_{SC}$/1kVA and $C' = C$/1 μF

From Fig. 5, the following conclusions regarding the THD_I behaviour can be drawn:

1. The THD_I function can be divided into two N_{PC} regions, namely the varying and constant regions. In the varying region, THD_I can be well approximated by a linear function. Other higher order functions are also eligible for this purpose, and should provide more accurate approximations, but we follow the model's simplicity as one of the key concerns.
2. THD_I depends on both S'_{SC} and C'. Therefore, an appropriate THD_I model should incorporate these parameters. Figure 5 reveals that as S'_{SC} increases, the THD_I line slope decreases and N_{PC} saturation point increases, and vice versa. For fixed S'_{SC}, the THD_I slope depends on C', that is, the smaller C' the larger slope and vice versa. This effect is more pronounced with lower S'_{SC} values.
3. For very small N_{PC}, the influence of C' can be neglected, i.e. THD_I depends only on S'_{SC}. Clearly, the THD_I curves meet at the same point for $N_{PC} = 1$, i.e. they have the same intercept value for given S'_{SC}.

Following these observations, THD_I can be modelled as

$$THD_I(N_{PC}, S'_{SC}, C') = \begin{cases} f(S'_{SC}, C')N_{PC} + g(S'_{SC}), & \text{for } N_{PC} < N_{PC}^{sat} \\ THD_I^{sat}(N_{PC}^{sat}, S'_{SC}, C'), & \text{for } N_{PC} \geq N_{PC}^{sat}. \end{cases} \tag{18}$$

The aim is to determine the slope function $f(S'_{SC}, C')$, intercept function $g(S'_{SC})$ and saturation point N_{PC}^{sat}. The saturated THD_I, denoted as $THD_I^{sat}(N_{PC}, S'_{SC}, C')$,, is a THD_I value at $N_{PC} = N_{PC}^{sat}$. From the third observation, $g(S'_{SC})$ depends only on S'_{SC}.

4.1.1 Determination of Slope Function

The slope value for each curve in Fig. 5 can be easily calculated from the simulation results. Since $f(S'_{SC}, C')$ is a continuous function, it can be approximated by a 2D polynomial

$$f(S'_{SC}, C') \approx P(S'_{SC}, C') = \sum_{m=0}^{M} \sum_{n=0}^{M} a_{mn} S'^{m}_{SC} C'^{n}. \tag{19}$$

The coefficients a_{mn} will be determined in the LS sense, i.e., the optimal coefficients a_{mn} can be obtained by minimizing the following error function:

$$E(S'_{SC}, C') = \sum_{S'_{SC}} \sum_{C'} \left(f(S'_{SC}, C') - P(S'_{SC}, C') \right)^2. \tag{20}$$

In (20), $S'_{SC} \in \{3000, 4000, 5000, 6000\}$ and $C' \in \{235, 340, 410, 500\}$. Error $E(S'_{SC}, C')$ is minimized by solving the following set of equations:

$$\frac{\partial E(S'_{SC}, C')}{\partial a_{pq}} = 0, \quad 0 \le p, q \le M. \tag{21}$$

Generally, higher order polynomials $P(S'_{SC}, C')$ can be used to approximate $f(S'_{SC}, C')$. However, since of the key goals is to propose a simple THD_I model, a first-order 2-D polynomial will be considered:

$$P^{(1)}(S'_{SC}, C') = \sum_{m=0}^{1}\sum_{n=0}^{1} a_{mn} S'^{m}_{SC} C'^{n} = a_{00} + a_{01}C' + a_{10}S'_{SC} + a_{11}S'_{SC}C'. \tag{22}$$

The details of derivation of $P(S'_{SC}, C')$ are given in [26] and will be omitted here. The final expression for $P(S'_{SC}, C')$ reads

$$P^{(1)}(S'_{SC}, C') = -0.7644 - 1.966 \times 10^{-3}C' + 1.893 \times 10^{-5}S'_{SC} + 3.124 \times 10^{-7}S'_{SC}C'. \tag{23}$$

4.1.2 Determination of Intercept Function

Once the slope function $f(S'_{SC}, C')$ is estimated, we can proceed with determination of the THD_I-intercept function (S'_{SC}) from (18). In order to retain the simplicity of model, $g(S'_{SC})$ will be modelled as a first-order polynomial:

$$g(S'_{SC}) = b_0 + b_1 S'_{SC}. \tag{24}$$

Coefficients b_0 and b_1 are obtained in the LS sense [26]:

$$g(S'_{SC}) = 94.151 + 1.539 \times 10^{-3}S'_{SC}. \tag{25}$$

4.1.3 Calculation of Saturation Point

Referring to Fig. 5, it can be concluded that the saturation point N_{PC}^{sat} depends on both S'_{SC} and C'. Therefore, we can apply the same rationale as in Sect. 4.1.1. We will also adopt a first-order polynomial

$$N_{PC}^{sat}(S'_{SC}, C') \approx Q^{(1)}(S'_{SC}, C') = c_{00} + c_{01}C' + c_{10}S'_{SC} + c_{11}S'_{SC}C'. \tag{26}$$

Coefficients c_{00}, c_{01}, c_{10} and c_{11} are obtained in the LS sense (details in [26]):

$$Q^{(1)}(S'_{SC}, C') = 73.606 - 1.232 \times 10^{-1}C' + 5.342 \times 10^{-3}S'_{SC} + 1.423 \times 10^{-5}S'_{SC}C'. \tag{27}$$

By combining (23), (25) and (27), the saturated THD_I can be obtained as

$$\begin{aligned} THD_I^{sat}(N_{PC}, S'_{SC}, C') = {} & 37.887 - 5.054 \times 10^{-2} C' - 1.151 \times 10^{-3} S'_{SC} - 7.175 \times 10^{-7} S'_{SC} C' \\ & + 2.422 \times 10^{-4} C'^2 + 1.011 \times 10^{-7} S'_{SC} - 6.646 \times 10^{-8} S'^2_{SC} C'^2 \\ & + 1.938 \times 10^{-9} S'^2_{SC} C' + 4.446 \times 10^{-12} S'^2_{SC} C'^2. \end{aligned} \tag{28}$$

From (18), (25) and (27), the final THD_I model reads

$$THD_I(N_{PC}, S'_{SC}, C') = \begin{cases} (-0.7644 - 1.966 \times 10^{-3} C' + 1.893 \times 10^{-5} S'_{SC} + 3.124 \times 10^{-7} S'_{SC} C') N_{PC} \\ \quad + 1.539 \times 10^{-3} S'_{SC} + 94.151, \text{for } N_{PC} < N_{PC}^{sat}(S'_{SC}, C'), \\ THD_I^{sat}(N_{PC}, S'_{SC}, C'), \text{for } N_{PC} \geq N_{PC}^{sat}(S'_{SC}, C'), \end{cases} \tag{29}$$

where $N_{PC}^{sat}(S'_{SC}, C')$ and $THD_I^{sat}(N_{PC}, S'_{SC}, C')$ are defined by (26) and (28), respectively. Once again, in the model, instead of S_{SC} and C, the p.u. values $S'_{SC} = S_{SC}/S_{SCb}$ ($S_{SCb} = 1$ kVA) and $C' = C/C_b$ ($C_b = 1$ μF) are used, respectively.

4.1.4 Case of Mixed Capacities

The proposed model assumes that all PCs in the cluster have the same capacitance. In practice, however, this is rarely the case, i.e. clusters may contain several PC groups with different PC capacitances. Therefore, the proposed THD_I model should be extended so that mixed capacitances are taken into account.

According to (29), THD_I can be expressed as

$$THD_I(N_{PC}, S'_{SC}, C') = (K_2 + K_4 S'_{SC}) N_{PC} C' + (K_1 + K_3 S'_{SC}) N_{PC} + K_5 S'_{SC} + K_6. \tag{30}$$

Coefficients K_i, i = 1, 2,…, 6, should be clear from (23) and (25).

For the sake of convenience, let us consider the non-saturated part of the THD_I curve. Note that the term $N_{PC}C'$ in (30) represents the total capacity of PC cluster for uniform capacitance C'. On the other hand, the total capacitance of PC cluster with M PC groups, each characterized by size N_{PCm} and capacitance C'_m, where m = 1,2, …, M, equals

$$C'_{tot} = \sum_{m=1}^{M} N_{PCm} C'_m. \tag{31}$$

Taking (31) into consideration, THD_I becomes

$$THD_I(N_{PC}, S'_{SC}, C') = (K_2 + K_4 S'_{SC}) \sum_{m=1}^{M} N_{PCm} C'_m + (K_1 + K_3 S'_{SC}) N_{PC} + K_5 S'_{SC} + K_6$$
$$= (K_1 + K_2 C'_{eq} + K_3 S'_{SC} + K_4 S'_{SC} C'_{eq}) N_{PC} + K_5 S'_{SC} + K_6, \quad (32)$$

where

$$C'_{eq} = \sum_{m=1}^{M} \frac{N_{PCm}}{N_{PC}} C'_m \quad (33)$$

represents the equivalent capacitance of one PC in the cluster.

Clearly, the THD_I model in the mixed capacitance case retains the original form; only the equivalent capacitance of one PC has to be calculated according to (33). The same holds for the saturation point and saturation value, which should be calculated according to (26) and (28), respectively, with C'_{eq} in place of C'.

4.1.5 Additional Factors that May Affect THD_I

This subsection addresses some additional issues that may affect the applicability of model (29) in practice.

Influence of the Pre-existing Voltage Harmonic Distortion

The supply voltage waveform at low voltage PCC is rarely a pure sinusoidal and as such it affects the reference signal. As pointed out in Sect. 3, the PC cluster of CCFTS is connected on the PCC where the initial THD_U exists, which has been incorporated in the simulation model. Now, a question arises: Whether the model accuracy will be deteriorated if the pre-existing THD_U differs from that taken in the simulation model? Measurements in NLBMB (Sect. 3.2) were conducted with different grid conditions than that in CCFTS, where, by different grid conditions, different S_{SC} and pre-existing THD_U are meant. Model (29) with the pre-existing THD_U recorded in the NLBMB building gives very close results. This, in turn, implies that varying the pre-existing THD_U (on low voltage level) within the range of common values 1.5–3 % [28] has insignificant impact on the model accuracy. In additional simulations, which have been carried out with greater pre-existing THD_U, namely up to 5 % (maximal allowed THD_U value according to IEEE 519 Standard), E_r has not exceeded 1.2 %. Hence, the pre-existing THD_U has not been taken into account as a parameter in the proposed THD_I model.

Impact of the Low Voltage Cable Cross-Section

The connection between the PC cluster and AC system is achieved through low voltage cables of cross-section in the range of 4 up to 16 mm^2. In our simulation model, we consider a 5 × 4 mm^2 cable, modelled by an equivalent "π" scheme and adequate resistance, inductance and capacitance. The applicability of the simulation model, and in turn the proposed model, is not constrained to this cable cross section because of small cable impedance in comparison with the AC source impedance.

4.1.6 THD_U Modelling

The THD_U values, obtained by measurements and simulations performed for N_{PC} in the range of 10–200 PCs per phase and S_{SC} = {3000, 4000, 5000, 6000, 7000} kVA, are presented in Fig. 5. Note that there is no upper limit for N_{PC}, but the selected PC cluster size is sufficient for analysis and conclusions. Also, the adopted S_{SC} range covers the most common S_{SC} values characteristic to PCCs at which the PC cluster is connected. As a matter of fact, the grid stiffness of 3000 kVA is rarely encountered, but it is included so as to make the analysis more general.

From Fig. 6, the Following Observations Hold

1. THD_U increases as N_{PC} increases. This is due to generated current of the PC cluster. Namely, as N_{PC} increases, the PC cluster draws more current from the mains and voltage distortion increases.
2. THD_U decreases as S_{SC} increases. Greater grid stiffness means greater grid capability to withstand the negative impact of generated harmonics.
3. The THD_U dependence on N_{PC} is not uniform within the considered N_{PC} interval and it can be divided into three regions. At certain number of connected PCs, the THD_U function changes its behaviour and further increasing of cluster size will result in a more pronounced THD_U growth.
4. As S_{SC} increases, the middle region narrows and shifts towards higher N_{PC} values. For very large S_{SC} values, it practically vanishes, and the THD_U function tends to be uniform within the whole N_{PC} interval (see the THD_U curve for S_{SC} = 7000).
5. Within each region, the THD_U can be well approximated by a linear function of N_{PC}. Taking these observations into consideration, the THD_U can be modelled as

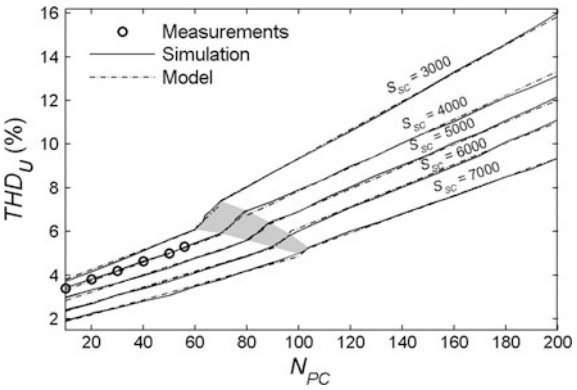

Fig. 6 Simulated THD_U values (*solid line*) for five considered S_{SC} values. *Circles* denote the measurements. In the middle region (*shaded*), the THD_U function changes its behaviour. THD_U model values, obtained using (37), are shown by *dash-dot lines*

$$THD_U(N_{PC}, S_{SC}) = f(S_{SC})N_{PC} + g(S_{SC}). \tag{34}$$

Our aim will be to determine functions $f(S_{SC})$ and $g(S_{SC})$ for each region, as well as the middle region boundaries $LB(S_{SC})$ and $RB(S_{SC})$. *LB* and *RB* stand for the left and right bounds of the middle region, respectively.

Functions $f(S_{SC})$ and $g(S_{SC})$ will be modelled by polynomials. The choice of polynomial model is motivated by Weierstrass's theorem, which states that any continuous function can be approximated by a polynomial within the considered interval. In addition, polynomial model is much more appropriate for analysis compared to exponential or some other model. Analytically

$$f(S_{SC}) \approx \sum_{i=0}^{P} k_i S_{SC}^i, \quad g(S_{SC}) \approx \sum_{j=0}^{Q} c_j S_{SC}^j, \tag{35}$$

where P and Q represent the polynomial orders, while k_i and c_j represent polynomial coefficients. The modelling problem now reduces to the estimation of parameters P, Q, k_i (i = 0,1, …, P) and c_j (j = 0,1, …, Q). Middle region boundaries $LB(S_{SC})$ and $RB(S_{SC})$ will also be approximated by polynomials, namely

$$LB(S_{SC}) \approx \sum_{i=0}^{B_L} l_i S_{SC}^i, \quad RB(S_{SC}) \approx \sum_{j=0}^{B_R} r_j S_{SC}^j, \tag{36}$$

where B_L and B_R represent the polynomial orders, and l_i and r_j represent polynomial coefficients to be estimated.

The derivation details of functions $f(S_{SC})$, $g(S_{SC})$, $LB(S_{SC})$ and $RB(S_{SC})$ can be found in [27]. The final THD_U expression reads

$$THD_U(N_{PC}, S_{SC}) =$$
$$\begin{cases} (-3.043 \times 10^{-6} S_{SC} + 5.44 \times 10^{-2}) N_{PC} - 4.527 \times 10^{-4} S_{SC} + 4.714 \\ \quad \text{for } N_{PC} \le LB(S_{SC}) \\ (-2.931 \times 10^{-7} S_{SC} + 1.059 \times 10^{-1}) N_{PC} - 1.348 \times 10^{-3} S_{SC} + 3.916 \\ \quad \text{for } LB(S_{SC}) < N_{PC} < RB(S_{SC}) \\ (-7.647 \times 10^{-13} S_{SC}^3 + 1.219 \times 10^{-8} S_{SC}^2 - 6.701 \times 10^{-5} S_{SC} \\ \quad + 1.767 \times 10^{-1}) N_{PC} - 5.264 \times 10^{-4} S_{SC} + 4.466, \text{for } N_{PC} \ge RB(S_{SC}) \end{cases}$$
$$LB(S_{SC}) = 1 \times 10^{-2} S_{SC} + 30$$
$$RB(S_{SC}) = -5 \times 10^{-7} S_{SC}^2 + 1.35 \times 10^{-2} S_{SC} + 34. \quad (37)$$

Note that $f(S_{SC})$ is a cubic function of N_{PC} in the right region, and linear function elsewhere, whereas g(S) is linear everywhere. On the other hand, boundaries $LB(S_{SC})$ and $RB(S_{SC})$ are linear and quadratic functions of S_{SC}, respectively. Dash-dot lines in Fig. 1 depict model results, showing exceptional matching between the simulations and the model.

4.1.7 Additional Factors that May Affect THD_U

The proposed model (37) can be further analysed by taking into account the effects described in the following subsections.

Effects of Cable Cross-Section

Cable PP-Y 5 × 4 mm^2, length of about 80 m, supplies the PCC of CCFTS. Simulation model and in turn analytical model (37) are obtained for such a cable. The maximal current capacity of the mentioned cable is I_{max} = 47 A. For a larger PC cluster, i.e., larger values of generated current, greater cable cross-section are needed. Hence, it is very important to analyse the THD_U dependence on the cable cross-section to see whether the introduction of cable cross-section as an additional parameter in model (37) is necessary.

For a given cable length and grid stiffness of S_{SC} = 4000 kVA, THD_U increases with the increase of the cable cross-section. This is due to the fact that at larger cross-section the distances between the neutral conductor and the phase conductors are increased leading to respective increase of the neutral conductor impedance. However, for different cable cross-sections, namely 5 × 6 mm^2, 5 × 10 mm^2, 5 × 16 mm^2 and 5 × 25 mm^2, which are very common in practice, the deviations of the THD_U values from model (37), expressed in terms of the RMS in Table 1, do not exceed 1.83 %.

For a cross-section of 5 × 25 mm^2 and grid stiffness of 6000 and 7000 kVA, the considered effect is much less pronounced, i.e., maximal deviations are 1.34 and

Table 1 RMS of deviation of simulated THD_U values (obtained for various cable cross-sections) from the model THD_U values. Fixed S_{SC} = 4000 kVA is considered

Cross-section (mm^2)	N_{PC}				
	10 (%)	50 (%)	100 (%)	150 (%)	200 (%)
5 × 6	0.10	0.21	0.39	0.55	0.71
5 × 10	0.16	0.29	0.51	0.72	1.03
5 × 16	0.23	0.38	0.72	1.08	1.42
5 × 25	0.35	0.73	1.15	1.40	1.83

1.07 %, respectively. Slightly larger deviations (3.63 %) are obtained for very low grid stiffness of S_{SC} = 3000 kVA. The influence of the cable cross-section on THD_U, therefore, can be practically neglected.

Effects of Pre-existing THD_U

The measured pre-existing THD_U values are incorporated within the simulation model, which was a base for developing the final mathematical model (37). However, in order to preserve the model's simplicity, the pre-existing THD_U has not been taken as a parameter. Now, a question of validity of such a decision arises. Model (37) for the case of pre-existing THD_U of 1.9 % (as opposed to 2.1 % adopted in the model), gives results very close to the measured ones, with a difference less than 0.2 %. Also, simulations carried out with the pre-existing THD_U values of 1.75, 1.82, 2.18 and 2.25 % and constant S_{SC} and N_{PC} values, show a slight difference between the obtained results (maximal discrepancy was 0.89 %). This point to the fact that common values of the pre-existing THD_U on the low voltage level (1.5–2.5 %) has insignificant impact on the model's accuracy.

Influence of Load-Side Parameters on THD_U

The simulation model used in our research takes into account the technology structure of modern PCs. From the power quality point of view, the PSU is the most significant PC component. More precisely, capacitors within the PSU (usually two capacitors connected in parallel) represent the major harmonic source, which can affect THD_I, as shown in Sect. 4.1, and its influence decreases with the increase of the PC cluster size. Simulations carried out in this study, that take into account a wide range of the PSU capacitances encountered in modern PCs (235–500 μF), show that the influence of the PSU capacitance on the THD_U can be neglected. Therefore, we have omitted it in the final THD_U model (37).

Table 2 RMSE versus S_{SC} and C

S_{SC} [kVA]	C [μF]			
	235	340	410	500
3000	2.87	1.88	2.19	2.49
4000	0.94	1.79	2.11	2.77
5000	1.55	2.36	2.47	3.12
6000	1.52	1.06	1.69	3.16

4.2 Verification of the Models Accuracy

To evaluate the performance of the THD_I model (29), the Root Mean Square Error (RMSE) is calculated for the values of S_{SC} and C given in Table 2. The maximal RMSE is 3.16 %, which is acceptable according to relevant standards.

For the values of S_{SC} and C characteristic to NLBMB (5800 kVA, see Sect. 3.2), the proposed model yields the THD_I values of 45.35, 47.51 and 46.97 %, per phase, which are very close to the measured ones.

The accuracy of the proposed THD_U model is also evaluated using the RMSE. The obtained RMSE values are 0.09, 0.09, 0.071, 0.08, 0.057 % for S_{SC} = 3000, 4000, 5000 and 6000 kVA, respectively. In addition, for the values of S_{SC} and N_{PC} (of the most loaded phase) characteristic to NLBMB (5800 kVA and 83 PCs, see Sect. 3.2), model (37) yields the THD_U value 5.14 %, which strongly confirms the validity of the proposed THD_U model.

5 Conclusion

Simultaneous operation of PCs can negatively affect the supply voltage and it is very important to evaluate their harmonic level. To that end, knowing the THD_I and THD_U values is profoundly important.

This study addresses the issue of THD_I and THD_U modelling due to PC cluster operation. Theoretical considerations and analysis of measurement results found in literature, for both single PC and PC cluster, imply that numerous parameters affect the THD_I and THD_U level. The analysis revealed some crucial shortcomings of the available THD_I and THD_U models, none of them being a comprehensive solution. Our intention was to develop THD_I and THD_U models suitable for practical engineering application. In line with that, the requirements of sufficient accuracy and mathematical simplicity had to be fulfilled. In other words, the model should include only major line side and load side parameters, such as the PC cluster size ($N_{PC} > 0$), the grid stiffness (range of 2000–6000 kVA represents most commonly found values in modern distribution grids) and the size of DC capacitor of the PC PSU (range of 235–500 μF represents most commonly found values in modern PCs). Many other parameters, such as frequency, phase (line) voltage RMS, dependence of active and reactive power on the phase voltage RMS, presence of

initial voltage distortion, low voltage cable cross-section and three-phase unbalance, may potentially affect both THD_I and THD_U. However, the conducted simulations have proved their minor impact. The proposed models are developed based on theoretical consideration regarding factors that affect THD_I and THD_U, measurements and simulations. The models coefficients are derived in the least square sense. The THD_I and THD_U calculation requires basic arithmetic operations only, which is convenient for engineering application. Therefore, it represents significant improvement over the existing models proposed in the literature. The models can be viewed as a low-cost alternative to specialized software for the power system analysis. The validity of the models is supported by additional measurement carried out in site characterized by grid conditions quite different from that used for model developing.

References

1. Katić VA, Dumnić B, Mujović S, Radović J (2004) Effects of low power electronics & computer equipment on power quality at distribution grid—measurements and forecast. In: Proceedings of international IEEE conference on industrial technology, Hammamet, pp 585–589
2. Mazin HE, Nino EE, Xu W, Yong J (2011) A study on the Harmonic Contributions of Residential Loads. IEEE Trans Power Delivery 26(3):1592–1599
3. Knežević JM, Katić VA (2011) The hybrid method for on-line harmonic analysis. Adv Electr Comput Eng 11(3):29–34
4. Bobric EC, Cartina G, Grigoras G (2009) Clustering techniques in load profile analysis for distribution stations. Adv Electr Comput Eng 9:63–66
5. Alshammari BM, El-Kady MA, Al-Turki YA (2011) Power system performance quality indices. Eur Trans Electr Power 21:1704–1710
6. IEEE Standard 519-1992 (1993) IEEE recommended practices and requirements for harmonic control in electric power systems. IEEE Press
7. IEC 61000-3-2 Standard (2002) Electromagnetic compatibility (EMC)—part 3-2: limits—limits for harmonic current emissions (equipment input current $\leq$ 16 a per phase). In: IEC 2002
8. Fuchs E, Masoum M (2008) Power quality in power systems and electrical machines. Elsevier Academic Press, Burlington, pp 19–20
9. Mansoor A, Grady WM, Chowdury AH, Samotyj MJ (1995) An investigation of harmonics attenuation and diversity among distributed single-phase power electronic loads. IEEE Trans Power Delivery 10:467–473
10. Mujović S, Katić VA, Radović J (2011) Improved Analytical Expression for Calculating Total Harmonic Distortion of PC Clusters. Electr Power Syst Res 81(7):1317–1324
11. EN50160 Standard (1994) Voltage characteristics of electricity supplied by public distribution systems. In: CENELEC
12. Fuentes J, Molina-Garcia A, Gomez E (2007) A measurement approach for obtaining static load model parameters in real time at the distribution level. Eur Trans Electr Power 17:173–190
13. Herraiz S, Sainz L, Corcoles F, Pedra JA (2005) Unified and simple model for uncontrolled rectifiers. Electric Power Syst Res 74:331–340
14. Herraiz S, Sainz L, Pedra JA (2003) Behaviour of Single-Phase Full-Wave Rectifier. Eur Trans Electr Power 13:185–192

15. Rawa MJH, Thomas MJH, Sumner M (2014) Background voltage distortion and percentage of nonlinear load impacts on the harmonics produced by a group of personal computers. In: Proceedings of the 2014 international symposium on electromagnetic compatibility 2014, Gothenburg, Sweden, pp 626–630
16. Emanuel AE, Janezak J, Pileggi DJ, Gulachenski EM, Root CE, Breen M, Gentile T (1994) Voltage distortion in distribution feeders with nonlinear loads. IEEE Trans Power Delivery 9:79–87
17. Mesas JJ, Sainz L, Sala P (2015) Statistical study of personal computer cluster harmonic currents from experimental measurements. Electric Power Compon Syst 43(1):56–68
18. Wu C-J, Hu C-H, Yin C-C, Chiu C-C (1998) Application of regression models to predict harmonic voltage and current growth trend from measurement data at secondary substations. IEEE Trans Power Delivery 13:793–798
19. Khan RAJ, Akmal M (2008) Mathematical modeling of current harmonics caused by personal computers. World Acad Sci Eng Technol 39:325–329
20. Patidar RD, Singh SP (2009) Harmonics estimation and modeling of residential and commercial loads. In: Third international conference on power systems, Kharagpur, India, paper ID-212
21. Katić VA, Mujović S, Radulović V, Radović J (2011) The impact of the load side parameters on PC cluster's harmonics emission. Adv Electr Comput Eng 11:103–110
22. Manjunatha S, Panduranga KV (2010) Assessment of distributed generation source impact on electrical distribution system performance. Adv Electr Comput Eng 10(2):135–140
23. Davidson CC (2011) Power transmission with power electronics". In: Proceedings of 14th international conference on power electronics and application, Birmingham, pp 1–10, Sept 2011
24. Dumnić B, Ostojić D, Katić V (2005) Power quality in case of a large number of nonlinear devices-measurements and forecast. In: Proceedings of international conference on power electronics, intelligent motion and power quality, Nuremberg, June 2005, pp 336–341
25. IEC Standard 61000-4-7 (2002) General guide on harmonics and inter-harmonics measurements and instrumentation for power supply systems and connected equipment, IEC, Geneva
26. Mujović S, Djukanović S, Radulović V, Katić V (2016) Multi-parameter mathematical model for determination of PC cluster total harmonic distortion input current. COMPEL: Int J Comput Math Electr Electron Eng 35(1):305–325
27. Mujović S, Djukanović S, Radulović V, Katić V, Rašović M (2013) Least squares modeling of voltage harmonic distortion due to PC cluster operation. Adv Electr Comput Eng 13 (4):133–138
28. Hansen S, Nielsen P, Blaabjerg F (2000) Harmonic cancellation by mixing nonlinear single-phase and three-phase loads. IEEE Trans Ind Appl 36:152–159

Energy Efficient Public Lighting—A Case Study

Maja Muftić Dedović, Nedis Dautbašić, Boško Drinovac and Samir Avdaković

Abstract In this paper energy efficiency in public lighting has been presented. Electricity consumption is analyzed according to input date taken from Public Company Roads of Federation of B&H (PCR FB&H). According to the analysis major consumers are classified and measures for rational consumption of electricity in public lighting are given. Analysis is carried out by replacing the existing lighting system by modern energy efficient lighting system (LED lighting), taking into account all technical and regulatory requirements. After that a techno-economic analysis of the installation of new lighting system is carried out with the necessary investment and time required to recoup the funds expended in an investment.

1 Introduction

Energy efficiency is an effective use of electricity in order to minimize the possible amount of electricity for the same work without losing comfort, standards or other economic activities. In order to implement energy efficiency and rationalization of electricity the trend is to go towards the replacement of conventional light sources with new technology that uses LED light sources. When selecting and purchasing new luminaires, economic and environmental factors should be considered.

M.M. Dedović (✉) · N. Dautbašić · B. Drinovac · S. Avdaković
University of Sarajeve, Sarajeve, Bosnia and Herzegovina
e-mail: mm14843@etf.unsa.ba

N. Dautbašić
e-mail: nd15231@etf.unsa.ba

B. Drinovac
e-mail: dbosko@jpcfbih.ba

S. Avdaković
e-mail: samir.avdakovic@etf.unsa.ba

M. Hadžikadić and S. Avdaković (eds.), *Advanced Technologies, Systems, and Applications*, Lecture Notes in Networks and Systems 3,
DOI 10.1007/978-3-319-47295-9_6

The new luminaires can be considered ecological and efficient if having the same effect with less power consumption [1]. Public lighting should allow such vision conditions, guaranteeing driving at night with the highest possible safety and maximum possible comfort. Also, important parameters that configure the selection of the light source are the color of light (color temperature), mean time to failure, the heating time, the temperature control of the working environment and the dimensions of the light source [2].

In recent times, application of LED light sources is in the great expansion. At the beginning of LED light implementation in the design of electrical lighting of the tunnel, these light sources are most often used to illuminate the interior zone of the tunnel. With the development of LED lighting, increasing efficiency and output brightness, it can be used in illumination of the threshold zone of the tunnel. As the threshold zone of the tunnel has the highest photometric requirements, therefore it is recommended to use light sources characterized by high power and light efficiency, long life, small dimensions in order to achieve the maximum photometric requirements. As mentioned features characterized the LED light sources, therefore, it is inevitably that their implementation is increasing. On the basis of present knowledge public lighting techniques, determined following quality criteria for a particular system of public lighting: the level of luminance - brightness of road surface, uniformity of roads surface luminance, the level of illumination of surrounding roads, limited glare, visual (optical) guidance [2, 3].

The basic solution of public lighting should identify classes of public lighting for individual roads, the basic lighting parameters required for specific roads, type of light source, and the basic geometry of the installation of public lighting [3].

Lighting criteria is achieved by a corresponding number of light sources, and by the application of the applicable technical regulations, rules, standards, guidelines and recommendations [4–24].

2 Energy Consumption Analysis

In this paper the power consumption of PCR FB&H is analyzed, which currently has 63 measurement locations in its jurisdiction. The subject of detailed analysis of consumer of PCR FB&H are 16 tunnels, 18 crossroads, 24 traffic lights, 4 traffic lights with crossroads and administrative building with a total annual consumption of 2,104,235.52 kWh. As the dominant consumers, tunnels and crossroads are singled out with 68 % of total electricity consumption, identified at the measurement locations corresponding to tunnels and 18 % of total consumption corresponding to the lighting on the crossroads (Fig. 1.).

The lighting in tunnels and crossroads represent about 90 % of electricity consumption of PCR FB&H, and by examining the available data bases are identified a total of 3027 luminaires (lighting device) of total installed power about 735.31 kW. For 1949 luminaires the technical characteristics are known and are related to lighting in tunnels (1743 pieces), lighting of crossroads (206 pieces) and the access

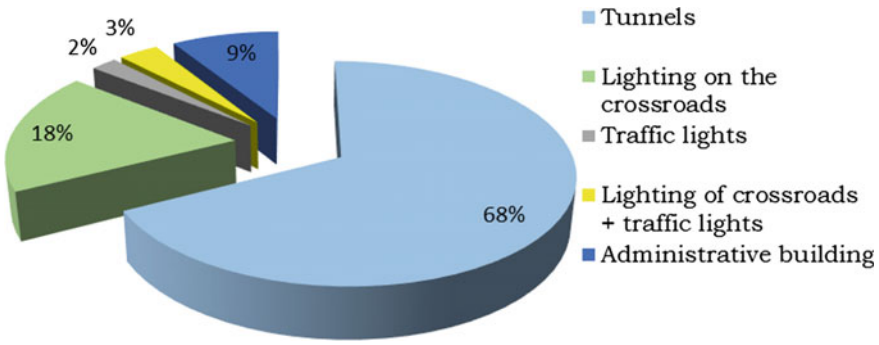

Fig. 1 Electricity consumption by consumer categories in 2014 (kWh)

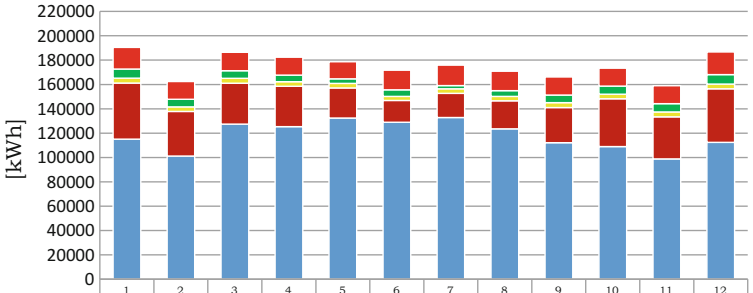

	1	2	3	4	5	6	7	8	9	10	11	12
Administrative building	17734	14496	15175.5	14614	14082	16227	16846.5	16022.5	14784.5	14750.5	14673	18562.5
Lighting of crossroads + traffic lights	7572	6255	6268	5459	3627	5351	2673	4725	6260	6662	6803	7791
Traffic lights	3945	3757	3953	3732	3833	3331	3705	3604	4110	3672	4044	3947
Lighting on the crossroads	46128.7	36701.1	33646.4	33182.35	24743.05	17867.2	19919.5	22984.7	28805.6	39349.3	34487.1	43911
Tunnels	115112.66	101193.7	127423.28	125403.83	132390.93	129014.52	132813.69	123569.56	112188.09	108953.7	98907.71	112490.85

Fig. 2 The monthly electricity consumption (2014) according to category (kWh)

tunnel lighting (70 pieces), while for 1008 pieces of lighting fixtures characteristics are currently not known. The total installed power of lighting fixtures (with the available characteristics) of PCR FB&H is 492.216 kW, which represents an average of 241,164 W/luminaire. So, for a total of 3027 luminaires (lighting devices) total installed power is approximately 735.31 kW.

The monthly electricity consumption (kWh) and monthly financial allocations (BAM) for year 2014 in each category are presented in Figs. 2 and 3. Consumers are sorted by categories:

- office building,
- traffic lights and lighting of crossroads,
- traffic lights
- lighting of crossroads and,
- tunnels.

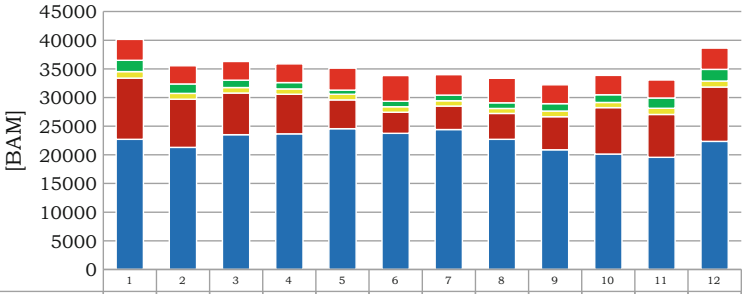

	1	2	3	4	5	6	7	8	9	10	11	12
Administrative building	3650.68	3190.52	3265.07	3244.96	3820.51	4493.5	3575.53	4271.06	3284.28	3380.66	3164.18	3727.53
Lighting of crossroads + traffic lights	1971.92	1637.87	1281.08	1125.57	728.26	946.53	966.11	971.18	1278.55	1357.11	1775.43	2026.36
Traffic lights	1123.4	1009.76	962.22	922.52	963.68	951.94	934.77	879.56	975.28	891.75	1100.05	1053.1
Lighting on the crossroads	10677.29	8417.04	7274.69	6891.41	5044.83	3692.09	4106.26	4525.58	5794.27	8096.66	7450.71	9489.26
Tunnels	22713.07	21287.13	23493.28	23663.03	24544.45	23733.25	24397.91	22683.95	20862.28	20134.07	19569.86	22327.8

Fig. 3 The monthly financial allocation for electricity (2014) according to category (BAM)

From Fig. 2. it is clear that the dominant consumers categories of PCR FB&H (on a monthly basis) are tunnels and lighting on the crossroads, while a much smaller part of consumption have remained for the other categories. From Figs. 2 and 3 it can be clearly identify that the electricity consumption and financial allocations of lighting on the crossroads are much higher during winter months compared to summer months as a result of differences in the length of day and night of the corresponding seasons. Unlike lighting on the crossroads, for tunnels can be seen the opposite situation where consumption of electricity in the summer months is slightly higher compared to the winter months.

3 An Outline of Methodological Approaches

3.1 Crossroads

Important parameters for lighting quality of crossroads for motorized traffic are:

- Horizontal illumination
- The linearity of lighting
- The density of traffic
- The importance of roads
- Problematic areas

Roads for motorized traffic are classified in six categories from ME1 to ME6 depending on the category of roads, the density and complexity of traffic.

Based on the classification of roads and recommendations for road lighting of different types of roads in the dry conditions on the road, in accordance with available input data, two groups i.e. ME3a "main distributor" and ME2 "strategic route" are singled out which include traffic crossroads analyzed in this paper.

Input data are taken from 18 measurement locations relating to lighting on crossroads (traffic intersections).

Lighting criteria for those two classes:

Class ME2:

- Average road surface luminance L_{sr} = 1.5 cd/m^2
- Longitudinal uniformity (of road surface luminance of a driving lane) U_0 = 40 %
- Longitudinal uniformity (of road surface luminance of a carriageway) U_1 = 70 %
- Threshold increment TI = 10

Class ME3b:

- Average road surface luminance L_{sr} = 1.0 cd/m^2
- Longitudinal uniformity (of road surface luminance of a driving lane) U_0 = 40 %
- Longitudinal uniformity (of road surface luminance of a carriageway) U_1 = 60 %
- Threshold increment TI = 15

In accordance with the proposed requirements and recommendations in order to reduce electricity consumption and innovation of the existing system of lighting, it is necessary to dismantle the existing lighting at all 18 measurement locations. So it is necessary to install new LED luminaires with different light sources on the existing poles. Replacement of lighting devices is submitted in accordance with EN 13201: 2005 Road lighting [7–11].

3.2 Tunnels

Highlighting the tunnel is significantly different from the illumination of the crossroads (road). The tunnels must be illuminated not only at night but also during the day, where the lighting requirements for daylight are considerably more complex than during the night. For illumination of the tunnel, night lighting is common, similar to other road illumination, while lighting the tunnel in day conditions requires special photometric calculations. Entering the tunnel, the driver is faced with the problem of "black hole" and the adaptation of his sight. The problem of "black hole" is a phenomenon that prevents the driver to see the inside of the tunnel when is relatively far from its entrance. Then there is a sudden change in the level of brightness, from brightness from the light out of the tunnel, to a very low level of

brightness in the tunnel (usually determined by the headlights of the vehicle). In such a big change of brightness level, the driver's eyes are slowly adapting. For quality luminance levels of tunnels it is very important to evaluated luminance of the access zone, section of road before the tunnel entrance.

Tunnels are divided into two groups:

- Long tunnels—tunnels longer than 100 m, or tunnels whose length is at least seven times greater than its width.
- Short tunnels—from 25 to 100 m; For tunnels shorter than 25 m is not necessary to install lighting equipment.

After the analysis and the calculations in this paper are presented for all 12 tunnels the replacement luminaires, their type and light sources, as well as the installation of the approach zone tunnel lighting.

Outdoor lighting in the access zone of the tunnel is selected according to the current regulations and recommendations:

- Luminaire: with symmetrical distribution of the light intensity and the possibility of luminous flux reduction at 50 %, resulting in a base night mode. Reduction of the luminous flux of the light source provides a longer life span of luminaires and reduce maintenance costs.
- Light source: LED, power 103, 120, 166, 180 W.

Lighting in adaption zone and the interior zone:

- Luminaire: with symmetrical distribution of the light intensity and the possibility of luminous flux reduction at 50 %, resulting in a base night mode.
- Light source: LED, power 34, 46 W.

Lighting of the threshold zone and an adaption zone is according to the operating modes presented in Table 1.

In Table 1 are presented for daylight three modes and depending on mode and the variations in luminance level of threshold zone. Therefore, it is necessary to perform the regulation of the luminous flux of luminaires and adjust the luminance levels of the individual zones in the tunnel.

Lighting in the threshold zone:

- Luminaire: with asymmetrical distribution of the light intensity "counter beam" and the possibility of luminous flux reduction at 45 %.
- Light source: LED, power 120, 166, 180 W.

Table 1 Modes of public lighting in tunnels

Daylight	I mode	Sunny day, all luminaires on with full capacity	100 % L_{th}
	II mode	Cloudy day, all luminaires in threshold zone on with reduced power	75 % L_{th}
	III mode	Sunset, every second luminaire in threshold zone on with reduces power, and every other luminaire off	50 % L_{th}

Lighting in an adaption zone:

- Luminaire: with asymmetrical distribution of the light intensity "counter beam" and the possibility of luminous flux reduction at 50 %.
- Light source: LED, power 73, 75, 103, 120, 166, 180 W.

Reducing the luminance level in the threshold zone can be achieved by reducing the luminance level of the access zone. To reduce the luminance level of access zones it is required darker facade of the tunnel. Energy-efficient illumination of the tunnel is also achieved by lighting control in steps. Luminance of access zone varies during the day throughout the whole year. Ideally, the luminance level of the first part of the threshold zone should be constant certain percentage of luminance level of the tunnel access zone. In terms of the long tunnels it should be at least six variations of the luminance level.

4 Techno-Economic Analysis—Results

4.1 Techno-Economic Analysis—Crossroads

In Table 2 is presented a new lighting system with modes and powers of the light sources used for modernization of lighting system and annually electricity consumption. It includes two modes, full mode (100 %, all luminaires turned on) and reduced mode (50 % one half of luminaires turned on and one half turned off). Reduced mode with 50 % of the luminous flux is assumed for the period from 23:00 to 04:30 h. So it is assumed that luminaires at crossroads operate for about 4100 h per year. For both modes operation time is 2050 h and then the average daily operation of the light source is 11.23 h. For the new lighting system, it is assumed the use of light sources with powers 18, 60, 75, 103 and 205 W. Based on available input data about maintenance costs, for more accurate techno-economic analysis, to the annual cost of electricity consumption are associated maintenance costs allocated for the crossroads.

Also in Fig. 4 are plotted significant differences in electricity consumption in kWh and in Table 3 are presented savings at crossroads in kWh/year and

Table 2 The new lighting system with modes and powers of the light sources used for modernization of lighting system and annually electricity consumption

New lighting system			
Mode (%)	Operation time (h)	Power (W)	kWh/god
100	2050	18, 60, 75, 103, 205	62,877.6
50	2050	18, 60, 75, 103, 205	31,438.8

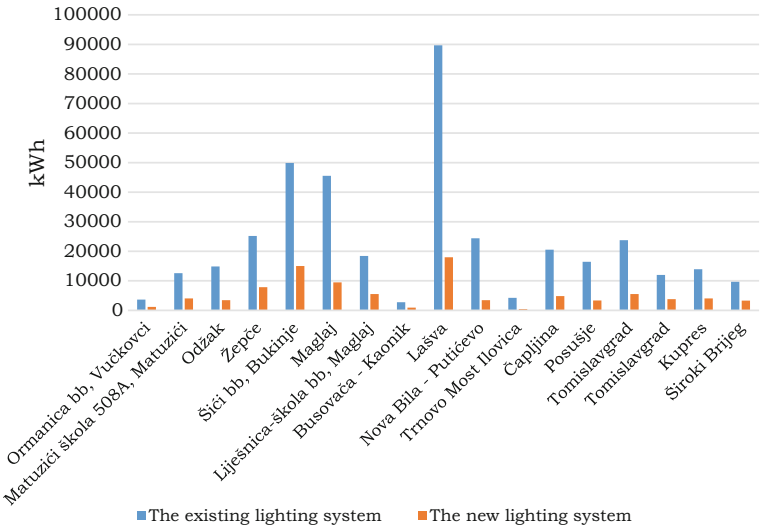

Fig. 4 Electricity consumption before and after the modernization of the respective measurement locations (crossroads)

Table 3 Saving at crossroads in kWh/year and BAM/year for 2014, with the investment for the installation of new lighting system and payback period taking into account maintenance costs

Locations	Saving		Investment	
	kWh/year	BAM/year	BAM	Payback period (year)
Lašva	71,717.25	15,825.404	38,386.14	2.43
Nova Bila—Putićevo	20,926.625	5222.3821	7381.95	1.41
Trnovo Most Ilovica	3800.75	866.96,656	984.26	1.14
Čapljina	15,713.875	1937.7356	10,334.73	5.33
Posušje	13,092.65	3535.9235	6529.82	1.85
Tomislavgrad	18,201	5643.5355	12,063.9	2.14
Tomislavgrad	8212.75	2165.5182	7512.78	3.47
Kupres	9877	3152.5942	8846.86	2.81
Široki Brijeg	6359	2226.9085	7238.34	3.25
Ormanica bb.	2477.65	1443.6334	2144.73	1.49
Matuzići škola	8549	2636.4294	8846.86	3.36
Odžak	11,415.625	3188.5591	7381.95	2.32
Žepče	17,364.75	5280.598	16,732.42	3.16
Šići bb, Bukinje	34,920.37	9457.2696	31,988.45	3.38
Maglaj	36,049.25	7905.7196	16,563.9	2.10
Liješnica-Maglaj	12,884	5297.0024	12,063.9	2.28
Busovača—Kaonik	1841.05	1185.4494	1736.21	1.46

BAM/year for 2014, with the investment for the installation of new lighting system and payback period taking into account maintenance costs.

4.2 Techno-Economic Analysis—Tunnels and Access Zones

Relations in electricity consumption before and after the modernization of the respective measurement locations in all tunnels are presented in Fig. 5. In Fig. 5 significant differences in electricity consumption expressed in kWh are clearly visible. Also in Table 4 the savings for all tunnels in kWh and BAM for 2014 are presented.

For more accurate techno-economic analysis, to the annual cost of electricity consumption are associated maintenance costs allocated for the tunnels and tunnel's access zones. Maintenance costs include regular maintenance and replacement of light sources for a total of 2587 luminaires in all tunnels. Also it is very important to emphasize that LED lighting maintenance costs only include costs for initial installation of new lighting system, all other costs are zero according to LEDs life expectancy of 50,000 h.

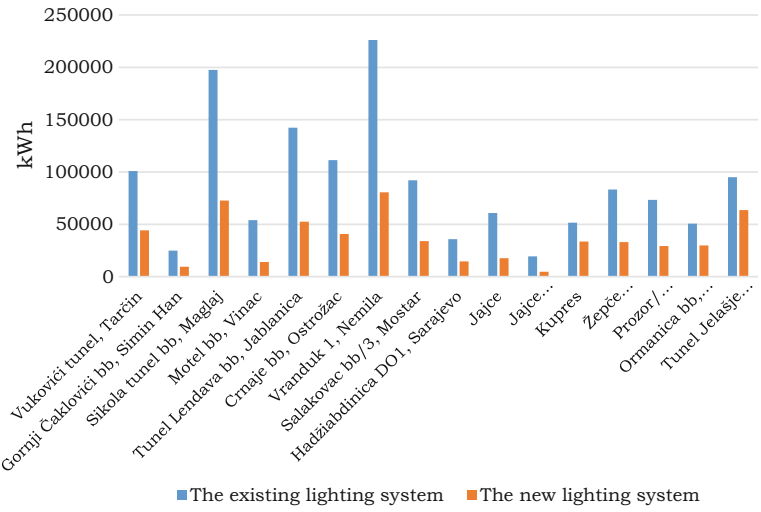

Fig. 5 Electricity consumption before and after the modernization of the respective measurement locations (tunnels and access zones)

Table 4 Saving in tunnels and access zones in kWh/year and BAM/year for 2014, with the investment for the installation of new lighting system and payback period taking into account maintenance costs

Locations	Saving		Investment	
	kWh/year	BAM/year	BAM	Payback period (year)
Vukovići tunel, Tarčin	56,714.52	24,671.45	139,400.44	5.65
Gornji Čaklovići bb	15,424.09	9519.352	124,615.24	13.09
Sikola tunel bb	124,781.92	66,829.25	261,878.17	3.91
Motel bb Vinac	40,060.56	8393.034	16,142.6	1.92
Tunel Lendava bb	89,742.61	25,087.08	141,977.66	5.66
Crnaje bb, Ostrožac	70,564.69	21,815.9	147,264.7	6.75
Vranduk 1	145,503	85,345.08	284,564.2	3.33
Salakovac	58,114.63	18,306.66	127,754.32	6.98
Hadžiabdinica	21,272.62	7751.985	79,726.14	10.28
Jajce	43,156	11,584.3	44,387.89	3.83
Jajce Skela	14,728	3877.42	12,106.95	3.12
Kupres	17,990	10,324.8	102,510.98	9.93
Žepče (Karaula)	50,203	17,766.87	133,678.02	7.52
Prozor/Rama	44,100	16,067.33	118,239.68	7.36
Ormanica bb	20,864.8	10,180.15	121,048.2	11.89
Tunel Jelašje M-17	31,446.96	11,823.01	141,821.16	12.00

Table 5 Powers and quantities of luminaires before and after the modernization of crossroads lighting system

The existing lighting system		The new lighting system	
Power (kW)	PCS	Power (kW)	PCS
98.54	440	30.67	440

Table 6 Saving in kWh/year and BAM/year for 2014, with the investment for the installation of new lighting system and payback period taking into account maintenance costs for crossroads and tunnels and corresponding access zones of tunnels

	Savings		Investment	
	kWh/year	BAM/year	BAM	Payback period (year)
Crossroads	293,402.595	76,971.628	196,737.2	2.55
Tunnels and access zone	844,667.4	349,343.7	1,997,116	5.72
Total	1,138,070	426,315.32	2,193,853.2	5.15

5 Conclusion

In Table 5 powers and quantities of luminaires, before and after the modernization of crossroads lighting system are presented. It is evident that the installation of a new lighting system with the retention of the same number of devices significantly reduces the lighting power expressed in kW. Table 6 presents final considerations in terms of economic viability of investment in the new lighting system, which include the crossroads and tunnels, as well as their access zones. This table present the summary of all analysis and calculations, so the annual savings for 2014 in kWh and BAM are, respectively, in the amount of 1,138,070 kWh and 426,315,328 BAM. Also here are presented the investments for the installation of alternative luminaires and light sources at all locations, and this investment is assumed to be 2,193,853.2 BAM. Payback periods for all crossroads and tunnels and access zones are obtained dividing values of investment with total annual savings and total number for payback period is about 5.15 years.

Carrying out the analysis of the results it is clear that the payback period is satisfying and justifies investment in the installation of a new lighting system. Also it is significant that after the modernization of the lighting system, installed power is significantly less than the installed power of the existing lighting system and this also proves a multiple profitability of investment. The main conclusion of this paper is that by implementation of modern lighting systems electricity consumption is reduced about 54 %, and the total costs for the consumption of electricity and maintenance is reduced by about 61 %.

References

1. Intelligent energy for Europe, Supply and environmental protection guidelines—efficient lighting, June 2012
2. Outdoor Lighting Guide, Institution of Lighting Engineers
3. Miomir B. Kostić Vodič kroz svet tehnike osvjetljenja Beograd 2000
4. BAS EN 12665:2012, Light and lighting—Basic terms and criteria for specifying lighting requirements
5. BAS CR 14380:2006, Lighting Applications—Tunnel Lighting
6. BAS EN 13032-1 + A1:2013, Light and lighting. Measurement and presentation of photometric data of lamps and luminaires. LED lamps, modules and luminaires
7. BAS CEN/TR 13201-1:2014, Road lighting—Part 1: Selection of lighting classes
8. BAS EN 13201-2:2005, Road lighting—Part 2: Performance requirements
9. BAS EN 13201-3:2005, Road lighting—Part 3: Calculation of performance
10. BAS EN 13201-4:2005, Road lighting—Part 4: Methods of measuring lighting performance
11. DIRECTIVE 2011/65/EU OF THE EUROPEAN PARLIAMENT AND OF THE COUNCIL —on the restriction of the use of certain hazardous substances in electrical and electronic equipment
12. Commission Regulation (EC) No 245/2009 of 18 March 2009 implementing Directive 2005/32/EC of the European Parliament and of the Council with regard to ecodesign requirements for fluorescent lamps without integrated ballast, for high intensity discharge

lamps, and for ballasts and luminaires able to operate such lamps, and repealing Directive 2000/55/EC of the European Parliament and of the Council
13. Directive 2005/32/EC of the European Parliament and of the Council with regard to ecodesign requirements for fluorescent lamps without integrated ballast, for high intensity discharge lamps, and for ballasts and luminaires able to operate such lamps
14. DIRECTIVE 2009/125/EC OF THE EUROPEAN PARLIAMENT AND OF THE COUNCIL of 21 Oct 2009 establishing a framework for the setting of ecodesign requirements for energy-related products (recast)
15. DIRECTIVE 2012/27/EU OF THE EUROPEAN PARLIAMENT AND OF THE COUNCIL of 25 Oct 2012 on energy efficiency
16. Directive 2002/95/EC of the European Parliament and of the Council of 27 Jan 2003 on the restriction of the use of certain hazardous substances in electrical and electronic equipment
17. DIRECTIVE 2006/95/EC OF THE EUROPEAN PARLIAMENT AND OF THE COUNCIL of 12 Dec 2006 on the harmonization of the laws of Member States relating to electrical equipment designed for use within certain voltage limits
18. Directive 2004/108/EC—electromagnetic compatibility
19. Green Paper/EC—provides guidance for use of LED technology in lighting stating that by the year 2020 should be 80 % of the lighting in the application of LED technology
20. CIE 88-2004 Guide for the Lighting of Tunnels and Underpasses; Publication CIE No 88; International Commission on Illumination: Vienna, Austria, 2004
21. CIE 140-2000 Road Lighting Calculations; Publication CIE No 140; International Commission on Illumination: Vienna, Austria, 2000
22. ANSI/IESNA RP-22-96 “American National Standard Practice for Tunnel Lighting”; American National Standards Institute, Illuminating Engineering Society of North America: New York, NY, USA, 1996
23. DIN 67524-1:2008 “Lighting of street tunnels and underpasses”
24. CEN Report CR 14380

Analysis of a Load Profile of the Public Company Roads of Federation Bosnia and Herzegovina

Nedis Dautbašić, Maja Muftić Dedović, Boško Drinovac and Samir Avdaković

Abstract This paper shows an analysis of the power consumption of PC Roads of FB&H, which currently has 63 measuring points in its jurisdiction, where electric power is received. The subjects of this analysis are consumers of Public Company Roads of Federation of Bosnia and Herzegovina (PC Roads of FB&H): 16 tunnels, 18 road lightings, 24 traffic lights, 4 traffic lights with additional lights and administrative building, with a total annual consumption. Electric power consumption will be classified by consumption in tunnels, road lightings, traffic lights and administrative building. This will determine the character of each consumers group and contribution of each group in the total consumption. Work and activities area of PC Roads of FB&H is the area of the Federation of Bosnia and Herzegovina, where currently two electric power companies exist: Public Enterprise Elektroprivreda B&H (PE EP B&H) and Public Enterprise Elektroprivreda HZHB (PE EP HZHB), which in the jurisdiction of JP Roads of FB&H supply electricity for different consumers. The paper presents a method of making the load curve and its basic indicators, which is presented for each category of consumers too.

1 Introduction

PC Roads of B&H take electric energy from PE EP B&H and PE EP HZHB at 63 measuring points. The dominant consumer of the electricity in PC Roads of FB&H are lightings. 68 % of total electricity consumption is by tunnels. 18 % of the total consumption is by road lightings, while 3 % of electricity consumption is by

N. Dautbašić (✉) · M.M. Dedović · S. Avdaković
Faculty of Electrical Engineering, University of Sarajevo, Sarajevo, Bosnia and Herzegovina
e-mail: nd15231@etf.unsa.ba

B. Drinovac
Public Company Roads of Federation of Bosnia and Herzegovina, Sarajevo, Bosnia and Herzegovina

M. Hadžikadić and S. Avdaković (eds.), *Advanced Technologies, Systems, and Applications*, Lecture Notes in Networks and Systems 3,
DOI 10.1007/978-3-319-47295-9_7

lighting areas with traffic lights. Traffic lights take 2 % of total consumption, while administrative building takes 9 % of the total consumption.

In this paper, an analysis of load curves for PC Roads of FB&H is done, which has 63 measuring points in total. While this analysis is performed, electric energy consumers are divided by consumption categories.

Daily load diagrams give a chronological dependence of power consumers and time (curve for one day). In terms of time periods load diagrams appear as daily, weekly, monthly and yearly diagrams, where the basis of all diagrams is daily diagram. The shape of the daily diagram depends on several factors such as the nature of the consumers area, the contribution of individual consumers in total consumption, in certain consumer area, season (summer and winter) etc. Daily diagram or power consumption, which is plotted on a diagram can be averaged value in 15 min, half an hour or whole hour [1–5].

Daily diagram is characterized by three main indicators:

- P_{pM}^{d} maximal daily load,
- P_{pm}^{d} minimal daily load and
- W_{p}^{d} total daily electricity consumption (area under the daily diagram curve).

2 Materials and Methods

Based on available data, total of six categories are identified: two high voltage categories (10 kV) and four low voltage categories (0.4 kV). Table 1 provides an overview of individual categories contribution in total consumption of electric energy.

Electricity consumption will be classified by consumption in tunnels, road lightings, traffic lights and administrative building. This will determine the character and contribution of each consumer group in the total consumption of electric energy. According to the recommendations of the USAID-REAP program, report on the load curve development PE EP HZHB, and report on completion of the

Table 1 Categories of electric energy consumers for measuring points which are in jurisdiction of PC Roads of FB&H

Category	Total number of customers	Electric energy consumption (kWh)
Administrative building (10 kV)	1	187968.00
Tunnels (10 kV)	2	423686.25
Tunnels (0.4 kV)	14	995776.75
Lightings (0.4 kV)	16	381726.00
Lightings and traffic lights (0.4 kV)	4	69446.00
Traffic lights (0.4 kV)	24	45633.00
Total	63	2104236.00

measurement cycle for the purpose of load curve development PE EP B&H, load curves analysis should include e following diagrams [6–8]:

- load diagram of each customer category at the sample level,
- normalized load diagram of each customer category,
- estimated load diagram of each customer category at the population level,
- load diagram of whole system (network),
- diagram of load duration,
- kWh diagram of each customer category,
- diagram of each customer category normalized to global consumption,
- group kWh diagram.

Based on collected data it is possible to identify the following values by consumer groups:

- maximal load P_{max} and maximal electric energy consumption W_{max},
- minimal load P_{min} and minimal electric energy consumption W_{min},
- P_{min}/P_{max} ratio,
- average load P_{avg},
- energy consumption W.

In order to obtain characterization of each diagram for simplifying typical behavior of each customer, different factors are calculated:

- Load factor (LF),
  It is the ratio of average and maximal load:

$$LF = m = \frac{P_{avg}}{P_{max}}. \tag{1}$$

- Simultaneity factor within the group (CF),
  Simultaneity factor within the group is the ratio of maximal load of the system (in this case PC Roads of B&H) and sum of all non-simultaneous maximal loads of each identified categories of this system:

$$CF = \frac{P_{\max\_system}}{\sum_{i=1}^{n} P_{imax}}. \tag{2}$$

- Factor of load contribution (POF),
  Factor of load contribution is the ratio of category load at the moment of maximal system load and maximal load of that category:

$$POF = \frac{P_i(t|P_{system}(t) = P_{\max\_system})}{P_{imax}}. \tag{3}$$

- Simultaneity factor of category and system (CPF),
  Simultaneity factor is the ratio of category load at the moment of maximal system load and maximal load of system:

$$CPF = \frac{P_i(t|P_{system}(t) = P_{\max\_system})}{P_{\max\_system}}. \tag{4}$$

For each analyzed consumption category the average value μ and standard deviation σ of consumption are calculated and number of samples for maximal error amounting to 5 % and confidence interval amounting to 95 % is calculated.

Average consumption value (μ) for category is ratio of sum of all category members and number of members in category [9–11]:

$$\mu = \frac{\sum_{i=1}^{n} P_i}{n}. \tag{5}$$

The standard deviation in statistics is an absolute measure of dispersion in the basic group. It tells us how much members together deviate from the arithmetic mean of the set, and in this case it is:

$$\sigma = \sqrt{\frac{1}{n}\sum_{i=1}^{n}(P_i - P_{avg})^2}. \tag{6}$$

The number of samples for each category is calculated according to the formula:

$$n = \left(\frac{\sigma}{\mu}\right)^2 \frac{z^2}{r^2}, \tag{7}$$

where is:

μ average consumption value (kWh),
σ standard deviation of consumption (kWh),
r maximal allowed error,
z standard normal variable (for confidence interval 95 % the amount of this coefficient is 1.96) and
n sample size.

3 Result and Discussion

Figures 1, 2, 3, 4, 5, 6 and 7 and Tables 2, 3, 4, 5, 5, 6, 7 and 8 show the results of analysis of available data, and based on them characteristic load curves and forward-defined coefficients are determined. The annual load curve of PC Roads of

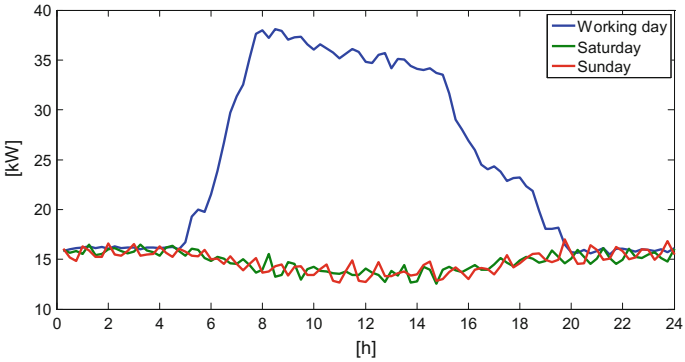

Fig. 1 The annual load curve PC Roads of FB&H for administrative building category (10 kV)

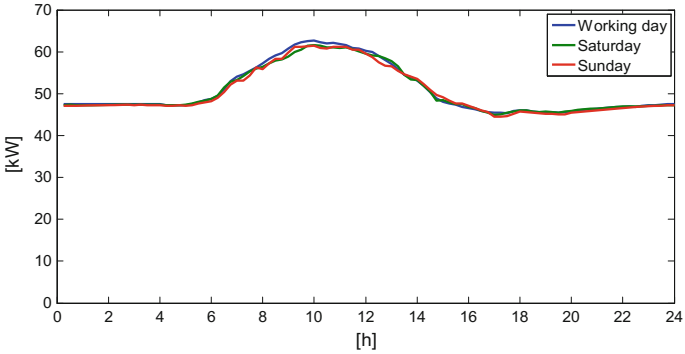

Fig. 2 The annual load curve PC Roads of FB&H for tunnels category (10 kV)

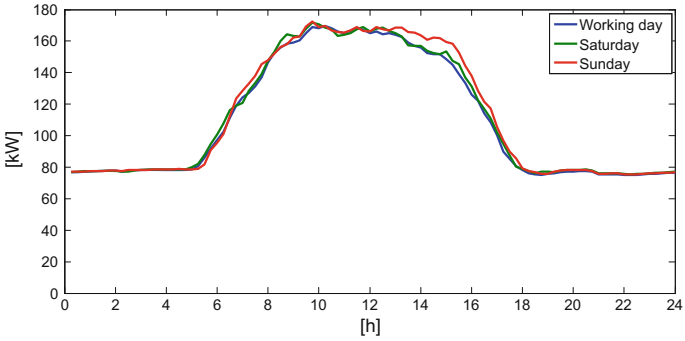

Fig. 3 The annual load curve PC Roads of FB&H for tunnels category (0.4 kV)

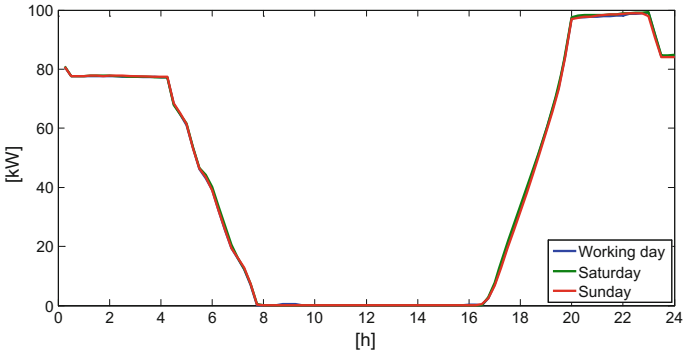

Fig. 4 The annual load curve PC Roads of FB&H for road lights category

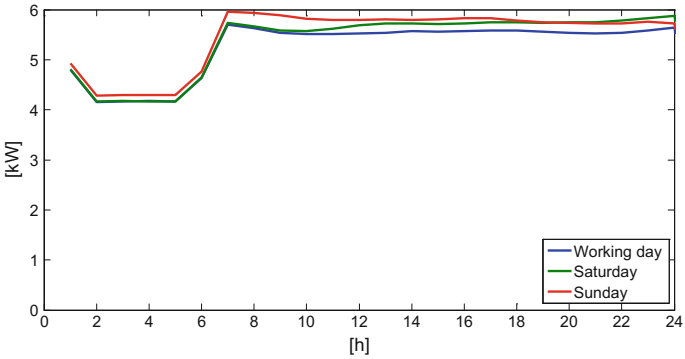

Fig. 5 The annual load curve PC Roads of FB&H for traffic lights category

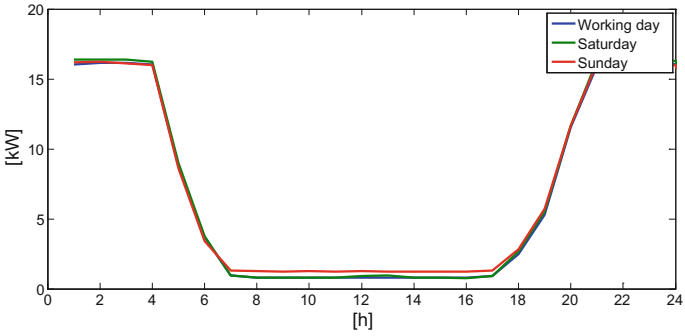

Fig. 6 The annual load curve PC Roads of FB&H for lightings and traffic lights category

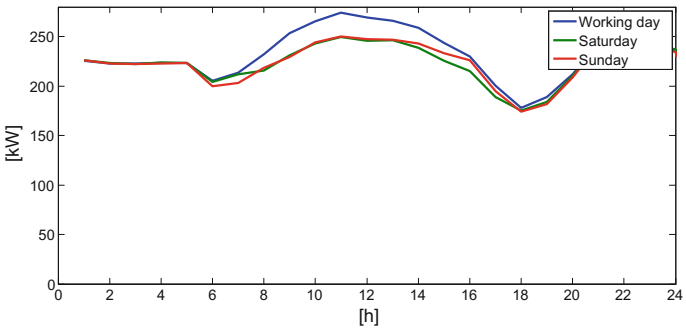

Fig. 7 The annual load curve PC Roads of FB&H

Table 2 Characteristic parameters of load curve for administrative building category (10 kV)

	P_{max} (kW)	P_{min} (kW)	P_{avs} (kW)	P_{avu} (kW)
Working day	38.113	15.502	24.671	21.839
Saturday	16.486	12.559	14.756	
Sunday	16.981	12.646	14.758	
	m	CF	POF	CPF
	0.5730	0.6944	0.9220	0.1282

Table 3 Characteristic parameters of load curve for tunnels category (10 kV)

	P_{max} (kW)	P_{min} (kW)	P_{avs} (kW)	P_{avu} (kW)
Working day	62.672	45.299	50.742	50.655
Saturday	61.587	44.949	50.519	
Sunday	61.407	44.515	50.354	
	m	CF	POF	CPF
	0.8083	0.6944	0.9869	0.2259

Table 4 Characteristic parameters of load curve for tunnels category (0.4 kV)

	P_{max} (kW)	P_{min} (kW)	P_{avs} (kW)	P_{avu} (kW)
Working day	169.76	74.885	110.22	110.73
Saturday	171.62	75.340	111.39	
Sunday	172.45	75.363	112.63	
	m	CF	POF	CPF
	0.6421	0.6944	0.9580	0.6025

Table 5 Characteristic parameters of load curve for road lights category

	P_{max} (kW)	P_{min} (kW)	P_{avs} (kW)	P_{avu} (kW)
Working day	99.168		41.182	41.212
Saturday	99.249	0	41.443	
Sunday	99.004	0	41.133	
	m	CF	POF	CPF
	0.4152	0.6944	0	0

Table 6 Characteristic parameters of load curve for traffic lights category

	P_{max} (kW)	P_{min} (kW)	P_{avs} (kW)	P_{avu} (kW)
Working day	5.9595	4.2878	5264	5310
Saturday	5.8777	4.1648	5379	
Sunday	5.7021	4.1593	5472	
	m		POF	CPF
	0.8910	0.6944	0.9263	0.0190

Table 7 Characteristic parameters of load curve for lightings and traffic lights category

		P_{max} (kW)	P_{min} (kW)	P_{avs} (kW)
Working day	16.147	0.7818	7.0481	7.1019
Saturday	16.405	0.7714	7.1883	
Sunday	16.252	1.2160	7.2846	
	m	CF	POF	CPF
	0.4329	0.6944	0.0481	0.0029

Table 8 Characteristic parameters of load curve PC Roads of FB&H

	P_{max} (kW)	P_{min} (kW)	P_{avs} (kW)	P_{avu} (kW)
Working day	274.17	178.07	232.14	229.815
Saturday	249.47	175.18	223.86	
Sunday	250.39	174.10	224.09	
	m	CF	POF	CPF
	0.8382	0.6944	1	1

FB&H for the administrative building category (10 kV) is shown in Fig. 1. It is clear that the characteristic curves for the non-working days are almost identical, while for the working days there are significant differences, the values are significantly higher during working hours (7–16 h). This is expected considering normal work activities of employees and involvement of consumers within the building during working hours.

The annual load curve PC Roads of FB&H for tunnels category (10 kV) and annual load curve PC Roads of FB&H for tunnels category (0.4 kV) are shown on Figs. 2 and 3. It is clear from these figures, that curves for all days during month/year are almost identical. It is expected considering fact that electric energy is constantly used in tunnels, and consumption depends on (defined) working modes. It is also clear that this consumption is intensified during day.

Also, expected values and diagrams are obtained for road lights, traffic lights and lightings & traffic lights categories (economy mode after 00:00 h). Load diagrams for these categories are shown on Figs. 4, 5 and 6. Tables 5, 6 and 7 provide parameters of shown diagrams for these three categories.

Summary characteristics for PC Roads of FB&H are shown on Fig. 7, where consumption during characteristic days can be observed clearly. It is slightly higher for the working days as a result of consumption in administrative building. Table 8. shows characteristic parameters of total load curve. The sum of non-simultaneous maximal loads of indentified categories amounts to 394.8517 kW.

4 Conclusion

Clear identification of characteristic load curves can help with demystifying own consumption, a clear insight into the characteristics of own consumers (as it is shown in this study on the examples of tunnels, lightings, etc.), and a clear and precise definition of the requirements for the preparation of documents for the electricity supply.

Also, these load curves can help potential suppliers for assessments and planning of electric energy consumption for its future customers, thus the very process of procurement of electricity and the future relations between the supplier and the customers can become a lot easier. Creation of load curves PC Roads of FB&H represents clear consequences of developing the electricity market in B&H and systematic approach to this issue in preparation for a future electricity supply on the open market.

References

1. Weber C (2005) Uncertainty in the electric power industry: methods and models for decision support. Springer Science, Berlin
2. Philipson L, Willis HL (2006) Understanding electric utilities and de-regulation, Second edition. CRC Press, USA

3. Harris C (2006) Electricity markets: pricing, structures and economics. Wiley, New York
4. Tešnjak S, Banovac E, Kuzle I (2009) Tržište električne energije, Graphis
5. Bommel W (2015) Road lighting: fundamentals, technology and application. Springer, Berlin
6. USAID-REAP (2011) Smjernica za izradu dijagrama opterećenja kupaca električne energije, regulatory and energy assistance
7. Public Enterprise Elektroprivreda B&H, Izvještaj o završenom ciklusu mjerenja za potrebu izrade krive opterećenja, 2015
8. Public Enterprise Elektroprivreda HZHB, Izviješće o izradi krivulje opterećenja, 2015
9. Wasserman L (2013) All of statistics: a concise course in statistical interference. Springer, Berlin
10. Gupta SC (2013) Fundamentals of statistics, seventh revised & enlarged edition
11. Devore JL (2015) Probability and statistics for engineering and the sciences, 9th edition. Brooks Cole, USA

Standardization in Bosnia and Herzegovina—Today's Approaches and Future Challenges

Mirjana Šućur and Dragan Ćućilo

Abstract The BAS Institute for standardization of Bosnia and Herzegovina (BAS) is the national (state) standardization body established under the Law on the Establishment of the Institute for Standardization of Bosnia and Herzegovina ("Official Gazette of BiH", No. 44/04) and the Law on Standardization of Bosnia and Herzegovina ("Official Gazette of BiH", No. 19/01). Institute is responsible for the preparation, adoption and publication of national standards, in accordance with the objectives and principles underlying BiH national standardization. In addition to the standardization activities, the Institute works on conformity assessment in the field of explosion protection in potentially explosive areas. These tasks are carried out by ExCommission whose secretary general is permanently employed at the Institute. The Institute was established and an information center. The Institute is engaged in the sale of standards as well. Within its jurisdiction, Institute is continually accomplishing its goals and objectives and actively participates in the representation of Bosnia and Herzegovina in the European and international standardization organizations. In this paper we will look at the importance of the process of preparing, adopting and publishing standards and other standardization documents, participate in the work of international and European committee/subcommittee.

1 Introduction

It is unthinkable in today's modern world that after finishing school engineers and other highly educated people have no knowledge of standards and standardization. In terms of educational needs, it is essential that the appropriate groups gain knowledge required for their specific professional function (e.g. developers, designers, production control engineers and/or production management engineers,

M. Šućur (✉) · D. Ćućilo
Institute for Standardization of BiH, Vojvode Radomira Putnika 34,
71123 Istočno Sarajevo, Bosnia and Herzegovina
e-mail: mirjana.sucur@bas.gov.ba

M. Hadžikadić and S. Avdaković (eds.), *Advanced Technologies, Systems, and Applications*, Lecture Notes in Networks and Systems 3,
DOI 10.1007/978-3-319-47295-9_8

process analysts, inspectors, etc.). Managers should also have a general knowledge on standards, especially in the areas of business strategy, regulations, social responsibility and sustainable development. It is also necessary to raise awareness on standardization as well as to gain knowledge on how standards can be used as a management tool. This particularly applies to the effects of the introduction and implementation of standards in all kinds of organizations (manufacturing companies, service companies, Research and Development centers, regulators etc.), as well as positioning products in the global market.

Since standards have a significant impact on almost all areas of life and business, learning about standards and standardization is a longstanding practice in developed countries. Academia offer different programs/courses covering the issues in the field of standardization, which are suitable for different professional orientations. Even less developed countries are paying more attention to this area. In a large number of developing countries standardization is included in a formal academic courses. Some of these countries even have special institutions for the training of students at different levels and in different areas of standardization (China, South Korea). In addition, the dialogue between academic institutions and national standardization bodies is necessary as well as the active involvement of academic institutions in the process of adoption of standards. The reasons are manifold, and the benefits are mutual, since:

- standards are the collective knowledge crystallized through consensus and as such can be used as a pedagogical device.
- nature, role and importance of standards in technology, trade, marketing and legal issues is, in itself, a topic that can be included in the curricula of various universities and business and law schools.
- standards can also be a subject of academic studies and research to explore the multiple links between the standards and innovation, international trade, business strategy, public welfare and sustainable development.
- standards also support management processes in academic institutions and their infrastructure.

2 International and European Organizations for Standardization in the Field of Electrical Engineering

IEC (*International Electrotechnical Commission*)
International Electrotechnical Commission IEC is one of the oldest Standards Organization which is a global non-profit organization that prepares and publishes international standards for all electrical, electronic and related technologies. IEC was founded in 1906 in London based on a resolution of the delegates of the International Congress of Electrical Engineering, held in St. Louis, USA, in 1904.

Members of IEC are the National Committees for electrical engineering from the participating countries. Technical work on the adoption of standards is carried out through Technical Committees (TCs) and Subcommittees (SCs). IEC covers all fields of electrotechnology, including electronics, magnetics and electromagnetics, electroacoustics, multimedia, telecommunications, energy producing and distribution, as well as related general areas including terminology and symbols, electromagnetic compatibility, measurement and performance, dependability, design and development, safety and the environment.

ISO (*International Organization for Standardization*)
International Organization for Standardization—ISO develops and publishes the largest number of international standards in the world. ISO was founded in 1947 by joining two organizations: ISA (International Federation of the National Standardizing Associations), which was founded in New York in 1926 and UNSC (United Nations Coordinating Committee), established in 1944.

ITU (*International Telecommunication Union*)
ITU is the leading United Nations agency for information and communication technology issues. It is the focal point for governments and the private sector in developing networks and services. For 145 years, ITU has coordinated the shared global use of the radio spectrum, promoted international cooperation in assigning satellite orbits, worked to improve telecommunication infrastructure in the developing world, established the worldwide standards that foster seamless interconnection of a vast range of communications systems and addressed the global challenges of our times, such as mitigating the impact of natural disasters and climate change and strengthening cybersecurity. ITU organizes worldwide and regional exhibitions and forums, such as ITU Telecom World, bringing together the most influential representatives of government, the telecommunications and ICT industries to exchange ideas, knowledge and technology for the benefit of mankind, and in particular the developing world.

CEN (*European Committee for Standardization*)
European Committee for Standardization—CEN (Comité Européen de Normalisation, Europäisches Komitee für Normung) is a European non-profit organization, based in Brussels, set up by under Belgian law. It was founded in 1961. CEN is the only recognized European organization responsible for planning, developing and adopting European standards in all spheres of economic activity, except for electrical engineering and telecommunications. CEN is business catalyst in Europe, removing trade barriers for European industry and consumers. Its mission is to foster the European economy in global trading, the welfare of all European citizens and the environment. Through its services CEN provides a platform for the development of European standards and other technical specifications. Of all European organizations CEN has been issuing the largest number of European standards and technical specifications.

CENELEC (*European Committee for Electrotechnical Standardization*)
European Committee for Electrotechnical Standardization—CENELEC was founded in 1973 as a result of the merger of two previous European organizations: CENELCOM (European Committee for the Coordination of Electrotechnical Standards in the Common Market) and CENEL (Comité Européen de Coordination des Normes Electriques). Today CENELEC is a non-profit technical organization set up by under Belgian law, based in Brussels.

The work of CENELEC is directed to:

- Satisfy the needs of the European industry and other stakeholders in the market place in the areas of standardisation and conformity assessment in the fields of electricity, electronics and associated technologies.
- Lead the improvement of all aspects of product quality, product safety, service quality and service safety in the fields of electricity, electronics and associated technologies, including protection of the environment, accessibility and innovation, and so to contribute to the welfare of society.
- Support IEC, the International Electrotechnical Commission, in achieving its mission on the global market.

CENELEC prepares standards, technical specifications, harmonized and other standardization documents for electrical and electronic components, devices, systems etc., as well as services in the field of electrical engineering, in order to regulate these areas and eliminate barriers to trade, create new markets, and reduce overall costs of products.

ETSI (*European Telecommunications Standards Institute*)
European Telecommunications Standards Institute—ETSI is an independent, non-profit organization, officially recognized by the European Union as a European Standards Organization in the field of information and communication technologies. Unlike CEN and CENELEC its membership is not limited to National Standards Bodies and National Committees. ETSI unites manufacturers, network operators, national administrations (usually the national standards bodies), service providers, research bodies, consumer groups and consultancies.

3 History of Standardization in Bosnia and Herzegovina

3.1 Standardization in Socialist Federal Republic of Yugoslavia

1977 Standardization Act (Official Gazette of SFRY, No. 38/77, 37/88, 23/91, 55/91)

After the disintegration of the former Yugoslavia and in accordance to the "Decree with the force of Law on adoption and application of federal laws which

shall be applied in Bosnia and Herzegovina as republic laws" Bosnia and Herzegovina has adopted

1992 Standardization Act—Revised text (Official Gazette of SFRY, No. 80/91).

3.2 Standardization in Bosnia and Herzegovina

(1992–1995)—Institute for Standardization, Metrology and Patents of Bosnia and Herzegovina (Official Gazette of RBiH, No. 18/92).

1996—Law on Administration and Administrative Organs in BiH (Official Gazette of RBiH, No. 17/96) establishes the Institute of Standardization, Metrology and Patents of Bosnia and Herzegovina.

In November 2000, the former High Representative Wolfgang Petrich issued a DECISION on future organization of standards, metrology, accreditation and intellectual property rights in Bosnia and Herzegovina (Official Gazette, No. 29/00), and in 2001, by passing the Law on the Establishment of the Institute for Standardization, Metrology and Intellectual Property of Bosnia and Herzegovina and the Law on Standardization of Bosnia and Herzegovina (BiH Official Gazette, No. 19/01):

2001—Institute for Standards, Metrology and Intellectual Property of Bosnia and Herzegovina (BASMP) was established—an independent institution as a state administration body.

2004—The Law on the Establishment of the Institute for Standardization of Bosnia and Herzegovina (BiH Official Gazette, No. 44/04)

According to the Law on Standardization of Bosnia and Herzegovina, in September 2004, the Institute for Standardization of Bosnia and Herzegovina (BAS) was established by dividing the Institute for Standards, Metrology and Intellectual Property of Bosnia and Herzegovina (BASMP). The final division of BASMP into three institutes, three independent administrative organizations, namely the Institute for Standardization, Institute of Metrology and the Institute for Intellectual Property was completed on 1 January 2007.

From 1 January 2007, the Institute for Standardization of Bosnia and Herzegovina operates as an independent state administrative organization and represents states national standardization body responsible to the Council of Ministers of Bosnia and Herzegovina [1].

4 Standardization of Bosnia and Herzegovina

4.1 What Is Standardization?

Standardization is defined as an activity of establishing, with regard to actual or potential problems, provisions for common and repeated use, aimed at the achievement of the optimum degree of order in a given context. The main characteristic of modern standardization is use of voluntary standards. Important benefits of standardization are improvement of suitability of products, processes and services for their intended purposes, prevention of barriers to trade and facilitation of technological cooperation. Application of standards is voluntary, unless their use is mandated by legislation/regulation or called up in a contract—then they become mandatory. The purpose of the standard is to set out clear and unambiguous provisions which facilitate trade and communication. To this end, a standard needs to be as detailed as necessary within the limits of its scope, take full account of current technology and science, be prepared with users and consumers acceptance in mind and be comprehensible to qualified users have not been directly involved in its drafting [2].

4.2 National Standardization in Bosnia and Herzegovina

The Institute for Standardization of Bosnia and Herzegovina was established according to the Law on the Establishment of the Institute for Standardization of Bosnia and Herzegovina ("Official Gazette", No. 44/04) as an independent state administrative organization for activities in standardization area. According to this Law, the Institute for Standardization of Bosnia and Herzegovina has taken over activities in the standardization area that were previously established according to the Law on the Establishment of the Institute for Standardization, Metrology and Intellectual Property ("Official Gazette", No. 29/00).

According to the Law on Establishing the Institute for Standardization ("Official Gazette", No. 44/04), the Institute for Standardization of BiH is a national scientific-professional institution responsible, in the field of standardization, to:

- propose standardization strategy in Bosnia and Herzegovina,
- prepare and publish BiH standards,
- represent Bosnia and Herzegovina in international and European organizations for standardization,
- perform tasks arising from international agreements and membership in these organizations,
- participate in the preparation of technical regulations,
- develop and establish an information system on standards and other related documents,
- promulgate BiH standards (BAS),

- organize and conduct specialized training of personnel in the field of standardization,
- become engaged in publishing activity in the field of standardization,
- participate in establishing and maintaining a system of certification and homologation in accordance with the European model,
- represent Bosnia and Herzegovina in European and international organizations for conformity assessment,
- organize education in the area of conformity assessment.

The Institute for Standardization of BiH is responsible for the adoption of BAS standards in Bosnia and Herzegovina. Aims of BiH national standardization are:

- facilitating international trade with prevention and elimination of barriers resulting from unfounded differences existing when conducting business at national level;
- increasing the level of safety, health and life protection, and environmental safety;
- improving purposeful exploitation of work, materials and energy in production processes;
- improving production efficiency along with management of diversity, conformity and interchangeability;
- improving the quality of products, processes and services, with establishing their characteristics enabling them to fulfill defined requirements or to serve a defined purpose.

The Institute for Standardization is a: Full member of:

- International Organization for Standardization—ISO (www.iso.org) since 1997 and
- European Institute for Telecommunications Standards—ETSI (www.etsi.org) since 1997.
- Associate member of: International Electrotechnical Commission—IEC (www.iec.ch) since 1997.
- European Committee for Electrotechnical Standardization—CENELEC (www.cenelec.eu) since 1999.
- European Committee for Standardization—CEN (www.cen.eu) since 2008 [2].

4.3 Participation in the Work of International and European Organizations for Standardization

The rights and obligations of the Institute in international and European organizations for standardization are a result of the contractual relationship and its membership status in these organizations. In accordance with its membership status, the Institute has the right to participate in the development of international and

European standards and other standardization documents and to vote at certain stages of its development. Delegates and delegations of the Institute have the right to participate in meetings of international and European TCs and SCs. The Institute has right to propose candidates for membership in the international and European WGs (working groups).

In addition, depending on its capabilities, the Institute can host meetings of international and European technical working bodies in Bosnia and Herzegovina, and hold the secretariats of international and European TCs and/or SCs.

As a full member of ISO and ETSI, the Institute has direct access to the working documents of all technical committees (TCs) and subcommittees (SCs). As an associate member of IEC, CENELEC and CEN, the Institute monitors their work as an observer (O-member), and therefore has the right but is not obliged to submit comments on the submitted documents.

Currently, the Institute is a P-member (permanent member) of the international subcommittee ISO/TC 34/SC 12, Sensory analysis, and O-member in 98 international committees/subcommittees, as well as O-member in 91 European Committees for Standardization.

4.4 Activities on the Adoption of Standards

Standardization work is carried out through the technical working bodies, technical committees (BAS/TCs) and working groups (WGs). Over 600 experts from all over BiH are involved in work of 50 technical committees with the possibility of permanently extending the scope of work, or accepting proposals for the establishment of new technical committees for the areas that are not covered by existing work. All stakeholders have the opportunity to submit their proposal to the Institute for the establishment of a Technical Committee in a new work area and the possibility to become involved in the work of the newly established and existing committees. Figure 1 shows the structure of stakeholders in the work of the technical committees as of 31 December 2015 [1]. International and European standards and other standardization documents have been adopted into BiH standardization system as well as national standards of other countries that have signed cooperation agreement with the Institute.

Adoption procedure is carried out in accordance with the Rules of Procedure for preparation, adoption and publication of BiH standards ("Official Gazette". No. 49/09) the Internal rules for Standardization (http://www.bas.gov.ba/button_91.html) that comply with the ISO/IEC Directives—Part 1 and 2; CEN/CENELEC Internal Regulations—Part 2 and 3; ISO/IEC Guide 21-1 and ISO/IEC Guide 21-2, and the Code of Good Practice for Standardization.

Methods for adoption of standards are:

- endorsement (pr);
- republication (ko);
- translation (pv).

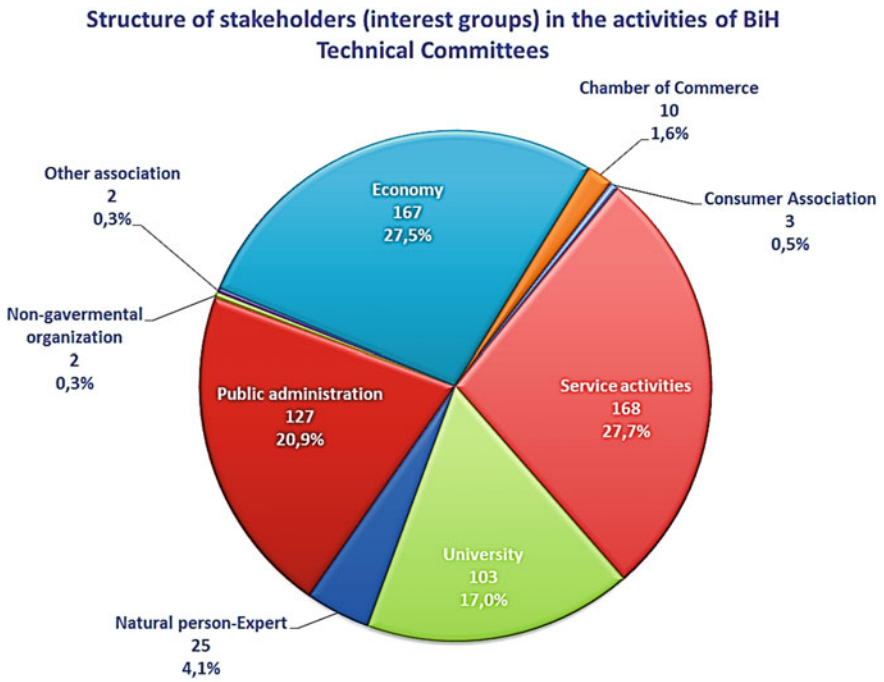

Fig. 1 Structure of stakeholders in the work of the technical committee

Endorsement method is one of the simplest methods of adoption because it does not require a reprint of the text of international or European standard.

Republication method is an adoption of international or European standards (including amendments and technical corrigenda) and its publication with BAS cover page.

Elements of BAS republication are:

- National title page of BAS standard;
- National foreword;
- National annexes at the end of the text of an adopted standard

Translation method

If BAS standard is a translation of international or European standard and has a BAS identifier, adopted international or European standard becomes a recognizable part of BiH standardization.

BAS standard, which is a translation of an international or European standard can be published as monolingual or multilingual edition. In both cases, BAS standard includes the following elements:

National title page of BAS standard;

- National foreword;
- Translation of international or European standard;
- National annexes at the end of the text of an adopted standard.

As of 31 December 2015, 236 standards have been adopted by translation method.

Original BAS standard is being developed by the Institute in the event that international standard does not exist in particular area or the existing international standard is unsuitable. Since the original standards may represent a technical barrier to trade, its development is limited to cases where there are few international or European standards for the particular standardization subject. As of 31 December 2015 the Institute has published 43 original standards.

BiH standards are developed by Technical Committees of the Institute for Standardization (BAS/TCs) in six stages:

Stage 1: Proposal stage
Stage 2: Preparatory stage
Stage 3: Committee stage
Stage 4: Enquiry stage
Stage 5: Approval stage
Stage 6: Publication stage.

For more details about the stages of the development of national standards see http://www.bas.gov.ba/images/upload/pdf/institut/Faze%20izrade%20standarda/bs_Faze%20izrade%20bosanskohercegovackih%20standarda_2016_bs.pdf (Table 1) [3].

Table 1 Overview of adopted national standards and other standardization documents as of 31 December 2015 [1]

Type of document	No. of adopted BAS standards and other standardization documents
BAS standards and other standardization documents	29,740
BAS standards and amendments	27,825
Other standardization documents	1915
European standards and amendments	20,512
Other European standardization documents	1075
International standards and amendments	8177
Other international standardization documents	843
Other national standards	165
Original BAS standards	43

4.5 An Example of Application of Bosnia and Herzegovina (BAS) Standards in Bosnia and Herzegovina

In the process of public procurement of Elektroprivreda BiH (Electric Utility of BiH) "Procurement of the substitution of ISAS system by TS 110/20/10 kV" general technical requirements that all available equipment must fulfill have been clearly stipulated. The subject of the public procurement of Elektroprivreda BiH is the reconstruction of the Hadžići transformer station TS 110/20/10 kV in the following extent: writing project documentation, procurement of protection and management equipment, SCADA system equipment, personal consumption equipment, storage batteries, electrical equipment erection, small-scale construction works, parametrization, functional performance testing and start-up of the equipment, all in accordance with the requirements of this tender documentation. Also, there are general technical requirements that all available equipment must satisfy and that should be complied with in the preparation of the Offer, during designing, equipment erection as well as parametrization and testing. The standards for designing, production, erection and performance testing of electrical equipment are the following:

- General standards: (BAS IEC 60038, BAS IEC 60050, BAS IEC 60445, BAS IEC 60617, BAS IEC 60664, BAS IEC 61082)
- Standards related to type testing: (BAS EN ISO/IEC 17025, BAS IEC 60068, BAS IEC 60255, BAS IEC 61000, BAS IEC 61850).

5 Conclusion

It should be emphasized as the final aim of the national strategy the Institute's practical endeavours in establishing effective and efficacious system of national standardization which would permanently enable that in due time every demand of the founder and members of the Institute, other interested parties and, generally, of the wider social community in our country be successfully complied with, and that necessary conditions be maintained for Bosnia and Herzegovina to join the European Union as quickly as possible. It is important to point out that the harmonization of Bosnia and Herzegovina standards and related documents with current European and international standards would promote development and competitiveness of Bosnia and Herzegovina's economy amidst growing international economic integration and necessity of sustainable growth, that is, it would help to eliminate the existing and prevent possible technical obstacles in economy.

In order to additionally upgrade the application of standards, it is necessary to devise financial modules which would significantly increase the number of standards in Bosnia and Herzegovina adopted by methods of translation to one of the three official languages in Bosnia and Herzegovina, work more on the promotion of

Bosnia and Herzegovina standardization system through expert counselling, so that all public as well as private-sector companies could grasp the importance of standards and therefore facilitate their dealings by properly applying standards and other standardization documents.

Also, it is public-sector companies that should especially recognize the significance of standards and involve more actively in the process of standardization and work of experts in the technical committees of the Institute for standardization of Bosnia and Herzegovina since by doing so they would have a direct influence upon the agenda of the TC, the content of the BAS standards as well as international standards in the process of their preparation that is in conformity to valid regulations, and they would also gain access to information, get a chance to make new business contacts and exchange knowledge, receive acknowledgement of their activities if actively involved in the process of standardization and, finally, they would have the opportunity to spread the culture and raise awareness of the standardization itself.

References

1. Annual Report of the Institute for Standardization of Bosnia and Herzegovina 2015
2. Edina Tanović, STANDARDIZACIJA - Priručnik za upotrebu u visokoškolskoj nastavi i permanentnom obrazovanju u poduzećima, Sarajevo 2014. god
3. http://www.bas.gov.ba/

A New Concept in the Design and Implementation of the Grounding Transmission Lines

Meludin Veledar, Zijad Bajramović and Adnan Čaršimamović

Abstract Lightning overvoltage cause the majority of outages in electrical transmission lines, mainly through a back flashover in the transmission system insulation. Key factors in reducing the number of back flashovers are: selection of route in design power lines, grounding, and increase of withstand insulation voltage and installation of metal oxide surge arresters along the transmission line. Reduction of grounding impedance is one of the most efficient ways to prevent the occurrence of back flashovers. The main issues with grounding in Bosnia and Herzegovina and the region are the wide range of specific resistivity in different soil types (10–10,000 Ωm), relatively high isokeraunic levels and high voltage lightning currents (in excess of 150 kA). The paper outlines the main features of own experimental research for reducing back flashovers by lightning current.

1 Introduction

During the 1970s and 1980s extensive research was carried out of the contribution of conductive materials in which grounding loops are backfilled [1], with the aim to reduce grounding impedance. Bentonite and red mud are mainly use as backfill material for grounding improvement. As transmission towers of 110 kV and higher voltages in our region are constructed in concrete foundations which may be used as base grounding, a study of the concrete samples under various conditions and the tower foundation as the grounding is performed. Many countries specifically monitor the proportion of reinforced concrete foundation in order to achieve the

M. Veledar · Z. Bajramović · A. Čaršimamović (✉)
Independent System Operator in B & H, Hamdije Čemerlića 2,
71000 Sarajevo, Bosnia and Herzegovina
e-mail: a.carsimamovic@nosbih.ba

M. Veledar
e-mail: meludin.veledar@gmail.com

Z. Bajramović
e-mail: z.bajramovic@elektroprivreda.ba

M. Hadžikadić and S. Avdaković (eds.), *Advanced Technologies, Systems, and Applications*, Lecture Notes in Networks and Systems 3,
DOI 10.1007/978-3-319-47295-9_9

appropriate values of grounding resistance and to ensure normal operation of the transmission line. Changes of steady-state resistance were monitored over an extended period of time. Intention of research, to analyze steady-state resistance of concrete, included application of grounding Type “A”. Positive results of grounding Type “A” initiated an experimental investigation of its impulse characteristics in 2012. All of the above, using bentonite, analysis taking into account contributions of concrete foundation and application of grounding Type “A”, have enabled a new approach in design and realization of transmission towers grounding. Better approaches to grounding definitely get bigger contribution to reduce outages in electrical transmission lines. as in abstract noted, in recent times application of location lighting system (LLC) may significantly improve route selection for new power lines to reduce back flashover. This paper below show more details of experimental research and their contribution to new approach for design and implementation to transmission lines grounding.

2 Bentonite

Tests of physical and chemical properties of bentonite such as water absorption and retention, possibility of mixing with other materials to achieve good resistivity of the bentonite suspension (approximately 2 Ωm) and the favourable pH factor (up to 10), and the resistance at higher temperatures, make possible the use of bentonite in improving the grounding. Bentonite powder in its raw state should contain approximately 80 % of montmorillonite which provides better swelling and better cat ion exchange. Such natural bentonite should be well crushed in order to allow better water dispersion in water solutions. The best degree of activation for such natural bentonite, in order to achieve optimal resistivity and pH value characteristics, is 3–5 % of sodium carbonate.

Bentonite as an additive for improving the properties of grounding systems may be used in the form of suspension or in powder form around the grounding. Obviously, the use of bentonite powder around the transmission system grounding greatly simplifies its use. Grounding systems with the bentonite powder must go through a stabilisation period for the bentonite powder to turn into a suspension through the effects of atmospheric precipitation. It is important to point out that the grounding system, even during this stabilisation period, shows better results when compared to an identical system constructed using the standard method and with excavated material. The expenditure of bentonite powder for grounding with bentonite suspension is 10–12 and 18 kg/m if using just powder.

The research [1, 2] established the following:

– Laboratory testing of bentonite performance under low and high temperatures, confirmed by test findings on actual grounding systems, has shown that bentonite should be buried at depths where the ground does not freeze, and that

increases in temperature resulting from short circuit currents do not result in changes of physical and chemical properties of bentonite.
– Laboratory testing of corrosive effect of bentonite on materials are in contact with it shows that corrosive effects are not significant. Visual comparison of grounding strips and samples used in field tests did not indicate any signs of corrosion. Also, exposure of PVC cables did not result in significant changes in water absorption or porosity of the insulating layer.
– Experimental testing of the effects of short circuit currents and lightning currents has shown that the physical and chemical properties of bentonite suspension remain unaffected.

Reduction in resistance of individual grounding strips and tubes using bentonite was achieved with the constant humidity not less than 50 % in the area surrounding the grounding system, low resistivity of bentonite, reduction of voltage transfer between the grounding and bentonite as well as between bentonite and the adjacent soil, which is not found in the formulas for calculating grounding resistance. Therefore, we can conclude that the reduction of grounding resistance is not a result of the changes in its geometry.

Experimental research of impulse response grounding with bentonite around grounding straps show that at currents around 2 kA impulse coefficients are not significantly different from that of the classical performance. Based on this, there is a conclusion that the reductions in steady-state resistance at power frequency current grounding with bentonite remain the same with pulse currents.

3 Concrite

In accordance with research of concrete cubes resistance, (please see below), the research of transmission towers foundations—as basic grounding—was done [3, 4]. A purpose-built experimental facility was created with grounding systems shown in Fig. 1. Changes of steady state resistance were monitored over an extended period of time for a specific Type “A” grounding system shown in Fig. 2 and its components, as well as a grid type grounding system—metal grid foundation.

Diagram of changes in steady state resistances is shown in Fig. 3. Previously conducted studies have been applied on actual transmission lines.

After analyses of the obtained results it can be concluded that the lowest grounding resistance is achieved in the grillage type grounding. No effects of protective bitumen coating on grounding resistance values were noted. Grounding resistance in grillage type grounding and the grounding strip around the tower foundation are changed proportional to the soil specific resistance. The differences between minimum and maximum resistances measured during testing are 1.5 and 1.8 respectively.

Change in resistance of the tower foundation base without grounding strips follow the same pattern, however the difference between minimum and maximum

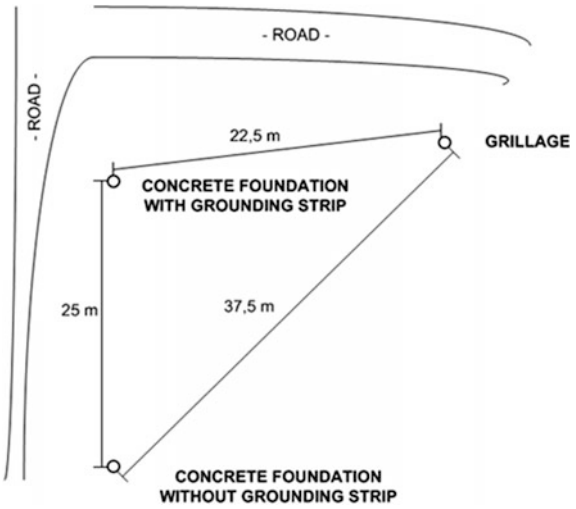

Fig. 1 Experimental facility

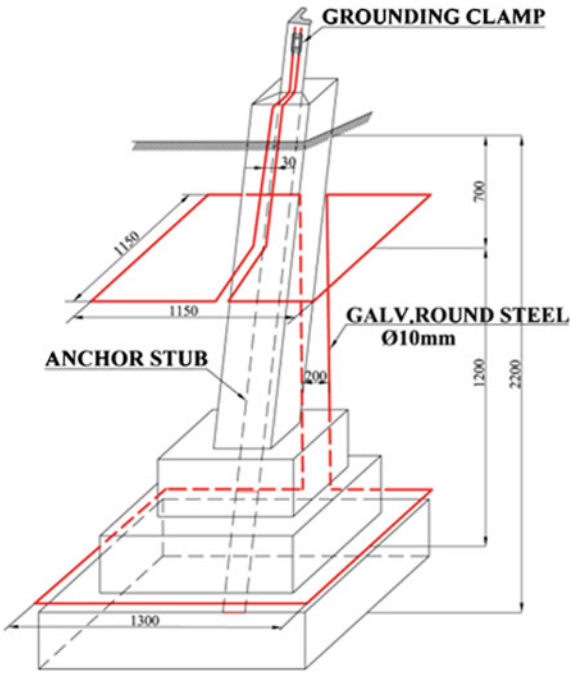

Fig. 2 Type "A" grounding system—here shown the foundation of one foot of the 110 kV tower with grounding strip around the foundation

resistance values was somewhat greater—approximately 2.5. This increase is the result of changes of the concrete resistance. Based on analysis of the entire period of measurement, it can be stated that the concrete stabilisation coefficient grew up to a value of 1.5 in the interval of 300–400 days after the construction of the foundation

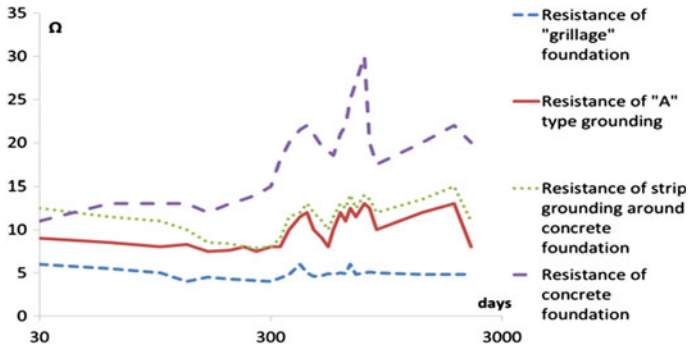

Fig. 3 Variation of steady state resistance for individual grounding systems at the experimental facility

and subsequently maintained that value with minor oscillations. Figure 3 shows that variations in steady state resistances of the grounding strip and the total resistance of Type "A" grounding system is far smaller than the resistance of the concrete foundation itself. Actually, the grounding strip greatly enhances the characteristics of the overall grounding resistance. Some international researches believe that atmospheric surges, passing through concrete in the tower foundation, diminish its mechanical properties.

This can be avoided by adding a grounding strip around the foundation. It has to be emphasised, the cost-effectiveness and simplicity of its installation around the foundation, as well as good inductive properties as a concentrated grounding solution from the aspect of its impulse characteristics. It is also necessary to mention research studies conducted in other countries [5–9] which confirm the importance of the use of concrete foundations as grounding.

In simultaneously monitoring the grounding systems at test site and at concrete samples placed in different environmental conditions [3]. Concrete samples were made of concrete with the same properties as that used in foundations of experimental grounding systems at test site.

Figure 4 shows the increase in resistance of the concrete under different environmental conditions in the first period and then tends to decrease over time. The largest increase was recorded for a concrete cube sample placed in a dry room, which is not a real situation for a grounding system.

Further analysis has shown that the sample immersed in water increased at 2.2 Ω m/day for the first 20 days, then 2.0 Ωm/day up to day 100, 0.7 Ωm/day up to 300 days, and to stabilize after 300 days. Samples placed in humid soil have increased at 0.36 Ωm/day for the first 80 days, then 0.9 Ωm/day for days 80–220, 0.04 Ωm/day for days 220–360 after which time the value settled, with only minor oscillations caused by changes in soil humidity.

According to [10, 11], after three to six months concrete will stabilise if exposed to normal humidity. Similar results were obtained through these tests, same as test carried out at test site on concrete samples and grounding foundations described in this paper.

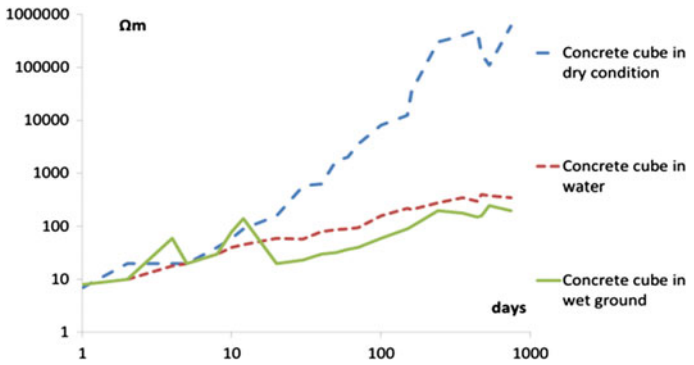

Fig. 4 Variation in resistance of concrete samples dimensions 10 × 10 × 10 cm under various conditions

4 Impulse Response of Type "A" Grounding System

The objective of this experiment was to determine the impulse characteristics of Type "A" grounding (Fig. 2). Experimental research on Type "A" grounding was carried out in 2012, at two locations [4, 12]:

- Test site shown in Fig. 1.
- Transmission tower on double 110 kV transmission line where Type "A" grounding was used on all four feet of the tower.

The diagrams in Fig. 5. show representative voltage and current diagrams in the course of measurement; Figs. 6 and 7 show characteristic details during the testing.

Experiments at test site were conducted twice, at two different times. Below are the test results of impulse response values for the grounding calculated using Zk = u(Tmu)/i(Tmi) and the impulse coefficient αk = Zk/Rs.

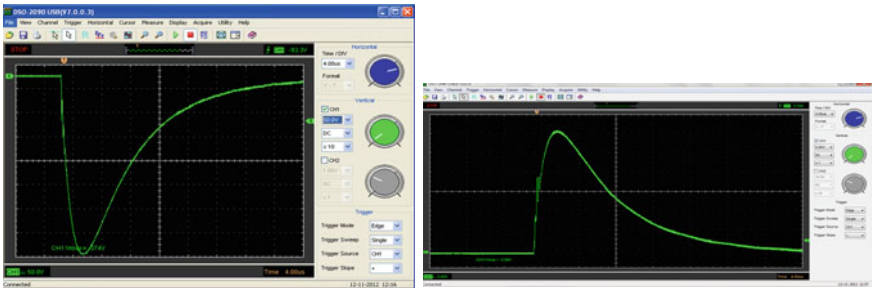

Voltage at the transmission tower grounding

Current at the transmission tower grounding

Fig. 5 Testing of complete Type "A" grounding without shield wire on the tower with single stage generator charge with voltage of 40 kV (Voltage at the transmission tower grounding current at the transmission tower grounding)

Fig. 6 Position of impulse generator during testing

Fig. 7 Connection of test voltage to the foot of the transmission tower

4.1 Experiments at Tests Site

Testing of complete Type "A" grounding (single foot) with one and two impulse generator stages—first test:

Mean impulse coefficient value 0.785 (four measurements)—single stage.
Mean impulse coefficient value 0.756 (five measurements)—two stages.
Total mean impulse coefficient value for all measurements 0.77 (nine measurements).
Testing of complete Type "A" grounding (single foot) with one and two generator stages—second test:
Mean impulse coefficient value 0.80 (four measurements)—single stage.
Mean impulse coefficient value 0.79 (four measurements)—two stages.
Total mean impulse coefficient value for all measurements 0.80 (eight measurements).

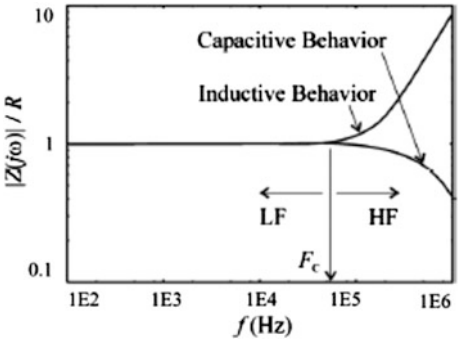

Fig. 8 Typical capacitive and inductive effect of grounding harmonic impedances in the high frequency range

4.2 Measurements at the Transmission Tower

Testing results when surge generator inject impulse current into the transmission tower foundation with complete grounding Type "A" system, when the ground wire was isolated from the tower top

Mean impulse coefficient value 0.820 (eight measurements).

Mean impulse coefficient value 0.812 (five measurements).

Total mean impulse coefficient value for all measurements 0.817 (thirteen measurements).

Impulse coefficients for the Type "A" grounding calculated from the measured values are less than 1, which confirms the fact that there exists a capacitive effect and that the inductive effect can be disregarded [13–15]. Figure 8 shows typical capacitive and inductive behaviour of grounding harmonic impedances in the high frequency range, in accordance with the literature [13].

5 Conclusion

Based on the above it can be concluded:

- Although not examined in detail, Lightning Localization System (LLS) is capable system that can efficiently and accurately locate cloud-to-ground and cloud-to-cloud lightning. Multi-annual statistics can help considerably to properly select the transmission line route from the aspect to decrees possible lightning struck to the power lines.
- Applications to increase withstand voltage of insulation and installation of metal oxide surge arresters along the transmission line significantly reduces the occurrence of back flashovers.
- The paper is mainly oriented to transmission line grounding. It is possible through these own experimental studies and world literature concluded that the use of bentonite, the contribution of the concrete construction of tower

foundation and applying grounding Type "A" can contribute to a significant reduction of resistance of transmission towers. By using the previous methods it is provided:

- Reinforced concrete foundation of transmission towers in the 110–400 kV transmission lines can be used as a sole grounding system in soils with lower resistance values (up to 300 Ωm).
- By adding the Type "A" grounding system, which does not require any further ground works, significant improvements are achieved: reduction in grounding resistance for transmission towers, no need to wait for the concrete to go through the stabilisation process as it is necessary when using only concrete tower footing, and substantial reduction of stress experienced by concrete foundations when exposed to lightning strikes.

Measurement of Type "A" grounding resistance for every tower, followed by a simple calculation, provides a value for equivalent resistance of each location. This primarily serves to test whether the measured resistance satisfies the required value and also provides a basis for calculating any additional grounding requirements.

References

1. ENERGOINVEST—Research and Development Centre for Electrical Energy (1982) Study—research into the possibility of using bentonite for grounding. JUGEL, "E"—IDV and IEO, SIZ Nauke BiH, Sarajevo 1982
2. Veledar M, Timic Z, Skok S, First Z (1982) Improvement of grounding properties by using bentonite. In: Proceedings: XXIX conference CIGRE, Paris
3. Dilberovic N, Veledar M, Pavlovic M (1989) Problems in transmission line grounding. In: Proceedings: CIGRE SC-22: transmission line open conference, Sarajevo, 1989, i Yugoslav committee of the international conference on large power networks—CIGRE, XIX conference of electrical engineers of Yugoslavia, Bled
4. Study: "Measurement of Steady state and Impulse Characteristics of Grounding under Laboratory Conditions, at the Experimental Facility and On Actual Transmission Lines", Report by Energoinvest IRCE—Oct/Nov 2012
5. Fagan EJ, Lee RH (1970) The use of concrete-enclosed reinforcing rods as grounding electrodes. IEEE Trans Ind General Appl IGA-6(3):337–348
6. Wiener P (1970) A comparison of concrete encased grounding electrodes to driven ground rods. IEEE Trans Ind General Appl IGA-6(4):282–287
7. Preminger J (1975) Evaluation of concrete-encased electrodes. IEEE Trans Ind General Appl IGA-11(6):664–668
8. Thapar B, Ferrer O, Blank DA (1970) Ground resistance of concrete foundations in substation yards. IEEE Trans Power Deliv 5(1):130–136
9. Sekioka S, Yamamoto K, Yokoyama S (1995) Measurement of a concrete pole impedance with an impulse current source. In: IPST'95—international conference on power systems transients, Lisbon, 3–7 Sept 1995
10. Lejrih VF, Gendin VJA. Electrical insulation properties of concrete under different exploitation conditions. Eljektričestvo 11/68
11. Flisovski Z (1979) Reinforced foundations as natural grounding for lightning protection installations. In: IX conference of JKG, Portorož

12. Veledar M, Bajramović Z, Čaršimamović S, Savić M, Hadžić O (2014) Impulse resistance for Type "A" grounding systems on transmission towers. In: Proceedings: XLV conference CIGRE, Paris
13. Grcev L (2007) Impulse efficiency of simple grounding electrode arrangements. In: 18th international Zurich symposium on EMC, Munich
14. Lightning Protection Edited by Vernon Cooray, The Institution of Engineering and Technology, Published by The Institution of Engineering and Technology, London, United Kingdom, # 2010 The Institutions of Engineering and Technology, First published 2010
15. Working Group 01 (Lightning) of Study Committee 33 (Overvoltage and Insulation Coordination) GUIDE TO PROCEDURES FOR ESTIMATING THE LIGHTNING PERFORMANCE OF TRANSMISSION LINES, CIGRE—Oct 1991

Solar and Wind Energy: EP B&H's Experiences on the Importance of Adequate Measurements

Ajla Merzić, Elma Redzić, Alma Ademović-Tahirović and Mustafa Musić

Abstract By intensifying the promotion of wind and solar energy potential in the world, a lot international databases have been developed, mostly based on relevant satellite images or recordings. In the case of Bosnia and Herzegovina (B&H) some databases exist. Comparative analyses between Elektroprivreda B&H (EP B&H) measurements on wind and solar energy potential and data from available databases have been analysed and compared. According to performed analysis in this paper, available databases are characterized by an insufficient data resolution, as well as under/overestimations due to the relief structure and local conditions at the sites of interest. Further, some important experiences from the ongoing measurement campaign performed by EP B&H, particularly in terms of wind power on high altitude abandoned areas and harsh weather conditions have been given in this article. Only measurements and evaluations performed in accordance to applicable standards and guidelines create preconditions for techno-economic evaluations of exploiting wind and solar power, with the final aim of building wind and photovoltaic power plants in the country.

A. Merzić · E. Redzić · A. Ademović-Tahirović · M. Musić (✉)
JP Elektroprivreda BiH d.d. Sarajevo, Vilsonovo šetalište 15,
71000 Sarajevo, Bosnia and Herzegovina
e-mail: m.music@elektroprivreda.ba

A. Merzić
e-mail: a.lukac@elektroprivreda.ba

E. Redzić
e-mail: e.turkovic@elektroprivreda.ba

A. Ademović-Tahirović
e-mail: al.ademovic@elektroprivreda.ba

M. Hadžikadić and S. Avdaković (eds.), *Advanced Technologies, Systems, and Applications*, Lecture Notes in Networks and Systems 3,
DOI 10.1007/978-3-319-47295-9_10

1 Introduction

It is widely recognized that the global over-reliance on dwindling fossil fuel resources is no longer sustainable, nor cost effective. Governments are designing energy and environmental policies to minimise their exposure to volatile international fossil fuel prices and reduce carbon emissions, particularly in the electricity power sector [1]. Thus, development and integration of renewable energy sources (RESs) is being promoted and intensified. Special attention is given to the use of wind and solar energy. Their use is associated with a number of characteristics, i.e.:

- clean energy source during operation;
- sustainable development;
- yearly growth of installed capacities worldwide;
- incentive systems (feed-in systems);
- research and development initiation;
- continuous decline in prices;
- interest of private investors, etc.

1.1 Power Generation Portfolio Structure in B&H

Total electricity generation in Bosnia and Herzegovina (B&H) is based on domestic coal fired thermal power plants (TPPs) and hydro power plants (HPPs), with a minimal participation from small HPPs (sHPPs) and a negligible involvement of photovoltaic power plants (PVPPs). Depending on the hydrology, usually 60 % of the electricity in the transmission system is generated from TPPs and the rest from HPPs. Such a generation capacity structure provides some advantages like safe and reliable supply, but is further linked to a quite negative impact on the environment, high emissions of pollutants and CO_2, inflexibility of the power generation portfolio, etc.

Promoting RESs and their use in the generation portfolio is a commitment in order to contribute to sustainable development plans and environmental preservation. Use of RESs is one of the strategic objectives of the European Union (EU) energy policy, expressed through the European energy legislation and required in all strategic documents related to energy issues, i.e. EU Strategy 2020, Energy Roadmap 2050 and Power Perspectives 2030. B&H has taken over many of these obligations through the transposition into its own legislation. In force is also an incentive system that subsidizes electricity generated from RESs [2].

1.2 On the Path to Sustainable Development—Objectives and Activities of EP B&H

In B&H, 3 power companies are active in the field of power generation, distribution and supply of electricity. Among them, by the total installed capacity in power generating facilities, as well as electricity production and the number of consumers, Public Enterprise Electric Utility of B&H (EP B&H) is the largest.

Having in mind commitments, own strategic objectives in regard to RESs implementation, as well as the importance of relevant inputs on measured data, EP B&H started an intensive campaign on wind and solar energy potential measurements across the country in 2009. By now, measurements of wind potential of different duration exist from 12 locations, whereas global solar radiation data is collected from 10 locations [3], which are shown in Fig. 1. Measurements are being performed according to applicable standards, i.e. [4] and guidelines, i.e. [5] with first-class equipment. Thus, met masts for wind potential measurements are equipped with at least 2 anemometers, one wind vane and air pressure, humidity and temperature sensors. Global solar radiation is collected from measurements performed by pyranometers. The main objective is to examine the potential and obtain relevant input data for assessing the techno-economic viability of electricity produced from wind and solar energy at selected locations and make possible business decisions.

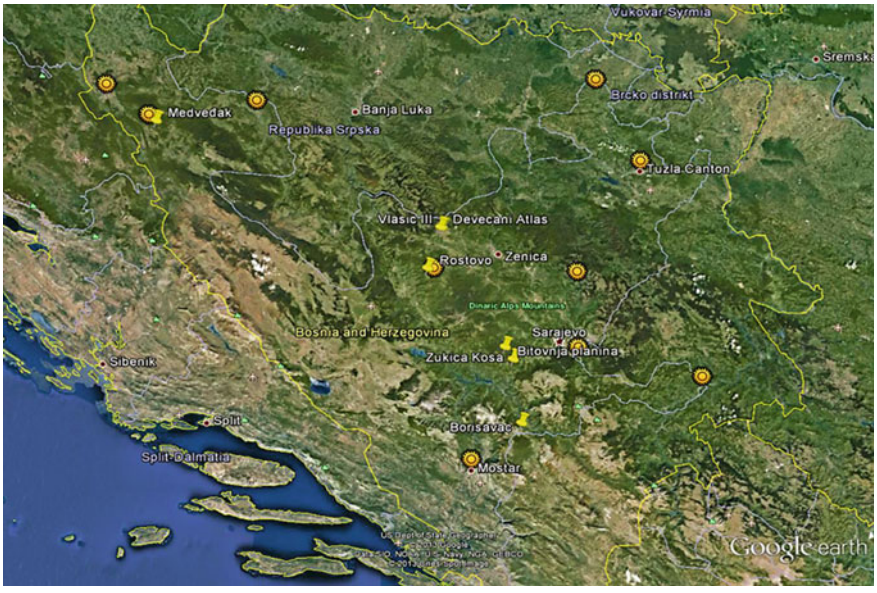

Fig. 1 Locations of EP B&H's solar and wind potential measurements

2 Solar Energy

2.1 Current Situation in B&H

In terms of solar potential, B&H disposes with 15 and 30 % more potential than Central and Northern Europe, respectively. For the purpose of generating electricity, in B&H solar energy is being used only in PVPPs. Conclusive with the end of June 2014, 19 PVPPs were in operation, with the total installed capacity of 1.55 MW and the average annual production of 2184 MWh [6]. In addition to existing facilities, the Register of RESs and cogeneration, which is created and maintained by the Federal Ministry of Energy, Mining and Industry announced further 220 projects to be constructed, with the total installed capacity of cca 37 MW.

Long-term solar irradiation measurements have not been performed in B&H so far. Parameters of the solar energy potential were mostly presented as results of assessments and estimations, according to which the annual insolation varied between 1240 kWh/m^2 in the north to 1600 kWh/m^2 in the southern regions [7, 8].

However, feasibility studies on investing into PVPPs are built on electricity generation assessments. Depending on the adequacy of the input data used, possible are significant variations in electricity generation estimations from the planned PVPPs, further leading to wrong estimates of economic parameters of the planned projects. Data used for feasibility assessments in B&H so far mostly relied on available databases. Some of those bases are PVGIS, Meteonorm, SoDa and Solargis, which mostly rest on satellite recordings, sometimes with an insufficient resolution.

2.2 Importance of Adequate Measurements—Comparative Analysis of Results Obtained from Measurements and Databases

For the purpose of this research, 9 spatially dispersed locations, where EP B&H performs measurements, have been chosen, as indicated in Fig. 1. Monthly data on solar insolation from the aforementioned 4 bases have been compared to measured results for a period of one year. Calculated are relative insolation deviations from meteorological databases in relation to the measured values on an annual level. Obtained results are presented in Fig. 2.

From results presented in Fig. 2 it could further be concluded that deviations from measured results are in a relatively acceptable range for locations such as Sanski Most, Sarajevo, Tuzla and Budozelje. Thus, average monthly insolations for these 4 locations have further been looked at into more detail. Significant deviations of the obtained monthly results with respect to annual values can be observed. Particularly interesting is the fact that during winter months, insolation results

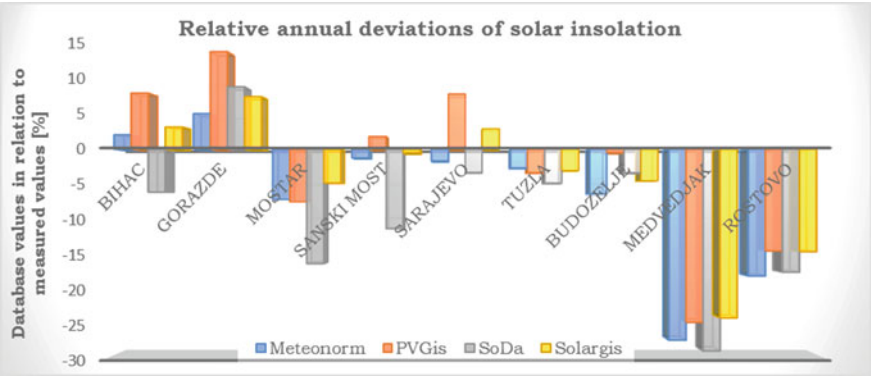

Fig. 2 Relative annual deviations of solar insolation

obtained from the 4 databases are significantly higher than the measured values, while the situation is reversed during summer months. Depending on the location and the basis considered, deviations can even reach −60 % in the winter and +20 % in the summer. Such a discrepancy during the winter period is partly a consequence of inadequate measurements due to snow and ice coverage of the pyranometer.

From these elaborations it can be concluded that relatively low annual deviations are also a consequence of an underestimation of the solar potential during the summer and an overestimation of the potential in the winter months. This fact is very important, particularly in terms of PVPP configuration planning, since irradiation data during certain months have an important impact on the selection of the optimal inclination angle that together with mutual shadings of the panels, outside temperature and panel heating/cooling significantly affect the overall electricity production of the PVPP during the year.

Considering that so far built PVPP in B&H are micro facilities with low amounts of individual installed capacities, such derogations do not cause large errors in production estimations and hence the feasibility of the plant. This is further supported by the fact that the incentive for such micro facilities in B&H is the highest. However, when planning PVPP of larger capacities, adequate inputs are essential, since overestimations in electricity production can bring into question the cost effectiveness of the project.

3 Wind Energy

3.1 Current Situation in B&H

In B&H no wind power plant (WPP) has been connected to the transmission network. Only one wind turbine is connected to the distribution grid with the

installed capacity of 300 kW. According to the Register of RESs and cogeneration, 12 WPPs are announced to be constructed resulting with a total installed capacity of over 630 MW.

Being aware of the importance of adequate input data, primarily wind potential measurements, most investors have started investigations at locations of interest. Only measurements performed in accordance with applicable standards, e.g. [4], and recommendations, i.e. [5], represent relevant input parameters for the development of wind energy projects and accordingly their feasibility assessment.

3.2 *Importance of Adequate Measurements*

As part of the project "BH Wind" [9] estimations of the wind potential in B&H have been made in year 2000, with the focus on its southern parts. It has been estimated that in this region 11 locations are very favourable and wind farms of total installed capacity of cca. 950 MW could be constructed. By now, different databases for wind potential estimations exist and can be used for indicative purposes. Example Fig. 3 shows the annual average wind speed map from the electronic Atlas for B&H (Atlas), from 1978 to 2007 [10, 11], with data based on the meteorological model MM5. These data emphasize the southern region of the country, too. But according to EP B&H's performed measurements, with some of them being presented in Fig. 1, analysed results accentuate some inland locations, as well. In this regard, even in the very beginning of researches and the selection of potential locations for met-mast installation and measurements, indicative figures

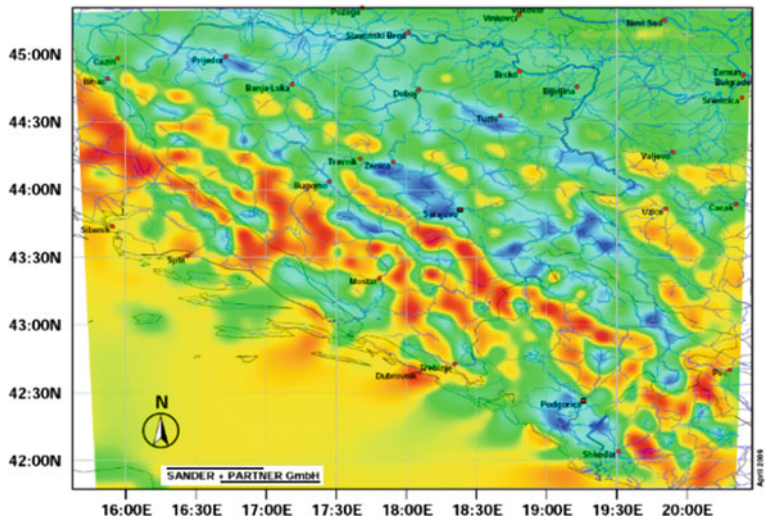

Fig. 3 Average annual wind speeds for B&H from the Atlas [10]

do not necessarily indicate to correct conclusions. Thus, other indicators and the terrain itself should be considered, too.

Long term databases like MERRA, NCAR, ERA, CFSR, etc. due to their nature, are mostly used for correlation purposes. Since the annual mean wind speed at any given site varies over the years, it is important to assess whether these values are above or below the long-term average, and address this information accordingly. For the purpose of a more detailed analysis, 2 inland sites have been selected, where EP B&H measures the wind potential and some comparisons have been made. Selected are points from the Atlas nearest to locations where measurements are being performed. Results are presented in Table 1. Both sites are at high altitudes, characterized by complex terrain and harsh weather conditions, especially emphasized for the Vlasic location. Due to such conditions, local wind flows as a consequence of differences in temperatures on the micro-location are present.

Those cannot be captured in available databases, which is why the importance of on-site measurements is being highlighted once again. For both locations a complete analysis of the measured results has been performed, including wind flow modelling, wind turbine layout optimisation and WPP annual energy production.

Taking into account measured values, Medvedjak location's specificity and long-term correlations, the estimated average wind speed at 80 m height resulted in 7.2 m/s, which is 13 % higher than the results from the Atlas.

However, measurements at high altitudes, even performed according to standards, carry considerable challenges and represent an insufficiently explored area. EP B&H has encountered challenges in this regard as anemometer icing despite sensor heating, equipment damage and even met-mast break down. This resulted with the underutilization of measured results and an increase of the uncertainty assessments.

Partial solutions are found in additional measurements by LiDAR and heated sonic sensors and anemometers, besides the standardized ones.

Table 1 Comparative results

Item	Vlasic	Medvedjak
Locality	Central part of B&H	Northwestern part of B&H
Terrain specification	Very complex	Complex
Altitude [m]	1788	970
Aver. temp. [°C]	4.2	9.6
Aver. wind speed [m/s]	7.02[a]	5.09[b]
Dominant wind direction range [°]	210–225	0–45
Aver. wind speed—Atlas [m/s]	5.18[c]	6.373
Dominant wind direction range—Atlas [°]	255–285	15–45

[a]at 92 m, [b]at 30 m, [c]at 80 m

Fig. 4 Met-mast covered in snow and ice

Difficult access during winter months represents also a big challenge, both during the measurement period (Fig. 4) as well as the WPP exploitation time in the future.

4 Conclusion

B&H disposes with significant solar and wind energy potential. The increasing integration of production units based on these resources is not in question, but given the current power generation portfolio structure in the country, it can be very challenging.

By elaborations presented within this article the importance of adequate input data has been demonstrated. Even for preliminary conclusions, data from available bases can lead to wrong assessments.

Deviations between measured solar radiation values and those from available databases may appear to be acceptable. However, by more detailed elaborations on a monthly basis, discrepancies can be very significant in the positive, as well as in the negative amount, which through mutual cancellation of the values results with annual deviations within tolerable limits.

Based on the performed analyses it has also been shown that at some locations the solar and wind energy potential presented in available meteorological databases is significantly underestimated. From the standpoint of the solar potential, such locations are e.g. Medvedjak and Rostov, located in the northwest and in the interior part of B&H, respectively, at relatively high altitudes.

EP B&H's experience on wind potential measurements at high altitudes with the aim of electricity production have shown that measurement results, especially wind speed and wind direction significantly different from those available in databases. The reason for that is mostly the local streaming that occurs during summer and winter months, due to a changing temperature field at the micro-site. These local flows significantly contribute to the overall wind potential power, even more than 10 % compared to values from available databases. In addition, these local wind flows are very often under an angle to the horizontal plane and require additional measurements using adequate equipment.

Further experiences are related to very demanding weather conditions at high altitudes, especially in the winter period. The required measuring equipment must be sufficiently robust, but at the same time measure with a low uncertainty. These two requirements are mutually opposed, thus the appropriate equipment selection is a very sensitive issue from the standpoint of data availability on the one hand and their quality on the other. This problem comes down to the optimization of the measuring equipment characteristics based on experiences in relation to the chosen site and a good compromise solution that will reconcile the two opposing conditions.

The impact of the terrain's complexity on the wind shear has also shown to be an important aspect for locations at high altitudes. At the Vlasic site, e.g. for heights over 60 m a sudden wind speed in-crease has been found, which can be explained by the minimal impact of the terrain orography on the wind flow at these altitudes.

References

1. CIGRE Working Group C1/C2/C6.18 (2013) Coping with limits for very high penetrations of renewable energy
2. Federal Ministry of Energy, Mining and Industry (2013) Law on the Use of Renewable Energy Sources and Efficient Cogeneration
3. Merzic A, Redzic E, Ademovic-Tahirovic A, Music M (2013) Wind and solar energy potential assessment in B&H based on real measurements and studies. In: The 4th international symposium on sustainable development—ISSD2013, Bosnia and Herzegovina
4. IEC 61400-12-1 (2005) Wind turbines—part 12-1, Power performance measurements of electricity producing wind turbines
5. MEASNET: Measuring Network of Wind Energy Institutes (2009) Evaluation of site-specific wind conditions, Version 1
6. Federal Ministry of Energy, Mining and Industry (2014) Register of renewable energy sources and cogeneration
7. Lukač A, Musić M, Turković E (2011) Indicative analysis of the measured solar potential results in Bosnia and Herzegovina. HRO CIGRE, Croatia

8. Federal Ministry of Energy, Mining and Industry—Experts Group (2008) Strategic plan and program of the energy sector development in the Federation of Bosnia and Herzegovina, Bosnia and Herzegovina
9. Musovic F (2005) Wind power plant projects in Bosnia and Herzegovina. Sarajevo, TKD Sahinpasic
10. Sander + Partner GmbH (2008) Electronic wind Atlas for B&H, Switzerland
11. Sander + Partner GmbH (2008) Regional re-analysis and the experts tool, Switzerland

Power Transformer Modeling from Differential Protection Aspect

Adnan Mujezinović, Maja Muftić Dedović, Nedis Dautbašić and Sead Kreso

Abstract Differential protection have the most important role in protection of power transformers from internal faults. This paper discusses the power transformer modeling from differential protection aspect. Firstly the paper describes a low frequency transient model of power transformer and parameters of given model. Cases of inrush current, short circuit in protection zone and over—excitation were simulated. Finally, in all cases the harmonic content of the differential current is analyzed and appropriate conclusions are given regarding the performance of differential protection on the basis of these analyzes.

1 Introduction

Power transformers are static electric machines whose primary role is to transform voltages and currents with propose of adjusting these values to transmission, distribution and consumption of electrical energy. Probability of occurrence of the internal fault in the power transformers is reduced to a minimum. Reason for this is that power transformers are electrical machines without any rotational elements, and are placed in the housing and dipped in quality insulating oils which have achieved excellent mechanical and dielectric properties [1]. Regardless that the probability of failure in the power transformer is very small, the occurrence of failure can cause significant economic and technical losses. Therefore proper design and setting of protection relay of the power transformers requires special attention.

A. Mujezinović (✉) · M.M. Dedović · N. Dautbašić · S. Kreso
Faculty of Electrical Engineering, University of Sarajevo, Zmaja od Bosne bb, 71000 Sarajevo, Bosnia and Herzegovina
e-mail: adnan.mujezinovic@etf.unsa.ba

M.M. Dedović
e-mail: maja.muftic-dedovic@etf.unsa.ba

N. Dautbašić
e-mail: nedis.dautbasic@etf.unsa.ba

M. Hadžikadić and S. Avdaković (eds.), *Advanced Technologies, Systems, and Applications*, Lecture Notes in Networks and Systems 3,
DOI 10.1007/978-3-319-47295-9_11

Transformer protection from internal faults must be set in such a way, that in case of failure react in a short time, turning off the power transformer from the network.

One of the fundamental protections of power transformers is a differential current protection. This protection works on the principle Kirchhoff law, by comparing the current that enters the transformer (current on the primary side of the transformer) and the current that comes out of the transformer (current on the secondary winding). Obviously, in normal operating conditions the primary and secondary current are different, therefore it is necessary to perform correction of a transformers current ratio and the current phase rotation [2].

In power substations measuring of the primary and secondary windings currents of the power transformer is done by using current transformers. Older versions of the differential protection relays of power transformers requiring additional current transformer for correction of a current ratio and phase rotation. Such embodiments are impractical, unreliable and expensive due to the need for additional transformation. Advances in computer technology and semiconductor devices have developed numerical protection that does not require additional current transformer for correction of current ratio and phase rotation of the power transformer. On numerical differential protection relay this is carried by software.

During an internal fault in the power transformer, the difference between the amplitude of the primary and secondary windings currents is substantial, and in that case it is necessary to turn off the power transformer from network with the appropriate circuit barker. From differential point of view, a similar scenario can occur during the switching on and sudden unload of power transformer, when magnetizing current flow on primary side of the power transformer and the protection relay can reacts unnecessary. Therefore, the differential protection of the power transformer must be able to distinguish between internal transformer faults, normal operation and saturation of the power transformer [3].

2 Power Transformer Model

In order to establish appropriate criteria for differential protection of transformers, it is necessary to establish an adequate model of the power transformer. For correct setting of the differential protection of power transformers analyzed phenomena such as inrush currents, various types of short-circuits and over—excitation, it is obvious that for this analysis should be used low-frequency transients transformer model proposed by CIGRE WG 33.02 [4]. Figure 1 shows a single phase transformer model used in this paper.

On Fig. 1 resistances R_1 and R_2 represents the losses in copper of primary and secondary winding of power transformer, respectively. Resistance R_{Fe} represents the power transformers core losses. Inductances L_1 and L_2 represent inductances of the primary and secondary winding of power transformer, while inductance L_μ represent ferromagnetic inductance and it is nonlinear.

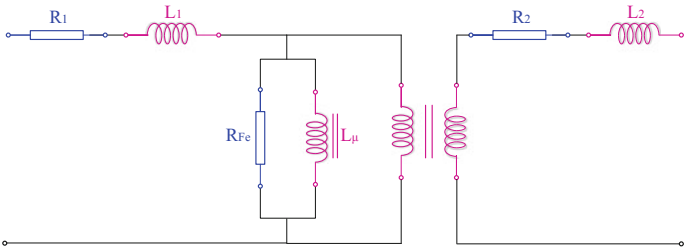

Fig. 1 Low frequency model of power transformer

All calculation in this paper was performed on the power transformer with parameters given in Table 1.

In order to conduct adequate analysis of the harmonic content of the differential current for analyze the setting of differential protection, it is necessary to properly present the nonlinear elements of the power transformer. Nonlinear characteristic of the ferromagnetic inductance is given on Fig. 2.

3 Simulation Results

In order to establish criteria for tripping of differential protection of power transformers it is necessary to perform analysis of harmonic content of the differential current in the special operating conditions of the power transformer. The criteria must be established in a way that differential protection of power transformer reacts when it comes to internal failure (failure within the protection zone), and in all other situations, regardless of the existence of differential current protection must not react. These specific situations, in which differential current occurs, and the differential protection is not supposed to react are mainly caused by nonlinear magnetization curve of the power transformer.

Also, the cause of the existence of differential current can be due to different load of current transformers on primary and secondary side of the power transformer. In such situations, one of the current transformers may result in saturation which causes differential current flowing through the differential protection. In this paper all simulation results and conducted analysis in this paper are conducted under the assumption that there is no saturation in any of the current transformers.

Table 1 Analyzed power transformer parameters [5]

Parameter	Value
Resistance R_1	0.529 (Ω)
Resistance R_2	0.144 (Ω)
Resistance R_{Fe}	5.75 (MΩ)
Inductance L_1	0.126 (H)
Inductance L_2	34.5 (mH)

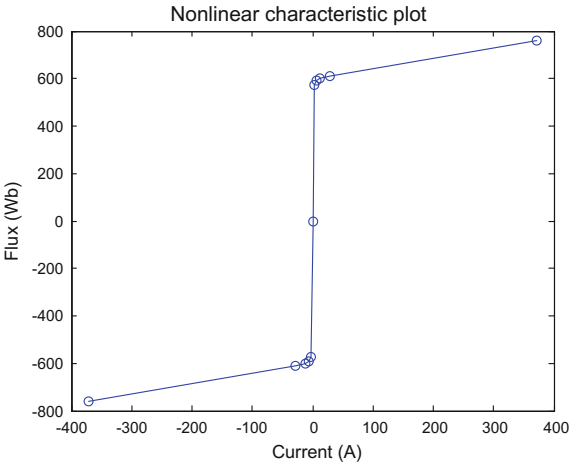

Fig. 2 Magnetizing reactance characteristics

4 Inrush Current

When power transformer is switched on, maximum value of the magnetic flux can be much higher from nominal value. In this case high inrush current can occur on primary side of power transformer [5–7] (Figs. 3 and 4).

In this case the secondary current of the power transformer is equal to zero, therefore the differential protection relay only receives current from the primary side of the power transformer. This current is typically several times higher than the current in the normal operation of the power transformer [8].

Figure 5 shows the waveform of the inrush current of the power transformer while Fig. 6 shows harmonic content of inrush current.

From Fig. 5 it is noticeable that waveform of the inrush current is highly distorted. Figure 6 gives harmonic content of inrush current from DC component to 7th harmonic, while numerical values of harmonic content for all analyzed cases are given in Table 2. From Fig. 6 it can be noted that the inrush current of power

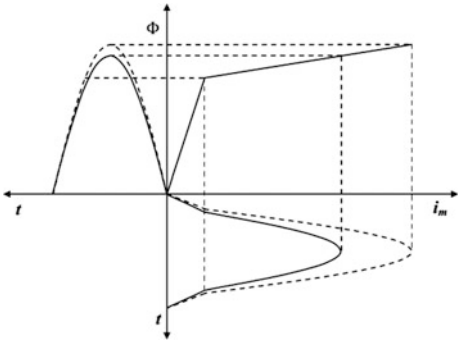

Fig. 3 The influence of magnetization curves on current waveform [7]

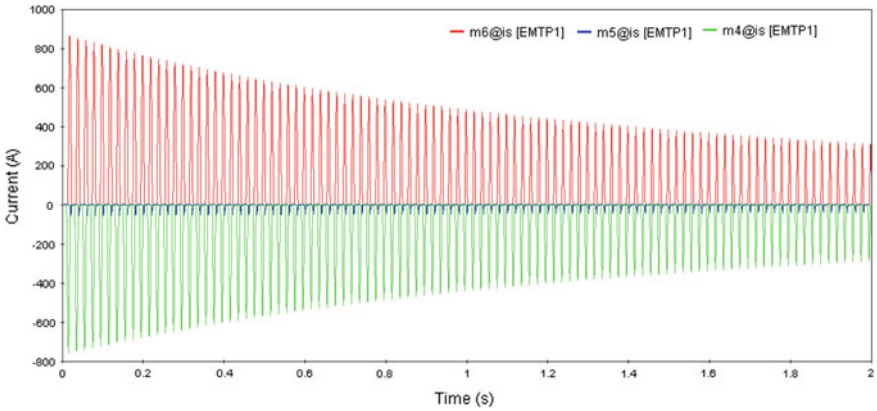

Fig. 4 Inrush current of analyzed power transformer

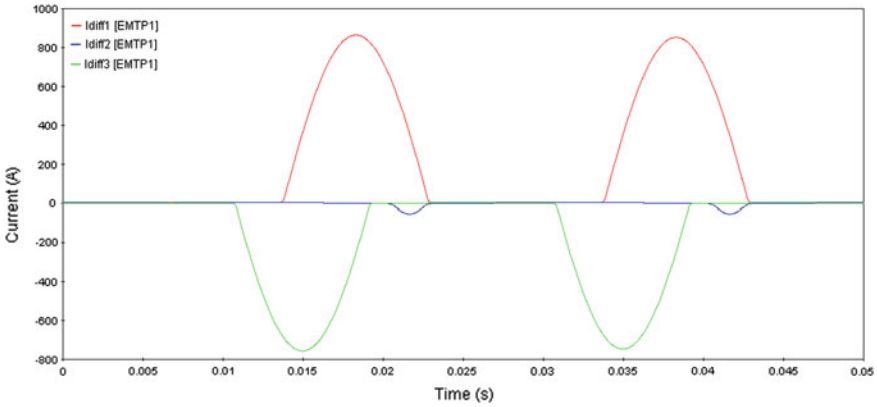

Fig. 5 Waveform of inrush current of analyzed power transformer

transformer has a large amount of current of second harmonic. This fact can be used to set the blockade of differential protection relay of power transformers. This type of blockade is called harmonic—current restraint.

Therefore, although in this case the differential current is equal to inrush current and is significantly larger than the tripping current of differential protection relay, relay should not react.

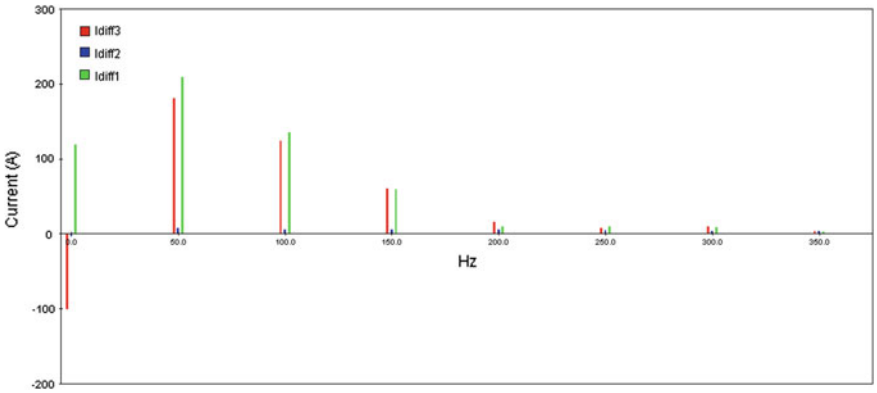

Fig. 6 Inrush current harmonic content

5 Short-Circuit in Protection Zone

When a fault occurs in the protection zone of differential protection, it is interesting to check the harmonic content of differential current. In this paper it was analyzed the three phase short-circuit in protection zone of power transformer differential protection. Differential current for this case is given on the Fig. 7.

As it can be seen from Fig. 7 differential current is significantly higher from differential protection reaction current. From this point of view, differential protection relay should react and switch off the power transformer from the network.

In order for differential protection to be able to differ the inrush current and internal fault current, it is necessary to carry out harmonic analysis of differential current. On Fig. 8 is given harmonic content of differential current from DC component to 7th harmonic. It can be noted that in case of three phase short circuit

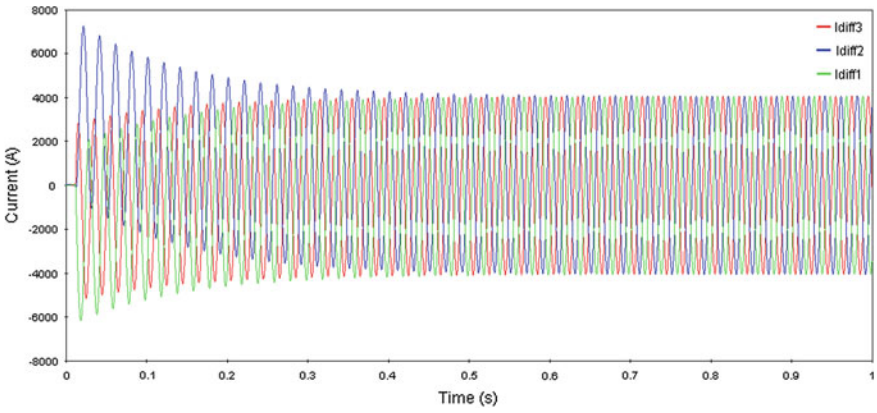

Fig. 7 Differential current for case of three phase short circuit in protection zone

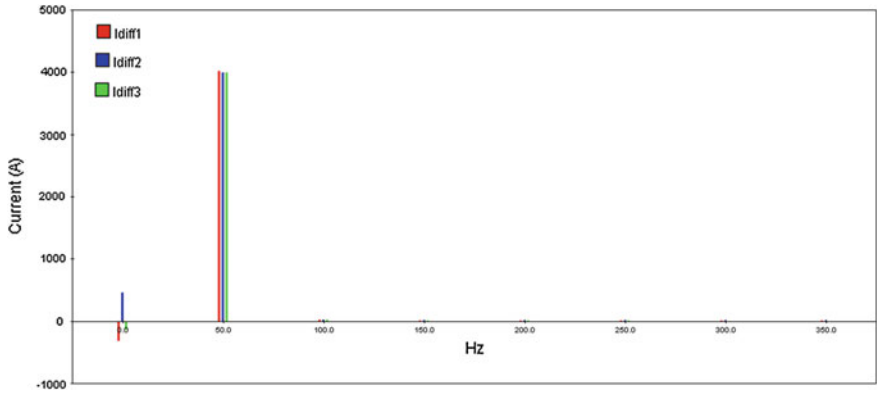

Fig. 8 Differential current harmonic content for case of three phase short circuit in protection zone

DC component and base harmonic component are accentuated, while higher order component are negligible. In this case because high order harmonic components of differential current are negligible, harmonic-current restrain will not react and differential protection will trip.

6 Over-Excitation

Another example in which a saturation of the power transformer core can occur, is the over-excitation. Over-excitation is caused by over voltages and/or under frequency conditions in power system [9]. Since, the over-excitation of power transformer produces exciting current on primary side of power transformer, the

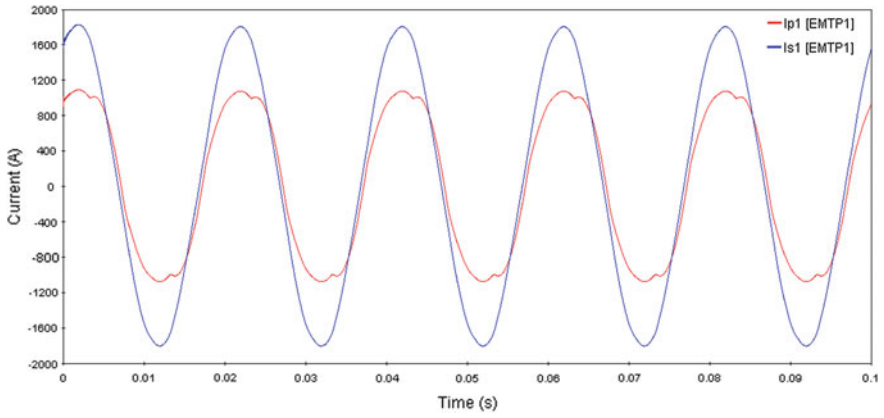

Fig. 9 Primary (I_{p1}) and secondary (I_{s1}) current of one phase for case of over-excitation

differential current will exist. In this paper over-excitation was modeled by assuming that applied voltage on the primary side is extremely high, 150 % [3]. For that case, on Fig. 9 shows primary and secondary current.

On Fig. 10 is given differential current for case of over-excitation.

Figure 11 gives the harmonic contest of the differential current in range of DC component to 7th order harmonics, for the case of over-excitation. From this figure it can be noted that 3rd and 5th order harmonics are accentuated. In this case, although there is a high value differential current (Fig. 10), due to the presence of high order harmonic components, harmonic—current restraint for 3rd and 5th harmonics [10] will react and differential protection relay will not trip.

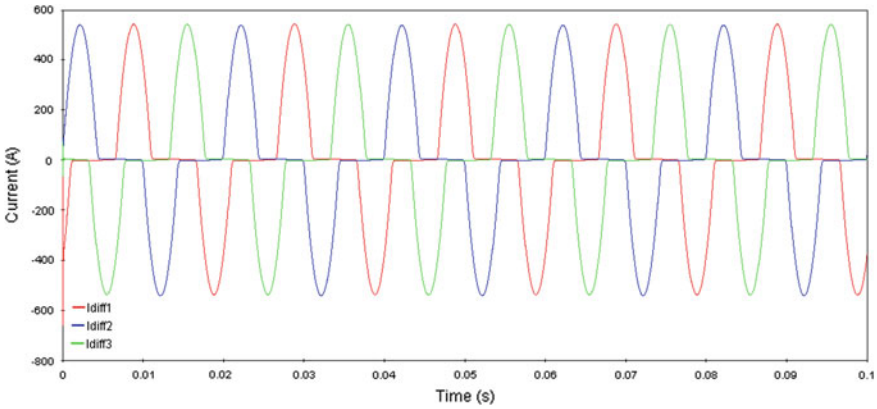

Fig. 10 Differential current for case of over-excitation

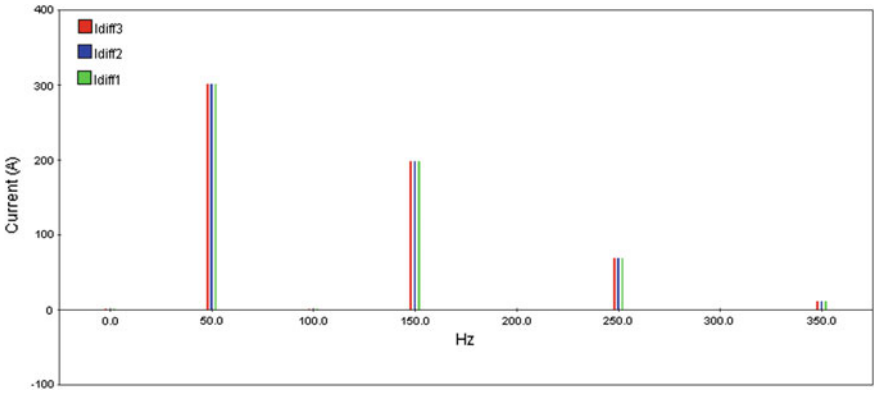

Fig. 11 Differential current for case of over-excitation

Table 2 Numerical values of differential current harmonic contest for all three cases

Harmonic		Inrush current (A)	Short-circuit (A)	Over-excitation (A)
DC	Phase 1	118.78	−320.9	0.55
	Phase 2	−3.28	461.97	−0.24
	Phase 3	−101.30	−142.38	0.47
1st	Phase 1	208.60	4013.77	300.55
	Phase 2	7.97	3995.64	300.54
	Phase 3	180.81	3997.36	300.52
2nd	Phase 1	135.36	24	0.78
	Phase 2	5.84	20.58	0.32
	Phase 3	123.39	16.18	0.65
3rd	Phase 1	59.18	5.45	193.08
	Phase 2	5.42	7.78	193.11
	Phase 3	60.62	5.50	193.09
4th	Phase 1	9.49	6.91	0.15
	Phase 2	5.12	6.27	0.07
	Phase 3	15.36	2.46	0.14
5th	Phase 1	9.92	4.92	68.71
	Phase 2	4.45	4.73	68.73
	Phase 3	7.04	3.10	68.73
6th	Phase 1	8.63	3.21	0.22
	Phase 2	3.94	3.79	0.10
	Phase 3	9.61	6.82	0.19
7th	Phase 1	1.95	3.77	10.74
	Phase 2	3.18	3.37	10.73
	Phase 3	3.86	1.42	10.72

7 Conclusion

Differential protection has an important role in protection of power transformers, and therefore it requires an application of very accurate and precise model for calculation of differential current. This paper presents low frequency power transformer model which is applicable for analysis of differential protection. Presented power transformer model was implemented on EMTP-RV. Calculations were conducted for specific cases which can occur during power transformer exploitation, and can have negative impact on differential protection functioning. Harmonic analysis was conducted on the results obtained by using presented model of power transformer in order to determine the blockade of differential protection relay. Based on a harmonic analysis conducted within this paper, it is evident that using the harmonic blockade of differential protection relay, an adequate protection of power transformer can be achieved.

References

1. Hosny A, Sood VK (2013) Phase angle pattern classifier for differential protection of power transformer. In: International conference on power systems transients (IPST), Canada, Vancouver
2. Alstom (2002) Guide on network protection and automation, 1st edn
3. Kang YC, Lee BE, Kang SH (2007) Transformer protection relay based on the induced voltages. J Electr Power Energy Syst 29:281–289
4. Chiesa N (2010) Power transformer modeling for inrush current calculation. Doctoral theses, NTNU
5. Tokić A, Madžarević V, Uglešić I (2005) Numerical calculations of three-phase transformer transients. IEEE Trans Power Deliv 20(4):2493–2500
6. Aktaibi A, Rahman MA (2012) Digital differential protection of power transformer using matlab. In: Katsikis VN (ed) p 1219
7. Tokić A, Uglešić I (2007) The numerical calculation of low frequency electromagnetic transient phenomena in power transformers. J Energy 56(5):584–607
8. Gajić, Z (2008) Differential protection for arbitrary three-phase power transformers. Doctoral dissertation, Department of Industrial Electrical Engineering and Automation, Lund University
9. Guzmán A, Zocholl S, Benmouyal G, Altuve HJ (2000) Performance analysis of traditional and improved transformer differential protection relays. In: 36th annual Minnesota power systems conference, Minneapolis, MN
10. ABB User Guide for Transformer Protection IED RET 670

Automatic Compensation Coil-Petersen Coil in Distribution Grid

Alija Jusić, Jasmina Agačević, Zijad Bajramović and Irfan Turković

Abstract The introductory part of the paper gives the basic theoretical considerations of the ways of neutral point treatment in distribution grids with special reference to the method of neutral grounding of distribution transformers by a compensation coil. The second part gives the analysis of the use of compensation coil as a future choice of neutral point grounding on the particular distribution grid TS 35/10 kV Bjelasnica. Also, the paper has conducted analysis of the available data and techno-economic analysis of neutral points grounding of transformers in TS 35/10 kV Bjelašnica in case of transformer neutral grounding by low ohmic resistor and in case of resonant neutral point grounding. In addition to the analysis of the (available) measured values, the adequate dynamic models of distribution grids are made by using the EMTP software package and calculations for neutral grounding by the compensation coil are done, as well as in the case of isolated grids, and a comparison of the results of ground fault currents was made.

1 Introduction

The main task of the electric power companies which carry out activities of production, distribution and supply of electricity, trade, representation and mediation in domestic and foreign markets of electricity, as well as other activities defined by the relevant documents, is to ensure the reliability of distribution systems and to meet the quality of supplied electricity in accordance with the regulations. With the

A. Jusić (✉) · J. Agačević · Z. Bajramović · I. Turković
Pritt Electical Utility Company, 71000 sarajevo, Bosnia and Herzegovina
e-mail: al.jusic@elektroprivreda.ba

J. Agačević
e-mail: jas.agacevic@elektroprivreda.ba

Z. Bajramović
e-mail: z.bajramovic@elektroprivreda.ba

I. Turković
e-mail: irfan.turkovic@etf.unsa.ba

M. Hadžikadić and S. Avdaković (eds.), *Advanced Technologies, Systems, and Applications*, Lecture Notes in Networks and Systems 3,
DOI 10.1007/978-3-319-47295-9_12

opening of the electricity market, Distribution System Operator (hereinafter referred to as DSO) is being imposed to a requirement for 'higher quality' electricity supply, which implies higher delivery reliability, and shorter de-energization intervals. In recent years there has been a rapid development of residential and commercial zones, tourist centres, etc., with a further trend of increase, and the general social development should be accompanied by the appropriate electricity infrastructure, which has resulted in the construction of new power lines (mostly cable), which significantly increases the overall value of capacitive current.

Increase of single-phase fault current makes the conditions for execution of 10 (20)/0.4 kV grounding and bringing the resistance propagation within the permissible limiting values defined in the relevant laws and regulations more difficult, which is directly related to hazardous voltage. All the above indicates the need for a special focus on the analysis of neutral point treatment, that is, neutral point grounding in the TS 110/x kV transformer stations (and TS 35/x kV until their final abandonment). Capacitive ground fault current in 10 kV isolated grid should not exceed 20 A, and in any case must not exceed 40 A with the shortening of shutdown period. In case of capacitive currents higher than 40 A, neutral point grounding should be made. Capacitive ground fault current in 20 kV isolated grid should not exceed 15 A, and in any case must not exceed 30 A with the shortening of shutdown period. In case of capacitive currents higher than 30 A, neutral point grounding should be done [1]. The 35 kV voltage distribution grids of JP Elektroprivreda BiH d.d. Sarajevo are typically grounded by a low ohmic impedance with the limitation of ground fault current at 300 A. Exceptionally, 35 kV branched cable grid is grounded in the way that the ground fault current is limited to a higher value (not higher 1000 A). In 20 and 10 kV grids the conditions are much more complicated, since the savings in lowering of isolation levels are not high, and there is also a danger of bringing grounding potential to the low voltage grid. The following is applied in these grids:

- isolation of the neutral point from the ground,
- grounding through a low ohmic impedance or,
- resonant neutral point grounding.

The right answer to the method of neutral point grounding can be given by over-all assessment of all the disadvantages and advantages of each solution. Having in mind a number of specific features that affect the choice of grounding method, it is difficult to recommend a solution which would satisfy all the requirements in terms of exploitation of the grids themselves for a longer period of time. In this paper, we will present the basic characteristics of the role and importance of automatic compensation coil in distribution grids as one of the methods for neutral point grounding [2, 3].

2 Use of Automatic Compensation Coil as a Future Choice for Neutral Point Grounding in Distribution Grids

2.1 Introductory Considerations of the Application of Automatic Compensation Coil as a Method of Neutral Point Grounding

A grid with compensated (resonant) grounding is a network in which the neutral points of power transformers are connected to the ground by the inductive reactance (the practice known as Petersen coil). When the capacitive single-phase fault current exceeds by regulations defined grid limiting values with the isolated neutral point, it loses its major advantage, namely the possibility of ground fault self extinction. In order to reduce capacitive ground fault current exceeding the limiting values, it is possible to connect the inductive reactance between the transformer neutral point and ground. In this way, the inductive currents compensate for capacitive ground fault current. The inductive reactance is adjusted so as to obtain resonance between it and the a serial line capacity per grid phase, so it is called a resonant grounding grid. Illustration of a single-phase ground fault in the case of neutral point grounding by Petersen coil with the vector diagram for the duration of ground fault is shown in Fig. 1.

The equivalent impedance viewed from the point of failure is defined as [4]:

$$\underline{Z}_0 = \frac{j3\omega L_{PR}\frac{1}{j\omega C_0}}{j\left(3\omega L_{PR} - \frac{1}{\omega C_0}\right)} \tag{1}$$

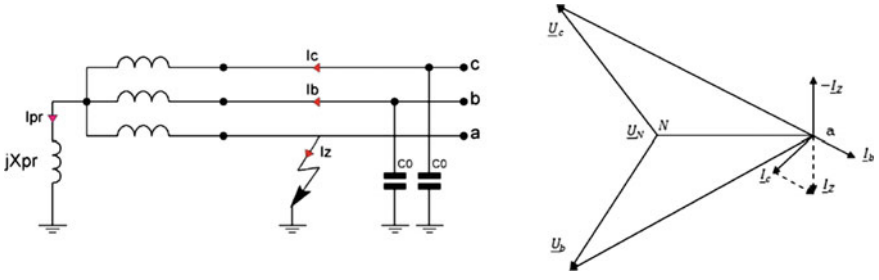

Fig. 1 Illustration of a single-phase ground fault in case of neutral point grounding by Petersen coil with vector diagram for the duration of ground fault

It is desirable that current I_PR which is approximately equal to the ground fault current in the grid Iz flows through reactance coil X_{PR}:

$$\mathrm{I}_{\mathrm{PR}} = \underline{\mathrm{I}}_{\mathrm{z}} - \underline{\mathrm{I}}_{\mathrm{b}} - \underline{\mathrm{I}}_{\mathrm{c}} \tag{2}$$

The condition of the resonant neutral point grounding formally comes down to: $3\omega^2 L_{PR} C_0 = 1$. Overall, total compensation is avoided in practice in order to prevent resonant surges that may occur in the interruption of phase conductors, and the coil in the neutral point is practically executed with the shunts or extensions with the projected (usually) nominal currents: 5; 10; 15; 20; 25; 30 A.

In case of failure, capacitive currents and currents of active conductivity of sound phases flow towards neutral point of the transformer. This also applies to all other sound transmission lines of the grid, that is, from the grid, the sum of current conductivity of all lines comes to the neutral point of the transformer. Through the faulty phase, in case of total compensation, only the active part of these currents and the active part of the coil current flow, that make up the ground fault current. Capacitive part of the ground fault current is compensated by the inductive coil current. The neutral point of the transformer, in case of ground fault, comes to the phase voltage of the grid, while the voltage of the sound phases come to phase to phase voltage, as is the case with the grids with the isolated neutral point.

Here the currents have the same flows as in an isolated grid, except that in the phase with the failure much lower ground fault current flows to the point of ground fault. This current is often called the residual ground fault current, and, in case of total compensation, consists only of active component.

In case of total compensation two instances may occur. The first instance is when the capacitive component of the ground fault current is higher than the inductive component of the coil current and when $L_p > \frac{1}{3\omega^2 C_0}$ and the second instance is when $L_p < \frac{1}{3\omega^2 C_0}$ that is, when the capacitive component of the ground fault current is lower than inductive. In the first case, we talk about „under compensated" grid, in the second case of "over compensated" grid. In this case, the reactive component of current also exists in the residual ground fault current.

Conditions for single-phase ground fault self-extinction, as one of the main advantages of these grids, primarily depend on the value of the ground fault current. In this case, it refers to the residual ground fault current. Conditions for ground fault extinction, after the causes of failure pass, also significantly depend on the speed of establishment of voltage on the phase that was out of order, so-called "reverse voltage", which aims to re-establish the ground fault. In incompletely compensated grids, reverse voltage has a pulsatile-oscillatory flow. With larger inaccuracies in compensation, reverse voltage may have an overvoltage up to 1.7. However, in this case the amplitude of the reverse voltage rises slowly and so reducing the possibility of ground fault re-establishment.

In the resonant grounded grids it is necessary to take into account the order of operations in manipulations of the grid. Compensation coil, at the moment of manipulation in the grid, can have a considerable magnetic energy, which must be emptied through small capacity power lines and other elements of the grid, which can cause significant overvoltage. Particularly large overvoltages can occur when two-phase ground faults are turned off, because the current in defective lines has the phase shift of 900 compared to the current in the coil, so a considerable magnetic energy can remain in the coil. Section B of this paper presents a model of real distribution grid TS 35/10 kV Bjelasnica, modeled in ATP-EMTP (Alternative Transients Program—EMTP) software package.

2.2 *Analysis of Single-Phase Fault in Distribution Grid Grounded by Resonant Grounding—Example TS 35/10 KV Bjelašnica*

In this section, the paper presents a model of real distribution grid TS 35/10 kV Bjelašnica modeled in ATP-EMTP (Alternative Transients Program—EMTP) software package. ATP—EMTP software package is used for computer analysis of electromagnetic phenomena caused by closure by switch operations, occurrence and elimination of short circuits, which is practically the standard in this field.

Computer modeling of elements and parts of distribution system was done for the purpose of analysis of transient phenomena in the selected distribution grid. The main elements used for the calculation of electromagnetic transients are given in Table 1.

Neutralization of ground fault current is done by installing a coil which is to be connected between the neutral point of the associated transformer substations and the ground. Reactance X_L is adjusted so as to be in resonance with the aerial capacity of lines X_{c0}, so that the remaining resultant ground fault current is of small amplitude. The active component of the current I_R, is obtained due to losses in the coil. Remaining ground fault currents are in the phase and they appear at the same time. If a ground fault occurs in the overhead grid (e.g. a breach through insulator), self-extinguishing may happen.

Table 1 Models of distribution grid elements

Grid elements	Block in ATP-EMTP
Source	“AC SOURCE”
Transmission lines model	“LINEPI3S”
Measurement of current and voltage	“OPEN PROBE”

When using the neutral point grounding by compensation coil, the goal is to choose a reactance coil $X_L = \omega L_N$ in a way to compensate for the reactance of aerial capacity of lines $X_c = \frac{1}{\omega C_z}$ which is the result of total aerial capacity of lines. In this case, the reactive part of zero impedance is equal to zero $X_N - X_C$. In case of total compensation $X_N = X_C$ it is said that the grid is configured and the current is only the result of operating losses in the coil and grid conductivity to the ground, which is most often overlooked. Reactance X_C is changed by every change in grid configuration. Therefore, to maintain the same amount of residual current it is also required to change the coil value.

Based on the above, this section will give the calculation of compensation coil values, with already known current value of the single-phase fault I_Z.

Total value of the ground fault current in 10 or 20 kV grid can be written according to the expression [5]:

$$I_z = \sqrt{3} \cdot \omega \cdot C_z \cdot U_L; \quad U_L = 10\text{kV} \tag{3}$$

2.3 The Results of Simulation of Neutral Point Treatment in TS 35/10 KV Bjelašnica by Ln Coil—TS Bjelasnica

Since the total value of the ground fault current in the TS Bjelasnica grid is equal to Iz = 136,54 A (according to the calculations done in PowerCad package), the above expression can be also used to do the calculation of the total value of aerial capacity of lines in the grid, which is:

$$\mathrm{C_z} = \frac{\mathrm{I_z}}{\sqrt{3} \cdot \omega \cdot \mathrm{U_L}} = 25.1\,\mu\mathrm{F}$$

Taking into account the condition of the ground fault current compensation, the calculation of the compensation coil for complete compensation can be made according to the expression:

$$\mathrm{L_N} = \frac{1}{3 \cdot \omega^2 \cdot \mathrm{C_z}} = 0.135\,\mathrm{H}$$

The model analyzes the worst case of single-phase fault from the aspect of coefficient of overvoltage that occurs at the beginning and the end of the line and

represents the fault that occurs in the phase conductor when the voltage in the phase in which the fault is simulated obtains the maximum value of phase voltage.

Therefore, the following diagrams are based on single-phase fault simulation when the voltage in phase A reaches the maximum value (Figs. 2, 3 and 4).

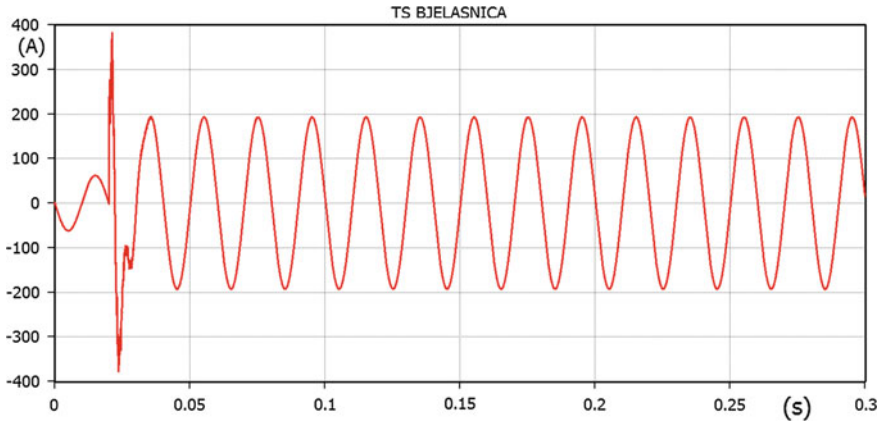

Fig. 2 Fault current—isolated grid

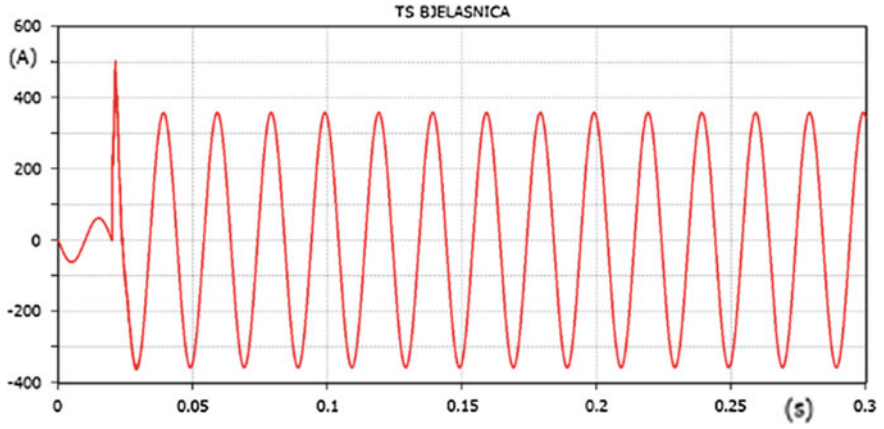

Fig. 3 Fault current—grid grounded by low ohmic metal resistor (Rn = 20 Ω)

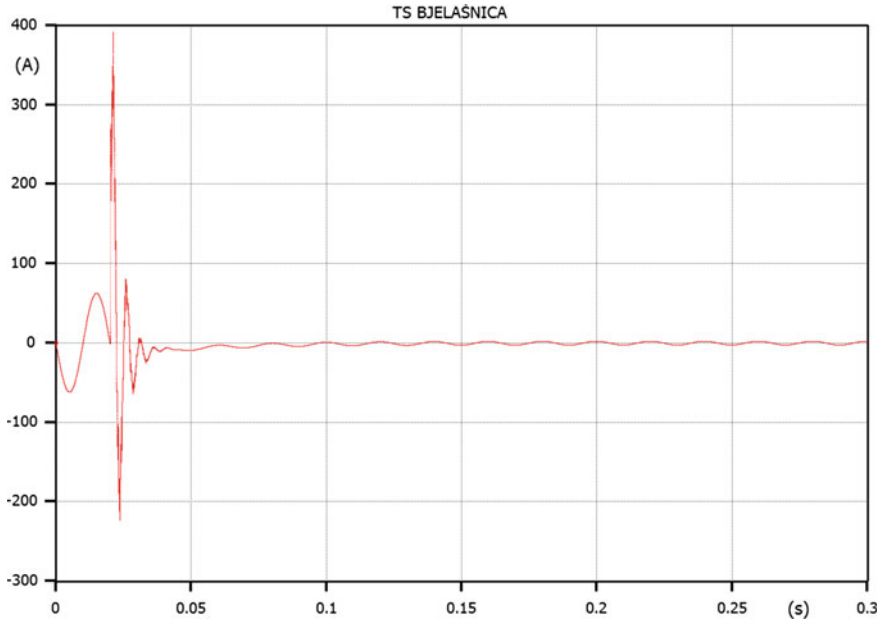

Fig. 4 Fault current—grid grounded by Peterson coil (L_N = 0.135 H)

2.4 Techno-economic Analysis of Application of TS 35/10 (20) KV Bjelasnica Neutral Point Grounding by Compensation Coil and Law Ohmic Resistor

By analyzing the available data, techno-economic analysis of the neutral points grounding of transformers in TS 35/10 (20) kV Bjelašnica was done, which is presented below. The analysis is done for the case of transformer's neutral point grounding by a low ohmic resistor and the case of resonant neutral point grounding.

- CASE I—neutral point will be done by using shared low ohmic metal resistor of 20 Ω value with a ground fault current limited at 300 A. Low ohmic resistor at the transformer neutral point should be connected by separate elements:
- Breaker—grounding device, with nominal voltage of 20 kV (so that equipment can meet the operating conditions when switching the grid from 10 to 20 kV voltage)
- 20 kV current measurement transformer
- single core power cable with 20 kV terminals.

35/10 kV, 4 MVA transformers are the group of Dy5 circuit with the neutral point on the bushing. It is necessary to provide overcurrent protection of the resistor for the neutral point grounding and to provide directional ground fault protection in water areas, so that the grid operating with grounded neutral point can eliminate the

mentioned output in a very short time. Ground fault will be manifested in the grounded grid as a single-phase short circuit. Grounding resistance on all TS 10/0.4 and 10 kV tower locations switching to grounded neutral point operation mode must be within the regulation framework required by the grounded grid.

CASE II—This case considers 35/10 kV transformer with 10 kV neutral point grounding by automatic compensation coil, with automatic compensation coils connected to the neutral points of power transformers, and create a parallel circuit with grid capacities. By regulating coil inductivity, the circuit is adjusted to the zero value of grid conductivity, so the value of the remaining current is small (depending on the setting). The remaining electricity consists also of a small value of the operating current due to coil ohmic resistance, and it is used for the selective work of protective devices.

For coils with continuous regulation, adjustment is done by shifting two cores using a motor drive controlled by an automatic regulator. The same has the option of manual control (locally) or remotely (via computer). The regulator operates continuously and adjusts the automatic compensation coil according to the grid conditions (Tables 2 and 3).

Table 2 Overview of investments needed for TS 35/10(20) kV Bjelašnica neutral point grounding by low ohmic resistor [6]

No.	Equipment description	Price BAM
1.	Resistor for 300 A transformer's neutral point grounding, 20 Ω	40.000
2.	Breaker-grounding device, for outdoor installation	2.600
3.	Pincer current measuring transformers	3.400
5.	Power cables and cable endings	5.500
4.	Purchase and adjustment of protection devices	20.000
5.	Adjustment of grounding devices on TS and power line poles[a]	50.000
Total		121.500

Table 3 Overview of investment needed for neutral point grounding of TS 35/10(20) kV Bjelasnica by compensation coil [6]

No.	Equipment description	Price BAM
1.	Compensation coil (2 pieces)	400.000
2.	Coil automatic regulation system (2 pieces)	100.000
3.	Relays for protection from high ohmic failures for two bus Sections (2 pieces)	30.000
4.	Other equipment	20.000
Total		550.000

3 Conclusion

Analyzing trends in the concept of transformer's neutral point grounding in MV grids in the region and some European countries, it is indicated that lately most attention is paid to neutral point grounding by compensation coils with automatic regulation.

In terms of techno-economic elaborations and comparison with other solutions (low ohmic grounding), in other countries the indicators of delivery reliability (undelivered electricity) are in favor of the proposals for this type of grounding (compensation coils).

Today there are no provisions in Bosnia and Herzegovina for distribution system operators to take into account the undelivered electricity as one of the parameters of techno-economic elaborations, so nowadays in BiH it is very difficult to justify this concept of neutral point grounding.

However, these indicators must be taken into account in long-term, and the proposals of this paper are aimed at the application of compensation coil as the primary mode of transformer's neutral point grounding in MV grids of JP EP BiH.

Developed European countries that have had low ohmic neutral point grounding in MV grids, due to consumers' requirements for reliable power supply, are switching to grounding by automatic adjustable compensation coil (e.g. Germany and France).

Often, the reasons are industrial consumption, technology and production processes sensitive to short interruptions in the power supply.

The price of the compensation coil with automatic regulation is a few times higher compared to the price of low homic resistors for neutral point grounding.

For the grids with low homic grounding and in the case of transferring to the compensation coil, the existing low homic resistor is being used (connected to the coil parallelly in order to increase the active component of fault current). These practical examples can be seen in the countries of our region.

References

1. BiH Electrical Utility Company (2011) TP-18_Technical recommendations for design and construction of grounding and grounding devices in power distribution grids and installations, Sarajevo
2. BAS EN 50522:2011 Earthing of power installations exceeding 1 kV AC
3. BAS HD 637 S1:2010 Power installations exceeding 1 kV AC
4. Nahman J (1980) Neutral point grounding in distribution grids, Beograd: Naučna knjiga
5. Ćućić R, Komen V, Đurović MŽ (2008) Neutral point concept in distribution networks. Eng Rev 28–2:77–89
6. BiH Electrical Utility Company (2016) Study-neutral point treatment in distribution grids, Sarajevo

Management of the Power Distribution Network Reconstruction Process Using Fuzzy Logic

Mirza Saric and Jasna Hivziefendic

Abstract This paper presents a fuzzy system for management of the power distribution network reconstruction process. The proposed system is based on Mamdani type fuzzy inference which is used to model reconstruction criteria. The system considers number of customers, rate of failure and age of distribution lines as input variables and provides output values used as criteria in a decision making process. The decision making process is based on the Bellman-Zadeh method in which decision making is performed by the intersection of fuzzy goals and constraints. In this paper, fuzzy logic is introduced as a system planning tool in order to account for weaknesses and imprecision of the traditional planning methods. The proposed model is presented as a logical decision making framework which can be used to evaluate and rank power distribution network reconstruction projects according to their ability to deliver long term benefits, both to the utility and customers.

1 Introduction

The power system is a complex and very capital intensive system which requires substantial investments in order to maintain predetermined quality standards and meet future energy and capacity needs. It is estimated that 30–40 % of total investments in the electricity sector is allocated to distribution systems [1]. The cost of electricity distribution constitutes a significant portion of the overall electricity cost [2]. The electricity distribution planning process requires that a large number of decisions be made within predetermined time and budget. Considering its strategic importance and the fact that the power system is very cost intensive, it is crucial to make the right decisions regarding planning management. Mistakes made during

M. Saric (✉)
JP EP BiH—d.d. Sarajevo, Sarajevo, Bosnia and Herzegovina
e-mail: m.saric@elektroprivreda.ba

J. Hivziefendic
International Burch University, Sarajevo, Bosnia and Herzegovina

M. Hadžikadić and S. Avdaković (eds.), *Advanced Technologies, Systems, and Applications*, Lecture Notes in Networks and Systems 3,
DOI 10.1007/978-3-319-47295-9_13

such processes can be very costly for decision makers and customers. Utilities make long term, ambitious investment plans which are evaluated by traditional planning techniques, based on load flow analysis [3]. However, network planning and project evaluation is a preference based decision making process which involves an assessment of a complex criteria [4]. Traditional approach neglects numerous planning criteria, which might result in misallocation of resources. Numerous judgments based on experience or expert opinion are crucial in decision making. Unfortunately, it is almost impossible to capture them all within the formulations of conventional optimizing models [5].

2 Power Distribution Network Planning Process

Certain managerial preferences are trade-offs, not hard constraints and need to be taken into considerations in order to make a balanced plan or decision [5]. Power distribution network planning requires analysis and management of large amount of data which need to be collected, processed and interpreted in a structured and systematic manner. The planning process requires that data be grouped to appropriate sets and subsets based on their attributes and characteristics. It is therefore justified to use advanced methods and tools to create a logical framework which will be used to determine a set of single valued criteria used for evaluation of electricity distribution network planning process. Such framework should include relative importance factors for each criteria which would be used to create a clear decision making algorithm. Their inclusion is not straightforward and it requires to use techniques designed for evaluation of qualitative aspects and vagueness or uncertainty [6] and multiple decision making criteria [3]. Fuzzy sets can be regarded as a tool which can be used to translate qualitative information into quantitative, crisp output [7].

Reference [8] shows that the main objectives of the planning process is the reduction of energy losses, voltage profile improvements, and the increase of reliability levels. Distribution planning process can be divided in two functional groups [9], namely exploitation (working) and construction and reinforcement planning. Reference [10] shows that distribution network process can be subdivided into following stages:

- problem identification which clearly defines applications and limits
- goals that need to be achieved
- identification of alternatives
- evaluations of alternatives
- selection of the best alternative
- make the final decision.

Figure 1 represents a simple illustration of the power distribution network planning process as described above. It shows various planning stages and their interaction.

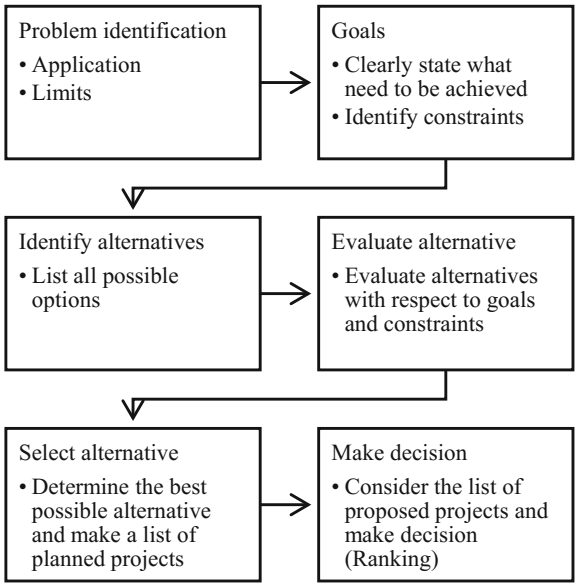

Fig. 1 Simple illustration of the electrical power network planning process

Review of research problems as well as models related to the planning of the power distribution network is provided in [2]. More recently, a comprehensive review of modern power distribution planning has been provided in [11] and it includes overview of modern models, methods and future research trends.

Decision making process relevant to network planning requires a logical, well-structured and easy to follow framework which can be used to categorize features of particular set and subset. Such framework is necessary in order to perform data interpretation and alternative raking. This kind of framework can hardly be defined within limits of classical set theory. Aristotelian binary logics does not offer an adequate framework required to model a wide range of practical engineering problems because a particular element x, either belongs to a set A ($\chi_A = 1$) or it does not belong to a set A ($\chi_A = 0$). Such a sharp (hard) approach to membership and boundary definition between two sets is not suitable for modelling various physical processes because it reduces real and natural process to discrete ones. Substantial number of authors highlight obvious advantages of fuzzy set models over the deterministic model for power system planning purposes. There is also enough evidence to argue that probabilistic approach is difficult to apply to planning problem because of the lack of significant data and because uncertainty is not random. Reference [12] observed that classical mathematical programming is not sufficient in many applications. This fact is especially true in the area of long term planning and strategy problems since the nature of these problems considers multiple objectives on one hand and uncertainly on another [12]. In traditional planning methods, many coefficients are modelled as crisp values and such crisp conditions can result in solutions which are not realistic [2].

Fuzzy approach appears to be appropriate to address these issues because it can provide significant information in a single fuzzy model, while traditional deterministic models need to include a large number of scenarios in order to produce the same result. Certain level of deviations or violations might be tolerated and might lead to substantial savings [2]. It is therefore justified to adopt a fuzzy approach and design a new framework capable to address these issues. Such framework should include relative importance factors for each criterion which would be used to create a straightforward decision making algorithm. It is expected that modern planning includes a number of other factors such as environmental issues, distributed generation, asset management, and quality of supply [3]. The power distribution network planning process also requires modelling of system attributes as network development criteria. Rigorous application of classical set theory to modelling of attributes and criteria leads to similar problems of artificial reduction to discrete values. This is not optimal because the given physical processes are continuous. In practice, these issues are overcome by the application of expert knowledge because the human mind has a remarkable capability to make decisions based on incomplete and approximate information.

3 Fuzzy Sets Operations and Properties

In a classical set theory, belonging or membership of an object to a set is precisely defined quantity. The object either belongs to a set or it does not belong to a set, which means that membership function can either take a value of 1 (an object belongs to a set) or 0 (an object does not belong to a set). If for example we define two sets A = {x|x is weekday} and B = x {x|x is weekend} and if we were constrained to the framework of classical Aristotelian logic, we would agree that Monday, Tuesday, Wednesday, Thursday and Friday belong to set A, while Saturday and Sunday belong to set B. The world is therefore either white or black. This binary description of membership can be represented mathematically with the following function [13]:

$$\chi_A(x) = \begin{cases} 1, & \text{for } x \in A \\ 0, & \text{for } x \notin A \end{cases} \tag{1}$$

$$\chi_B(x) = \begin{cases} 1, & \text{for } x \in B \\ 0, & \text{for } x \notin B \end{cases} \tag{2}$$

However, human perception is quite different as it adopts a softer approach to boundary conditions. Fuzzy logic, as a mathematical tool, recognizes such approach to membership concept. It considers the values of graded (partial) membership, which can assume values between 0 and 1 and can, therefore, be used to model human perception. Fuzzy set, therefore, can be described as an extension of classical set theory with softer transition from one membership function to another.

Similarly, classical sets can be defined as a special case of a fuzzy set where all membership grades equal to 1. Friday, in this case, is still a working day, but only until the end of business hours. The weekend starts on Friday afternoon and therefore, in fuzzy terms, we could define Friday as an element of fuzzy set, described by membership function having a value of 0.66 in set A, and 0.33 in set B. Similarly, we can define Sunday with a membership of 0.66 in set B and 0.33 in set A. If we consider a classical set A of the universe U, a fuzzy set A is defined by a set or ordered pairs, a binary relation as [14]:

$$A = \{(x, \mu_A(x)) | x \in A, \mu_A(x) \in [0, 1]\} \tag{3}$$

In this case, $\mu_A(x)$ is a function called membership function and it specifies the grade or degree to which any element x in A belongs to the fuzzy set A. This definition associates, with each element x in A, a real number $\mu_A(x)$ in the [0, 1] interval, which is assigned to x. The mapping of a fuzzy set to a universe of membership values is performed using a function-theoretic form [13]. If universal set X is a finite set $X = \{x_1, x_2, \ldots, x_n\}$ and μ_i is a membership function of x_i in A, then a fuzzy set A can be represented as [14]:

$$A = \frac{\mu_1}{x_1} + \frac{\mu_2}{x_2} + \cdots + \frac{\mu_n}{x_n} = \sum_{i=1}^{n} \frac{\mu_i}{x_i} \tag{4}$$

Members $\frac{\mu_i}{x_i}$, $i = 1, 2, \ldots, n$ represent degree of membership μ_i of the element x_i to a fuzzy set A. If X is an infinite and continuous set, rather than discrete, with elements x (X, then fuzzy set A can be represented as [14]:

$$A = \int_{x \in X} \frac{\mu(x)}{x} \tag{5}$$

Let us define two fuzzy sets A and B on the universe X as shown in Fig. 2. The basic fuzzy set operations can be defined as:

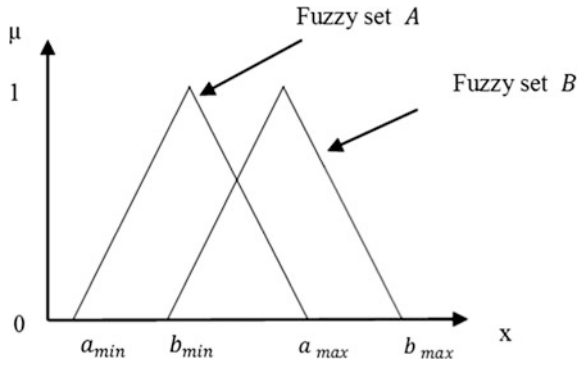

Fig. 2 Graphical representation of fuzzy sets A and B

- Union:

$$\mu_{A\cup B}(x) = \mu_A(x) \vee \mu_B(x) \tag{6}$$

Graphical representation of union of fuzzy sets A and B is shown in Fig. 3. In the Eq. 6 the sign $\vee$ represents the maximum operator, which means that union can be represented as:

$$\mu_{A\cup B}(x) = \mu_A(x) \vee \mu_B(x) = \max\{\mu_A(x), \mu_B(x)\} \tag{7}$$

- Intersection

$$\mu_{A\cup B}(x) = \mu_A(x) \wedge \mu_B(x) \tag{8}$$

Graphical representation of the intersection of fuzzy sets A and B is shown in Fig. 4. In the Eq. 8 the sign $\wedge$ represents the minimum operator which means that intersection can be represented as:

$$\mu_{A\cup B}(x) = \mu_A(x) \wedge \mu_B(x) = \min\{\mu_A(x), \mu_B(x)\} \tag{9}$$

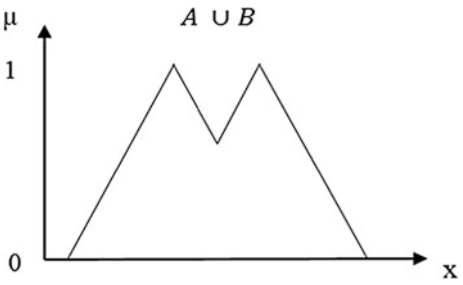

Fig. 3 Graphical representation of the union of fuzzy sets A and B

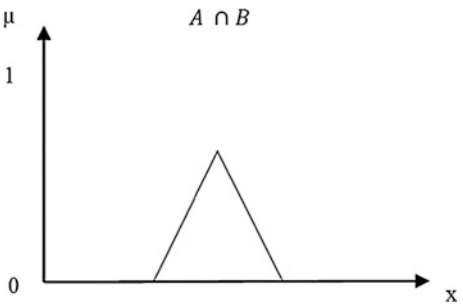

Fig. 4 Graphical representation of the intersection of fuzzy sets A and B

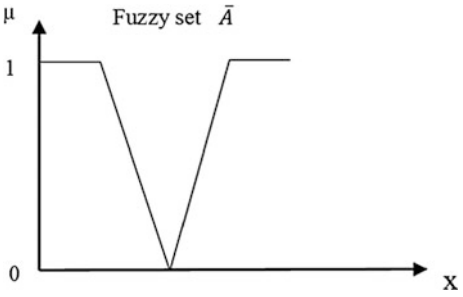

Fig. 5 Graphical representation of fuzzy set $\bar{A}$ (complement of A)

- Complement:

$$\mu_{\bar{A}}(x) = 1 - \mu_A(x) \tag{10}$$

Graphical representation of the complement of fuzzy set A is shown in Fig. 5.

All operations on classical sets are also true for fuzzy sets, apart from the excluded middle axioms. This property in the case of classical sets can be represented as $A \cup \bar{A} = X$ and it represents the fundamental difference between fuzzy and classical sets because a fuzzy set and its complement can overlap. Therefore, in the case of a fuzzy set, it can be written that:

$$A \cap \bar{A} \neq 0 \quad \text{and} \quad A \cap \bar{A} \neq X \tag{11}$$

Fuzzy sets display the same properties of crisp sets. Some of the most common properties are [13]:

- Commutativity

$$A \cup B = B \cup A \tag{12}$$

$$A \cap B = B \cap A \tag{13}$$

- Associativity

$$A \cup B(B \cup C) = (A \cup B) \cup C \tag{14}$$

$$A \cap (B \cap C) = (A \cap B) \cap C \tag{15}$$

- Distributivity

$$A \cup (B \cap C) = (A \cap B) \cap (A \cup C) \tag{16}$$

$$A \cap (B \cup C) = (A \cap B) \cup (A \cap C) \tag{17}$$

- Idempotency

$$A \cup A = A \quad \text{and} \quad A \cap X = A \tag{18}$$

- Identity

$$A \cap 0 = 0 \quad \text{and} \quad A \cap X = X \tag{19}$$

- Transitivity

$$\text{If} \quad A \subseteq B \quad \text{and} \quad B \subseteq C \quad \text{then} \quad A \subseteq C \tag{20}$$

- Involution

$$\overline{\overline{A}} = A \tag{21}$$

4 Fuzzy Models and Methods for Electrical Distribution Network Planning

Fuzzy apporach has been extensively used in distribution system planning [15], reconfiguration [8] and DG allocation problems [16]. Reference [17] develops a robust possibilistic mixed-integer programming method for planning applied to municipal electric power systems considering the uncertatitny. Fuzzy models for decision making behave more like expert systems than fuzzy control algorithms because they are modelled by human expert knowledge and can only be confirmed by testing their outcomes. Fuzzy models for decision making are implemented as control algorithms. Using crisp values as inputs and outputs of fuzzy rule based models in decision-making, significantly limits their ability to support decision-making [18]. Reference [5] found that there are three main reasons for incorporating expert systems in the planning process. First is the guidance of the decision making procedure by the knowledge and experience built up over many years by system planning engineer. Secondly, expert systems can be exploited to make the models more viable. Finally an extension and innovation is carried out within the expert system.

Reference [19] reports specification of fuzzy logic based knowledge modelling for development of decision support system which would be used to assist utility engineers in medium term outage planning. Reference [5] describes a long range power system expansion planning program which is an optimizing program and uses dynamic programming for tracking an optimal expansion strategy, a rule based

decision making mechanism to incorporate engineering and fuzzy set theory has which is used to define decision making procedure. Reference [17] proposes a fuzzy multi-criteria group decision-making method for power distribution system planning evaluation. It considers technology, economy, society and environment as evaluation aspects with 8 evaluation criteria. This contribution determined that the engineering practice is more complex since quantitative values of criteria are often difficult to determine. Additional criteria need to be determined and modelled. There is therefore a considerable gap between existing model and what is required in order to represent other important aspects of modern distribution system planning and create practical and robust expert system which can be extensively used in practice. Reference [20] presents a computational system used to assist decision makers in the process of the power distribution network planning and designs a single objective optimization model with technical and economic considerations, a multi-objective model which considers various aspects and, finally, a fuzzy mathematical programming model which takes into consideration fuzzy goals and constraints. Reference [21] develops a fuzzy method used to improve operational planning efficiency of the distribution network, based on indices of economic feasibility and service quality. Reference [22] presents a fuzzy knowledge-based approach for reliability planning purposes as it makes the assessment of circuit configuration and hazards and assigns each section and feeder a relative risk index by expressing the configuration variables mathematically using fuzzy logic. Reference [23] defines mathematical operations by the extension principle and proposes the way to model the partial correlation between variables and that fuzzy numbers provide a good way to include non-statistical uncertainties in the decision making process.

Reference [3] describes a method for the power distribution network planning which considers load growth, distributed generation, asset management, quality of supply and environmental issues by using a number of discrete evaluation criteria within a multi criteria decision making (MCDM) environment to examine and assess the trade-offs between alternative solutions. Reference [3] demonstrates suitability of MCDM techniques to the distribution planning problem and highlight how evaluating all planning problems simultaneously can provide substantial benefits to a distribution company. Reference [24] introduces comprehensive evaluation hierarchy which includes system security, reliability, economic profit, supply capability and derivative capability. The proposed model is based on fuzzy sets, introduced in order to account for the lack of suitable quantitative evaluation method to the connection model. Evaluation includes indices such as maximum short circuit current, maximum voltage drop, voltage shift, ASAI and SAIDI which are described by fuzzy sets. This paper shows that it is possible to identify key elements influencing network planning and evaluate connection modes quantitatively.

Fuzzy approach has been used in a few closely related fields such as power system stability and control, load forecasting, monitoring, diagnosis and market

design [25]. A fuzzy reasoning approach is also used in numerous papers written on the topic of the service restoration, which is a multiple-objective problem with some objectives contradictory to each other [26]. Reference [27] discusses a new expert model for decision making process in electrical outage management while [28] shows a fuzzy expert system for the integrated fault diagnosis. Reference [29] designed a fuzzy model which can be used in the management of the water supply system planning process. Reference [30] develops a decision-making fuzzy control model for small and medium enterprise, which can be used in an ambiguous environments to train company's strengths and develop long term strategy. Reference [31] presents the improvements of the fuzzy load models with the application of fuzzy clustering techniques for the distribution networks planning.

5 Model Development

Figure 6 shows a simplified structure of the proposed systems and interaction of its major components while Fig. 7 show a simple graphical representation of Mamdani type inference. Three major attributes, namely the number of customers, rate of failure and age of distribution line, are evaluated in two separate, Mamdani type inference models. In the first model, reconstruction criteria is evaluated according to

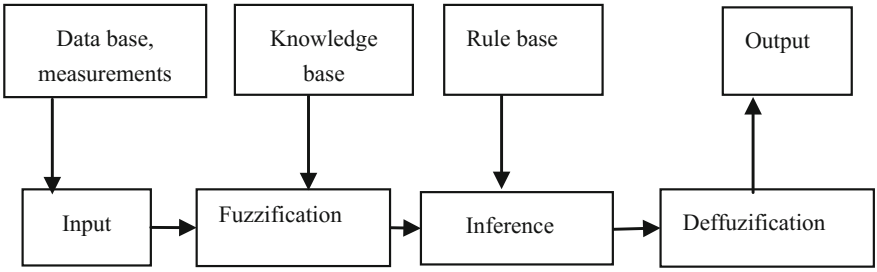

Fig. 6 Simple graphical representation of the proposed fuzzy systems

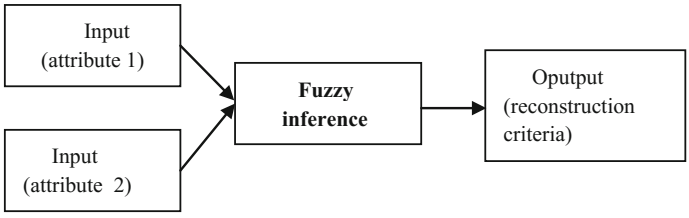

Fig. 7 Graphical representation of Mamdani type fuzzy inference

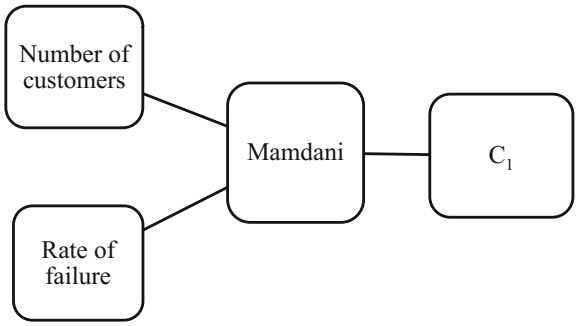

Fig. 8 Model 1-criteria based on number of customers and failure rate

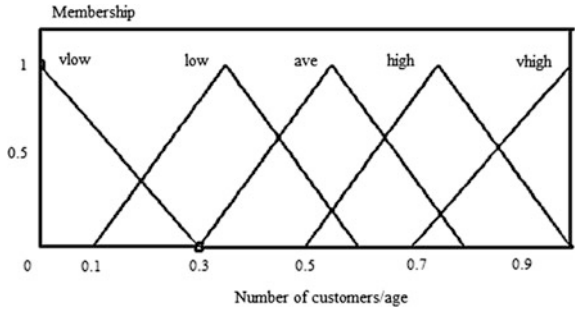

Fig. 9 Fuzzy set representation of number of customers and age

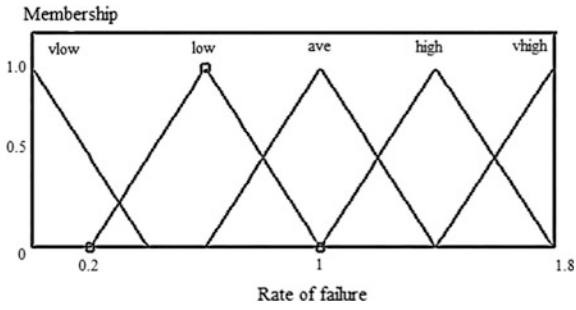

Fig. 10 Fuzzy set representation of failure rates

the logics shown in Fig. 8. The number of customer data (first input variable) and quantitative measure of failure rates (second input variables) are both represented by fuzzy sets, as shown in Figs. 9 and 10. The output value of the first Mamdani type model represents the value of the first planning criteria C1. In the second Mamdani type inference model, the input attributes are age of distribution power line and respective failure rates. These two attributes are combined according to the logic shown in Fig. 12 and provide the output variables of fuzzy system which is used to estimate the condition of the line in question. This output variable represents the second reconstruction criteria, C2.

Electricity outages are unwelcome and unpleasant events which, apart from inconvenience, might cause serious damages. Number of customers served by network section (power line) is a quantitative criteria which considerably influences the risk for utility in the case of service interruptions. If a power line serves large number of customers and if its failure rate is high, then risk faced by utility is high. This type of infrastructure should be given priority considerations during the service restoration and reconstruction planning process. This system attribute is fuzzified as shown in Fig. 9. In proposed model, customer number values are normalized into 0–1 range, where 1 is maximum, corresponding to 1000 customers and 0 is minimum, corresponding to 0 customers. This attribute is combined with rate of failure value, in order to obtain C1. This attribute is represented by fuzzy set as follows:

$$\mathrm{NC} = \{\mathrm{A}_1, \mathrm{B}_1, \mathrm{C}_1, \mathrm{D}_1, \mathrm{E}_1\} \tag{22}$$

$$\mathrm{NC} = \{\text{very low, low, average, high, very high}\} \tag{23}$$

The second attribute used as input in this model is rate of failure, given by λ. Conductor aging and deterioration is a physical and chemical process which causes irreversible alterations of conductor mechanical and electrical properties. Major factors which determine the speed of such deteriorations are temperature, pollution, quality of storage and installation and finally, loading conditions which considerably contribute to conductor heating. System security depends on security and performance of its individual components. Reliability considerations are important part of planning and development process. In proposed model, the probability of an event is represented by rate (intensity) of failure defined as [32]:

$$\lambda = \frac{\text{number of failures}}{\text{number of components} \times \text{number of years}} \tag{24}$$

It was shown in [32] that the average and maximum sustained failure rates for cables and overhead lines are (0.93/100 km, year) and (1.81/100 km, year) respectively. Values for overhead lines are used in model, represented by set (shown in Fig. 10):

$$\mathrm{RF} = \{\mathrm{A}_2, \mathrm{B}_2, \mathrm{C}_2, \mathrm{D}_2, \mathrm{E}_2\} \tag{25}$$

$$\mathrm{RF} = \{\text{very low, low, average, high, very high}\} \tag{26}$$

Third attribute is modelled according to the same logic, with 1 being the maximum value corresponding to 60 years of age. It is shown in Fig. 9 and can be represented by a fuzzy set in following way:

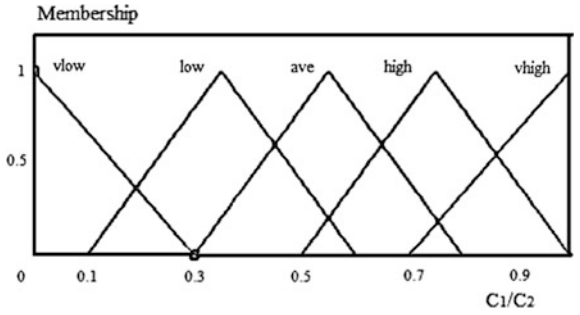

Fig. 11 Fuzzy set representation of the output variables

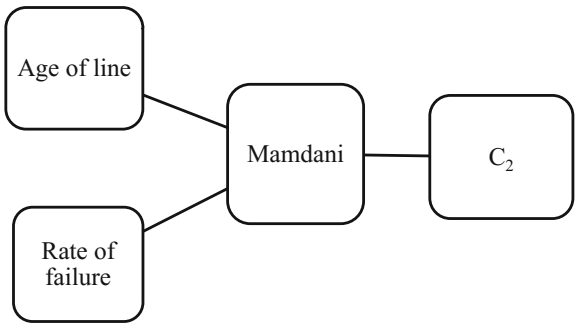

Fig. 12 Model 2-criteria based on the distribution line condition

Table 1 Fuzzy rules for models 1 and 2

Rate of failure	Number of customers/age				
	Vlow	Low	Ave	High	Vhigh
Very low	VL	VL	L	L	L
Low	VL	L	A	H	VH
Average	L	A	H	H	VH
High	L	A	H	H	VH
Very high	L	A	H	VH	VH

$$\mathrm{AGE} = \{\mathrm{A}_3, \mathrm{B}_3, \mathrm{C}_3, \mathrm{D}_3, \mathrm{E}_3\} \tag{27}$$

$$\mathrm{AGE} = \{\text{very low}, \text{low}, \text{average}, \text{high}, \text{very high}\} \tag{28}$$

Finally, output variables, C_1 and C_2 as shown in Fig. 11 are used as criteria in power network reconstruction process and are represented by following fuzzy sets (Fig. 12):

$$\mathrm{C}_1 = \{\mathrm{A}_4, \mathrm{B}_4, \mathrm{C}_4, \mathrm{D}_4, \mathrm{E}_4\} \tag{29}$$

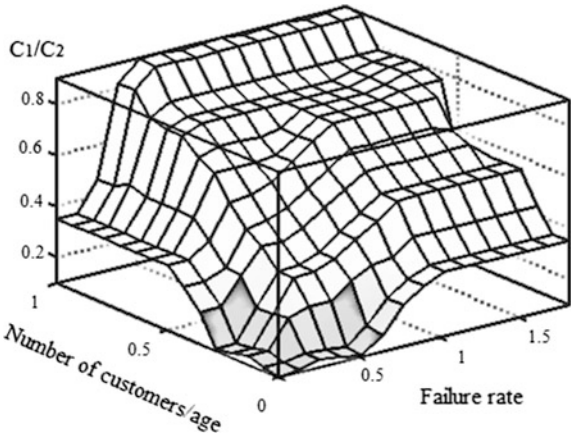

Fig. 13 Surface viewer

$$C_1 = \{\text{very low, low, average, high, very high}\} \tag{30}$$

$$C_2 = \{A_5, B_5, C_5, D_5, E_5\} \tag{31}$$

$$C_2 = \{\text{very low, low, average, high, very high}\} \tag{32}$$

Table 1 shows n x m IF…AND…THEN rules, where n and m are the numbers of elements of input variable sets, giving a total of 25 rules. These rules are used to obtain the output variable described by the sets C_1 and C_2. Rules are the same in both models. Final simulation results can be summarized in surface viewer shown in Fig. 13 which, for a given value of number of customers (or age) and rate of failure, returns the value C_1 and C_2 respectively.

Control output value are used to grade entire network according to these criteria, thus providing a model for project selection and priority ranking. This method is particularly useful in applications such as distribution network planning, where large amount of data need to be processed.

6 Application Example

Figure 14 shows a single line diagram of a simple power distribution system. The values relevant for application demonstration are listed in Table 2. It can be seen that crisp values are obtained as criteria for ranking distribution system reconstruction project. Proposed system can be used as a business analysis/intelligence tools and decision making support tool. The list of possible criteria is obviously not exhausted by the attributes proposed in this model. It is possible to extend the existing model to include any other criteria required by decision maker. One of the characteristics associated with planning problem is the trade of between different

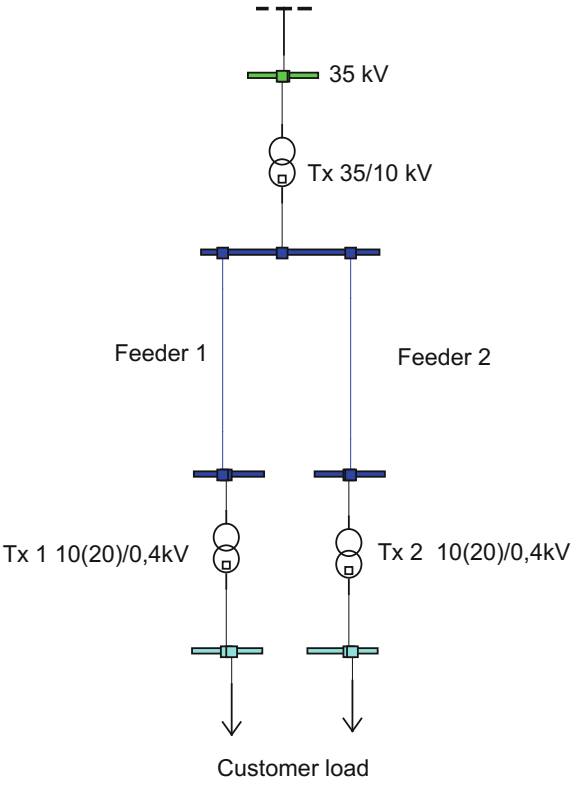

Fig. 14 Single line diagram of simple power distribution network

Table 2 Model application results

Line name	Number of customers	Failure rate (km, year)	Age of the line (years)	Criteria 1	Criteria 2
Feeder 1	481	1.2	18	0.71	0.55
Feeder 2	111	0.8	48	0.28	0.75

planning criteria. One possible way to resolve the conflict between criteria is use of fuzzy MCDM. In order to make decision it is necessary to construct a decision making matrix M where each column represents a particular alternative and each row corresponds to a particular criteria.

More formally, each element of a decision making matrix M represents a ranking of an alternative X_i with respect to a criteria C_j. For the case of m criteria (C_1, C_2, …, C_m) an n alternatives (X_1, X_2,…, X_n), decision matrix M is [29]:

$$M = \begin{array}{c} \\ C_1 \\ C_2 \\ \vdots \\ C_m \end{array} \begin{array}{c} \begin{array}{cccc} X_1 & X_2 & \ldots & X_n \end{array} \\ \begin{bmatrix} x_{11} & x_{12} & \ldots & x_{1n} \\ x_{21} & x_{22} & \ldots & x_{2n} \\ \vdots & \vdots & \vdots & \vdots \\ x_{m1} & x_{m2} & \ldots & x_{mn} \end{bmatrix} \end{array} \tag{33}$$

For fuzzy set of goals $G_{g,}$ where r is the number of goals, it can be written that:

$$G_g = \sum_{i=1}^{n} \frac{\mu_{Gg}\left(x_{gi}\right)}{X_i}_{g=1}^{g=r} \tag{34}$$

Similarly for constraints fuzzy sets C_c, where h is the number of constraints, it can be written that:

$$C_c = \sum_{i=1}^{n} \frac{\mu_{Cc}\left(x_{r+c,i}\right)}{X_i}_{c=1}^{c=h} \tag{35}$$

Decision set is given by the intersection of fuzzy goals and fuzzy constraints and can be represented as follows [29]:

$$D = G_g \cap C_c = \sum_{i=1}^{n} \frac{\mu_{Gg}\left(x_{gi}\right)}{X_i}_{g=1}^{g=r} \bigcap \sum_{i=1}^{n} \frac{\mu_{Cc}\left(x_{r+c,i}\right)}{X_i}_{c=1}^{c=h} \tag{36}$$

Fuzzy sets intersection is defined according to [29]:

$$D = G_g \cap C_c = \min \left[\min_{g=1,r}\left(\mu_{Gg}\left(x_{ij}\right)\right), \min_{c=1,h}\left(\mu_{Cc}\left(x_{ij}\right)\right) \right] \tag{37}$$

7 Conclusion

Fuzzy logic control and MCDM have developed rapidly since 1970 and have been a very vibrant field of research. This is a mature field and there are still numerous areas where fuzzy logic could be applied. Availability of fuzzy criteria is necessary for application of fuzzy MCDM. Including uncertainty in the process of decision making optimizes the social cost of network expansion and is therefore beneficial for electricity customers and society. This paper presented a simple fuzzy system used for management of the power distribution network reconstruction process. The proposed model considers set of the criteria based on the number of customers served by the line, rate of failure and age. The decision making process is based on the Bellman-Zadeh method in which decision making is accomplished by the intersection of fuzzy goals and constraints. Output values of the proposed fuzzy

system are used inputs to decision making matrix (criteria). It is argued that this paper makes a contribution toward more effective management of power distribution network planning process and that there is an opportunity to further investigate the application of fuzzy control in the process of power distribution network planning.

References

1. Rudnick H, Harnisch I, Sanhueza R (1997) Reconfiguration of electric distribution system. Revista facultad de ingenieria, U.T.A. (Chile), 4:41–48
2. Khator SK, Leung LC (1997) Power distribution planning: a review of models and issues. Power Syst IEEE Transac 12(3):1151–1159
3. Espie P, Ault GW, Burt GM, McDonald JR (2003) Multiple criteria decision making techniques applied to electricity distribution system planning. In: Generation, transmission and distribution, IEE proceedings, vol 150, no 5, pp 527,535, 15 Sept 2003
4. Zhang T, Zhang G, Ma J, Lu J (2010) Power distribution system planning evaluation by a fuzzy multi-criteria group decision support system. Int J Comput Intell Syst 3(4):474–485
5. David AK, Zhao R (1991) An expert system with fuzzy sets for optimal planning [of power system expansion],". IEEE Trans Power Syst 6(1):59–65
6. Miranda V, Matos MACC (1989) Distribution system planning with fuzzy models and techniques. Electricity Distribution, 1989. CIRED 1989. 10th international conference on, vol 6, pp 472, 476, 8–12 May 1989
7. El-Sayed MAH, Seitz T, Montebaur A (1994) Fuzzy sets for reliability assessment of electric power distribution systems, Circuits and Systems. In: Proceedings of the 37th midwest symposium on, vol 2, no, pp 1491, 1494, 3–5 Aug 1994
8. Bernardon DP, Garcia VJ, Ferreira ASQ, Canha LN (2009) Electric distribution network reconfiguration based on a fuzzy multi-criteria decision making algorithm. Electr Power Syst Res 79(10):1400–1407. ISSN 0378-7796
9. Prenc R (n.d.) Alokacija distribuiranih izvora električne energije u mreži ODS-a HEP ODS d. o.o.—DP Elektroprimorje Rijeka Viktora Cara Emina 2, 51 000 Rijeka
10. Neimane V (2001) On development planning of electricity distribution networks. Doctoral dissertation, Royal Institute of Technology, Department of electrical engineering, power engineering, Stockholm
11. Georgilakis PS, Hatziargryriou ND (2015) A review of power distribution planning in the modern power systems era: models, methods and future research. Electr Power Syst Res 121:89–100
12. Slowinski R, Teghem J (1990) Stochastic versus fuzzy approaches to multiobjective programming under uncertainty, Dordrecht. Kluwe, The Nederlands
13. Ross TJ (2010) Fuzzy logic with engineering applications. 3rd edition. Wiley, New York
14. Bojadziev G, Bojadziev G (2007) Advances in fuzzy systems: applications and theory. 2nd edition, vol 23, World Scientific Publishing Co. Pte. Ltd, Singapore
15. Yu L, Li YP, Huang YP (2016) A fuzzy-stochastic simulation-optimization model for planning electric power systems with considering peak-electricity demand: a case study of Qingdao, China, Energy, vol 98, 1 Mar 2016, pp 190–203. ISSN 0360-5442
16. Soroudi A (2012) Possibilistic-scenario model for DG impact assessment on distribution networks in an uncertain environment. IEEE Trans Power Syst 27(3):1283–1293
17. Zhou Y, Li YP, Huang GH (2015) A robust possibilistic mixed-integer programming method for planning municipal electric power systems. Int J Electr Power Energy Syst, 73:757–772. ISSN 0142-0615

18. Piskounov A (2003) Fuzzy rule-based models: decision-making vs control. In 12th IEEE conference on fuzzy systems. FUZZ '03, vol 1, pp 96, 101, 25–28 May 2003
19. Egwaikhide OI (2000) Fuzzy modeling of uncertainty in a decision support system for electric power system planning. Fuzzy Control, Advances in Soft Computing 6:387–396
20. Kagan N, Adams RN (1992) A computational decision support system for electrical distribution systems planning, CompEuro'92. Proceedings of the computer systems and software engineering, pp 133,138, 4–8 May 1992
21. Cavati CR, Ekel PY (1998) "A fuzzy decision making for the distribution systems planning," Power system technology. In: Proceedings. POWERCON '98. 1998 International conference on, vol 1, pp 233, 236, 18–21 Aug 1998
22. Cavati CR, Ekel PY (1998) A fuzzy decision making for the distribution systems planning," Power system technology. In: Proceedings POWERCON '98. 1998 international conference on, vol. 1, pp 233, 236, 18–21 Aug 1998
23. Dimitrovski AD, Matos MA (2000) Fuzzy engineering economic analysis [of electric utilities]. Power Syst IEEE Transac 15(1):283–289
24. Feng P, Ming Z, Min Z (2009) An evaluating hierarchy for distribution network based on fuzzy evaluation. In: Transmission & distribution conference & exposition: Asia and Pacific, pp. 1, 4, 26–30 Oct 2009
25. Momoh JA, Tomosevic K (1995) Overview and literature survey of fuzzy set theory in power systems. IEEE Transac Power Syst 10(3)
26. Hsu Yuan-Yih, Kuo Han-Ching (1994) A heuristic based fuzzy reasoning approach for distribution system service restoration. IEEE Trans Power Delivery 9(2):948–953
27. Banan K, Khanmohammady S, Hoseiny SH (2005) New expert model for decision making process in electrical outages management. In: International conference on intelligent agents, web technologies and internet commerce
28. Lee HJ, Park DY, Ahn BS, Park YM, Park JK, Venkata SS (2000) A fuzzy expert system for the integrated fault diagnosis," Power delivery. IEEE Transac 15(2):833, 838
29. Spago S (2009) Fuzzy model for decision making in management of the water supply network renewal and development process (in Bosnian). University Dzemal Bijedic, Mostar
30. Jia Z, Gong L, Han J (2009) The application of fuzzy control in strategic decision-making of small and medium enterprises," Measuring technology and mechatronics automation. ICMTMA '09. International conference on, vol 2, pp 602,605, 11–12 Apr 2009
31. Cartina G, Grigoras G, Bobric EC, Comanescu D (2009) Improved fuzzy load models by clustering techniques in optimal planning of distribution networks. In: PowerTech, 2009 IEEE Bucharest, pp 1, 6, June 28 2009–July 2 2009
32. Roos F, Lindah S (2004) Distribution system component failure rates and repair times—an overview. In: Nordic distribution and asset management conference 2004, Finland

Software Tool for Grounding System Design

Adnan Mujezinović

Abstract The purpose of the grounding systems is to ensure safety of substations equipment and personnel in and outside of substation at the maximum fault cur-rents. In order to properly perform their function, grounding system should have low resistance, thus limiting the potential values at the ground surface during the highest values of fault currents. This paper presents mathematical models on which developed software tool for calculation of the grounding system parameters is based. Modules of the developed software tool were used to conduct some calculations which are typical for designing of the grounding systems.

1 Introduction

When designing high voltage substations of all voltage levels, special attention must be paid to the performance of the grounding system. Grounding systems with low grounding resistance is the basis for reliable, secure, and functional operation of the substation [1]. Addition to reliable and safe operation of the substation another important aspect is the safety of personnel inside as well as outside of the substation. [2, 3]. Basic precondition for successful design of grounding system is knowledge of the characteristics of the soil where grounding systems are buried. A precise calculation of the grounding system parameters doesn't allow making an equivalency between non-homogenous and homogenous soil with apparent value of soil resistivity [4].

Grounding systems are composed of the horizontal, vertical and inclined galvanic connected unisolated conductors that in most practical cases form very complex geometries [5]. Length and position of the grounding system conductors depends on the substations gear disposition, surrounding soil resistivity and available space. Due to the large number of different geometric shapes of grounding systems, a simple analytical equation doesn't provide satisfactory accuracy in most

A. Mujezinović (✉)
Faculty of Electrical Engineering, University of Sarajevo, Sarajevo, Bosnia and Herzegovina
e-mail: adnan.mujezinovic@etf.unsa.ba

M. Hadžikadić and S. Avdaković (eds.), *Advanced Technologies, Systems, and Applications*, Lecture Notes in Networks and Systems 3,
DOI 10.1007/978-3-319-47295-9_14

practical cases. Nowadays, design of the grounding system relies on the use of numerical methods for field calculation [6].

In modern literature different numerical approach has been proposed for model-ling grounding systems like finite difference method (FDM), finite element method (FEM) [6–8] and boundary element method (BEM) [9–14]. First two mentioned methods are not suitable for modeling grounding systems because of specific geometry of the problem. Greater weakness of these two methods is need for discretization of entire domain (semi—infinite domain) and great differences in size between subdomains that need to be discretize (small ratio of the radius—length). All this leads to the great matrix systems that need to be solved which is time consuming. On the other hand, by using boundary element method only boundaries of the domain need to be discretized and there is no need for discretization of the infinite boundary. In this paper for modeling grounding system in homogeneous and stratified soil boundary element method was used.

2 Soil Resistivity Measurement

One of the main input data for the grounding system parameters calculation is soil resistivity and soil stratification. Soil resistivity varies from location to location, and should be determined by measurement on each individual location. Soil resistivity can be measured by using numerous methods described in ANSI/IEEE Std. 81-2012 [15]. Most common used method is Wenner's four-probe method. This method is characterized by simplicity, relatively large depth of the measurement and high immunity to noise which could cause a measurement error [5]. On the other hand, interpretation of the results obtain by this method can be complex and require usage of the optimization technique.

2.1 Wenner's Measurement Method

Measurement circuit of the Wenner's methods is composed of four probes, volt-meter, ampermeter and source which frequency is different from the industry frequency, as showed on the Fig. 1.

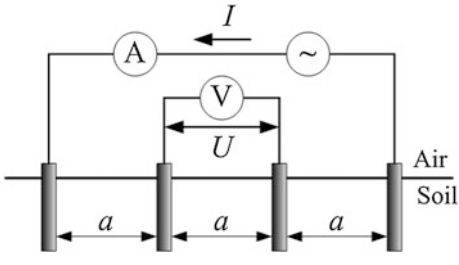

Fig. 1 Wenner's four-probe measurement method

This method is based on the injection of current by current (outer) probes, and voltage drop on voltage (inner) probes are measured by voltmeter. Current injected in the soil is measured by ampermeter. From measured values and distance between probes apparent soil resistivity can be easily calculated by using following relation [16, 17]:

$$\rho(a) = 2\pi a \frac{U}{I} \tag{1}$$

where: a is distance between two adjacent probes, U is value of voltage that is measured on voltmeter and I is value of current measured on amperemeter.

Apparent soil resistivity is equal to the soil resistivity only if soil is homogenous. In order to determine whether the soil is homogeneous, several measurements need to be conducted at different electrode distances. In practice homogenous soil is rear, therefore it is necessary to assume that the soil is layered. When using multi-layer soil model following assumptions must be introduced:

- soil is composed of finite number of layers,
- thickness of all soil layer is finite except for to the lowest layer whose thickness is assumed to be infinite,
- each soil layer is electrically homogeneous [18].

In most practical situations it is sufficient to assume the double layer soil. For double layer soil, apparent soil resistivity can be calculated by using following relation:

$$\rho(a) = \rho_1 \left[1 + 4 \sum_{i=0}^{\infty} \left(\frac{\beta^i}{\sqrt{1 + \left(\frac{2ih}{a}\right)^2}} - \frac{\beta^i}{\sqrt{4 + \left(\frac{2ih}{a}\right)^2}} \right) \right] \tag{2}$$

where h is thickness of the upper layer and β is reflection coefficient that can be calculated as:

$$\beta = \frac{\rho_2 - \rho_1}{\rho_2 + \rho_1} \tag{3}$$

where ρ_1 is soil resistivity of upper layer of soil and ρ_2 is soil resistivity of lower layer of soil.

As it can be noted from Eqs. (2) and (3) apparent soil resistivity is function of three unknown parameters (soil resistivity of upper layer ρ_1, soil resistivity of lower layer ρ_2 and thickness of upper layer h). These three unknown parameters are essential data for proper calculation grounding systems parameters. To determine unknown parameters optimization calculation techniques must be used. Solution of the problem can be obtained by minimizing square error between measured and calculated data [19].

$$f(\rho_1, \rho_2, h) = \sum_{i=1}^{N} \left(\frac{\rho_i^m(a) - \rho_i(a)}{\rho_i^m(a)} \right)^2 \tag{4}$$

where ρ_i^m is apparent soil resistivity given by Eq. (1) and ρ_i is the soil resistivity given by relation (2) and N is number of conducted measurements.

2.2 Gradient Method

Problem presented above is the unconstrained nonlinear optimization problem. Therefore, for minimization of square error function some optimization technique must be employed. In this paper, problem was solved iteratively by using gradient descent method. According gradient descent method, iterative scheme for calculation of unknown parameters has the following form:

$$\begin{Bmatrix} \rho_1^{k+1} \\ \rho_2^{k+1} \\ h^{k+1} \end{Bmatrix} = \begin{Bmatrix} \rho_1^{k} \\ \rho_2^{k} \\ h^{k} \end{Bmatrix} - \gamma \cdot \nabla f \tag{5}$$

where k is number of iteration, γ is constant (0.005 according to [15]) and ∇f is gradient vector of square error.

All components of the gradient vector can be found in [15]. Iterative procedure stops when variation of square error function between two adjacent iterations is lower than premised value.

Presented mathematical model for interpretation of soil measurement data was tested on measured data for two locations listed in Table 1.

Comparison of calculated and measured results for Location 1 is given on Fig. 2.

Value obtained for soil resistivity of upper layer, soil resistivity of lower layer and thickness of the upper layer are given in Table 2.

Table 1 Measurement results

Distance (m)	Location 1	Location 2
	Soil resistivity (Ωm)	
1	79.1	147
2	140	89.7
4	229	78.9
6	271	54.6
8	224	52.9
10	234	45.4

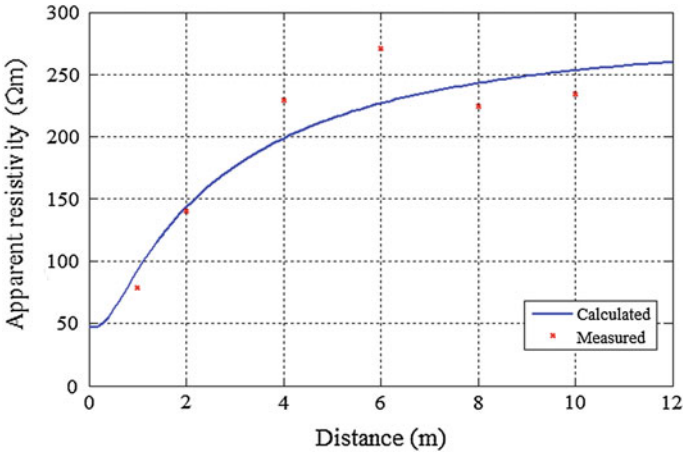

Fig. 2 Comparison of measured and calculated results

Table 2 Results of the calculation

Parameter	Location 1	Location 2
	Value	
ρ_1 (Ωm)	163.31	46.67
ρ_2 (Ωm)	50.75	282.26
h (m)	1.175	0.52

3 Grounding System Parameter Calculation

The electrokinetic phenomena of fault current flow from grounding system to the surrounding soil can be described by Fredholm's integral field equation of the first kind:

$$\varphi(\boldsymbol{q}) = \rho \int_{l} \sigma(\boldsymbol{p}) G(\boldsymbol{p}, \boldsymbol{q}) dl \tag{6}$$

where $\varphi(\boldsymbol{q})$ is the potential of the observation point $\boldsymbol{q}$, $\sigma(\boldsymbol{p})$ is the grounding system current density, ρ is the soil resistivity, $G(\boldsymbol{p},\boldsymbol{q})$ is the Green's function for the adopted soil model and l is the length of the grounding system conductor (grounding system conductor length is much larger then radius therefore radius of grounding conductor can be neglected). For homogeneous soil Green's function have the form:

$$G(\boldsymbol{p}, \boldsymbol{q}) = \frac{1}{4\pi} \left(\frac{1}{|\boldsymbol{p} - \boldsymbol{q}|} + \frac{1}{|\boldsymbol{p}' - \boldsymbol{q}|} \right) \tag{7}$$

where $|\boldsymbol{p}\text{-}\boldsymbol{q}|$ is the Euclidian distance between source point $\boldsymbol{p}$ and observation point $\boldsymbol{q}$ and $|\boldsymbol{p}'\text{-}\boldsymbol{q}|$ is the Euclidian distance between reflected source point $\boldsymbol{p}'$ (point place above ground at height which is equal to the depth below the ground surface of the original source point) and observation point $\boldsymbol{q}$.

For layered soil different Green's functions must be used. Form of the Green's function for layered soil depends of the soil model and the position of the field point and source point [10, 11]. In this paper layered soil was treated by Green's function for homogeneous soil and potential value was corrected by using correction factors given by [20].

Integral field Eq. (6) can be solved numerically by using indirect boundary element method. According to the BEM procedure after discretization of the grounding system geometry and collocation method at the point, potential of the observation point in the discrete form can be written as:

$$\varphi(\boldsymbol{q}) = \rho \sum_{e=1}^{n_e} \sum_{m=1}^{n_g} \sum_{i=1}^{n} \left(\sigma_i^e \cdot \psi_i(\xi_m)\right) G^e(\xi_m, \boldsymbol{q}) \det J(\xi_m) w_m \tag{8}$$

where n_e is the number of boundary elements, n_g is the number of Gauss—Legendre's integration points, n is number that dependents on the geometry and current density approximation, $\det J(\xi)$ is determinate of Jacobean matrix, $\psi_i(\xi)$ is used shape function, w_m is m-th weighting coefficient.

Fault current I_F that enters into grounding system leaks to the surrounding soil. This can be written in the following form:

$$\sum_{e=1}^{n_e} \sum_{i=1}^{n} \left(\sigma_i^e \cdot \psi_i(\xi_m)\right) l_i = I_F \tag{9}$$

Since, all conductors of the grounding system are on the same potential φ_G, previous equation can be written in the following matrix form [21]:

$$\begin{bmatrix} R_{11} & R_{12} & \cdots & R_{1n_{cp}} & -1 \\ R_{21} & R_{22} & \cdots & R_{2n_{cp}} & -1 \\ \vdots & \vdots & \ddots & \vdots & \vdots \\ R_{n_{cp}1} & R_{n_{cp}2} & \cdots & R_{n_{cp}n_{cp}} & -1 \\ l_1 & l_2 & \cdots & l_{n_{cp}} & 0 \end{bmatrix} \cdot \begin{Bmatrix} \sigma_1^e \\ \sigma_2^e \\ \vdots \\ \sigma_{n_{cp}}^e \\ \varphi_G \end{Bmatrix} = \begin{Bmatrix} 0 \\ 0 \\ 0 \\ 0 \\ I_F \end{Bmatrix} \tag{10}$$

The matrix Eq. (10) is solved iteratively by using GMRES algorithm. Previously presented mathematical model was used for calculation of the grounding system parameters of two grounding systems of typical geometry.

3.1 Case Study 1

Presented mathematical model was used for calculation of the 10(20)/0.4 kV substation grounding system. Analysed grounding system is placed in homogeneous soil and is composed of the two contours placed at the different depth, four grounding electrodes connected to inner contour. Geometry of analysed grounding system is given on the Fig. 3.

Value of the fault current was assumed to be 300 A and soil resistivity is 100 Ωm. Results of the value of the potential distribution on the earth surface and touch voltage distribution is given on the Figs. 4 and 5, respectively.

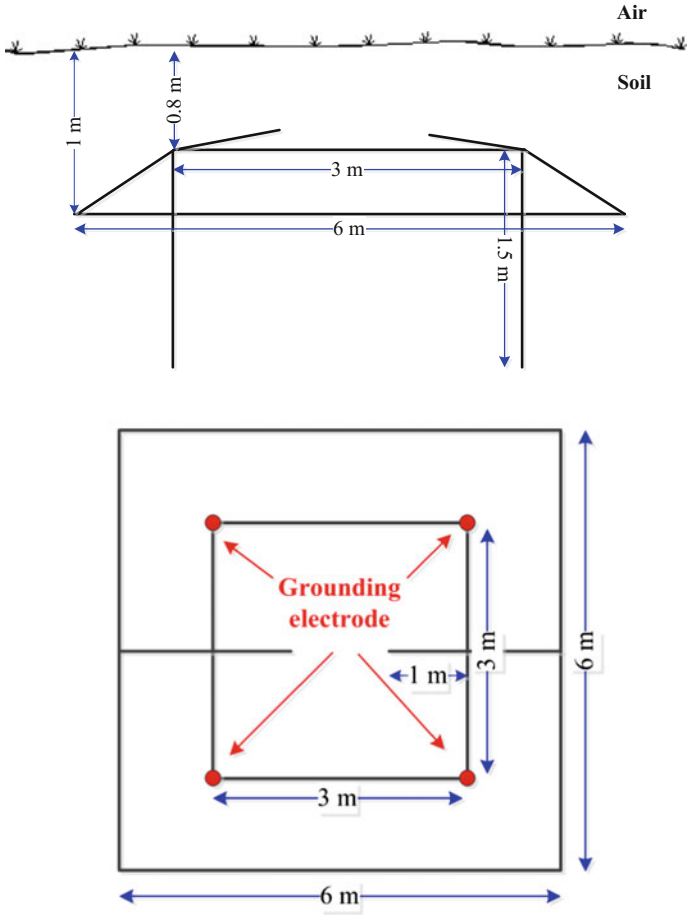

Fig. 3 Geometry of analysed grounding system

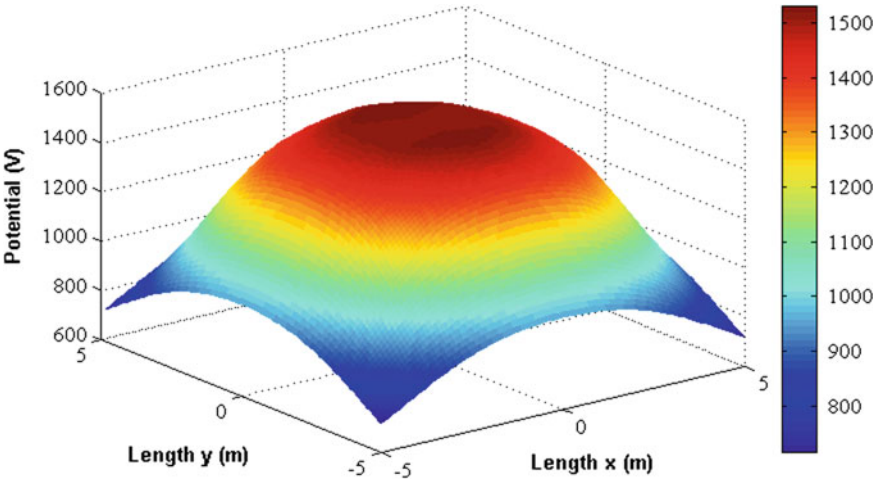

Fig. 4 Potential distribution on the earth surface

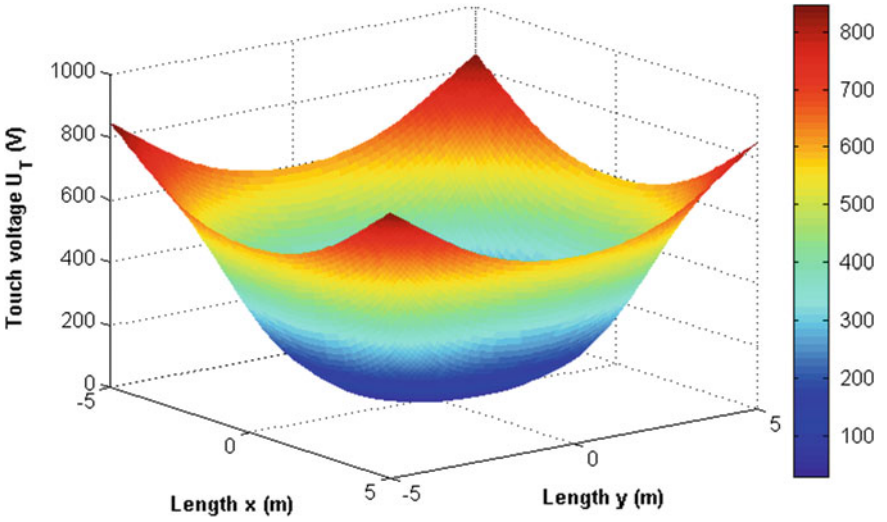

Fig. 5 Touch voltage distribution

Results of the GPR and grounding resistance obtained by the presented model were comparison with results obtained by using analytical approach. Comparison of the results is given in Table 3.

Table 3 Comparison of the results

	Presented model	Analytical model
Grounding resistance	5.208 Ω	8.08 Ω
GPR	1562.6 V	2424 V

3.2 Case Study 2

Previously analysed geometry is typical for the distribution network substations. In high voltages substations grounding system are mostly design in form of mesh. Therefore, in this section calculation of the grounding system parameters of the mesh geometry was calculated. Geometry and dimensions of the analysed grounding system is given on the Fig. 6.

Value of the fault current was assumed to be 10 kA. Soil was assume to be double layered where resistivity of upper layer is 75 Ωm and thickness of the upper layer is 2 m, and soil resistivity of lower layer was 150 Ωm. Results of the value of the potential distribution on the earth surface is given on the Fig. 7 while comparison of the grounding resistance and GPR with analytical approach is given in Table 4.

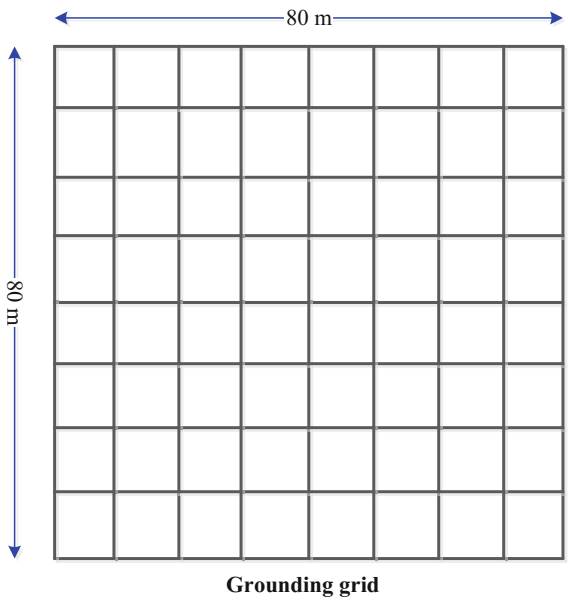

Fig. 6 Geometry of analysed grounding system

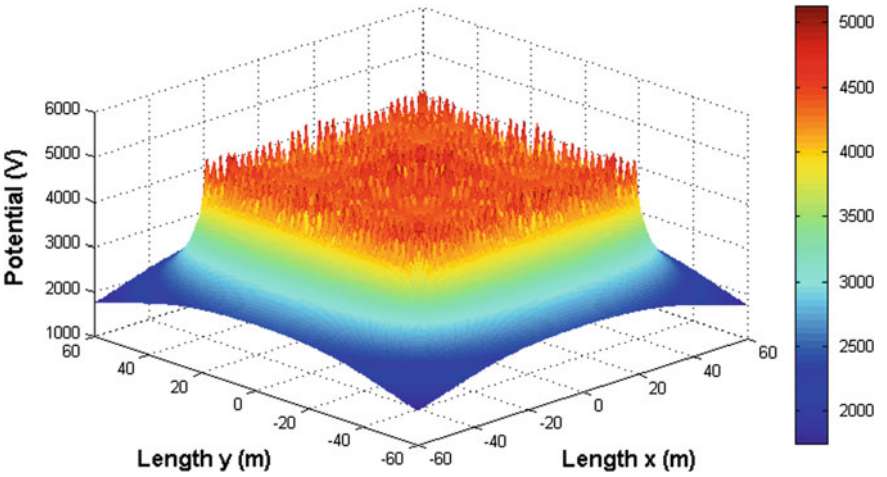

Fig. 7 Potential distribution on the earth surface

Table 4 Comparison of the results

	Presented model	Analytical model
Grounding resistance	0.446 Ω	0.460 Ω
GPR	4.459 kV	4.460 kV

4 Calculation of the Transferred Earth Potentials

In urban area situation can be further complicate due to other metallic infrastructure in the vicinity of grounding systems such as metallic pipelines, rails, metallic fences. When in the vicinity of the grounding system is other metal infrastructure, flow of the fault current through the grounding system may cause unwanted transfer of earth potential. In this situation transferred earth potential must be calculated.

Presence of the passive electrode requests the upgrade matrix Eq. (10) in order to calculate the potential of passive electrode. Since there is no leaking of the current from passive electrode into the surrounding soil, it can be written [22]:

$$\sum_{e=1}^{n_e}\sum_{i=1}^{n}\left(\sigma_i^{ePAS}\psi_i(\xi_m)\right)\cdot l_i^{ePAS}=0 \tag{11}$$

Previous equation is necessary to add on the matrix Eq. (10), in order to calculate potential of the passive electrode. New matrix equation has the following form [22]:

$$\begin{bmatrix} R_{11} & R_{12} & \cdots & R_{1n_{cp}} & -1 & 0 \\ R_{21} & R_{22} & \cdots & R_{2n_{cp}} & -1 & 0 \\ \vdots & \vdots & \ddots & \vdots & \vdots & \vdots \\ R_{n_{cp}1} & R_{n_{cp}2} & \cdots & R_{n_{cp}n_{cp}} & 0 & -1 \\ l_1 & l_2 & \cdots & 0 & 0 & 0 \\ 0 & 0 & \cdots & l^{PAS}_{n_{cp}} & 0 & 0 \end{bmatrix} \cdot \begin{Bmatrix} \sigma^e_1 \\ \sigma^e_2 \\ \vdots \\ \sigma^e_{n_{cp}} \\ \varphi_G \\ \varphi_P \end{Bmatrix} = \begin{Bmatrix} 0 \\ 0 \\ \vdots \\ 0 \\ I_F \\ 0 \end{Bmatrix} \tag{12}$$

4.1 Case Study 3

In this section calculation example of the transfer of earth potential on the railway tracks close to the grounding system, was conducted. Geometry of analysed system is given on the Fig. 8. Grounding system and railway tracks are placed in homogeneous soil with resistivity 100 Ωm. Value of the fault current was assumed to be 3 kA.

Potential distribution on the earth surface and distribution of touch voltage are given on the Figs. 9 and 10, respectively.

Results of calculation of the grounding resistance, GPR and potential of the passive electrode are given in Table 5.

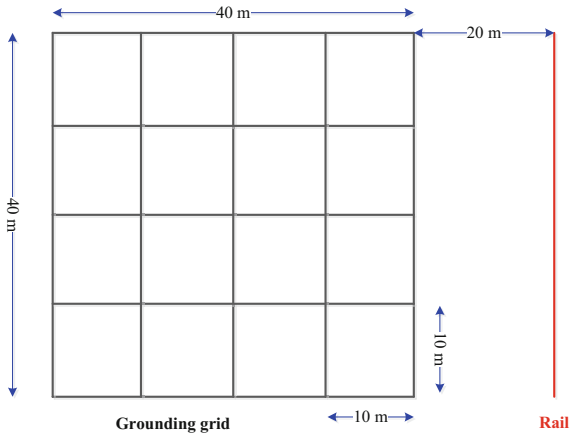

Fig. 8 Geometry of analysed problem

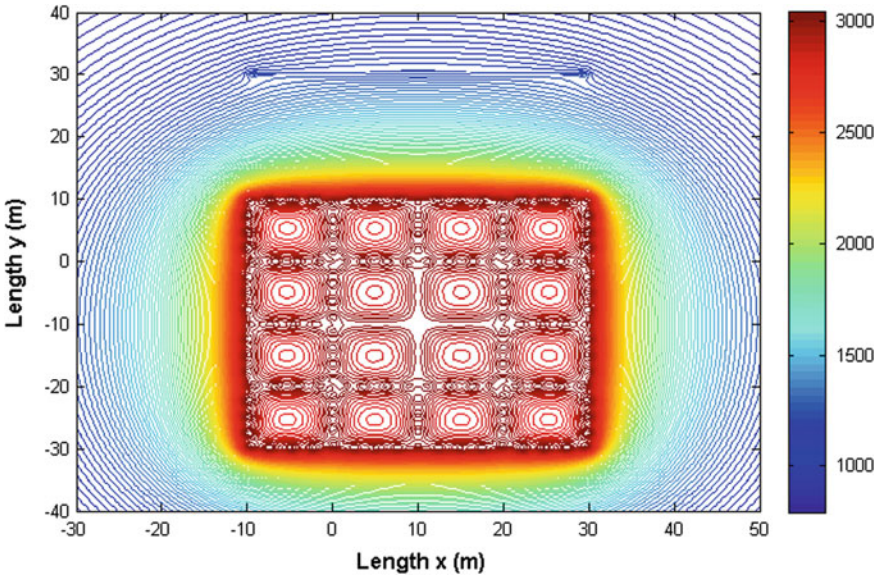

Fig. 9 Potential distribution on the earth surface

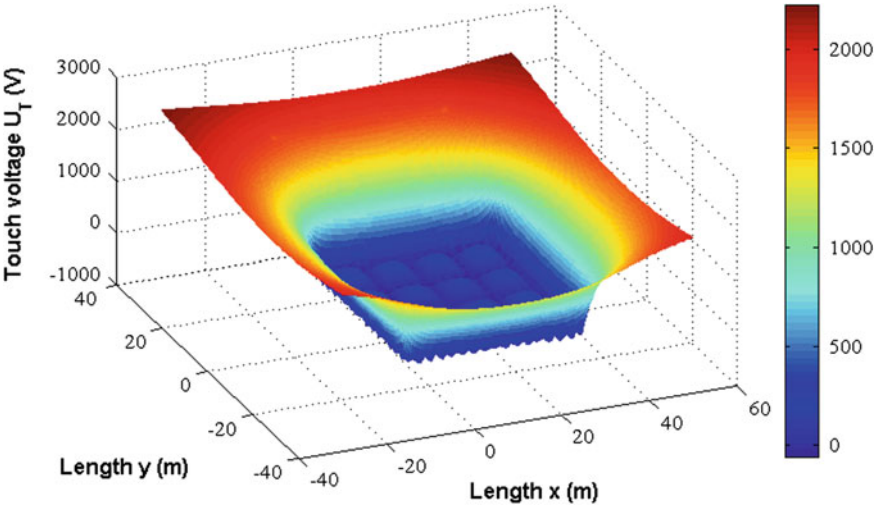

Fig. 10 Touch voltage distribution

Table 5 Results of the calculation

Parameter	Presented model
Grounding resistance	0.999 Ω
GPR	2999.94 V
Passive electrode potential	1212.71 V

5 Conclusion

In this paper, mathematical models of the software tool for grounding system analysis and design has been presented. Given models were used for analysis and calculations of layered soil parameters, potential distribution on the earth surface and touch voltage distribution for cases when grounding system is placed in homogeneous and double layered soil. Also, calculation of the transferred earth potential was done when other metallic infrastructure is placed in the vicinity of grounding system. These calculations are essential for grounding system analysis and design.

References

1. Mujezinović A (2011) Analysis of discontinuity of electrical conductivity of soil on grounding resistance. Thesis, Faculty of Electrical Engineering, University of Sarajevo, MSc (in Bosnian)
2. Lukovac L (2014) Analysis of measurement and test methods for grounding system of high-voltage substation with a focus on the measurement of grounding resistance in high voltage substations. Thesis, Faculty of Electrical Engineering, University of Sarajevo, MSc (in Bosnian)
3. IEEE Std. 80-2000, "IEEE Guide for Safety in AC Substation Grounding", IEEE, New York, 2000
4. Haznadar Z, Berberović S, Vujević D, Markovinović D, Žanić N, Žic Z (1981) Touch Voltage and Grounding System Potential Distribution in Power Systems. Journal of Energy 30(7–8):303–312 Zagreb
5. Kokoruš M, Mujezinović A (2014) Computer aided design of the substation grounding system. In: International conference on high voltage engineering and application (ICHVE), Poznan
6. Mujezinović A, Muharemović A, Muharemović A, Turković I, Bajramović Z (2012) Application of finite element method in calculation of large and complex grounding systems. In: IEEE international conference and exposition on electrical and power engineering (EPE). Romania, Iasi, pp 688–692, Oct 2012
7. da Luz MVF, Dular P (2007) Analytical and finite element modeling of grounding system. IX International Symposium on Lightning Protection SIPDA, Brazil, Foz do Iguacu
8. Nahman J, Paunovic I (2007) Effect of the local soil nonuniformity upon performances of grounding grid. IEEE Trans Power Deliv 22(4)
9. Bottausicio O, Zucco M (2000) A numerical model for the design of complex grounding systems. In: 9th international IGTE symposium on numerical field computation. Austria, Graz, pp 258–263
10. Berberović S, Haznadar Z, Štih Ž (2002) Method of moments in analysis of grounding systems. Eng Anal Boundary Elem 27(3):351–360
11. Colominas I, París J, Navarrina F, Casteleiro M (2012) Improvement of the computer methods for grounding analysis in layered soils by using high - efficient convergence acceleration techniques. Adv Eng Softw 44(1):80–91
12. Navarrina F, Colominas I, Casteleiro M (2003) Why Do Computer Methods For Grounding Analysis Produce Anomalous Results? IEEE Trans. on Power Delivery 18(4):1192–1202

13. Colominas I, Navarrina F, Casteleiro M (2007) Numerical Simulation of Transferred Potentials in Earthing Grids Considering Layered Soil Models. IEEE Transaction on Power Delivery 22(3):1514–1522
14. Zildžo H, Muharemović A, Matoruga H, Mujezinović A (2011) Application of coupled 1D and 2D isoperimetric discontinuous boundary elements in the calculation of large grounding systems. XXIII International Symposium on Information, Communication and Automation Technologies, Sarajevo
15. IEEE Std. 81-2012. (Revision of IEEE Std. 81-1983) "Guide for measuring earth resistivity, ground impedance, and ground surface potentials of a ground system", Dec. 2012
16. Muharemović A (2004) Electrical measurement. University of Sarajevo, Sarajevo, Faculty of Electrical Engineering
17. Muharemović A, Đokić B (1999) Electric soil resistivity measurement method on the depth up to 100 m in desert conditions. In: 4th conference Bosnia-Herzegovina committee of CIGRE, Neum, Sept 1999
18. Milun S, Gotovac S (1989) Static Analysis of Results of Vertical Electrical Sounding on Horizontally Inhomogeneous Soil. Journal of Electrotechnics 32(3–4):247–252 Bograd
19. Dawalibi F, Blattner CJ (1984) Earth Resistivity Measurement Interpretation Technique. IEEE Trans Power Appar Syst 103(2):374–382
20. Nahman J, Paunovic I (2010) Mesh Voltages at Earthing Grids Buried in Multi-layer Soil. Electr Power Syst Res 80(5):556–561
21. Zildž H (2004) Computer Methods in Power Engineering. University of Sarajevo, Sarajevo, Faculty of Electrical Engineering
22. Zildzo H, Muharemovic A, Turkovic I, Matoruga H (2009) Numerical Calculation of Floating Potentials for Large Earthing System. XXII International Symposium on Information, Communication and Automation Technologies, Sarajevo

Bosnia and Herzegovina's Power System: From the First Luminaires to the Modern Power System. Part I: History

Samir Avdaković, Anes Kazagić, Mirsad Hadžikadić and Aljo Mujčić

Abstract This two-part chapter presents historical overview of the development of Bosnia and Herzegovina's (B&H) power system with its trends and challenges in the future. B&H has a very wealthy and turbulent history of power system development which went through different development phases over time. It is possible to single out some very successful and progressive phases during more than 120 years. A very interesting period in this area is the period up to the First World War, when development of B&H power industry followed the development trends in Europe and USA. Also, the period after the Second World War presents a period of intensive construction of power plants, transmission and distributions grids, and an intense increase of power consumption. At the end of the twentieth century, the B&H power system experienced a significant destruction and power consumption in 2010 came again to the level of consumption from 1991. Today, B&H power system has been renewed and became a modern power system which is the part of the European power system. Also, in this paper we present some important dates and events related to the development of B&H power system, as well as trends and challenges in the sector of power distribution and power generation systems, with presentation of related specific technical indicators.

S. Avdaković (✉)
University of Sarajevo, Zmaja od Bosne bb, Kampus Univerziteta,
71000 Sarajevo, Bosnia and Herzegovina
e-mail: samir.avdakovic@etf.unsa.ba

A. Kazagić
EPC Elektroprivreda BiH d.d. Sarajevo, Vilsonovo Setaliste 15,
71000 Sarajevo, Bosnia and Herzegovina
e-mail: a.kazagic@elektroprivreda.ba

M. Hadžikadić
Complex Systems Institute, UNC Charlotte, Charlotte, USA
e-mail: mirsad@uncc.edu

A. Mujčić
Univesity of Tuzla, Tuzla, Bosnia and Herzegovina
e-mail: aljo.mujcic@gmail.com

M. Hadžikadić and S. Avdaković (eds.), *Advanced Technologies, Systems, and Applications*, Lecture Notes in Networks and Systems 3,
DOI 10.1007/978-3-319-47295-9_15

1 Introduction

Bosnia and Herzegovina (B&H) has a long tradition in the area of electrical engineering. The use of electricity in B&H began in 1888 and it is possible to identify different periods of power system development through the history. Rich with significant coal reserves and water potentials, B&H, over the decades, was subject of interest of professional and scientific community, as well as different investors. Innovation and diligence of B&H experts in the area of electrical engineering was recognized at the end of the 19th century, when in collaboration with engineers from Europe they started working on a relatively complex projects for this time period. Also, general economic conditions that prevailed in different periods in Europe and the world, had an impact to the intensity of power sector development in B&H, so the project implementations (electrification of settlements, construction of power plants, etc.) were not always in accordance with the project plans. Available resources in B&H are still not fully utilized, and the construction of new power plants currently has no significant intensity. These and similar projects now represent a development opportunity for B&H and all activities in this area (especially in the exploitation of water resources) should be accelerated. The short analysis of the available data related to the development of B&H power system is presented in this paper. First, the data concerning the development of the power sector in B&H has been compared with available data on the development of power sector in the other countries, and the results show that the development of B&H power system generally follows the trends from Western Europe and USA. The data of B&H power consumption in the period from 1946 to 2010 is also presented in this paper, from which it is possible to identify different periods of intensity in power consumption. Since the power consumption is closely related to the overall social development, periods of significant social and economic progress can be recognized from this data.

The rest of the paper is organized as follows: significant dates and events related to the development of power systems are presented in Sect. 2 (based on [1–3]), while Sect. 3 presents some specific indicators and technical details related to B&H power system (based on [4–7]. A review of current affairs and future challenges is presented in Sect. 4, while Sect. 5 is reserved for conclusions.

2 Development of Power Systems—Significant Dates and Events

In the decades-long history, development of power systems is marked with significant dates and events. Although A. Volta in 1799 (Fig. 1) finds first electrochemical cell (electrical battery) [1], the efforts of scientists and engineers made a breakthrough only more than 70 years later, when Z. Gramme (Fig. 1) constructed the first DC electric generator (according to [2] in 1873) in 1872. This discovery

Fig. 1 Alessandro Volta (1745–1827), Zénobe Gramme (1827–1901), Thomas Alva Edison (1847–1931) (http://en.wikipedia.org/)

enabled the production of relatively large amount of electrical power compared to the active power which then could be extracted from electrochemical elements. This generator had all characteristics of today's DC generators [1]. Edison, ten years later (1882) installs lighting in the narrow part of the New York network using DC voltage—110 V, which is considered the beginning of the era of distribution power networks [1]. Two years ago (1880), Edison patented a practical and simple system of distribution of electricity using the main and secondary lines. Principles of this system (based on Edison research) represent the basic principles for power distribution in cities and settlements which are still used. Edison's efforts, as well as efforts of other scientists in this period, yielded results at the end of 1882, putting into operation the first public power plant with six DC generators of active power of approximately 90 kW in the Pearl Street, New York.

Two years after the commissioning of the new power plant, the distribution network has already connected about 11,000 light fixtures and about 600 electric motors. At the same time in Germany, Desprez and Muller have put into work DC power transmission between the town of Miesbach and Munich using the 2000 V network. Electricity in Miesbach is produced by Gramme power generator of about 1.4 kW. In the next few years a large number of DC power plants were built, but with a relatively small power of generators that are able to meet the demand for electricity of a few buildings and lighting.

In 1888, Nikola Tesla (Fig. 2) published his discovery of multi-phase asynchronous motor based on rotating magnetic field, which was a turning point in terms of the application of alternating current. Tesla's patents included the multi-phase generators, multi-phase transformers, multi-phase power transmission, as well as multi-phase and single-phase asynchronous motors. The event that took place in 1891 in Germany, which was related to a successful first AC power transmission from Laufen to Frankfurt, with a total length of 179 km and 12 kV voltage level, presented a real impetus to the development of three-phase alternating system.

Fig. 2 Nikola Tesla (1856–1943) (http://en.wikipedia.org/)

By the end of the 19th century both, DC and AC systems, still existed and there was a need for unification/standardization. In 1895, Nikola Tesla put into operation three two-phase generators (3.7 MW and 2.4 kV) on Niagara Falls, which was the first 'large' hydro power plant (HPP) in the world. The intensive industrial development had an impact on an increase of power demand, which required higher voltage levels of transmission grid.

In the period up to the Second World War generator power and voltage levels of transmission power lines were in a growing trend. 110 kV networks began operating in Germany and the United States before the Second World War, while in the USA in early twenties a network of 220 kV was put into operation. The highest voltage level before Second World War was in the area of Los Angeles (287.5 kV). 400 kV network comes in 1952 with putting into operation a 1000 km long transmission line between HPP substations Harsprangert and Hallsberg (Sweden).

In 1957, in the USSR, 500 kV transmission line was put into operation, and in 1965, in Canada, 735 kV transmission line was also put into operation. Development of the transmission using a DC high-voltage begins in 1954 by commissioning of 100 km long, 100 kV cable line on the Baltic Sea. Immediately after that, in 1963, 470 km long ± 400 kV DC transmission line was put into operation in the USSR [3].

3 Development of B&H Power System

The development of power industry in our country largely followed the trends and technical developments in Western European countries and the USA. According to written documents in B&H, the beginning of electrification was first recorded in 1888 in Zenica (construction of the first electric lighting), and the first public

thermal power plant (TPP) of 220 kW was built in 1895 in Sarajevo [4]. The first HPP in B&H was built in 1899 on the river Pliva with capacity around 7 MW (Elektrobosna), and it was the largest hydroelectric plant in Europe in that period (according [5]). Six small hydropower plants were built during this period:

- Elektrobosna Jajce,
- Plava voda Travnik,
- Kanal Una Bihać,
- Krušnica Bosanska Krupa,
- Trapisti (Delibašino selo, Banja Luka) and
- Hrid Sarajevo,

These hydropower plants, with the existing smaller power plants, met the power demand [5]. Until 1918, there had been a total of 47 power plants in operation, 6 of them were HPP and 41 TPP with total capacity of 17,007 kW. Only 1.1 % of the villages in B&H, in 1919, were electrified. Table 1 provides an overview on the number and installed capacities of power plants in B&H by the end of 1918 (based on [4]). The total number of power plants in B&H by the end of 1938 was 77, with total capacity of 34 MW. A more detailed overview is provided in Table 2 (according to [4]). The period between the two world wars in B&H, as well as in other countries of the world, was characterized with economic crisis, high unemployment and not so intensive economic development. In the context of the development of power industry, efforts were recorded to increase the installed capacity of TPP in mines. There are also records of efforts of municipal governments to build smaller municipal power plants and to electrify villages.

Also, private entrepreneurs continued activities to build power plants in B&H (HPP Kraljeva Sutjeska, 1921; HPP Čajniče, 1928; HPP Široki Brijeg, 1935; HPP Ljuta—Konjic, 1936; HPP Bugojno, 1938). According to the assessment of water resources, which was compiled in 1921 in the former Yugoslavia, B&H had approximately 595 MW or 23 % of total water resources in Yugoslavia [4].

Electrification of settlements in our country was carried out continuously with changing intensity during this period: in 1945, 16 % of the settlements were

Table 1 Power plants constructed up to 1918 [4]

Administrative unit (county)	Number of power plants			Power plants generating capacity		
	HPP	TPP	Total	HPP (kW)	TPP (kW)	Total (kW)
Banja Luka	1	12	13	535	1891	2426
Bihac	2	2	4	256	675	931
Mostar	–	–	–	–	–	–
Sarajevo	1	11	12	3	1646	1649
Travnik	2	10	12	6500	3491	9991
Tuzla	–	6	6	–	2010	2010
Total B&H	6	41	47	7294	9713	17007

Table 2 Power plants constructed up to 1938 [4]

Administrative unit (county)	Number of power plants		Power plants generating capacity			
	HPP	TPP	Total	HPP (kW)	TPP (kW)	Total (kW)
Banja Luka	4	13	17	7644	3059	10703
Bihac	2	3	5	200	1150	1350
Mostar	2	2	4	22	2540	2562
Tuzla	–	12	12	–	5513	5513
Doboj	–	9	9	–	1638	1638
Sarajevo	2	13	20	4207	4683	8840
Zenica	2	8	10	280	3135	3415
Total B&H	12	65	77	12353	21663	34021

Table 3 Construction of line in B&H [6]

[kV]	Name	Year
10	TE Sarajevo-Ilidža i TE Kreka-Tuzla	1920
30	Mostar–Metkovic	1927
35	Kreka–Solana Simin Han	1930
110	Zenica–Doboj	1948
220	Mostar-HE Zakucac	1958
400	Tuzla-Ugljevik-Ernestinovo and Mostar–Konjsko	1976

electrified, while in 1980 this percentage has risen to 93 % [6]. Along with the electrification and growth of power consumption, transmission network development was also continued, connecting production facilities with centers of consumption. In the early twenties of the last century the lines of voltage levels of 5, 6 and 10 kV were in operation, and an overview of the construction of the first lines of higher voltage levels is presented in Table 3 (according to [6]). The most important power facilities were built in the period after Second World War until the end of the eighties. They are characterized with significant power capacity and large construction works. HPP-s and TPP-s built in this period are presented in Table 4.

It should be noted that the after the reconstruction and modernization of some power plants presented in Table 4 available capacity has increased, and some of the power plants are out of operation. B&H power system is one of the smaller systems in Europe and is connected to the power systems of neighboring countries (and other members of the UCTE-ENTSO-E (European Network of Transmission System Operators for Electricity).

Currently, control of B&H power system is the responsibility of the Independent System Operator of Bosnia and Herzegovina (ISO) and together with the Slovenian

Table 4 Power plants constructed in the period from1945 to 1990 [4]

HPP			TPP		
Name	Capacity (MW)	Year	Name	Capacity (MW)	Year
Trebinje I	2 × 54 + 1 × 60	1968	Tuzla I	64	1964
Dubrovnik	2 × 105	1965	Tuzla II	100	1966
Trebinje II	1 × 8	1981	Tuzla III	200	1971
Čapljina	2 × 215	1979	Tuzla IV	200	1974
Rama	2 × 80	1968	Tuzla V	215	1978
Jablanica	6 × 24	1955	Kakanj I	64	1956
Grabovica	2 × 57	1982	Kakanj II	64	1960
Salakovac	3 × 70	1982	Kakanj III	110	1969
Mostar	3 × 25	1987	Kakanj IV	110	1977
Jajce I	2 × 24	1957	Kakanj V	230	1988
Jajce II	3 × 10	1954	Gacko I	300	1983
Bocac	2 × 55	1981	Ugljevik I	300	1985
Total	1.725	–	Total	1.957	–

and Croatian power systems makes control block SLO-HR-BIH within the UCTE network. By connecting the first and second synchronous zones UCTE (10.10.2004.), the B&H power system became again an important transit system. Today (2015), the total installed capacity of power plants in B&H is 3963.96 MW (HPP 2048 MW and TPP 1765 MW). The installed capacity of small hydropower plants in B&H is 59.73 MW, while 91.23 MW are installed in industrial power plants [7].

The power consumption in B&H showed significant growth in the period from 1970 to 1990, after which as a result of the war, the whole country, its economy and the entire power system suffered significant destruction. In 2010, power consumption in B&H reached 1990 levels (Fig. 3), and the period from 1995 to 2005 presents a period of intensive restoration of the power system. Today, the B&H power system is a part of the European interconnected power system with almost all the features of modern power system.

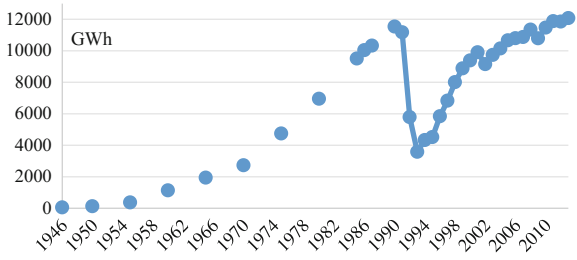

Fig. 3 B&H power consumption in the period between 1946 and 2013 [8]

4 Conclusion

B&H power sector, in its decades-long tradition, went through different periods and intensities of development. Based on available data it is possible to identify two very intense periods of development. The first period of intensive development in this area is the period up to the First World War (1888–1918) when significant number of power plants were built. After First World War the development in power sector has low-intensity, and after Second World War B&H has experienced an expansion in this area. In the period from 1945 to 1988 the most important power plants which are mostly still in operation were built. Constructions of these power plants (such as HPP Jablanica, HPP Rama, etc.) were very complex projects and they represent very serious construction works. Unfortunately, history has not been kind to B&H, and as a result of this the power system in the past experienced total destruction. However, diligence and expertise of B&H engineers always exceeded these problems by finding adequate solutions to the challenges that were before them. Major trends and challenges that have been identified for the B&H power system are explained in [9].

References

1. Požar H (1983) Snaga i energija u elektroenergetskim sistemima. Informator, Zagreb
2. Wikipedia
3. Rajakovic N (2002) Analiza elektroenergetskih sistema I. Elektrotehnički fakultet Beograd, Beograd
4. Rajakovic N (1988) 100 godina električne energije u Bosni i Hercegovini. Elektroprivreda Bosne i Hercegovine, Sarajevo
5. Komisija/povjerenstvo za očuvanje nacionalnih spomenika BiH (http://kons.gov.ba/)
6. http://elprenosbih.ba/
7. Državna regulatorna komisija za električnu energiju (DERK) http://www.derk.ba/
8. Avdakovic S, Muftic Dedovic M, Dautbasic N Impact of air temperature on active and reactive power consumption—Sarajevo case study. Int J Environ Res (under review)
9. Avdakovic S, Kazagic A, Hadzikadic M, Mujcic A (2016) Bosnia and Herzegovina power system: From the first luminaires to the modern power system. Part II: Trends and challenges. In: International symposium on innovative and interdisciplinary applications of advanced technologies (IAT), Neum, Bosnia and Herzegovina, 26–29 May 2016

Bosnia and Herzegovina Power System: From the First Luminaires to the Modern Power System. Part II: Trends and Challenges

Samir Avdaković, Anes Kazagić, Mirsad Hadžikadić and Aljo Mujčić

Abstract This two-part chapter presents historical overview of the development of Bosnia and Herzegovina's (B&H) power system with its trends and challenges in the future. B&H has a very wealthy and turbulent history of power system development which went through different development phases over time. It is possible to single out some very successful and progressive phases during more than 120 years. A very interesting period in this area is the period up to the First World War, when development of B&H power industry followed the development trends in Europe and USA. Also, the period after the Second World War presents a period of intensive construction of power plants, transmission and distributions grids, and an intense increase of power consumption. At the end of the twentieth century, the B&H power system experienced a significant destruction and power consumption in 2010 came again to the level of consumption from 1991. Today, B&H power system has been renewed and became a modern power system which is the part of the European power system. Also, in this paper we present some important dates and events related to the development of B&H power system, as well as trends and challenges in the sector of power distribution and power generation systems, with presentation of related specific technical indicators.

S. Avdaković (✉)
University of Sarajevo, Zmaja od Bosne bb, Kampus Univerziteta,
71000 Sarajevo, Bosnia and Herzegovina
e-mail: samir.avdakovic@etf.unsa.ba

A. Kazagić
EPC Elektroprivreda BiH d.d. Sarajevo, Vilsonovo Setaliste 15,
71000 Sarajevo, Bosnia and Herzegovina
e-mail: a.kazagic@elektroprivreda.ba

M. Hadžikadić
Complex Systems Institute, UNC Charlotte, Charlotte, USA
e-mail: mirsad@uncc.edu

A. Mujčić
Univesity of Tuzla, Tuzla, Bosnia and Herzegovina
e-mail: aljo.mujcic@gmail.com

M. Hadžikadić and S. Avdaković (eds.), *Advanced Technologies, Systems, and Applications*, Lecture Notes in Networks and Systems 3,
DOI 10.1007/978-3-319-47295-9_16

1 Introduction

Development of power systems over time following different organizational forms of the entire power sector, different ownership structure and organization of large power companies. In the last two decades, significant impact on the power sectors had the restructuring, deregulation and opening of the electricity market. Developed countries have significant experience in this area, while in B&H, some of these processes are still ongoing. On the other hand, requirements for more intensive construction and the use of renewable energy are set and for B&H, so that today in B&H large number projects are in preparation (wind power plant, photovoltaic power plant, etc.). Also, an interesting scientific and technical analysis can be found in the areas of establishing a system for monitoring power quality, the integration of electric vehicles in power systems, and generally, applications of new technology in all segments of power distributions and generation systems.

This paper is the continuation of [1]. Trends and challenges in power distribution systems is discussed in Sect. 2, while Sect. 3 deals with trends and challenges in power generations. Section 4 is reserved for concluding remarks.

2 Trends and Challenges in Power Distribution Systems

Power distribution systems worldwide in recent years experienced significant changes. By integrating a large number of distributed generators, distribution networks becoming a (relatively) more complex distribution systems. Also, increasingly stringent requirements related to power quality require from the operators to change the current approach, significant investment in the power distribution system and the application of modern measurement and control devices. These changes are also apply to power distribution systems in B&H. However, achieving the desired level or the value of certain parameters is not possible overnight, so that many activities are long-term processes with significant investments.

The above-mentioned processes have led to major changes in the way the organization and functioning of the power distribution companies, as well as their relationship with the consumers. The quality of services that companies provide customers increasingly gaining in importance. With the introduction of regulations and standards governing the quality of services in distribution, as well as systems for measuring and monitoring the quality parameters, power distribution companies are encouraged to raise the power quality and services. On the other hand, distribution system operators pay special attention to the losses of electricity, which is an important technical and economic indicator.

2.1 Losses in Power Distribution Systems [2]

The power losses in distribution system have a significant influence on the efficiency of the whole electricity supply system. Based on [2], for some European country average losses in transmission networks are between 1 and 2.6 % and the losses in distribution networks are between 2.3 and 11.8 %. Today, the power losses in distribution system JP EPBIH is about 10 %, while the total power losses for B&H have a slightly higher percentage (taking into account the indicators of other two operators in B&H). Structure of power losses in distribution systems JP EPBIH is presented in Table 1. These indicators are the result of the measurement data, appropriate models of distribution network and load flow and losses calculations. As can be seen, the most significant losses in JP EPBIH were identified in the low voltage networks (about 61.68 %). This is an expected result given that the average length of the low voltage network is relatively large (about 3.2 km/transformer).

In the other words, JP EP BIH in 2011 was 7543 transformer substations 10(20)/0.4 kV and the total length of low voltage network about 24,190 km. Also, transformers represent significant sources of power losses (about 22.68 %), in particular transformer iron losses (16.20 %). This is a result of the installation of large number power transformers with higher values of rated powers. Finally, losses in power distribution systems, JP EP BiH in the period from 1996 with trends and projections to 2030 is presented on Fig. 1.

Table 1 Structure of losses in power distribution systems JP EPBIH

	MWh	%
Losses in distribution lines 35 kV	10,579.11	2.67
Losses in distribution lines 20 kV	1,888.53	0.48
Losses in distribution lines 10 kV	49,543.39	12.49
Lossse in transformers (iron losses)	64,262.93	16.20
Losses in transformers (copper losses)	25,704.88	6.48
Losses in low-voltage grid	244,622.45	61.68
Total	396,601.29	100

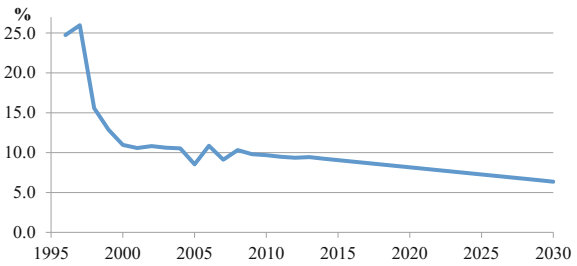

Fig. 1 Losses in power distribution systems, JP EP BiH trends and projections by 2030 [9]

Very high level of power losses in distribution networks in the period from 1996 to 2000 was the consequence of the war destruction. The planned implementation of systematic measures in the coming period would lead to the level of power losses about 6 %. System measures include the implementation of modern system of measurement (AMR), shortening the length of the low voltage network, reactive power compensation, etc.

2.2 *Quality of Electric Power Supply—Reliability Indices [3]*

A strong impetus for companies to achieve the required level of quality is the introduction of financial penalties that companies have to bear in cases when some specific indicators does not meet the quality standards. In JP EPBIH, since 2005 is established a system for monitoring quality of electric power supply—reliability indices (System Average Interruption Duration Index (SAIDI), System Average Interruption Frequency Index (SAIFI)). Reliable supply of electricity is one of the most important parameters of quality of electricity supply. According to most of the world statistics of operating events, 80–90 % of the interruption of power supply occurs in the distribution system. Therefore, the greatest responsibility for the reliability of power supply goes to the operators of the distribution systems.

Reliability indices SAIDI and SAIFI for JP EP BiH (trends and projections by 2030) are presented in Figs. 2 and 3. Compared to EU countries, reliability indices

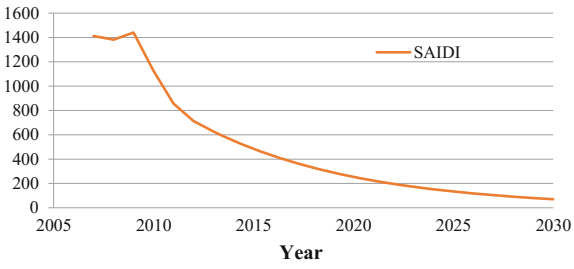

Fig. 2 SAIDI (minutes per end consumer), JP EP BiH trends and projections by 2030 [9]

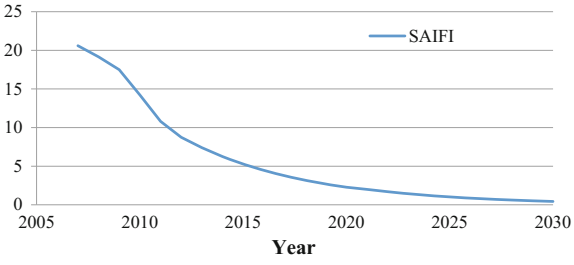

Fig. 3 SAIFI (number of interruptions per customer), JP EP BiH trends and projections by 2030 [9]

of the distribution network of EP BIH (SAIFI/SAIDI = 8.75/713, for 2011) are significantly higher of the reliability indices achieved in the European Union. For example, in Slovenia 2011: SAIFI/SAIDI = 2.79/203, in Austria 2010: SAIFI/SAIDI = 0.66/31.77. In order to raise the level of security to a higher level, it is requires significant investments in construction and modernization of distribution network.

3 Trends and Challenges in Power Generation

Power generation system, mainly based on coal, is not compatible with international climate targets [4]. Problems which power sector based on coal face today are conducted with high CO_2 emissions comparing to lower CO_2-intensive energy resources, particularly various renewable energy sources (RES). Furthermore, criteria of power generation cost efficiency give more and more an advantage to the RES options (wind, solar, hydro) compared both to coal-based power generation and combine cycle gas turbine (CCGT) power plants. Environmental sensitivity issue and consequent stronger requirements posed to fossil-fueled power plants in relation to reduction of SO_2, NO_x and dust emissions, according to industrial emissions directive (IED), along with CO_2 taxes, significantly contribute to the above mentioned negative trend of cost effectiveness of conventional fossil-fueled power plants.

In the other hand, safe, reliable and sustainable energy supply is becoming one of the greatest challenges for the World [5, 6]. Key decisions have to be taken to drastically reduce carbon dioxide (CO_2) emissions and fight climate change. In 2007, the European Council adopted energy and climate change objectives for 2020 [5], i.e. to reduce greenhouse gases (GHG) emissions by 20 %, rising to 30 % if the conditions are adequate, to increase the share of renewable energy to 20 %, and to make a 20 % improvement in energy efficiency, what is stated in the Directive 2009/28/EC. However, Europe's energy systems are adapting too slowly. The security of internal energy supply is undermined by delays in investments and technological progress. Currently, only 45 % of European electricity generation is based on low-carbon energy sources, mainly nuclear and hydropower. Parts of the European Union (EU) could lose more than a third of their generation capacity by 2020 because of the limited life time of these installations. This means replacing and expanding existing capacities, finding secure non-fossil fuel alternatives, adapting power systems to renewable energy sources (RES) and achieving a truly integrated internal energy market [5]. In addition, thermal energy storage technologies coupled with renewable energy are also actively utilized for CO_2 reduction for different kinds of applications, such as heating, ventilation, and air-conditioning areas, for example see [6]. The European Council has also given a long-term commitment to the decarbonisation path with a target for the EU and other

industrialized countries of 80–95 % cuts in GHG emissions by 2050, as stated in Energy roadmap 2050 [7]. In 2011, the European Commission set out sectorial CO_2 reduction trajectories with a mid-term view on 2030 to steer the decarbonisation of the economy on a manageable and cost-effective course. For the power sector, a CO_2 reduction range of between 54 and 80 % was proposed by 2030 compared to 1990 levels. It was analyzed in details in Power Perspectives 2030 [8], to response what is required between today and 2030 to remain on a pathway to a decarbonized power sector by 2050. For power industry, efforts are needed to substantially increase the uptake of RES, high-efficiency cogeneration, district heating and cooling. Use of RES is one of the strategic objectives of the EU energy policy. Two important factors attached to their use are reduction of negative environmental impacts and decrease of dependence on fuel and electricity import [9, 10].

Although significant efforts have been undergone and are still ongoing to provide perspectives for clean coal based power generation (CCT—Clean Combustion Technologies) [11], power system of EU indisputably goes toward an energy transition (Ger: Energiewende), driven by the relevant EU legislation launched and forced by the need to reduce carbon emissions and to mitigate climate change. It is predicted that coal will lose its dominant role and keep only minor contribution in the future energy mix. In its Fifth Assessment Report, the Intergovernmental Panel on Climate Change (IPCC) also sees coal-based power generation as having no long-term prospects [12]. From the other side, the growing number and amount of renewables in the supply mix create transmission imbalances that need to be managed [13]. The gradual climb out of the global economic crisis means unnecessary investment in infrastructure must be avoided. Thus, in the future low-carbon power system, it is reasonable to place future efficient, environment friendly and flexible coal-based power plants serving as one of alternatives for the meeting the peak loads and secure reserve. Otherwise, despite of such a scenario for 2050 and beyond, the present trends all current estimations suggest that coal will keep its dominant role in the next 5–10 years. It is particularly expressed globally due to Chinese industrial expansion and progress of coal projects, although China has shown growing interest in market-based CO_2 pricing and is expected to establish a nationwide emission trading system by 2016 [11, 14]. Thus, coal will even reach its maximum use in the next few years. In the mid-term, focused on 2020 and 2030, problem of slow energy transition from high CO_2 coal-based power generation to low-carbon technologies, e.g. in Germany, may seriously treat the set decarbonisation goals, mainly due to high cost energy path, pointing the way to a more competitive energiewende, pivoting away from a focus solely on renewables development toward a more balanced approach. Furthermore, possible expansion of nuclear energy for base load is not so realistic option even in long-term due to highly expressed risk of nuclear power plants from security aspect.

Considering the issue with carbon intensive coal-based power generation to be enhanced in the next period, various ways of reducing coal-based power generation

are currently under discussion. In Europe these include reforming the European Emissions Trading System the introduction of minimum efficiency levels or stricter flexibility requirements, national minimum prices for CO_2 emissions allowances, capacity mechanisms, a residual emissions cap for coal-fired power plants, CO_2 emissions performance standard, and network development planning that respects climate targets. These proposals apply to both new and existing coal-fired power plants. It should be kept in mind that these are just the operational and economic issues and measures. However, a holistic sustainable concept is required for future power system, as discussed in the next chapter.

3.1 Power Generation System of EPBiH—Current State

Power utility EPBiH is a typical power utility in South-East Europe. Annual electricity generation is near 8000 GWh and it comes from two coal-fired TPP, i.e. TPP Tuzla (1 × 100 MW + 2 × 200 MW + 1 × 225 MW) and TPP Kakanj (2 × 118 MW + 1 × 235 MW), three large hydro power plants (HPP), i.e. HPP Neretva (6 × 30 MW + 2 × 57 MW + 3 × 70 MW), with a minimal participation from small HPP (sHPP), approximately 1 %. Both TPP use domestic low-rank coal, and consume approximately 6,500,000 t per year. The current generation capacity structure of 70 %:30 % in favor of TPP provides some advantages like safe and reliable supply, but further penetration of RES into the generation portfolio is a commitment in order to contribute to the long-term sustainable development plans of the company and to comply with the European targets for reduction of GHG emissions as well as pollutant emissions. EPBiH supplies electricity to near 750,000 consumers in B&H, via its distribution network operated by the EPBiH´s distribution company, organized in five regional distributive parts. Furthermore, EPBiH exports about 20 % of electricity. Annual production of heat energy, generated in cogeneration power units of TPP Tuzla and TPP Kakanj, is approximately 400 GWh. The thermal energy for heating is supplied over long-distance district heating systems to the consumers in the city of Tuzla and city of Lukavac (from TPP Tuzla) and city of Kakanj (from TPP Kakanj). A part of the generated heat (steam) is supplied from TPP Tuzla to the process industry in Tuzla region [15]. Total annual emission of CO_2 in year 1991 was 9,500,000 t. Today the situation is more favorable, given that the six blocks with the lowest efficiency are decommissioned and all other existing coal-based power units have been reconstructed and modernized in the period between 2002 and 2012. Consequently, energy efficiency in TPP of EPBiH is increased for 30 % compared to the 1990 level; from 24 % up to the current 31 %. Projection of net efficiency of existing power units in Tuzla TPP and Kakanj TPP until their decommissioning as well as overall net efficiency of thermal power units of EPBiH is given in the Fig. 4.

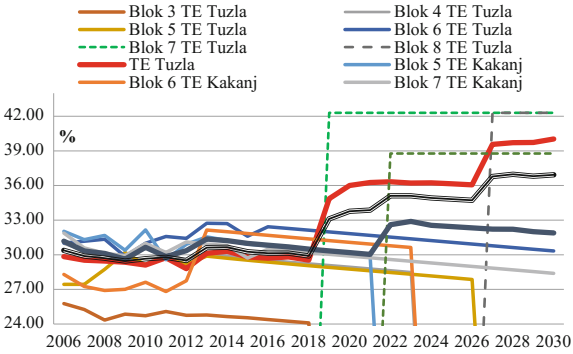

Fig. 4 Projection of overall net efficiency of thermal power plants of EPBiH by 2030

3.2 EPBiH Power Generation Development Targets with Long-Term Projections by 2030 and 2050

Despite these energy efficiency improvements achieved during the last fifteen years, EPBiH is facing new challenges; requirements for further energy efficiency improvements and CO_2 emissions reduction, mandatory for the company to keep and improve its position on the market and comply with the energy efficiency and environmental regulation, as well as low-carbon future. Considering the expected annual power demand until year 2030, as well as the planned generation portfolio development, a further step towards sustainability and generation portfolio optimization is projected, in order to reach specific energy and decarbonisation targets. The generation portfolio expansion is based on EPBiH plans for construction of new generation facilities in future, considering the necessity for replacement capacity to be constructed instead of existing TPP units planned to be decommissioned by 2030. In EPBiH's long term plans, the dynamics of decommissioning old TPP is already defined and stated in the company's strategic document Long-term strategic development of EPBiH. The choice of all other facilities commissioning dynamics is subject of analyses, regarding sustainability and decarbonisation criteria and is performed by experts from the company, see for example [15].

Additional aspects which have been considered are current investment plans for DeSOx and DeNOx facilities, in order to fulfill obligations according toLarge Combustion Plants Directive (LCPD) and Industrial Emission Directive (IED), Directive 2009/28/EC and Directive 2012/27/EU, and provide further operation of TPP units. The development plan results in new TPP projects, HPP projects, WPP projects, PVPP projects and biomass projects (BPP). Replacement of existing coal-based power units with new, more efficient and carbon capture and storage (CCS)-ready power units is essential in the development plan. At this moment, considering the planned consumption growth as well as exhausted life time and low efficiency of TPP units, a new generation facilities are planned to be built. Commissioning of replacement TPP unit in TPP Tuzla (TPPTU7—450 MW) is

planned for 2021, and in TPP Kakanj (TPPKU8—300 MW) in 2023. Those units will be CCS ready, which will be taken into account, depending on scenario.

The development plan also includes cogeneration expansion for heating/cooling purposes, both in TPP Kakanj (new 170 MWh for long-distance district heating of Zenica city and new 300 MWh for long-distance district heating of Sarajevo city) and in TPP Tuzla (new 200 MWh for Tuzla and new 60 MWh for long-distance district heating of Zivinice city). For further reduction of CO_2 emissions, co-firing coal with biomass is planned at all EPBiH's TPP [15–17].

According to this biomass co-firing plans, co-firing coal with biomass is planned at all existing EPBiH's TPP; projected to use of 7 %w of biomass for average operation for 3000 h annually. Also, for new TPP units, higher amounts of biomass are planned to be co-fired, up to 25 % annually, depending on considered scenario. According to these plans, overall net efficiency of thermal power plants of EPBiH reaches 40 % in 2030, see Fig. 4, while overall CO_2 emissions from TPP falls down from the current 1140 kg/MWh to 950 kg/MWh in 2030, see Fig. 5.

Furthermore, EPBiH experts have made the plans and projections for power generation development by 2050 [18]. Three different scenarios have been analyzed, with different portfolio structures, in order to define measures to be taken to achieve defined CO_2 cuts:

(a) 55 % CO_2 cut compared to 1991 level—low CO_2 cut scenario (LOW CO_2 CUT)
(b) 65 % CO_2 cut compared to 1991 level—medium CO_2 cut scenario (MID CO_2 CUT)
(c) 80 % CO_2 cut compared to 1991 level—high CO_2 cut scenario (HIGH CO_2 CUT).

Table 2 shows installed capacities in EPBiH power system in 2050 for three considered scenarios. As can be seen, some thermal capacities planned in low CO_2 cut scenario would not be built in MID and HIGH scenarios while they would be replaced mostly by new HPP and wind parks.

Accordingly, power generation from fossils (coal), which in low scenarios accounts 8.7 TWh in 2050, would be drastically decreased for HIGH CO_2 cut scenario, falling down to 3.5 TWh. In the same time, electricity generation from hydro and wind will be increased significantly for HIGH CO_2 cut scenario, reaching 57 % share of hydro and 15 % share of wind in total electricity generation in 2050

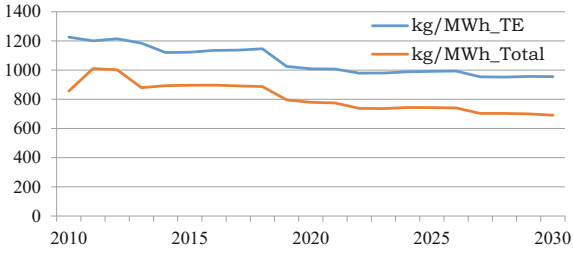

Fig. 5 Projection of reduction of CO_2 emissions from TPP of EPBiH by 2030 (kg CO_2/MWh)

Table 2 Comparison of installed capacity in MW in 2050 for all scenarios

	Low CO_2 cut	Mid CO_2 cut	High CO_2 cut
TPP	1500	1200	750
HPP	950	1200	1600
sHPP	150	190	250
WPP	550	800	950
Solar	100	150	300

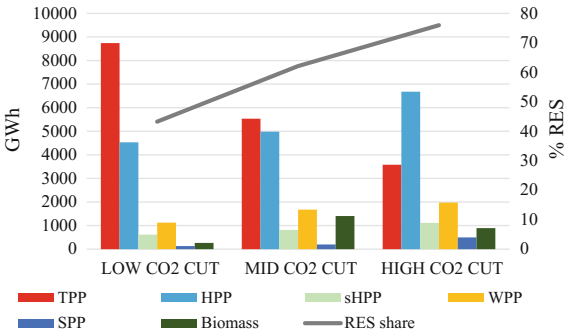

Fig. 6 Electricity generation by sources and RES share for considered scenarios

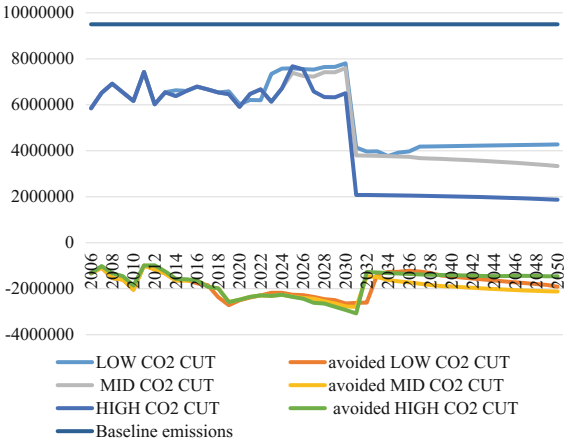

Fig. 7 Annual projections of CO_2 emissions and avoided CO_2 emissions for all scenarios (tones CO_2 per year)

for HIGH CO_2 cut scenario, see Fig. 6. Consequently, in HIGH CO_2 cut scenario, annual CO_2 emissions in 2050 falling down below 2,000,000 tones, which is more than double lower emissions compared to LOW CO_2 cut scenario, see Fig. 7.

In relation to emissions in 1990, 80 % of CO_2 reduction is achieved in HIGH CO_2 cut scenario compared to 55 % cut in LOW CO_2 cut scenario. According to the Multicriteria Assessment Analysis (MSA) performed [18], no matter what relation between weighting factors is considered, HIGH CO_2 cut scenario is preferable both from the environmental and economical aspect, since economic indicator is sum of CAPEX, OPEX and CO_2 fees indicators.

4 Conclusion

In this paper we present the trends and challenges of some parameters relating to power distribution and power generations systems of JPEPBIH. It is clearly that the indicators today are not the best and that the upcoming period requires significant investment and the application of new technologies. The fact is that Bosnia and Herzegovina has a great potential of RES, and that it is possible to sustainably exploit the available capacity for the drastically reduced the environmental impact of the power sector. Also, for new TPP units which will be commissioned, which are necessary for consumption coverage when generation from RES is low, the environmental aspect is included. For that purpose, in order to have sustainable future power generation system in 2050, those units are planned to cogenerate heat and electricity which would additionally contribute to decrease overall emissions on district heating coverage area. Also, the cost-efficient use of fuel will be the maximum in accordance with the best available techniques, and biomass co-firing should contribute to the ultimate goal.

References

1. Avdakovic S, Kazagić A, Hadzikadic M, Mujcic A (2016) Bosnia and Herzegovina power system: from the first luminaires to the modern power system. In: Part I: history, international symposium on innovative and interdisciplinary applications of advanced technologies (IAT), Neum, Bosnia and Herzegovina 26–29 May 2016
2. Avdaković S, Bećirović E, Karadža J, Gruhonjić Š, Redžić N, Kruščica S, Kasumović E, Penava I (2013) Analiza postojećeg stanja i mjere za unapređenje postupaka identifikacije i lokalizacije gubitaka električne energije u elektrodistributivnim mrežama JP Elektroprivreda BiH DD Sarajevo. JP EP BiH
3. 'Dugoročni plan razvoja JP Elektroprivreda BiH do 2030. Godine'
4. IEA Statistics (2014) CO_2 emissions from fuel combustion—highlights. International Energy Agency, 2014 Edition
5. European Commission (2011) Energy 2020. European Union, Brussels, Belgium
6. European Climate Foundation (2010) Energy roadmap 2050. European Union, Brussels, Belgium
7. Wang RZ, Yu X, Ge TS, Li TX (2013) The present and future of residential refrigeration, power generation and energy storage. Appl Therm Eng 53(2):256–270
8. European Climate Foundation (2011) Power perspectives 2030. European Union, Brussels, Belgium
9. Boston A (2013) Delivering a secure electricity supply on a low carbon pathway. Energy Policy 52:55–59
10. Blum H, Legey FLL (2012) The challenging economics of energy security: ensuring energy benefits in support to sustainable development. Energy Econ 34:1982–1989
11. Carpenter AM (2014) R&D programmes for clean coal technologies, CCC/244, ISBN 978-92-9029-566-2, IEA Clean Coal Centre
12. IPCC (2013) Climate Change 2013: the physical science basis, contribution of working group I to the fifth assessment report of the intergovernmental panel on climate change. Cambridge University Press, Cambridge, United Kingdom and New York, NY, USA

13. Sorknæs P, Lund H, Andersen AN (2015) Future power market and sustainable energy solutions—the treatment of uncertainties in the daily operation of combined heat and power plants. Appl Energy 144:129–138
14. Li Y, Lukszo Z, Weijnen M (2015) The implications of CO_2 price for China's power sector decarbonization. Appl Energy 146:53–64
15. Kazagić A, Merzic A, Redzic A, Music M (2014) Power utility generation portfolio optimization as function of specific RES and decarbonisation targets—EPBiH case study. Appl Energy (Elsevier) 135:694–703
16. Kazagić A, Smajević I (2009) Synergy effects of Co-firing of woody biomass with Bosnian coal. Energy (Elsevier) 34:699–707
17. Smajević I, Hodzic N, Kazagić A (2014) Lab-scale investigation of middle-Bosnia coals to achieve high-efficient and clean combustion technology. Therm Sci 18(3):875–888
18. Kazagic A, Redzic A, Merzic A, Music M (2015) Sustainability assessment of measures to meet long-term GHG cut targets for a conventional power utility. In: 10th international conference on sustainable development of energy, water and environmental systems—10. SDEWES Dubrovnik 2015, 27 Sept–03 Oct 2015 (Paper accepted for publishing in Elsevier's journal Energy)

The Relationship Between GDP and Electricity Consumption in Southeast European Countries

Enisa Džananović and Sabina Dacić-Lepara

Abstract Energy plays an important role in the economic development. The aim of this study was to investigate the relationship between GDP per capita and the electricity consumption on 2000–2014 time series for some of the countries of Southeast Europe (B&H, Croatia, Greece, Serbia, Slovenia, Romania and Bulgaria). The annual data for GDP per capita and electricity consumption are obtained from several online available official databases. Comparative analysis showed that in the reference period GDP per capita (19,900 (17,600–21,500) EUR/capita) and electricity consumption (50.51 ± 3.82 TWh) in Greece was significantly higher than the GDP per capita and electricity consumption in all other analyzed countries ($p < 0.005$). A strong, statistically significant positive correlation between GDP per capita and electricity consumption was found in all analyzed countries except in Serbia, (Rho = −0.407; $p = 0.131$ NS). The highest coefficient of determination [r-square (r^2)] having a value of 0.9051 has been identified for Bulgaria, while the lowest coefficient r^2 was identified for Serbia (0.238). Bosnia and Herzegovina has a very close relation between GDP and electricity consumption, ($Rho = 0.885; p = 0.00001$) while the coefficient of determination r^2 was 0.8436. In other words, for the reference period 2000–2014, about 84 % changes in electricity consumption in B&H can be described by changes of GDP. The obtained results show a very close relationship between the GDP per capita and electricity consumption for selected countries.

E. Džananović · S. Dacić-Lepara (✉)
JP Elektroprivreda BiH, Vilsonovo šetalište 15, 71000 Sarajevo, Bosnia and Herzegovina
e-mail: s.dacic@elektropriverda.ba

E. Džananović
e-mail: en.dzananovic@elektroprivreda.ba

M. Hadžikadić and S. Avdaković (eds.), *Advanced Technologies, Systems, and Applications*, Lecture Notes in Networks and Systems 3,
DOI 10.1007/978-3-319-47295-9_17

1 Introduction

Identification of the major factors affecting the electricity consumption and a full understanding of the characteristics of own consumption enables better analysis and forecasts of the future needs. Seasonal variations in the electricity consumption are closely related to the changes in temperature (for a large number of power systems), while long-term analysis suggests a relatively strong correlation between economic growth and the electricity consumption [1]. Energy plays an essential role in an economy, so the relationship between energy consumption and economic growth is now well researched in the literature. Lots of literatures are based on the questions that whether economic growth leads to energy consumption or that energy consumption is the engine of economic growth. Hence many studies have attempted to test for causality between energy and economic growth. The literature has conflicting results and there is no consensus either on the existence or the direction of causality between electricity consumption and economic growth [1]. The answer to this question has important implication for the policy makers [2]. However, if the causality runs from energy consumption to GDP, this indicates an energy dependent economy such that energy is a stimulus for GDP growth, implying that shortage of energy may negatively affect economic growth or may cause poor economic performance [1]. Some studies suggest a bi-directional long-run causality between electricity consumption and economic growth [3]. Quality of identification of factors affecting the electricity consumption depends on the available data quality and quantity. Some data (such as GDP) are recorded on an annual (or quarterly) level, so the time series analysis require observation of long period of time. However, in the case of Bosnia and Herzegovina, the continuity of the time series was interrupted during the Bosnian war in 90s of the last century, and any analysis for a longer period of time is quite difficult. Different approaches to data analysis can be found in [4–10], where the authors in different ways and mathematical approaches analyze the impact of various factors on the electricity consumption.

In this paper, the relationship between GDP and electricity consumption is determined by using real data for some of the countries of Southeast Europe and a descriptive analysis, comparative analysis and linear regression, i.e. correlation approach. It is known that some of these countries are in the process of transition with very specific political relations and unstable economic conditions. Also, the considered time period from 2000 to 2014 includes the global economic crisis, which did not pass by these countries. However, regardless of the above, for most of the considered countries a very close relation between GDP and electricity consumption is identified.

The remainder of this paper is organized as follows. Sect. 2 presents the data employed and a briefly overview of the applied methodological approach. The empirical results with an adequate discussion are reported in Sect. 3, while concluding remarks are given in Sect 4.

2 Data and Applied Methodological Approach

2.1 Data

This study uses annual time series data for the 7 Southeast European countries which include Bosnia and Herzegovina, Croatia, Greece, Serbia, Slovenia, Romania and Bulgaria. The annual data for GDP and electricity consumption are obtained from the different sources. There for, the annual data for GDP per capita and electricity consumption of Croatia, Greece, Serbia, Slovenia, Romania and Bulgaria are obtained from the official database [11]. The data on GDP per capita of Bosnia and Herzegovina are obtained from multiple sources [12, 13]. The GDP is expressed in EUR per capita, while the electricity consumption is expressed in units of Gigawatt hours (GWh). Since the available data for GDP per capita of B&H was expressed in USD per capita, the data is converted in EUR per capita according to the average exchange rate of USD/EUR in Bosnia and Herzegovina for 2008, and minor errors due to data conversion are possible. Data on electricity consumption in B&H are provided from the official report of the Independent System Operator (ISO B&H).

2.2 An Analysis Using Linear Regression

Based on [4], the interdependence between GDP and electricity consumption using linear regression is given as: $y = ax + b$, where y-represents electricity consumption, x denotes GDP per capita and a and b are the respective regression coefficients.

Correlation refers to any of a broad class of statistical relationships involving dependence, though in common usage it most often refers to the extent to which two variables have a linear relationship with each other. "Correlation does not imply causation" is a phrase used in statistics to emphasize that a correlation between two variables does not imply that one causes the other [14].

The Pearson's correlation coefficient is defined as $r = \sigma_{xy}^2/\sigma_x\sigma_y$, where σ_{xy}^2 represents the covariance of the x and y time series, while σ_x and σ_y are the standard deviations of x and y, respectively. This coefficient is sensitive only to a linear relationship between two variables (which may exist even if one is a nonlinear function of the other). r-square (r^2) is a coefficient used for evaluation of the representativeness of the regression model, which is based on analysis of the respective variance [4]. It is defined as the ratio of the sum of squared deviations interpreted by regression and the total sum of squares of deviations. *Rank correlation* coefficients, such as *Spearman's rank correlation* (*often denoted by the Greek letter* ρ (Rho) or as r_s) measures the extent to which, as one variable increases, the other variable tends to increase, without requiring that increase to be represented by a linear relationship. In other words, it measures the strength of association between two ranked variables. It is common to regard this rank

correlation coefficient as alternative to Pearson's coefficient, used either to reduce the amount of calculation or to make the coefficient less sensitive to non-normality in distributions. The Spearman's correlation coefficient is defined as $Rho = cov(rg_x, rg_y)/\sigma_{rg_x}\sigma_{rg_y}$, where $cov(rg_x, rg_y)$ represents the covariance of the rank variables, while σ_{rg_x} and σ_{rg_y} are the standard deviations of the rank variables.

Although there are no hard and fast rules for describing correlational strength [15], correlation is an effect size and so we can verbally describe the strength of the correlation using the guidelines suggested in [16]:

- $0.00 \leq |r| \leq 0.19$ very weak correlation
- $0.20 \leq |r| \leq 0.39$ weak correlation
- $0.40 \leq |r| \leq 0.59$ moderate correlation
- $0.60 \leq |r| \leq 0.79$ strong correlation
- $0.80 \leq |r| \leq 1.00$ very strong correlation.

2.3 Methodology

Statistical analysis were performed with the software SPSS version 16.0. The distribution of variables was tested by Shapiro-Wilk test. Values with normal distribution were expressed as mean ± standard deviation, while those with non-normal distribution were shown as median and interquartile range. The Kruskal-Wallis (i.e. Mann-Whitney U) test was used for comparison of variables with non-normal distribution, while the normally distributed variables were compared by using ANOVA test. For normally distributed variables, correlations were assessed by Pearson's test, while for those with non-normal distribution correlations were assessed by Spearman's test. *P*-values less than 0.05 were considered statistically significant.

3 Results and Discussion

In this section the main results and findings of our analysis performed for the selected data sets are presented. To analyze and illustrate the impact of GDP/capita on electricity consumption, the data from Southeast European countries for the period 2000–2014 is used. This period is wide enough to justify the use of these data for the determination of relationship between GDP and electricity consumption in Southeast European countries.

Comparative analysis (see Table 1 and Fig. 1) showed that in the period from 2000 to 2014 the GDP per capita in Greece (19,900 (17,600–21,500) EUR/capita) was significantly higher than the GDP per capita in all other analyzed countries (2800 (1774–2936) EUR/capita for B&H, 3900 (3000–4200) EUR/capita for

Serbia, 4900 (3600–5300) EUR/capita for Bulgaria, 6100 (4500–6400) EUR/capita for Romania, 10,200 (9400–10,600) EUR/capita for Croatia and 17,300 (15,400–17,700) EUR/capita for Slovenia) ($p < 0.005$).

Comparative analysis (Table 1 and Fig. 1) showed that in the period from 2000 to 2014 the electricity consumption in Greece (50.51 ± 3.82 TWh) also was significantly higher than the electricity consumption in all other analyzed countries (10.74 ± 0.89 TWh for B&H, 12.18 ± 0.78 TWh for Slovenia, 14.43 ± 1.43 TWh for Croatia, 26.50 ± 1.56 TWh for Bulgaria, 27.29 ± 1.04 TWh for Serbia and 39,461 ± 2,72 TWh for Romania) ($p < 0.005$). Note that the for these analysis are not used data of electricity consumption per capita, as was the case for GDP, but the total electricity consumption in each country.

The trend of change in GDP per capita and trend of change in electricity consumption during the period 2000–2014 is shown on Fig. 2. Figure 2 shows permanent, depending on each country smaller or greater growth of GDP per capita and electricity consumption until 2008 when the global economic crisis appeared. At that time the GDP per capita recorded smaller or greater fall in all analyzed countries. In Greece the fall continued until the end of 2013, while in 2014 GDP per capita recorded an increase of 1.17 %. Although that in the period from 2008 in almost all analyzed countries the fall in electricity consumption was also observed, the fall was much milder and lasted considerably shorter.

The correlation between the electricity consumption and GDP for all analyzed Southeast European countries for the period from 2000 to 2014 determined by using the linear regression approach, is presented in Fig. 3.

Obtained regression coefficients a and b for all analyzed countries are given in Table 2. The Pearson's correlation coefficient r which represents statistical measure of the strength of a linear relationship between paired data, Spearman's correlation coefficient r which represents measure of the strength of a monotone association between two variables, and the coefficient of determination r-square (r^2) which is used for evaluation of the representativeness of regression model, for all analyzed countries are also given in Table 2.

By analyzing the Fig. 3 and coefficients in Table 2. it can be concluded that in the period from 2000 to 2014, in all analyzed countries except in Serbia there was a strong, statistically significant positive correlation between GDP per capita and electricity consumption ($r = 0.947$; $p = 0.0000008$ for Croatia, Rho $= 0.905$; $p =$

Table 1 The comparative values of GDP per capita and electricity consumption for selected countries

		B&H	Croatia	Greece	Serbia	Slovenia	Romania	Bulgaria
TWh	Mean ± SD	10.74 ± 0.89	14.43 ±1,43	50.51 ± 3.82	27.29 ± 1.04	12.18 ± 0.78	39.461 ± 2.72	26.50 ± 1.56
GDP/capita	Median (25–75) %	2800 (1774–2936)	10,200 (9400–10,600)	19,900 (17,600–21,500)	3900 (3000–4200)	17,300 (15,400–17,700)	6100 (4500–6400)	4900 (3600–5300)

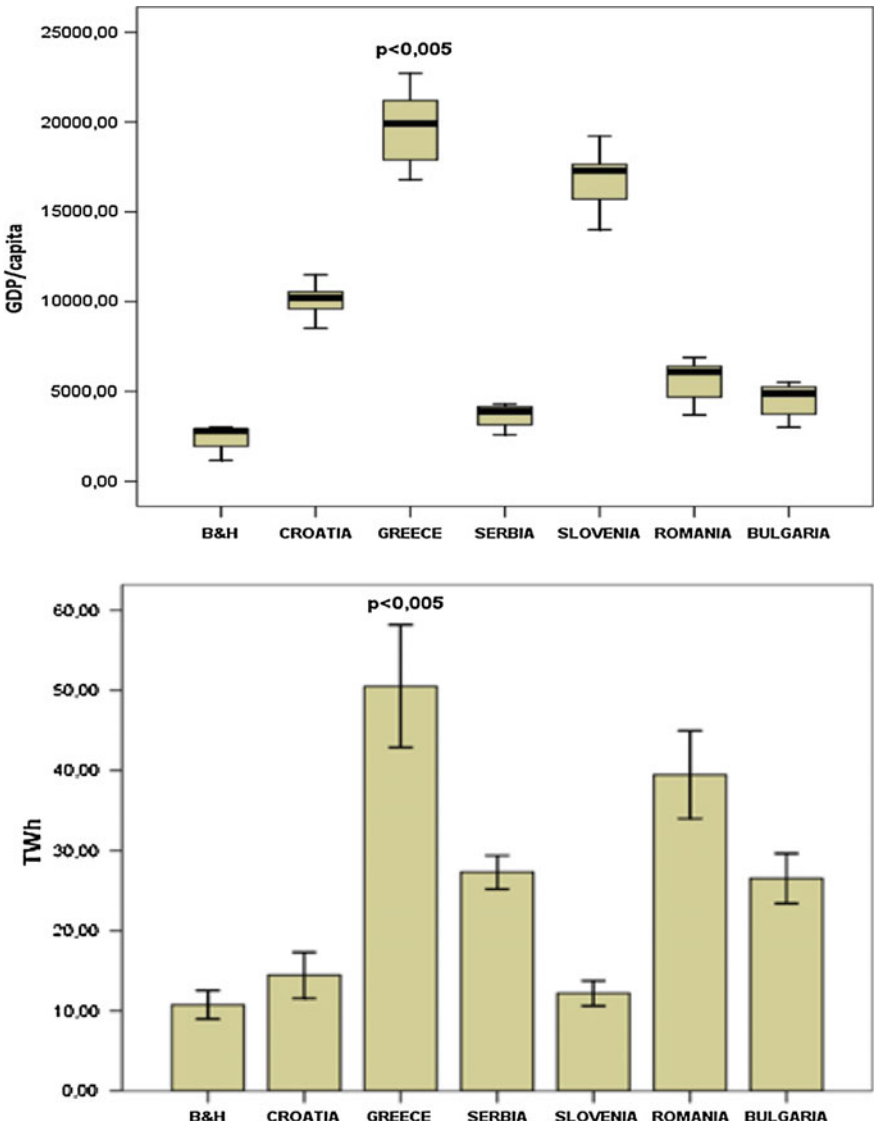

Fig. 1 The comparative values of GDP per capita and electricity consumption for selected countries

0.000003 for Bulgaria, r = 0.890; $p = 0.000008$ for Romania, Rho = 0.885; $p = 0.00001$ for B&H, r = 0.736; $p = 0.002$ for Slovenia and r = 0.672; $p = 0.006$ for Greece.

By analyzing the Fig. 3 and coefficients in Table 2 it can be concluded that in the period from 2000 to 2014, in all analyzed countries except in Serbia there was a

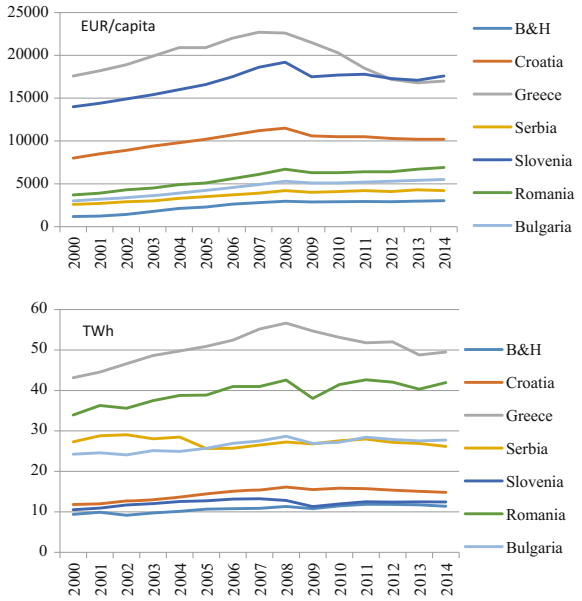

Fig. 2 The trend of change in GDP per capita and electricity consumption during the period 2000–2014

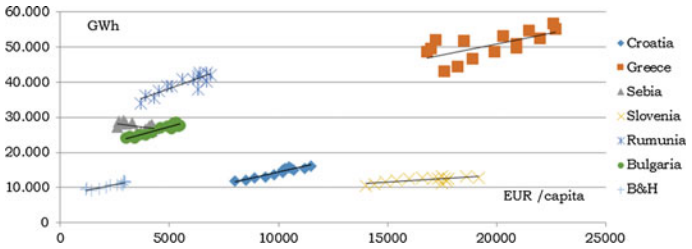

Fig. 3 Correlations between GDP and electricity consumption for selected countries

Table 2 $y = ax + b$ equation coefficients, r, *Rho* and r^2

	a [GWh/(EUR/capita)]	b (GWh)	r	ρ (Rho)	r^2	p
B&H	1.2161	7828.5		0.885	0.8436	0.00001
Croatia	1.4063	329.47	0.947		0.8968	0.00000008
Greece	1.2442	26049	0.672		0.4522	0.006
Serbia	−0.8506	30.396		−0.407	0.2380	**0.131; NS**
Slovenia	0.3804	5807.9	0.736		0.5421	0.002
Romania	2.2217	27,050	0.890		0.7930	0.000008
Bulgaria	1.6913	18,872		0.905	0.9051	0.000003

strong, statistically significant positive correlation between GDP per capita and electricity consumption ($r = 0.947$; $p = 0.00000008$ for Croatia, Rho $= 0.905$; $p = 0.000003$ for Bulgaria, $r = 0.890$; $p = 0.000008$ for Romania, Rho $= 0.885$; $p = 0.00001$ for B&H, $r = 0.736$; $p = 0.002$, for Slovenia and $r = 0.672$; $p = 0.006$ for Greece). This practically means that in the analyzed period in all countries, except in Serbia increase in GDP was accompanied by the rise in electricity consumption (and vice versa). As it is shown on Fig. 1, the only country between analyzed Southeast European countries where it has been observed a negative correlation coefficient between variations in GDP per capita and electricity consumption was Serbia, but this correlation wasn't significant (Rho $= -0.407$; $p = 0.131$).

In this paper, the relationship between GDP per capita and electricity consumption is determined by using real data for some of the countries of Southeast Europe and a descriptive analysis, comparative analysis and linear regression, i.e. correlation approach. These approaches do not imply causation, and causation wasn't the subject of this study. It is known that some of these countries are in the process of transition with very specific political relations and unstable economic conditions. Also, the considered time period from 2000 to 2014 includes the global economic crisis, which did not pass by these countries.

However, regardless of the above, for most of the considered countries a very close relation between GDP and electricity consumption is identified. Also, it is clear that the dependence of electricity consumption in relation to GDP is not the same for all countries, and the unstable political and economic conditions makes this relationship appear to be significantly different for various countries.

4 Conclusion

In this paper, a descriptive analysis, comparative analysis, and linear regression, i.e. correlation approach are applied to analyze the impact of GDP per capita on the electricity consumption in some Southeast European countries, based on the available data. These approaches do not imply causation. Although used methodology approaches are relatively simple approaches for this type of analysis, from the results we can conclude that there are different reciprocal influences between the observed variables. The most significant correlations were identified for the new EU members, and this can be interpreted as the result of systemic measures and intensive economic growth. On the other hand, the lowest correlation coefficient was identified for Serbia. In addition to being the lowest, it is the only one with a negative sign, which means that only in Serbia changes in GDP were inversely proportional to the changes in electricity consumption Also, the relatively low correlation coefficient was identified for Greece which is most likely a result of the unstable economic, social and political situation in the country.

What are the reasons for such results, why among the analyzed countries occurs differences in correlation between the two variables, as well as the causality issue are the tasks to be dealt with in our future research.

References

1. Acaravci A, Ozturk I (2010) Electricity consumption-growth nexus: evidence from panel data for transition countries. Energy Econ 32(3):604–608
2. Sheng-Tung C, Hsiao-I K, Chi-Chung C (2007) The relationship between GDP and electricity consumption in 10 Asian countries. Energy Policy 35(4):2611–2621
3. Zortuk M, Asutay M, Bayrak S (2015) The relationship between electricity consumption, real gdp and employment in G-7 Countries: seasonal panel unit roots and cointegration mode. J Energy Technol Policy 5(4):50–62
4. Moghaddas-Tafreshi SM, Mahdi F (2008) A linear regression-based study for temperature sensitivity analysis of Iran electrical load. In: IEEE international conference on industrial technology, pp 1–7
5. Avdakovic S, Ademovic A, Nuhanovic A (2012) Insight into the properties of the UK electricity consumption using a linear regression and wavelet transform approach. Elektrotehniški Vestnik / Electrotechnical Review 79:278–283
6. Fung WY, Lam KS, Hung WT, Pang SW, Lee YL (2006) Impact of urban temperature on energy consumption of Hong Kong. Energy 31:2623–2637
7. Avdakovic S, Ademovic A, Nuhanovic A (2013) Correlation between air temperature and electricity demand by linear regression and wavelet coherence approach: UK, Slovakia and Bosnia and Herzegovina case study. Arch Electr Eng 62(4):521–532
8. Hou Qiang (2009) The relationship between energy consumption growths and economic growth in China. Int J Econ Finan 1(2):232–237
9. Chima CM, Freed R (2011) Empirical study of the relationship between energy consumption and gross domestic product in the U.S.A. Int Bus Econ Res J 4:101–114
10. Soytasa U, Sarib R (2003) Energy consumption and GDP: causality relationship in G-7 countries and emerging markets. Energy Econ 25:33–37
11. http://ec.europa.eu/eurostat/web/products-datasets/-/tsdec100
12. Granić G, Zeljko M, Morankić I, Martinez JA, Olano M, Jurić Ž (2008) Studija energetskog sektora u BiH. Energetski institut Hrvoje Požar, Soluziona, Ekonomski institut Banjaluka, Rudarski institut Tuzla
13. http://www.tradingeconomics.com/bosnia-and-herzegovina/gdp-per-capita
14. Aldrich J (1995) Correlations genuine and spurious in Pearson and Yule. Stat Sci 10(4):364–376
15. Comanac A, De Medici L, Capone M, Millis AJ (2008) Optical conductivity and the correlation strength of high-temperature cooper oxide superconductors. Nat Phys 4:287–290
16. Evans JD (1996) Straightforward statistics for the behavioral sciences. Brooks/Cole Publishing Company, Pacific Grove

Wireless Networking for Low Power Sensor Networks

Migdat I. Hodžić and Indira Muhić

Abstract In this paper we set the scene for new low power wireless sensor network protocol and architecture suitable for field implementation in the context of general wireless networking as well as Internet of Things (IoT), and a variety of security, defense or general campus applications, where the wireless sensor power expenditure is critical. The sensor network we propose is divided into sub-nets which account for sensor geographical "congregation" due to a prescribed or an ad hoc deployment, depending on the situation at hand. We consider a geographically fixed and static (not-moving-sensors) network which is a dynamic one in a sense that the relationships between the sensor nodes (local and global) is a dynamic one (such as which sensor is "in charge" at any given time). We propose (i) new approach to low power sensor wireless protocol as well as (ii) an introductory description of the simulation environment to test protocol's effectiveness. The paper is a part of an ongoing research.

1 Introduction

Many wireless sensor field and campus applications include deployments of networks of low power sensors with extended lifetimes. Their mission is to detect and report a wide variety of environmental and physical properties including but not limited to acoustic, seismic, magnetic, temperature, pressure, humidity, local and global positioning. Recent developments in various classic and Nano-technologies [1–9], show the advance in producing such sensors. The advantages of reduced physical scale coupled with extended life include improved redundancy, lower cost, simplified deployment and improved stealth profile—just to name a few. The reduced physical scale of the modern sensors and deployment parameters indicate that communication between components will be primarily wireless communications. While wired

M.I. Hodžić (✉) · I. Muhić
International University of Sarajevo, Sarajevo, Bosnia and Herzegovina
e-mail: mhodzic@ius.edu.ba

M. Hadžikadić and S. Avdaković (eds.), *Advanced Technologies, Systems, and Applications*, Lecture Notes in Networks and Systems 3,
DOI 10.1007/978-3-319-47295-9_18

deployments may have some utility, wireless deployments represent a more general solution and wired deployments may be considered as a subset of the wireless solution space.

Designers of conventional wireless networks have developed solutions to various problems associated with actually communicating efficiently in the wireless media. Few have addressed any solutions with respect to a reduced (minimal) energy paradigm. In fact, current protocols and implementations are not sufficient to support the proposed low energy sensor network deployments.

Conventional network protocols are highly inefficient for low power applications and new low consumption and long life methodologies must be developed. Most data communication networks (such as WiFi) typically have 5 layers. These layers are not, in themselves, essential to good communications but are simple abstractions that divide the implementation into distinct self-contained objects. While they represent good overall programming practice, the layer distinctions introduce a certain amount of overhead and create restrictions that may not be useful in a more passive environment [14–17].

The fundamental roles of each merge when we examine the basic restrictions of long life and low energy. Among other considerations, the entire network design needs to incorporate the concept of Passivity (silence)—so an entirely new protocol suite may be required. The objective of this paper is to introduce and propose a simple cross-layer networking protocol suitable for a network of low cost wireless sensors, with finite energy requirements and extended lifetimes, which will collect, aggregate, compress, fuse and deliver data to a final consumer. The overall network will "self-organize" and utilize some proprietary encryption technology. Each deployment collection is delivered with its own private encryption and will require minimum maintenance. Normally the network will be in a "Silent Communication" state. Once an event triggers one or more sensors, there will be a flurry of communication, using the internal encryption. All information will be stored redundantly on multiple nodes, completely encrypted, until requested by the consumer which is decrypted only at its final destination. Typical sensor data packets are short and the corresponding network protocol should be independent of sensor type or data content. In this paper we describe:

1. New protocol methodology based on our novel approach of "relative time domain sensor networking", resulting in a short "sensor event trail" which will minimize communication required. The wireless network we are proposing is a self organizing network which is normally in "Silent or Sleep" mode. An event somewhere in the network area triggers a short burst of network activity. Data reporting traffic is generated causing "event network trail" after which the network will go back to a silent (sleep) mode. During the event reporting, certain network functions are performed, such as sensor "wake up", routing data locally and globally, via specific sensors "in charge" called Master Sensors. Depending on the type of trigger event and resulting communications and reporting (number of sensors alarmed, sensor signal strength, intruder trail duration, and additional required data), the network may reconfigure its basic

infrastructure based on the series of events to adapt more effectively for better throughput, time and power expenditure. Each sensor communication time is divided arbitrarily into Time Divisions, TDs, which are divided into equal size blocks. These blocks represent intervals when a sensor may transmit. Designated Masters may arbitrate time ration assignments, and these may change as the network reconfigures itself after an event trigger. The need for conserving power and greatly limiting message traffic will make the protocol quite different from the existing wireless sensor protocols. New architecture and protocol offer real advantages when sensor power is critical and when sensor deployment may be an ad hoc within a geographical, secured or campus area [10–13]. We also propose:

2. A simulation tool to simulate various network topologies, trajectories and protocols, as well as doing protocol trade-off analysis. This tool is suitable for analyzing both small and large wireless sensor network and communication, where the network consists of various kinds of intelligent sensors grouped in self-organizing smaller subnets. The simulation tool will be adopted of the sensor type, network topology and protocols. We will describe this tool in a follow up paper. Some potential practical applications are as follows:

   (i) Deployments in "signal polluted" environments (industrial, home, campus, auto, manufacturing).
   (ii) Personal area network applications (patient's health monitoring, firefighters, police, sport activities).
   (iii) Commercial remote security monitoring such as in industrial, data centers, distribution centers, industrial mines, special facilities, etc.
   (iv) Military applications such as protected bases, battlefield deployments behind enemy lines, air dropped sensor "fields", etc.
   (v) In particular we see many applications in the newly emerging area of Internet of Things (IoT) where wireless sensors will play a key role in many areas.

2 Technical Objectives

One fundamental property of low-power/long-life systems may be summarized as follows: do nothing until there is something to do! For example, conventional networks are noisy and broadcast their presence on a regular basis. This can be easily transformed into a physical location—detection is much too easy. Therefore, any design of a communication protocol should incorporate "Silence" and "Passivity" attributes as major considerations. An additional side benefit of silence is that energy is conserved when no work is preformed. Because of this, arbitrary deployments of the sensor network must be capable of virtually instant self-organization. Each sensor must be self sufficient, capable of identifying neighbors and responding to them. The onboard software must support dynamic

re-configuration heuristics. A fundamental criterion for all network objects should be: Everyone listens—speak only when absolutely necessary and only what is necessary. This response may be triggered by a command query or as the result of some other threshold event trigger. Transmission duplication should be avoided at all costs by appropriate message queue pruning and general housekeeping. Knowledge about what ones neighbors are saying can reduce redundant reports. Sensor nodes should maintain a world view that includes immediate neighbors and an abstraction of the outlying neighborhoods as reported by their local neighbors. This is essential in calculating the most efficient transmission paths from any node to any other node in the universe of neighborhoods. The general structure of a network is presented in Sect. 3. Next we define key design criteria which we consider for our methodology, as well as a protocol testing.

2.1 Major Design Criteria

(i) Low power consumption to extend sensor service life. Every bit transmitted consumes the scarce resource of battery power; therefore the protocol should utilize as small a packet size as possible with variable size packets.
(ii) Minimal transmissions to minimize risk of detection. In addition to making the packets as small as possible, the number of transmissions should be kept to a minimum. This will save power and also reduce the risk of detection by unauthorized agents.
(iii) Self-organization and adaptability, to reduce the need for control from the outside. This self-organization will further reduce network transmissions and save energy. Onboard self-diagnostics will be used to evaluate overall system performance and self-tune power output to optimize energy utilization.

2.2 Protocol Testing Goals

(i) Identify several protocols and their variants. Evaluate their potential value relative to the design criteria above.
(ii) Create a computer model with heuristics for a generic low energy wireless sensor network. Allow for the simulation of power drain, varying deployment topologies, environmental barriers, varying power output capabilities, etc.; include simulation of several different sensor types. We will be mostly concerned with sensor variable output power which can be used in heuristics addressing sensor network changing scenarios, as well as limited local memory and computation capabilities. All of this will be analyzed using our simulator. Some specific sensor examples based on the above assumptions will be analyzed and simulated.

(iii) Build the Wireless Sensor Network Simulator and prepare protocol variations for testing. The simulator will simulate the behavior of sensor nodes in all aspects of a real network environment. This will include different intrudertrajectories, number of activated sensors, different intruder velocities and different sensor field scenarios.

(iv) Create object oriented deployment spaces including design of the data and control packet structures required.

(v) Implement a time depended state machine that will simulate the properties of the wireless media access including message packet propagation delays. This will include Time Cycle stepping as well as Time Slot stepping.

(vi) Construction of sensor network topologies for testing and evaluation, include multiple frequency data channeling to minimize transmission collisions and hidden node interference. Each sensor should be able to communicate with its neighbors on different channels/frequencies. The specifics will be determined by each sensor node during the self-configuration phase. This also lends itself to a more mobile, adaptive network configuration capability. The template is used to format your paper and style the text. All margins, column widths, line spaces, and text fonts are prescribed; please do not alter them. You may note peculiarities. For example, the head margin in this template measures proportionately more than is customary. This measurement and others are deliberate, using specifications that anticipate your paper as one part of the entire proceedings, and not as an independent document. Please do not revise any of the current designations.

(vii) The simulator will have a graphical interface, so it can show the location of nodes being simulated, their associations as well as the message traffic between them. Network arrays will be built using direct placement through drag and drop, or random topological deployment simulating automated seeding. Sample collections will obtain properties from select lists of features. Logs of node and system status and activity will be created for analysis. Configuration profiles will be saved in a local file folder so they may be reloaded for future runs or used as a base for testing parameter changes. Test runs will save logs of programmable events and overall system status for later analysis. This will allow repeatable tests with changes in protocol, sensor attributes and other environmental parameters. Thus testing will be conducted in a controlled manner allowing repeatability for verification purposes. Statistics of various sorts, including but not limited to traffic volume, energy consumption, propagation time, and time to gather information from nodes, will be generated.

(viii) Use the Simulator to evaluate the protocol's performance.

(ix) Test and document self-organizing heuristic properties such as speed of network organization and expenditure of energy for the sensors. Derive sensor lifetimes (bit life or bit capacity) based upon energy cost per bit. Calculate network effectiveness.

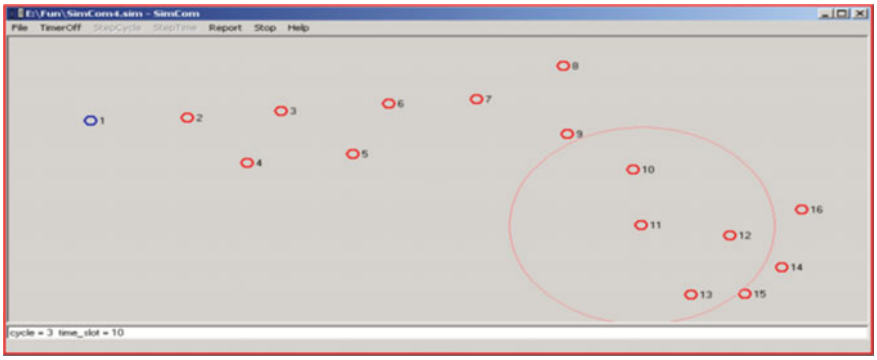

Fig. 1 Illustration of sample wireless simulator GUI

(x) Vary error rates and topology to determine network cohesiveness under changing environmental conditions.
(xi) Determine protocol performance in unreliable environments. Analyze the effect of redundancy on longevity. Provide operational boundary estimates and analyze impact on energy utilization and conservation.
(xii) Save statistical and parametric simulation data for further analysis.
(xiii) Include comparisons of different protocol models. The GUI is to be built for the Microsoft Windows or Android operating system. Figure 1 shows a sensor nodes GUI built as an illustration for this paper.

3 Low Power Sensor Network Protocol

The low power wireless sensor network is divided into sub-nets to account for sensor geo displacement and "congregation" due to a prescribed or ad hoc deployment (Figs. 2, 3 and 4), as required by a particular application. In order to describe network protocol operation we will introduce the following networking and protocol terms.

3.1 Networking Terms

LNm—Local Network number **m**, which is a collection of fixed number of sensors forming a sensor locale, where **m = 1,2,…,N**.
Sn,m—Sensor **n** within a particular **LNm**. Sensor may have limited local intelligence and memory, and a specific physical protocol as considered in Sect. 3.3.

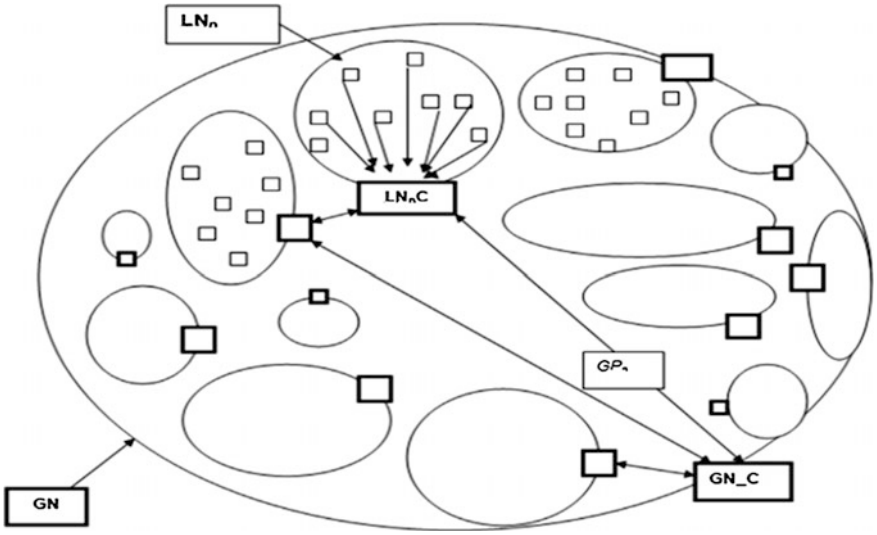

Fig. 2 Illustration of sample wireless simulator GUI

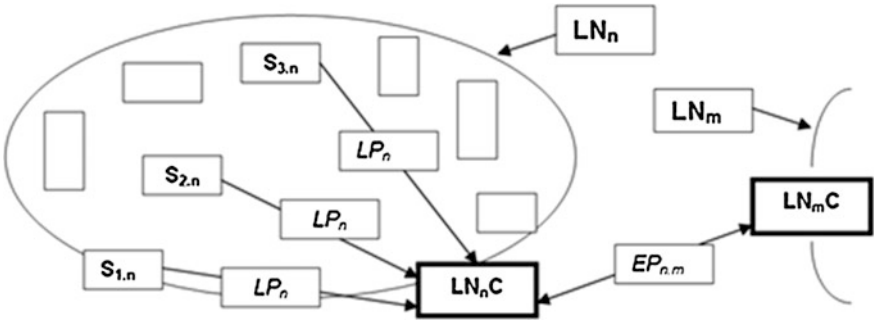

Fig. 3 A local wireless sensor network topology (**LNn**)

GN—Global Network, which is a collection of all **LN**'s hence consisting of all the deployed sensors, performing a data collection.
LNmC—Local Network **m** Control sensor is "in charge" (a Master) of communication within and outside of **LNm**. This function is negotiable by the other sensors in **LNm**. An event may trigger (based on some metrics) this function to be renegotiated.
GNC—A Global Network Control sensor node is, in charge of the overall data reporting and communication. This may also be a negotiable function.

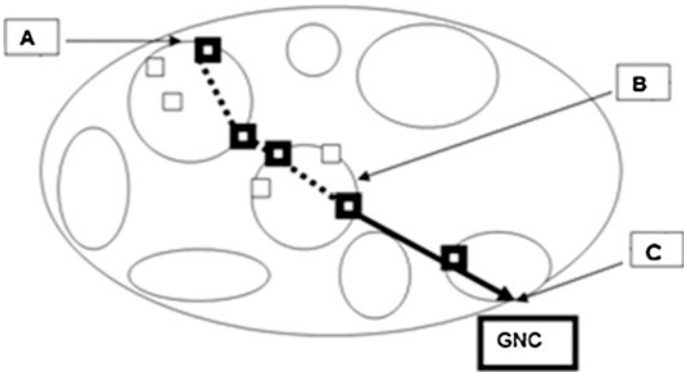

Fig. 4 Event network trail

3.2 Wireless Communication Protocols Terms

LPm—Local Wireless Sensor Protocol is a communication protocol internal to **LNm, i.e.** between any sensor Sn,m and **LNmC**. It needs to be as simple as possible, employed as infrequently as possible, with the lowest energy possible. This protocol is explained more in detail in theupcoming paper.
$\mathbf{EP_{p,q}}$—External Wireless Local Sensor Protocol is a communication protocol between $\mathbf{LN_p}$ and $\mathbf{LN_q}$. This protocol can be either Bluetooth or Wi-Fi standard protocols.
$\mathbf{GP_p}$—Global Protocol between $\mathbf{LN_p}$ and **GNC.** It can be implemented as any of $\mathbf{EP_{p,q}}$ protocols.

3.3 Network Operation

Here we consider a fixed and static (not-moving-sensors) network but it is a dynamic one in the sense that the relationships between the sensor nodes will be dynamic (such as which sensor is "in charge" at any given time; see also below). The network is self-organizing and we envision the following basic situations:

1. Network Initialization (sensors not collecting data)
   (a) Synchronize (time) sensors throughout the network. This function may be performed periodically to maintain network integrity. Simulation will be a reliable tool in determining how often to repeat this function.
   (b) Establish relationships (Master/Neighbor/Slave) among sensors based on pre-assigned criteria, such as sensor physical layer consideration, accuracy, battery life, memory, etc.
   (c) Forming of **LNm** and "Master" sensor "in charge", i.e. **LNmC**. This may be simply pre-determined based on the nature of the final network application.

(d) Test communications throughout the network to make sure that all the sensor nodes are responding and are "healthy". This is a responsibility of **GNC**.
(e) All of the above Initialization functions will be integrated into our final $\mathbf{LP_m}$, $\mathbf{EP_{p,q}}$ and $\mathbf{GP_p}$ protocols.

2. Following initialization, the network will go silent until an event triggers data gathering and reporting.
3. An event will trigger a short network activity and data reporting traffic (causing "event network trail" in Fig. 4) after which the network will go back to a quiet mode. During the event reporting the following functions will be performed:

(a) All the reporting sensors will route their communications from within sub networks, i.e. **LNm**, through sensors in-charge, **LNmC**, to **GNC** using short packets and $\mathbf{LP_m}$, $\mathbf{EP_{p,q}}$ and $\mathbf{GP}_p$ protocols.
(b) Depending on the type of trigger event and resulting communications and reporting (number of sensors alarmed, sensor signal strength), the network may re-adjust internal structure to address the next event more effectively.

3.4 Wireless Protocol Description

The design of the **LP** protocol came from a synthesis of our own ideas and ideas gleaned from existing successful network protocols. The need for conserving power and greatly limiting message traffic will make the protocol quite different from existing protocols. The following is a description of our initial considerations as far as the structure of these protocols. We will use a generic description for **LP** protocol as an illustration as to how a particular subnet **LNm** is formed and how individual sensor nodes are given roles (such as Master **LNmC**) within the subnet (see also Figs. 2 and 3). The details of **LP** will be discussed in our future work after the simulator is fully implemented and several particular protocols fully tested. Initially, it is assumed that all nodes are Masters and Neighbors of themselves. There may be two general situations:

1. Node has no neighbors in the protocol tables

(a) Broadcast request for Slaves

i. If another Master's request received

- Negotiate Master-hood domain number
  - Generated Random domain number
  - Highest domain number becomes Master

- If it becomes a Slave
- Transmit neighbor list to new Master

(This may be just itself!)

2. Node has neighbors

(a) It is Master

i. All of his neighbors are Slaves of his domain

(b) It is Slave

i. To only one Master
ii. May be connected to other Slaves and Masters

- Some neighbors may belong to other Master domains
- Another Master will consider him an Ambassadorial Slave, able to forward messages to and from different Master domains.

In any case, the above scheme results in a particular sensor node in a subnet $\mathbf{LN_m}$ becoming a Master or $\mathbf{LN_mC}$ control node. As stated earlier, this can be re-negotiated following some network event that can trigger it and cause the network to reconfigure itself.

Basic Relative Time Domain Description

1. Time is divided arbitrarily into Time Divisions (TD's). A TD belongs to one or more Master domains (i.e. one or more $\mathbf{LN_m}$**'s**). As Slave sensor units are added or lost, the time division of an $\mathbf{LN_m}$ domain is adjusted accordingly.
2. TD's are divided into equal size blocks. These blocks represent intervals when a sensor may transmit. Masters ($\mathbf{LN_mC}$**'s**) arbitrate duration assignments.

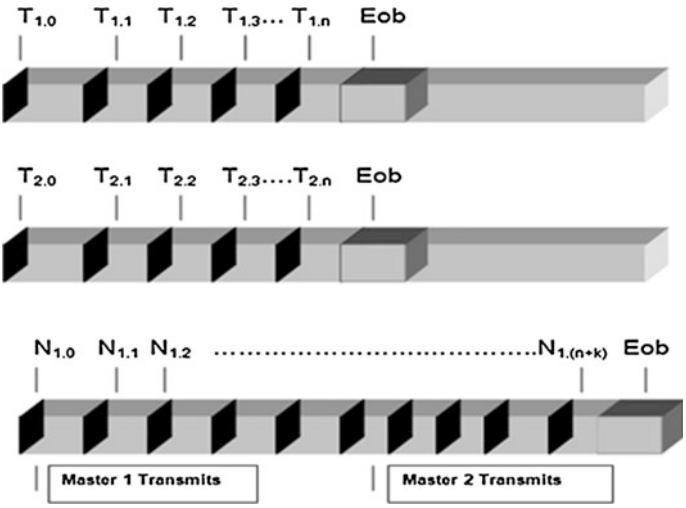

Fig. 5 Simplified relative time domain structure of LP protocol

3. Time in the TD is always relative and is marked by a numerical time stamp by each sensor unit that broadcasts.
4. Everyone listens when not transmitting, and adjusts their internal time to the time in the last block received. Since each next block is clock relative to a predecessor (without absolute time reference), it insures message sequencing will undergo the least possible collision and boundary failures. This will maximize overall energy efficiency in the local network by eliminating excessive synchronization transmissions due to high traffic collisions.
5. A time block belongs to a Master domain (i.e. $\mathbf{LN_m}$). When two domains overlap, the $\mathbf{LN_mC's}$ will negotiate time block sequences and they will coalesce into a single mutually inclusive TD (Fig. 5).

4 Protocol Simulator

Based on the general description of the protocol in Sect. 3, we now lay the ground for the Protocol Simulator, and propose to:

(i) Build protocol modules and integrate them into the simulator. The modules will be easy to switch for testing.
(ii) Test the basic packet flow. This will be done using typical network configurations (Table 1). Using the same configurations for testing will ensure fair comparison and interpretation of the results.
(iii) Evaluate overall network capabilities with several pre-designed scenarios (Table 1). Purpose of the first scenario—single node configuration in Table 1 is to test an isolated node, for the scenario of minimal network is to test basic network configuration, for the scenario of compact network is to test establishment of Master/Slave relationships and minimizing of traffic flow and for the scenario number 4 where configuration is done for realistic network purpose is testing real network. The protocol candidates will be implemented and a weighted statistics generated for each protocol. The protocols simulation results will summarize several typical wireless network topologies and corresponding protocols with their properties deduced from the simulations.

Table 1 Network configuration summary

Scenario	Node	Proximity
1	50	Nodes can communicate with a few neighbors
2	50	Distribution wide enough that nodes can only communicate with a few neighbors
3	50	Distribution wide enough that nodes can only communicate with a few neighbors
4	50	Distribution wide enough that nodes can only communicate with a few neighbors

Table 2 Network protocol scenarios

Scenario	Node	Proximity
Initial net config.	50	Nodes can communicate with a few neighbors
Report neighborhoods to a control node	50	Distribution wide enough that nodes can only communicate with a few neighbors
Report event to control node	50	Distribution wide enough that nodes can only communicate with a few neighbors
Request information from a specific node	50	Distribution wide enough that nodes can only communicate with a few neighbors

(iv) Simulate, test and optimize the protocols. Here we will be focused on fine tuning and optimizing protocols based on the results obtained in (iii) above. Various scenarios (Table 2) and statistics will be used to judge the performance of the network per LP, EP and GP protocols. Purposes of the four scenarios in Table 2 are testing basic configuration, report global net information to a control node, testing asynchronous information gathering ability and testing efficiency between two network nodes.

(v) Implement proposed protocols in the wireless sensor nodes of the Simulator. The message format will be defined and the command and parameters specified.

(vi) Implement the message transmission and receiving mechanism allowing sensor nodes to transmit messages, in their time slots, and to receive messages as they are heard and process them as is appropriate.

(vii) Gather network performance statistics (number of messages, their size, time required to accomplish tasks, and any failures). These statistics will be used to evaluate the performance of the protocols. The outcome of this will be protocol candidate's analysis, which will summarize best protocol candidates for further fine tuning.

(viii) Further test most promising protocols. In this task we will continue simulating and testing couple of best performing protocols which came out of Task (vii). This will be an iterative process (Fig. 6) whereas we will iterate the network configurations and protocols to achieve the best results from the point of view of technical goals stated in Sect. 3.

(ix) Further test the best performing protocol. Here we will choose a single best performing protocol so far, which will then be simulated, tested and

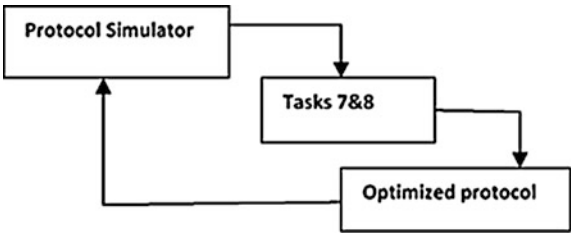

Fig. 6 Iterative process for protocol testing

fine-tuned even further. In the process we will redefine network configurations and again iteratively arrive at the best protocol structure.

5 Conclusion

In this paper we introduced new low power sensor wireless networking methodology. In particular:

(A) We introduced efficient wireless network topologies which will allow for effective wireless low-power sensor protocols.
(B) Developed introductory and innovative wireless communication protocol that can operate effectively in low power sensor networking. The final result is expected to be a stable and reliable protocol capable of accommodating a wide variety of network topologies. It will be easily scalable such that it can accommodate existing and future low power sensors.
(C) Our simulator will continuously aid in getting to this goal.
(D) Describe a concept of an elegant and user-friendly simulation environment with a GUI for analyzing and testing various wireless networks, including low-power wireless sensor network. This simulation environment will be easily scalable and will produce useful networking and protocol analysis and statistics.

References

1. Gowens J, Eike J (2010) Networked sensors: armor for the future forces. In: Proceedings of 2010 SPIE aero sense conference
2. Tarannum S (2011) Wireless sensor networks. InTech
3. Yang W (2012) Sensor array. InTech
4. Upadhayay V, Agrawal S (2010) Application of wireless nano sensor networks for wild lives. Nano Commun Netw 1:3–19
5. Park S, Kim J (2006) A nano operating system for wireless sensor networks. In: ICACT 8th international conference advanced communication technology, vol 1
6. Yu R, Watteyene T (2015) Reliable, low power wireless sensor networks for the internet of things. Linear Technology Corp, Whitepaper
7. Doherty L, Simon J (2012) Wireless sensor network challenges and solutions. Microwave J 1:22
8. Hodzic M, Brennan J (2000) Adaptive digital wireless communications network apparatus and process. US Patent No. 6
9. Altwies T, Hodzic M et al (2003) A method and architecture of an event transform oriented operating environment for a personal mobile display system. US Patent Publication
10. Hodzic M, Altwies T. (2010) A method and architecture that allows wireless devices or appliances to communicate in a cooperative thin-client networking environment. Internal communication

11. Krendzel A (2012) Wireless mesh networks: efficient link scheduling, channel assignment and network planning strategies. InTech
12. Yang D, Liu F (2010) A survey on internet of things. Atlantis Press, Amsterdam
13. Friese I. Challenges from the identities of things. Discussion group within Kantara Initiative
14. Said O (2013) Towards internet of things: survey and future vision. Int J Comput Netw (IJCN) 5(1)
15. Abdelwahab S (2014) Enabling smart cloud services through remote sensing: an internet of everything enabler. IEEE Internet Things J 1(3)
16. Zanell A (2014) Internet of things for smart cities. IEEE Internet Things J 1(1)
17. Pande P (2014) Internet of things—a future of internet: a survey. Int J Adv Res Comput Sci Manage Stud 2(2)

Feasibility of Biomass Co-firing in Large Boilers—The Case of EPBiH Thermal Power Plants

Admir Bašić, Enisa Džananović, Anes Kazagić and Izet Smajević

Abstract This paper investigates the possibilities and the sustainability of "biomass for power" solutions on a real power system. The case example is JP Elektroprivreda BiH d.d.—Sarajevo (EPBiH), a typical conventional coal-based power utility operating in the region of South East Europe. Biomass use is one of the solutions considered in EPBiH as a means of increasing shares of renewable energy sources (RES) in final energy production and reducing CO_2 emissions. This ultimately is a requirement for all conventional coal-based power utilities on track to meet their greenhouse gas (GHG) cut targets by 2050. The paper offers possible options of biomass co-firing in existing coal-based power plants as a function of sustainability principles, considering environmental, economic and social aspects of biomass use. In the case of EPBiH, the most beneficial would be waste woody biomass and energy crop co-firing on existing coal-based power plants, as suggested by biomass market analyses and associated technological studies including lab-scale tests. Four different options were considered, based on different ratios of biomass for co-firing: 0 %w-reference case, 5, 7 and 10 %w of biomass. The CO_2 parameter proved to be a key sustainability indicator, effecting the most decision making with regard to preference of options from the point of economy and sustainability. Following up on the results of the analyses, the long-term projection of biomass use in EPBiH has shown an increase in biomass utilization of up to 450,000 t/y in 2030 and beyond, with associated CO_2 cuts of up to 395,000 t/y. This resulted in a 4 % CO_2 cut achieved with biomass co-firing, compared to the 1990 CO_2 emission level. It should be noted that the proposed assessment model for biomass use may be applied to any conventional coal-based power utility as an

A. Bašić (✉) · E. Džananović · A. Kazagić · I. Smajević
Vilsonovo šetalište 9, 71000 Sarajevo, Bosnia and Herzegovina
e-mail: ad.basic@elektroprivreda.ba

E. Džananović
e-mail: en.dzananovic@elektroprivreda.ba

A. Kazagić
e-mail: a.kazagic@elektroprivreda.ba

I. Smajević
e-mail: i.smajevic@elektroprivreda.ba

M. Hadžikadić and S. Avdaković (eds.), *Advanced Technologies, Systems, and Applications*, Lecture Notes in Networks and Systems 3,
DOI 10.1007/978-3-319-47295-9_19

option in contributing to meeting specific CO_2 cut targets, provided that the set of input data are available and reliable.

1 Introduction

Co-firing biomass and bio-waste in coal-fired power plants is one of the most straightforward biomass applications in the short-to-medium term, as set out in the European Commission's White Paper on Energy for the Future: Renewable sources of energy [1]. The main reason for the use of biomass as a co-fuel is its dual role in greenhouse gas (GHG) mitigation, by being a substitute for fossil fuels (bio-energy) and a carbon sink [2]. Fuels derived from biomass contain less sulphur, ash and trace elements as well. Current research on co-firing is focused on controlling combustion behaviour, emissions, corrosion, agglomeration, and fouling-related problems. Biomass used for combustion in industrial-scale furnaces must meet a number of criteria, including: availability throughout the year to ensure security of supply, high density to minimize transportation costs, a sufficiently high heating value and an acceptable price [2]. As reported by Baxter et al. [3] and Koppejan [4], wood residues meet these requirements.

In the last decade, significant progress was made in the utilization of biomass in coal-fired power plants. Over 250 units worldwide have either tested or demonstrated co-firing of biomass or are currently co-firing on a commercial basis [5]. Coal is often replaced with up to 30 % of biomass by weight in pulverised coal based power plants, as in Belgium, Canada, Denmark, Finland, the Netherlands, Sweden, United Kingdom, Germany, Poland and the United States. Most of these projects refer to co-firing biomass with high-rank coal (both bituminous and anthracite), while availability of projects on biomass co-firing with low-rank sub-bituminous coal and lignite is more scarce, like the project involving Greek lignite reported in the work by Kakaras [6]. Estimates made by Poyry for the International Energy Agency (IEA) World Energy Outlook suggest that there is a certain potential for biomass sufficient to replace a 10 %th of coal in all coal-based power plants in the world [7]. Furthermore, progress is made in application of different types of municipal solid waste as a fuel in coal-based power plants (solid recovered fuel—SRF or refuse derived fuel—RDF, including their gasification). However, along with research, development and demonstration projects and technologies, economic and social issues of biomass to power solutions have to be investigated as well, to achieve sustainable biomass-based power systems.

2 State-of-the-Art

The co-combustion of biomass or waste with a base fuel in a boiler is a simple and economically suitable way to replace fossil fuels and utilise waste [8]. In addition to that, co-combusting in a high-efficient power station means utilising biomass and waste in a process with a higher thermal efficiency than what other ways had been possible, as reported by Leckner [9]. However, due to transportation limitations, the additional fuel will only supply a minor part (less than a few hundred MW fuel) of the energy in a plant. As according to the same author there are several options of "biomass for power" in large combustion plants, as for example:

- co-combustion with coal in pulverised or fluidised bed boilers,
- combustion on added grates inserted in pulverised coal boilers,
- combustors for added fuel coupled in parallel to the steam circuit of a power plant,
- external gas producers delivering its gas to replace an oil,
- gas or pulverised fuel burners.

Biomass can further be used for reburning in order to reduce NO_x emissions [10], or for after-burning to reduce N_2O emissions in fluidised bed boilers. A combination of fuels can give rise to positive or negative synergy effects, of which the interactions between S, Cl, K, Al and Si are the best known, which may give rise to or prevent deposits on tubes [11], or may have an influence on the formation of dioxins [9].

Co-combustion has a number of potential advantages. A brief list, as reported by Leckner [9], is given below:

- reduction of CO_2 emissions from fossil fuels,
- increased use of local fuels,
- conversion of biomass and waste fuels with a high efficiency and under controlled environmental conditions,
- there are no formal size limitations, although there are certain economic restrictions on how far voluminous and disperse materials such as biomass and waste can be transported, which can limit the size of a plant using such fuels,
- seasonal variations inherent in some biofuels can be adequately handled, because the ratio of the added to the base fuel can easily be scaled down from its maximum value,
- less complicated than other alternative conversion methods for biofuels and, hence, potentially economically advantageous,
- the amount of added fuel employed can be adjusted to the availability of biofuels and wastes within a reasonable transportation distance from the conversion plant, and
- possible positive synergy effects with different fuels can be utilised.

Disadvantages can also be expected in form of:

- the costs of some additional equipment or treatment processes need to be considered,
- the threat of harmful influence on the power plant, caused by the added fuel,
- possible negative synergy effects if the added fuel has some extreme properties (like some wastes) or if the combination of fuels is unfavourable, and
- lack of experience, as reflected from two of the above points.

Better knowledge of these effects may help the positive ones to be used and the negative ones to be avoided [9].

Over the last decade many research studies were conducted in order to investigate the biomass co-firing phenomenon. As an example, Wang et al. [12] evaluated the combustion behaviour and ash properties of a number of renewable fuels, like rice husk, straw, coffee husk and RDF derived from municipal waste. The work used a drop tube furnace to evaluate the combustion behaviour and ash properties of biomass, waste derived fuels, pine and coal. Kupka et al. [13] investigated the ash deposit formation during the process of co-firing coal with sewage sludge, saw-dust and refuse derived fuels in a drop tube furnace, to optimize biomass co-firing blends. Williams et al. [14] investigated the emission of pollutants from solid biomass fuel combustion. Emissions and ash-related problems were investigated in the Bosnian case as well, by co-firing Bosnian coal with waste woody biomass [15, 16], where some specific benefits and synergy effects were observed. Co-firing Bosnian coal with woody biomass in existing coal-fired power plants is hence considered a perspective combustion technology in the Bosnian case. Examples of biomass co-firing can be found in other industries as well, like in the example of biomass co-firing in the cement industry, as reported by Mikulcic et al. [17].

When it comes to GHG emissions and policy related issues, which present important supporting tools when considering more extensive biomass use, further considerable research can be found as well. GHG and pollutant emissions coming from the energy sector are very high today, which forces countries all over the world to take cost-effective steps for their mitigation, by creating adequate policies [18, 19]. CO_2 storage in underground reservoirs can result in very low—perhaps even near-zero—net GHG emissions, depending on the share of biomass used as input and its CO_2 signature, as reported by Aitken et al. [20]. Royo et al. [21] developed a methodology applied to the Spanish case, by which a significant biomass co-firing potential and a subsequent GHG emission reduction could be achieved over large territories.

Overall, the given examples illustrate that research in biomass co-firing has so far mainly been performed in order to optimize the fuel mix through minimizing ash-related problems and emissions. Biomass co-firing in large power plants is mainly considered in reducing CO_2 emissions, improving security of supply and reducing operational costs by fuel cost optimization. However, less attention was given to economy and sustainability issues of biomass co-firing solutions, where authors found only some related work. As an example, Umar et al. [22] investigated

the market response to six sustainability-related topics, thereby identifying several key factors for consideration by the government. The research involved an electronic and conventional postal dissemination of questionnaires to palm oil producers in Malaysia. Samsatli et al. [23] gave a novel MILP formulation of the Biomass Value Chain Model (BVCM), which accounts for the economic and environmental impacts associated to the end-to-end elements of a pathway: crop production, conversion technologies, transport, storage, local purchase, import (from abroad), sale and disposal of resources, as well as CO_2 sequestration by carbon capture and storage (CCS) technologies and forestry. It supports decision-making around optimal use of land, biomass resources and technologies with respect to different objectives, scenarios and constraints. Objectives include minimizing the cost, maximizing the profit, minimizing GHG emissions, maximizing energy/exergy production or a combination of these. The main contribution of this work is reflected in demonstrating the additional merit of biomass co-firing in this specific case and its contribution to economy and sustainability.

3 System Under Consideration—EPBIH Utility

3.1 General Description of the System Under Consideration—EPBiH Power Utility

The analyses performed in this work are demonstrated on an example of a real power system. The case example is JP Elektroprivreda BiH d.d.—Sarajevo (EPBiH), a typical conventional coal-based power utility operating in the region of South East Europe. EPBiH is part of the Energy Community of South-East Europe (SEE) and is situated in Bosnia and Herzegovina (BiH). The total power output of EPBiH amounts to approximately 8000 GWh/y and is generated at two coal-based thermal power plants (TPP), i.e. TPP Tuzla and TPP Kakanj, three large hydro power plants (HPP) on the river of Neretva, and a small number of small HPPs (sHPP) with a share of approximately 1 %.

Table 1 provides an overview of some basic information for existing TPPs addressed in the case study. The data is later on used as input parameters for the calculation and assessment of sustainability indicators. Both TPPs use indigenous low-rank coal, consuming about 6,500,000 t/y and generating around 6,500,000 tCO_2/y. Annual output of heat generated at the cogeneration units of TPP Tuzla and TPP Kakanj accounts for approximately 400 GWh/y [24].

Table 1 Basic data on existing TPP units of EPBiH

Generation facilities	Installed capacity [MW]	Efficiency [%]	Domestic fuel cost [€/10^6kcals]	Variable O&M costs [€/kW per month]	Fixed O&M costs [€/kW per month]	Planned retirement year
TPP Tuzla unit 3	100	24.78	2.99	1.00	2.7	2018
TPP Tuzla unit 4	200	30.13	3.09	1.37	2.4	2021
TPP Tuzla unit 5	200	29.88	2.82	0.72	2.6	2030
TPP Tuzla unit 6	223	32.73	2.86	0.41	1.4	2030
TPP Kakanj unit 5	118	31.55	2.78	0.65	3.5	2023
TPP Kakanj unit 6	118	32.14	2.72	0.39	2.0	2030
TPP Kakanj unit 7	230	30.93	2.68	0.67	7.3	2030

3.2 Development Targets for Thermal Power Plants of EPBiH

Over the past ten years, the total net efficiency of EPBiH's power plants has increased from 24 to 31 %. This was accomplished by applying specific measures such as decommissioning old thermal power units (4 × 32 MW in TPP Kakanj and 2 × 32 MW in TPP Tuzla) and modernising all of the other existing coal-based power units. At the same time, CO_2 emissions were reduced from 9500,000 t/y (1990) to the current level of 6,500,000 t/y [24].

EPBiH, however, is still facing challenges despite the improvements made. Requirements for further energy efficiency and CO_2 emission reduction measures are mandatory for the company to keep and improve its position on the market. It should also help the company comply with the energy efficiency and environmental regulation, as well as give support to the low-carbon future. Based on the planned generation portfolio development and an annual power demand projection until 2030, a new generation portfolio was optimized and projected in order to reach specific energy and decarbonisation targets. The portfolio expansion took into account plans of EPBiH to construct new generation facilities, while at the same time taking into consideration the requirements for replacement capacities. Replacement capacities are considered with respect to TPPs planned to be decommissioned by 2030. The dynamics for their decommissioning are defined as part of the Long-term development plan of EPBiH. The choice of the commissioning dynamics of all other TPP associated facilities is subject to analysis, performed with regard to sustainability and decarbonisation criteria, partially conducted as part of this work as well. Additional inputs involve the current investment plans for desulphurization (DeSOx) and denitrification (DeNOx)

facilities, planned in order to address obligations arising from the Large Combustion Plants Directive (LCPD) and Industrial Emission Directive (IED) (Directive 2009/28/EC, Directive 2012/27/EU).

The development plan will overall result in new TPP, HPP, wind power plant (WPP), photovoltaic power plant (PVPP) and biomass power plant (BPP) projects. To effect further CO_2 emissions reduction, co-firing coal with biomass is planned in all EPBiH TPPs [24].

3.3 *Biomass for EPBiH Power Plants—Resourcing*

The residues of the wood processing industry, agricultural and forest residues, as well as dedicated energy crops, are among the most abundant sources of energy in Europe. Making use of forest and agricultural residues in the power industry does not only help replace a certain amount of fossil fuels, but it also helps reduce their disposal in the environment, cutting down emissions of the greenhouse gas CH_4 (by avoiding biomass decomposition). Additional benefits include new job creation in establishing the required biomass supply chain (collection, transportation) and an overall better perspective for the development of energy, forestry and agriculture in the country.

Biomass has a significant potential as a source of energy in BiH. It is estimated that the total annual technical biomass energy potential in BiH is over 33PJ, which is equivalent to more than 3 million of BiH lignite [25]. The most significant source of biomass for energy production in BiH is waste woody biomass originating from forestry (forest residues), as well as from the wood industry (wood chips, sawdust). Agricultural residues have a significant energy potential in BiH as well and are mainly located in the northern, central and southern parts of the country. Several assessments of the BiH biomass potential were performed so far and the results of one of these studies (EU/FP6/INCO/ADEG), reported by Schneider et al. [25], are presented in Table 2.

Table 2 Data on annual potential of biomass in BiH (FP6 Project ADEG), [25]

	Available amounts (per year)	Energy potential [PJ]	Origin
Biogas from farms	200,000 m^3	0.51	Agriculture
Fruit growing waste	211,257 t	0.74	Agriculture
Grains residues	634,000 t	8.88	Agriculture
Leguminous plants and oil seeds remains	3858 t	0.04	Agriculture
Woody waste from industry	1,142,698 m^3	7.53	Forestry
Firewood	1,466,973 m^3	13.2	Forestry
Woody residues from forestry	599,728 m^3	2.62	Forestry
Total technical potential		33.52	

BiH has also certain conditions suitable for the cultivation of fast-growing energy crops. This option is currently subject to research and power plants are one of the potential beneficiaries of such a CO_2 neutral fuel.

3.4 Biomass Market

Biomass market in BiH is not developed enough at the moment to supply PE EP BiH with required amount of biomass. Introducing pellets and briquettes for heating private apartments started a small market of biomass but that is not enough to secure needed amounts of biomass for PE EP BIH, and prices are still unstable. It can be expected that both the supply and prices will be constant if the demand is constant. Biomass market in BiH is a typical representative of the new market. For example, in the project in EP BiH it was assumed that the price would be approximately 16.00 €/t, but when the project started, the price of wooden biomass was five to six times higher than expected. The reason for this is that there is no established market, and when the demand increased, the supply did not change. But if the demand was constant, the supply would increase and the new price would be formed, as presented in Fig. 1. Based on the market research, the assumed price of biomass would be 6.00 KM/GJ.

One of possible solutions for PE EB BiH is to form a long term contract with suppliers, such as forest companies in BiH, just like, for example, HEP (electrical energy company in Croatia) did and secured approximately 400,000 t/a of biomass. The seller has product placement, and the buyer has constant prices, a sufficient amount of biomass and a safe supplier. However, the biggest potential for biomass

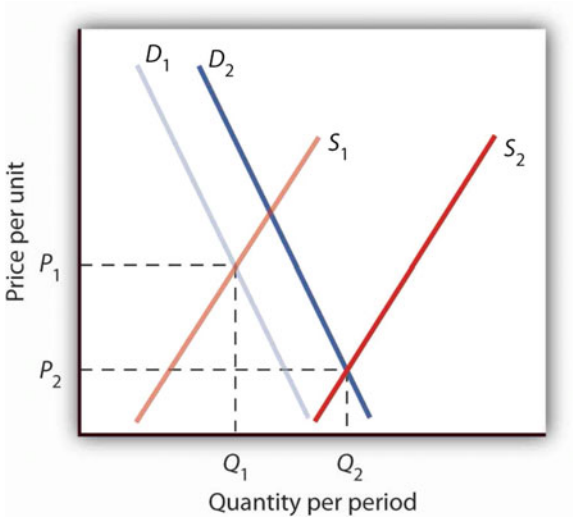

Fig. 1 Biomass price

is inside PE EP BiH, for coal mines to grow energy crops. It is best to grow Miskantus; one hectare can replace up to 9000 l of fuel.

3.5 *Projections and Biomass Co-firing Options in the Case of EPBiH*

It is anticipated that the future of coal-fired power plants will only be certain if their CO_2 emissions are below 550 kg/MWh. In order to fulfill such conditions in a long-term view and in the absence or delay of CCS implementation and development, the new coal-fired power units of EPBiH are required to reach a net efficiency of 43 %, using at the same time 25 % of biomass.

The first steps of introducing biomass in the power generation portfolio of EPBiH were already made. After years of laboratory research, the implementation of a pilot project trial run on the TPP Kakanj Unit 5 in April 2011 has proven a technological viability of using at least 7 %w of waste woody biomass (sawdust) mixed with specific brown coal, as reported by Smajevic et al. [26]. The method involved first mixing biomass and coal on the coal depot, transporting the mixture by the belt conveyor to the bunker and the mills, and injecting it into the boiler through existing coal burners. This method of direct co-combustion allows a use of 7-10 % of biomass in the fuel mix without causing any operational problems, in the case of TPP Kakanj. Other forms of co-combustion, allowing higher shares of biomass in the mixture (10–30 %), are also considered. These involve indirect mixing and co-combustion of the fuel blend in the boiler via biomass gasification or special biomass burners.

Overall, a projected use of 7 %w of biomass at all power units of EPBiH, used at an average rate of 3000 h/y, would reduce the total CO_2 emissions of EPBiH by 4 %, as reported by Smajevic et al. [26]. EPBiH has therefore announced plans to introduce biomass into its generation portfolio, in order to reach long-term CO_2 cuts. These are concurrent with plans of energy efficiency improvements and the construction of new more efficient thermal power plants [24]. According to the plan, by the end of the planning period covered by the Long-term development plan of EPBiH, it is technologically feasible and therefore can be planned to exploit biomass in existing and new thermal power units of EPBiH. The projected share of biomass in the fuel mix is indicated in Table 3.

Therefore, the primary objective of biomass use in existing and new power units of EPBiH in the coming years is to reduce CO_2 emissions, as well as to optimize fuel and operation and maintenance (O&M) costs. The 2030 projections show that there is a technological potential for the TPPs of EPBiH to have an annual power generation of up to243 GWh at existing and 885 GWh at new units coming from biomass. Taking only a 50 % of the estimated fuel consumption at the new units alone, an annual volume of at least 225,000 t/y in long-term biomass use would be achieved.

Table 3 Projection of the biomass share in the fuel mix of EPBiH thermal

	Power from biomass [MWe][a]	Annual generation [MWh][a]	Annual biomass consumption [t][b]	Annual CO_2 cut [t]
Kakanj TPP unit 5 (118 MWe)	7.5	24,000	16,000	18,500
Kakanj TPP unit 6 (118 MWe)	7.5	24,000	16,000	18,500
Kakanj TPP unit 7 (230 MWe)	17	54,000	35,000	40,000
New Kakanj TPP unit 8 (450 MWe)	75	225,000	130,000	115,000
Tuzla TPP unit 4 (200 MWe)	16	45,000	30,000	36,000
Tuzla TPP unit 5 (200 MWe)	16	45,000	30,000	36,000
Tuzla TPP unit 6 (223 MWe)	17	45,000	35,000	40,000
New Tuzla TPP unit 7 (450 MWe)	110	330,000	160,000	140,000
New Tuzla TPP unit 8 (450 MWe)	110	330,000	160,000	140,000
Existing units	81	243,000	162,000	188,000
New units[c]	295	885,000	450,000	395,000

[a]The projection of power and power generation based on energy from biomass, is projected based on a share of 7 %w of biomass in the mixture with coal for existing units and a 25 % share of biomass in the mixture for new units, along with an operating rate of 3000 h/y under the regime of co-combustion at each unit (for the remaining time of the year the units are operated on coal only)
[b]Annual consumption of biomass for the projected power generation and net efficiency of a given unit, and for an average net calorific value of biomass of 14,000 kJ/kg
[c]If a CCS technology is not implemented

4 Financial Assessment od Biomass Co-firing Options in Case of a EP BiH Power Plant Kakanj

4.1 Methodology

In this research we used the following scientific methods: statistical methods, comparative methods, the method of analysis, synthesis methods, and we also used scientific methods to collect data necessary to carry out the necessary conclusions. The detection method was used in determining the truth of individual facts. The comparative method was used for comparing prices of fuel and biomass, and fees for pollution in Croatia and EU. The methodology applied in financial analysis is common for projects in PE EP BiH and is compliant with the methodology of international financial institutions and economic theory.

4.2 Inputs for Analysis—Case of TPP Kakanj

Thermal power plants vary according to technological characteristics and according to the type of applied technology implementation of co-firing, which will have different impact on business results. A project like this one will have an initial investment, an impact on costs of, for example, the material for production, maintenance, emission of pollutants, and, less likely, an impact on NUS products, administration and other costs. For the analysis, the results and conclusions from project in PE EP BiH will be used. The project of co-firing of biomass and coal is performed in TPP Kakanj, Unit 5, but because of the characteristics of Unit 5 and Unit 6, the conclusions can be applied to Unit 6. The main objective of the pilot project was to test the possibility of introducing the practice of co-firing biomass and coal in order to reduce CO_2 emissions. The conclusions important for economic analysis are that the amount of biomass burned cannot exceed 7 % of the total amount of coal, calculated by weight, at 3000 h. Co-firing in this volume does not require any additional investments and realizes the positive environmental aspects. Biomass could be mixed with coal at existing depots in the framework of the existing principles of homogenization of coal at the depot, and, most importantly, the production of energy does not depend on the quantities of biomass.

For better performance and longer life expectancy for analyses, Unit 6 is used for the analysis, and this Unit is observed isolated from TPP. There are two options for Unit 6: to implement co-firing biomass and coal or not.

For this analysis, net book value of assets is used as an initial investment. Due to conclusions that an additional investment for co-firing is not needed, the initial investment is the same for both options. The difference is in the variable costs. The biggest change will be in the material for production. This cost is about 40 % of all costs in EP BiH, and coal is about 60 % of all costs of the thermal power plant. Savings of 1 % in these costs mean savings of over 1.5 million in TPP Kakanj. The introduction of biomass will directly affect the reduction of emissions, and therefore a reduction in costs related to air pollution.

According to experimental testing with 7 % w biomass and 3000 operating hours per year, the results are:

- Reducing CO_2 emissions by about 8.5 %,
- Reduction of SO_2 emissions by about 3.6 % and
- Reduction of NO_x by about 2.3 %.

Based on the above information and based on expected emissions, we can calculate savings for the financial analysis. Moreover, in this analysis the expectation of additional increase of fees and new fees for CO2 should be considered. Biomass is CO_2 neutral fuel and is recognized as renewable energy, so it is important to note that co-firing of 7 %w biomass in coal will reduce emission of CO_2 for about 8.5 %. For example, in Croatia, the fee for CO_2 emission is 18 kn/t and 100 kn/t if pollution is more than allowed. Similar regulation will be developed

in BiH in the near future, and this cost can be partially avoided with co-firing of biomass and coal.

The fixed expenses should be the same for both options. Maintenance facilities and operational readiness are of utmost importance, but it is proven there will be no negative effects on production processes. In TPP Kakanj, co-firing will not change the depreciation and salaries, and it is expected that there will be no changes of other costs.

TPP generate income from electrical energy, thermal energy, NUS products, renting equipment and other unexpected revenues. Co-firing will have an impact on income from electrical energy, so it can be assumed that other revenues will be the same with or without co-firing. Income from electrical energy will be changed trough incentive price for renewable energy which is regulated by law. For complete financial analysis, private and social costs and the benefits of the project have to be calculated. It is most difficult to valorise social costs, but the society and the State recognized it and that is why there is the incentive price.

4.3 Results of Economic Parameters

The final decision about realization of co-firing depends on the results of financial analysis. For this purpose we made a cash flow and a projection for two options for Unit 6 TPP Kakanj: Option 1—traditional, Option 2—co-firing. Both options can be used only for this project because it is calculated isolated from other units and TPP. For the analysis the static and dynamic indicators have to be calculated, but the most realistic and the only ones presented are IRR and NPV (Fig. 2).

The first analysis was conducted in 2013 and based on market information at that time. The investment is not needed, coal would be substituted with biomass and biomass is more expensive than coal. Tax for pollution is lower for Option 2 but not significantly since biomass is more expensive than coal. It follows that electrical

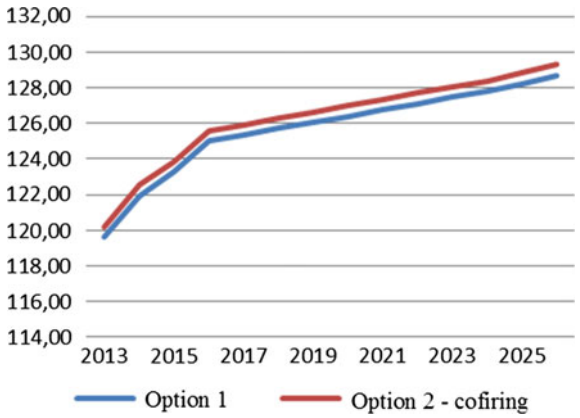

Fig. 2 Production cost

energy from co-firing biomass and coal is more expensive (Fig. 1. Production cost) for about 1 % for market conditions in 2013 (biomass price and pollution fee).

In spite of the higher production cost, the decision about the implementation of the project can be made based on the financial analysis with included calculations of all revenues, including the revenues for electrical energy with the incentive price for renewable energy. PE Elektroprivreda will choose the project with better results (Table 4; Figs. 3 and 4).

Implementing the project of co-firing, PE EPBiH would have a higher annual profit as long as biomass price is lower than 9.80 KM/GJ, as shown in Fig. 4. It needs to be noted that the information about the net profit and the loss can be interpreted only with a remark that this projection for Unit 6 is isolated from TPP and the net book value is calculated as an investment.

Table 4 Economic indicators

	Option 1	Option 2
Pay-back period	–	13
Rate of return	1.90	3.56
Reproduction rate	9.31	10.96
NPV	-18440797	5813825
IRR (%)	−2.30	0.69

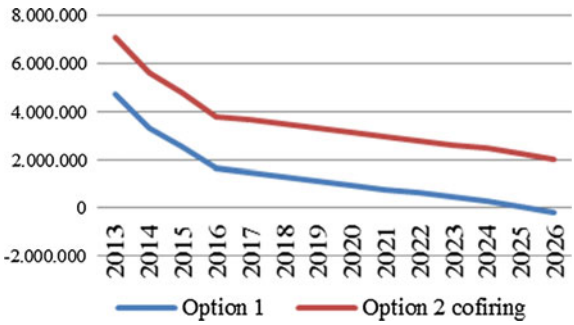

Fig. 3 Net profit/loss

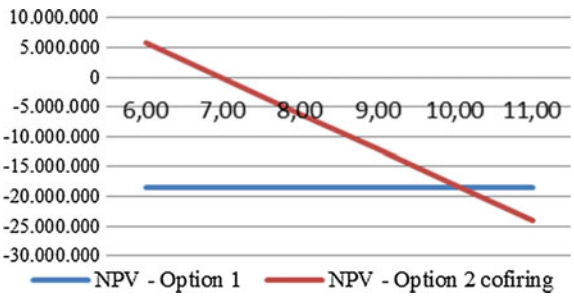

Fig. 4 Biomass price and NPV

Now, when results in 2016 are analyzed, it can be seen that coal and biomass price, depreciation and other costs are unchanged, but there have been many changes in the electrical energy market since 2013.

Electrical energy price suffered unexpected decline and in March the price was 50 KM/MWh. Laws in BiH are changed and there is more competition. Many companies/consumers are leaving EP BiH and buying electrical energy from other suppliers. The price for households is not changed, but this price is calculated based on electric energy from hydro and thermal power plants. Nowadays, it is more profitable to buy electric energy for 50 KM/MWh and not produce it in TPP. Reduced production causes the same fixed cost, and the higher price per unit, which was approximately 130.00 KM/MWh in TPP Kakanj for the period January–April. If the price of electric energy of 60.00 KM/MWh is assumed in the financial analyses, the result for Unit 6 will be negative and the net loss will be higher than 30 mil KM/a.

PE Elektroprivreda BiH recognized this problem and the solution for this is offered in the two projects: District heating systems of cities Visoko, Breza, Vogošća and Sarajevo from TPP Kakanj cogeneration units and Project of co-firing biomass and coal.

Both projects are in a phase of feasibility study. Heating will secure more production, lower pollution and lower costs per unit, and feasibility study will show whether it is worth investing in that project. The second project is related to co-firing of biomass and coal. For this project, the incentive price for renewable energy is the most important.

In BiH in 2016, the incentive, guaranteed price for energy from biomass by law is 31,292 KM/MWh. For Unit 6 in TPP Kakanj, it means that 9 % of annual energy would be generated from biomass, and for this energy TPP Kakanj would get the stimulating price of 31,292 KM/MWh.

Market changes just confirmed that co-firing of biomass and coal would diversify the risk and reduce the negative effects of lower price electric energy or other expected negative effects, such as an increase of coal price, pollution taxes and similar. Figures 5 and 6 can show what has happened in the last three years,

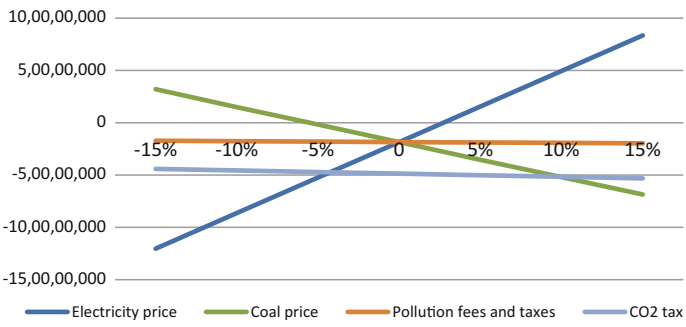

Fig. 5 Sensitivity analysis—option 1

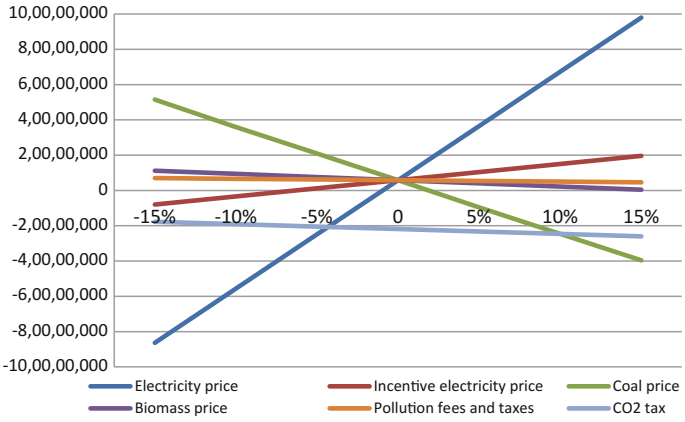

Fig. 6 Sensitivity analysis—option 2 cofiring

and what else may happen in next period. When observing economic indicators and the risk for TPP in terms of the unstable market, now, even more than before, the conclusion is obvious: PE Elektroprivreda should implement the project of co-firing.

5 Conlusions

In the last decade, significant progress was made in the utilization of biomass in coal-fired power plants. While many research studies were conducted to investigate the biomass co-firing phenomenon, like ash-related problems or emissions, far less attention was given to the investigation of sustainability of "biomass for power" solutions, and to the economy as well. In this work, the assessment is performed for EPBiH, a typical conventional coal-based power utility operating in the region of South East Europe.

On the basis of the performed analyses, it was concluded that the CO_2 parameter proves to be a key sustainability indicator in the considered case, effecting the most decision making with regard to the preference of biomass co-firing options from the point of economy as well as sustainability. Market changes just confirmed that co-firing of biomass and coal would diversify the risk and reduce the negative effects of lower price of electric energy or other expected negative effects, such as an increase of coal price, pollution taxes, etc.

The results demonstrate the additional merit of biomass co-firing for this specific case and its contribution to sustainability. The model presented in the paper can be applied to any power utility provided that the set of input data is available and reliable.

References

1. European Commission (1997) Energy for the future: renewable sources of energy. White paper for a community strategy and action plan. ec.europa.eu/energy/library/599fi_en.pdf. Accessed June 2015
2. Wischnewski R, Werther J, Heidenhof N (2006) Synergy effects of the co-combustion of biomass and sewage sludge with coal in the CFB combustor of Stadtwerke Duisburg AG. VGB Power Tech 86(12):63–70
3. Baxter LL, Rumminger M, Lind T, Tillman D, Hughes E (2000) Cofiring biomass in coal boilers: pilot- and utility-scale experiences. In: Biomass for energy and industry: 1st world conference and technology exhibition, Seville
4. Koppejan J (2004) Overview of experiences with cofiring biomass in coal power plants. IEA Bioenergy Task 32, Netherlands
5. KEMA (2009) Technical status of biomass co-firing. IEA Bioenergy Task 32, Netherlands
6. Kakaras E (2000) Low emission co-combustion of different waste wood species and lignite derived products in industrial power plants. XXXII Krafwerkstechnisches colloquium: Nutzungschwierigerbrennstoffe in kraftwerken, Dresden, pp 37–46
7. International Energy Agency—IEA (2014) World energy outlook 2014. IEA Publications, Paris
8. Williams A, Pourkashanian M, Jones JM (2001) Combustion of pulverised coal and biomass. Prog Energy Combust Sci 27(6):587–610
9. Leckner B (2007) Co-Combustion: a summary of technology. Therm Sci 11(4):5–40
10. Hodzic N, Kazagic A, Smajevic I (2016) Influence of multiple air staging and reburning on NO_x emissions during co-firing of low rank brown coal with woody biomass and natural gas. Appl Energy 168:38–47
11. Kazagic A, Smajevic I (2009) Synergy effects of co-firing of woody biomass with Bosnian Coal. Energy 34(5):699–707
12. Wang G, Silva RB, Azevedo JLT, Martins-Dias S, Costa M (2014) Evaluation of the combustion behaviour and ash characteristics of biomass waste derived fuels, pine and coal in a drop tube furnace. Fuel 117:809–824
13. Kupka T, Mancini M, Irmer M, Weber R (2008) Investigation of ash deposit formation during co-firing of coal with sewage sludge, saw-dust and refuse derived fuel. Fuel 87(12):2824–2837
14. Williams A, Jones JM, Ma L, Pourkashanian M (2012) Pollutants from the combustion of solid biomass fuels. Prog Energy Combust Sci 38(2):113–137
15. Kazagic A, Smajevic I (2007) Experimental investigation of ash behavior and emissions during combustion of Bosnian coal and biomass. Energy 32(10):2006–2016
16. Kazagic A, Smajevic I (2008) Evaluation of ash deposits during experimental investigation of co-firing of bosnian coal with woody biomass. 40. KraftwerkstechnischesKolloquium: KunftigesBrennstoff- und Technologieportfolio in der Kraftwerkstechnik, 2008. Dresden 2:238–249
17. Mikulcic H, von Berg E, Vujanovic M, Duic N (2014) Numerical study of co-firing pulverized coal and biomass inside a cement calciner. Waste Manage Res 32(7):661–669
18. Fan J, Zhao D, Wu Y, Wei J (2014) Carbon pricing and electricity market reforms in China. Clean Technol Environ Policy 16(5):921–933
19. Klemes JJ (2010) Environmental policy decision-making support tools and pollution reduction technologies: a summary. Clean Technol Environ Policy 12(6):587–589
20. Aitken ML, Loughli DH, Dodder RS, Yelverton WH (2015) Economic and environmental evaluation of coal-and-biomass-to-liquids-and-electricity plants equipped with carbon capture and storage. Clean Technol Environ Policy 18(2):573–581
21. Royo J, Sebastian F, Garcia-Galindo D, Gomez M, Díaz M (2012) Large-scale analysis of GHG (greenhouse gas) reduction by means of biomass co-firing at country-scale: application to the Spanish case. Energy 48(1):255–267

22. Umar MS, Jennings P, Urmee T (2014) Sustainable electricity generation from oil palm biomass wastes in Malaysia: an industry survey. Energy 67:496–505
23. Samsatli S, Samsatli NJ, Shah N (2015) BVCM: a comprehensive and flexible toolkit for whole system biomass value chain analysis and optimisation—mathematical formulation. Appl Energy 147:131–160
24. Kazagic A, Merzic A, Redzic E, Music M (2014) Power utility generation portfolio optimization as function of specific RES and decarbonisation targets—EPBiH case study. Appl Energy 135:694–703
25. Schneider DR, Duic N, Raguzin I, Bogdan Z, Ban M, Grubor B, Stefanovic P, Dakic D, Repic B, Stevanovic Z, Zbogar A, Studovic M, Nemoda S, Oka N, Djurovic D, Kadic N, Bakic V, Belosevic S, Eric A, Mladenovic R, Paprika M, Delalic N, Lekic A, Bajramovic R, Teskeredzic A, Smajevic I, Dzaferovic E, Begic F, Lulic H, Metovic S, Petrovic S, Djugum A, KadricDz Hodzic N, Kulic F, Kazagic A, Gafic A (2007) Mapping the potential for decentralised energy generation based on RES in Western Balkans. Int Sci J Therm Sci 11 (3):7–26
26. Smajevic I, Kazagic A, Music M, Becic K, Hasanbegovic I, Sokolovic S, Delihasanovic N, Skopljak A, Hodzic N (2012) Co-firing Bosnian coals with woody biomass: experimental studies on a laboratory-scale furnace and 110 MWe power unit. Therm Sci 16(3):789–804

Numerical Simulation of Air-Water Two Phase Flow Over Coanda-Effect Screen Structure

Hajrudin Dzafo and Ejub Dzaferovic

Abstract Application of numerical methods to assess the hydraulic performance of the screen Coanda-effect is investigated. This research project focused on flow observation and CFD simulation in the zone around the Coanda-effect screen. Numerical model is developed for clear water conditions. This model allows prediction of water discharge through the Coanda-effect screens, allowing to estimate the performance of the screen changes caused by variations in parameters screen design. Flow over the Coanda-effect screens can be modeled using the energy equation for spatially varied flow with decreasing discharge. Since the flow is supercritical, computations begin at the top of the screen and proceed in the downstream direction. The next phase of this PhD-research project is planned to be realized in cooperation with the Water Resources Research Laboratory, U.S. Bureau of Reclamation, Denver-Colorado (USA), where is performing experimental tests for improving Coanda-effect screen Technology, as coupling numerical and physical modeling for analysis of flow in structures with Coanda-effect screens. This can provide progress in better understanding of this phenomenon of flow. This article deals with experimental research and numerical simulations of specific phenomena in fluid flow called Coanda effect, which is important engineering application in the water intake structures of the small hydro power projects.

1 Introduction

This article shows how numerical modeling tool can be used to observe flow patters around the Coanda-effect screen in water intake structure for small hydro power plants in the mountain streams.

H. Dzafo (✉) · E. Dzaferovic
University of Sarajevo, Vilsonovo setaliste 9, Sarajevo, Bosnia and Herzegovina
e-mail: h.dzafo@elektroprivreda.ba

E. Dzaferovic
e-mail: dzaferovic@mef.unsa.ba

M. Hadžikadić and S. Avdaković (eds.), *Advanced Technologies, Systems, and Applications*, Lecture Notes in Networks and Systems 3,
DOI 10.1007/978-3-319-47295-9_20

The "Coada effect" is named after Henri-Marie Coanda, a Romanian scientist, who first identified the effect in 1910, and involves the tendency of fluids to follow a surface. The Coanda effect is natural phenomena, means the tendency of a fluid to attach itself to a curved wall and to attach fluid from the surroundings. Flow passes over the crest of the weir, across a solid acceleration plate, and then across the screen panel, which is constructed of wedge-wire with wires oriented horizontally, perpendicular to the flow across the screen. As the flow passes over this surface, the shearing action of the bars combined with the Coanda effect, separates the flow, as shown in Fig. 1.

The CFD model presented in this article will be used to analyze the sensitivity a of the Coanda-effect screen performance to variations in several screen design parameters.

The objective of this research project was to evaluate the capacity of the Coanda-effect screen.

The CFD simulation have been performed on the same geometry and compared with experiments performed by Wahl [1], in order to defined the equation for correct prediction of the capacity of the Coanda-effect screen, repeated in the past to basic hydraulic parameters, such as the Froude, Reynolds and Weber numbers of the flow over the screen. From the same researcher Wahl [2], conducted extensive laboratory tests and developed a numerical model that can be used to predict Coanda-effect screen capacity and analyze the influence of design parameters, as presented in Fig. 2.

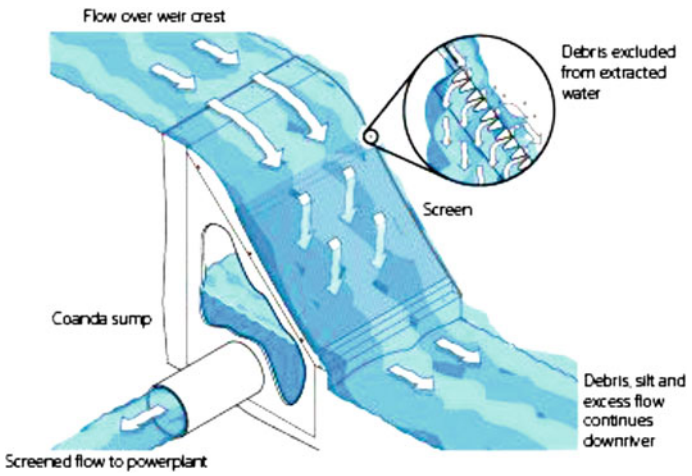

Fig. 1 Water intake structure of the small hydro power plant with the Coanda-effect screen. *Source* http://www.aquashear.com

Fig. 2 The Coanda-effect screen tested in the hydraulic laboratory. *Source* [2]

2 Assessment of Flow Conditions (Supercritical Flow)

The Froude number provides the relationship between flow velocity and flow depth, and helps assess the energy conditions of water flow.

The Froude number is defined as the ratio of gravitation forces to inertial forces:

$$f = \frac{gravitation\ gravitational\ forces}{inertial\ forces}$$

Critical flow occurs when F = 1; there is a perfect balance between the gravitational and inertial forces. Supercritical flow is shallow and fast, and occurs when F > 1.

The concept of critical flow is not an easy one to impart, but some understanding of it is necessary to understand the full range of flow conditions that may exist in area.

Stream flow cannot go on accelerating in the natural river environment. Changes in (critical) flow, from sub-critical to super-critical, can be assessed by calculating the Froude number: This is done using the following equation:

$$f = \frac{v}{(gxd)(g \cdot d)^{1/2}}$$

where:

F Froude number of flow,
v velocity of flow (m/s),
g gravitational acceleration (9.8 m/s),
d depth of flow (m).

Depth and gravity are the key factors in determining critical flow. Flow velocities across the screen are typically 2–3 m/s, they increase over acceleration plate before screen panel, and Froude numbers of flow through the screen can vary from 2 to 30 or greater. By the same author [1], developed a theoretically based model for hydraulic performance of Coanda-effect screens. This model predicts the discharge through the screen and overflow off the screen.

Discharge through the screen is a function of the depth of water above the screen face, the with of the slot and a coefficient [2]. Water flow through a model of the Coanda-effect screen is investigated using a computation fluid dynamics (CFD) method by authors [3].

3 CFD Model for Prediction of Hydraulic Flow Performance

In this project, the results of CFD obtained by using FLUENT software will be compared with the data of physical model. Also, the CFD results needs to be compared with results of empirical relationship presented by other researchers.

The purpose of this PhD research project is to compare the results of numerical model with measured results obtained from fiscal model of the actual project. "Improving Coanda-Effect Screen Technology" from Water Resources Research Laboratory, U.S. Bureau of Reclamation, Denver-Colorado (USA).

There is created 3D-model of Coanda-effect screen water intake structure with geometric parameters identical experimental physical model, as shown in Figs. 3 and 4.

The numerical grid shown in Figs. 5 and 6 was generated.

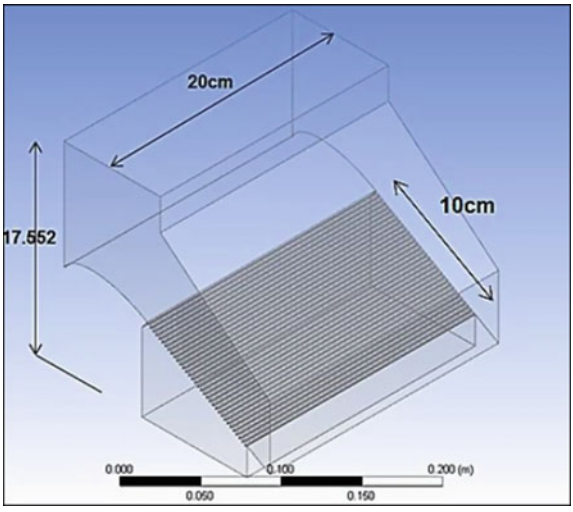

Fig. 3 The Coanda-effect screen water intake 3D model

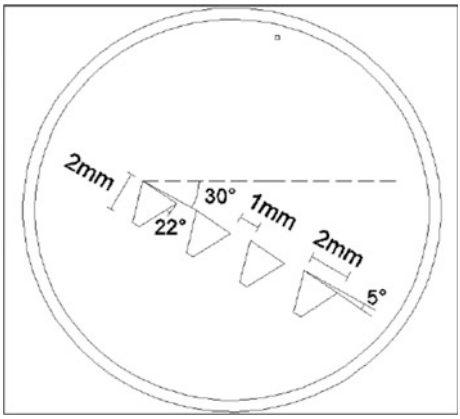

Fig. 4 The geometrical parameters of the screen details

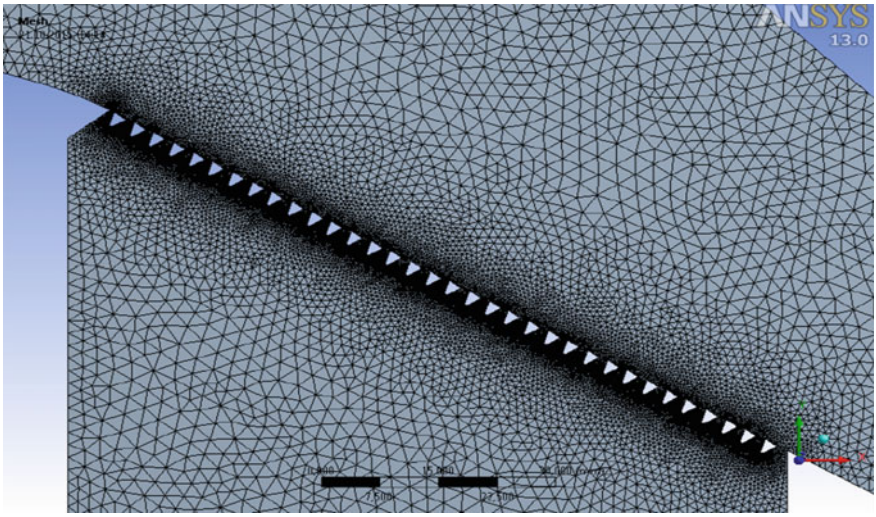

Fig. 5 Numerical grid around the Coanda-effect screen

4 Results and Discussion

As will be shown in Fig. 7, the flow characteristics between each two individual wires and velocity flow distribution from the beginning of the screen to the end are presented. For consistency, all of the results this presented from numerical modeling, should be verified and validated in order to compare with experimental results, to provide detailed information about the velocity and other parameters of interest such as the Froude number at different locations. Figure 7 presents the distribution of the velocity magnitude in the first half of the flow through the Coanda-effect screen, under these input data.

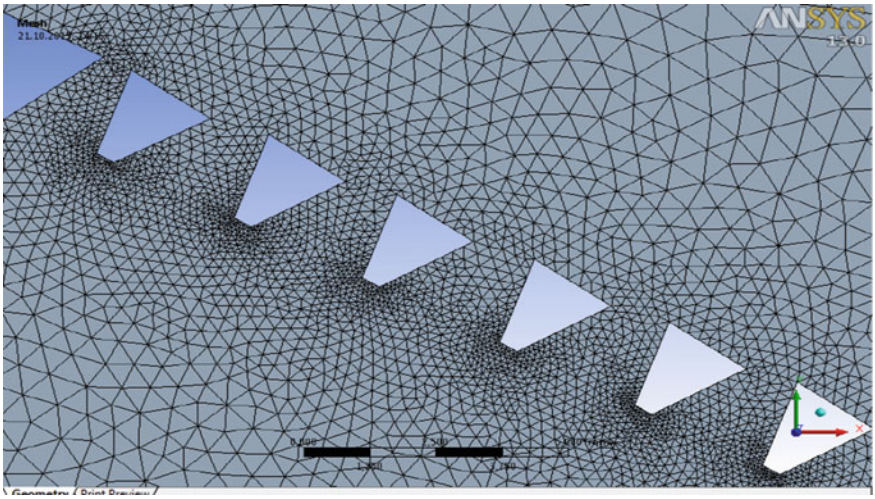

Fig. 6 Numerical grid with details around individual wires of the Coanda-effect screen

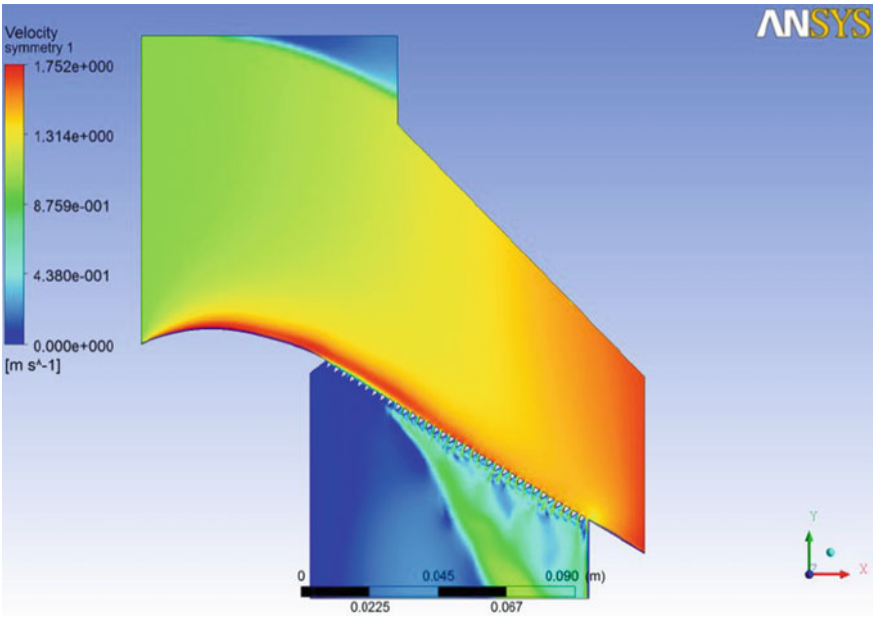

Fig. 7 The numerical grid with details around individual wires of the Coanda-effect screen

References

1. Wahl TL (2013) New testing of coanda-effect screen capacities. Poster presentation on HydroVision International 2013, Denver, CO, 23–26 July 2013
2. Wahl TL (2003) Design guidance for coanda-effect screens. Bureau of Reclamation, Technical Service Center, Water Resources Research Laboratory, Denver, CO
3. Dzafo H, Torlak M, Dzaferovic E (2014) Numerical modelling and geometry analysis of water intake structure with Coanda effect screen. In: 18th seminar on hydropower plant, Vienna Hydro 2014, (Edited by Vienna University of Technology, Institute for Energy Systems and Thermodynamics), pp 867–875

The Use of Concrete for Construction of the Roads and Railways Superstructure

Mirza Pozder, Sanjin Albinovic, Suada Dzebo and Ammar Saric

Abstract The superstructure of roads (road and railway) is used to transmit traffic load on the subsoil. The world is increasingly used of concrete pavement during the construction of roads, and the sleeper during the construction of the railway. Applying Life Cycle Cost Analysis (LCCA) it is possible to compare the long-term economic benefits when using concrete compared to traditional materials. The use of concrete in order to build roads in Bosnia and Herzegovina still does not have a big expansion. Using the experiences and research of other countries can justify its implementation in Bosnia and Herzegovina.

1 Introduction

The superstructure of roads (road and railway) is used to transmit traffic load on the subsoil. The design of these elements can be quite different depending on a number of factors.

The paper gives an overview of the possibilities of concrete as a supporting element of roads in Bosnia and Herzegovina. By comparing the existing research, emphasized the advantages and disadvantages of its implementation.

M. Pozder (✉) · S. Albinovic · S. Dzebo · A. Saric
Department of Roads and Transportation, Faculty of Civil Engineering, University of Sarajevo, Sarajevo, Bosnia and Herzegovina
e-mail: pozder.mirza@hotmail.com

S. Albinovic
e-mail: sanjin.albinovic@gmail.com

S. Dzebo
e-mail: suada.dzebo@gf.unsa.ba

A. Saric
e-mail: ammar.saric@hotmail.com

M. Hadžikadić and S. Avdaković (eds.), *Advanced Technologies, Systems, and Applications*, Lecture Notes in Networks and Systems 3,
DOI 10.1007/978-3-319-47295-9_21

2 Flexible Versus Rigid Pavements

A pavement structure consists of multiple layers of different materials. The primary task of pavement is to receive the impact of traffic load, and stresses of the traffic load reduce to acceptable levels in order to prevent damage of subgrade.

Traditionally, the pavement is divided into flexible (asphalt) and rigid (concrete) pavement. The basic elements of flexible pavements are bound asphalt layers placed over the unbound granular material, while in the case of solid bonded, asphalt layers replaces concrete slab.

In the case of flexible pavements, the load of the vehicle at a depth of subgrade transfers based on the interaction of grain granular materials. This has the consequence that the flexible pavement have a low bending strength. On the other hand, for rigid pavements vehicle load at a depth of subgrade transfers due to high bending strength concrete slabs (Fig. 1).

The most common defects of flexible pavements are cracks and permanent deformation (rutting). The cracks are the result of exceeding stress to the tension under asphalt layers. The permanent deformation (rutting) is the property of flexible pavement and manifest as depressions in zones crossing the wheels of vehicles.

The most common damage to rigid pavements are cracks due to fatigue. They are the result of stress ratio (flexural strength vs. plate strength).

When asked the question what type of pavement is better, it is difficult to answer, because both types have advantages and disadvantages. The problem of choice cannot be solved on the basis of a single criterion.

Overall, the engineering differences between flexible and rigid pavements are:

- service life of flexible pavements is almost twice less than concrete,
- construction costs of flexible pavements are less than concrete,
- maintenance costs of rigid pavements are lower than in flexible,
- in case of flexible pavements transfer loads directly dependent on the characteristics of the layers, while for rigid transfer of load depends almost entirely of concrete slabs characteristics,

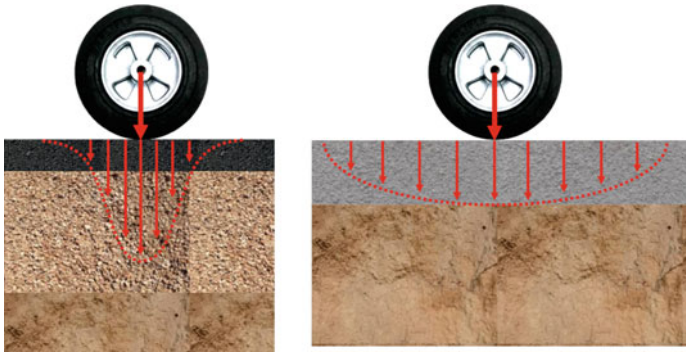

Fig. 1 Comparison of the stress transmission in flexible and rigid pavements

– bearing capacity depends on the characteristics of each layer (flexible) while in case of concrete depends on the slab properties,
– the flexible pavement deflection basin offers a significantly downward, while the concrete is shallower and wider,
– flexible pavement have less elasticity modules (less load-bearing), while in the case of concrete is significantly higher.

2.1 LCCA Analysis

LCCA (Life Cycle Cost Analysis) is procedure to perform comparisons of long-term economic value alternative, and the results of these analysis can be very useful for management structures.

According to AASHTO Guide for Design of Pavement Structures [1], LCCA analysis pavements includes all costs, both direct and indirect, which it can meet the manager within a single lifetime pavement. Roughly, the cost can be divided into the following categories: construction costs, the costs of the agency that manages the pavement, user costs and expenses related to environmental impacts. The cost of the agency that manages the pavements are maintenance costs, rehabilitation, etc., while the users costs are travel time and accidents, etc. [1].

Results of the analysis depends on the accuracy of input data, and considering that this is a long-term analysis, the greatest degree of uncertainty related to the cost of materials, the discount rate etc.

For a period of 40 years, in the case of low-intensity traffic load, flexible pavement are profitable. Limit when rigid pavement become more cost-effective is more then 12,000–14,000 vehicles per day. Cost effectiveness is increased with the increase of the share of heavy traffic load in the vehicle structure. Sensitivity analysis showed that the profitability of the most affected economic parameters (discount rate, the price of materials) and the uncertainty related to this connection, and to a lesser extent, maintenance and external effects [2].

For example studies conducted in India, for time project period of 20 years with a discount rate of 10 %, showed that construction costs are 28 % higher in concrete than in the case of application of flexible pavements. However, LCCA analysis showed that the rigid pavement is 20–25 % cheaper than flexible in the project period. Longer service life of rigid pavements (over 30 years) relative to the flexible (maximum 20 years old) indicates that after the end of the planning period of 20 years, which is selected in the analysis, rigid pavement certainly last 10 years more. In this case concrete pavement are lot favorable [3].

So, if the initial financial cost of construction is less with flexible pavement, if you take out all the other external effects in the budget, it can be concluded that the

rigid pavement affordable provided that the road higher intensity of traffic load (for rigid pavements greater fuel savings, they are safer, lower operating expenses, lower noise and emission of pollutants). All of these external effects when anticipated in calculations bring economic benefits in favor of concrete pavements.

2.2 *The Possibility of Using Concrete Pavements in Bosnia and Herzegovina*

Statistically, Bosnia and Herzegovina, is 100 % applied flexible pavement. Rigid pavement applicable only on toll stations on highways and at some gas stations. Comparing these examples in relation to the entire road network, their use is insignificant.

The possibility of using concrete pavements in the future can be analyzed through SWOT analysis (Fig. 2).

The fact is that rigid pavement require a higher initial investment costs than flexible, which ultimately results in lower financial feasibility of the project. However, if we observe the entire cycle life of rigid pavement, which is significantly longer than the flexible, then, the economic feasibility, achieve significant benefits.

Also, the fact is that the economic benefits are the function of traffic load, (the intensity and structure). In this regard, the greatest benefits can be achieved on highways. In particular, the rigid pavement are more favorable when it comes to "special" cases such as tunnels. The possibility of using rigid pavements in tunnels increases the safety, especially for "long" tunnel (fire risk).

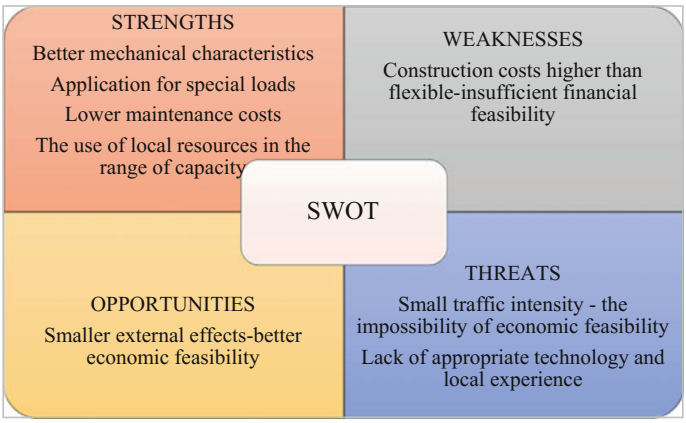

Fig. 2 SWOT analysis of the possible application of concrete pavements

3 Concrete Use as a Support Element in the Superstructure of Railway Lines

Railway track is road for railway traffic and it is made of two rails on a standard distance, which are connected with tackle for transversely sleepers.

This kind of track can be laid in a crashed stone ballast or on a stable surface (track structure without crashed stone ballast).

In rail systems, passage vehicle made load, transfers through rails and tackle on a sleepers, ballast and finally on a foundation ground—subgrade. The biggest stress suffered by rails and therefore it is the most important part of system to choose, depending on the load.

However, it is very important to properly choose all other elements of a superstructure, especially appropriate type of sleepers.

On the type of sleepers (wooden, concrete, steel) largely depends choice of tackle type, ballast material, as well as the shape of ballast.

3.1 Choosing the Type of Sleepers

From the point of choosing correct type of sleepers, in engineering practice in our country, there is choice between two types of transversely sleepers: wooden and concrete.

In order to make the correct choice we must: consider all the pros and cons of both types of sleepers, their participation in load transfer and the way in which that load is taken. Table 1 shows the main advantages/disadvantages of concrete sleepers compared to wooden sleepers.

In the past, the wooden sleepers were priced more favorable compare to concrete sleepers. However, the recent product technology process improvement, the lack of high-quality natural materials for wooden sleepers production, as well as increasingly stringent environmental requirements in terms of used materials for their impregnation, concrete sleepers have a lower price than wooden.

The biggest drawback of concrete sleeper is its much greater weight of approximately 300 kg (which is three to four times higher than for wooden sleepers) and that requires mechanized laying and maintenance.

High-quality materials of substructure and its good construction is very important for concrete sleepers which leads to an increase in initial investments. Slightly larger initial investments are compensated through longer life cycle of concrete sleepers[1] as well as through reduction of maintenance costs.

[1]The average life cycle of wooden sleepers without impregnation is 10 years, or 30–40 with impregnation, and concrete sleepers is 50–60 years.

Table 1 Advantages and disadvantages of concrete sleepers compared to wooden sleepers [4]

Advantages	Disadvantages
Weather conditions proof	Nonelastic as a rail base
High strength	Sensitive to strike
Freedom in design	Sensitive to aggressive water
Fireproof	Requires mechanized laying and maintenance
Suitable for CWR[a] because of higher weight	

[a]Continuous welded rail

3.2 LCCA Analysis

Comparing the results of this analysis can identify the biggest expenses and efficient solution for long term, which leads to reducing overall costs.

However, problem is the fact that in most cases the analysis is still limited to the direct costs, the so-called "plan costs", such are construction, maintenance, renewal costs and the value of assets.

In the mid-1990s, by many state governments, it was generally accepted to reduce maintenance costs and make short term savings. This caused bad railway track condition which resulted in the increase travel time and vague timetable, so subsequent cost of urgent railway track repair, in long term, were greater than the achieved savings.

For these reasons, lately using of LCCA tries to encompass more and more of these unplanned costs, so that the analysis considered costs shown in Fig. 3 [5].

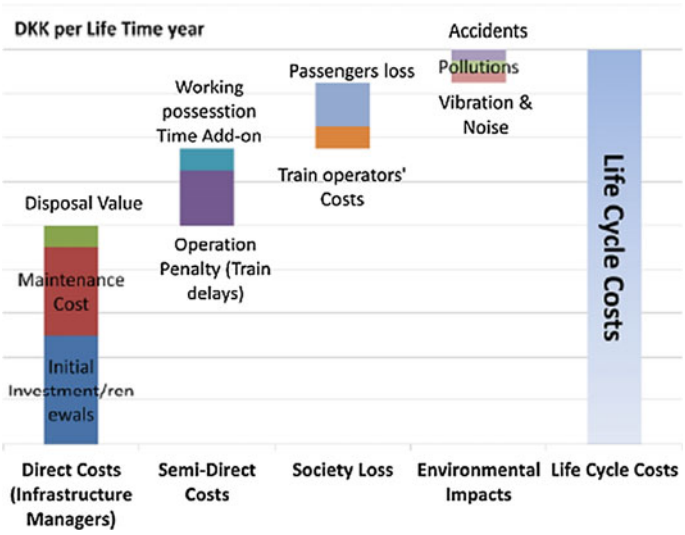

Fig. 3 The total cost in the life cycle

Table 2 Input data for LCCA of wooden and concrete sleepers

Description	Concrete sleepers	Wooden sleepers
Lifetime (years)	35	25
Cost (per km of railway track)	4500	4000
Packing every (years)	5	3
The upper limit functionality without maintenance (years)	12	9

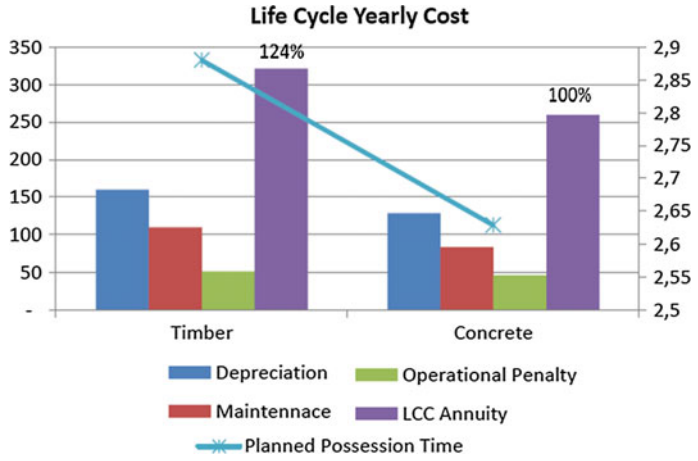

Fig. 4 The results of the LCCA analysis for comparison wooden and concrete sleepers

As an example, results of LCCA analysis carried out for choosing the sleeper type, are presented here.

It is made a comparison between the wooden and concrete sleepers, and to simplify the analysis, assume the same initial railway track quality. Input data that were used in the analysis are shown in Table 2. Based on the rate of 2.0 %, LCCA annuity is shown in Fig. 4 [5].

Based on the results of the analysis may be noted that concrete sleeper, in LCCA perspective, much better investment and wooden sleepers are ultimately to 24 % more expensive than concrete, because of increased costs of the frequent maintenance.

3.3 Railway Tracks Without Ballast

Because of increasing demands in terms of speed, traffic volume and traffic safety, as well as reducing the environmental impact which classic railway tracks with ballast cannot satisfy or in very difficult way, discussed some new design in terms railway tracks without ballast.

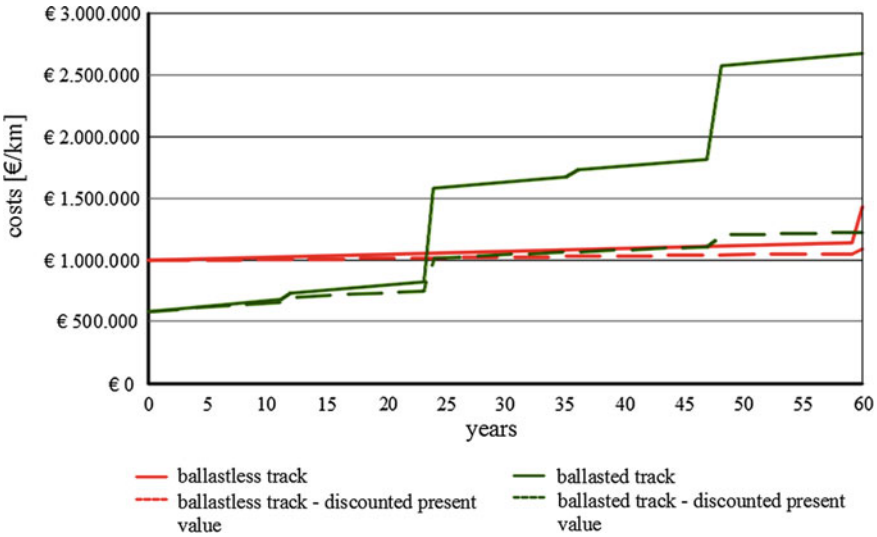

Fig. 5 The results of LCCA of rail track with ballast and without ballast

On these railway tracks, instead of ballast as the support element, more stable materials such as asphalt or concrete are applied.

Railway tracks systems without ballast have many advantages over conventional systems such as: greater stability of the track, precise geometric design, travel comfort, the availability of track, long lifetime and low maintenance cost with little preventive work or not preventive work at all.

The biggest disadvantage of these structures is much higher price than the price of classic railway tracks, which is around 350 EUR/m′ [6].

Also, construction of these structures required high load capacity of the substructure.

All this ultimately leads to increased initial investment of 20–40 %.

According to LCCA analysis results (Fig. 5) it can be seen that the construction of railway track without ballast is in long term much favorable than classic railway systems with ballast [7].

4 Conclusion

Rigid pavement application in Bosnia and Herzegovina has a future, especially on the high rank roads (highways) and special purpose structures. The fact is that investors are interested in direct financial benefits (because external effects benefits will not return directly to the investor), so in this respect flexible pavement are more applicable. However, if we consider the economic benefits through the life cycle, it can be assumed that rigid pavement has justified application.

Because of increasing demands in terms of loads and travel speed, it is necessary to use concrete as a supporting element in the railway superstructure.

Therefore, in the future, it is necessary to continue with the activities of replacing wooden with concrete sleepers on the existing railways as part of major repairs, as well as start to use new technologies in production of environmental friendly sleepers and railway tracks without ballast.

The application of the system of railway track without ballast is necessary to consider at the newly designed railways, but especially in tunnel reconstruction, which have many advantages in terms of track construction height, water drainage and so on.

References

1. American Association of state Highway and Transportation, Guide for Design of Pavement Structures, 1993
2. Pozder M (2015) Fleksibilne naspram krutih kolovoznih konstrukcija, Simpozij betonske saobraćajnice, Građevinski fakultet u Sarajevu
3. Sampark Grameen (2006) Publication. National Rural Roads Development Agency, India
4. Albinović S (2015) Primjena betona kao nosivog elementa u gornjem stroju željezničkih pruga, Simpozij betonske saobraćajnice, Građevinski fakultet u Sarajevu
5. Hausgaard E (2013) Planning framework for railway phase based. In: Trafikdage-Transport Conference at Aalborg University
6. Esveld C (1999) Slab track: a competitive solution. TU Delft, Netherlands
7. RHEDA (2000) The ballast less track with concrete supporting layer, RAIL.ONE GmbH Pfleiderer track systems, Neumarkt, Germany. www.railone.com

CAD—GIS BIM Integration—Case Study of Banja Luka City Center

Nikolina Mijic, Maksim Sestic and Marko Koljancic

Abstract This article provides a sneak peak of ongoing technology integration efforts targeting fields of computer aided design and drafting (CAD), geographic information systems (GIS) and building information modeling (BIM). CAD enables ad hoc drawing and sketching spatial plans. GIS adds geospatial component to it, making your drawings and associated objects spatially aware. BIM goes one step further and establishes relationships between the drawing objects, making them more "intelligent" and suitable for future processing and analyses. With each step data classification requirements increase dramatically, so is the time required to complete one. Most users focus merely on just a single of aforementioned components, be it CAD, GIS or BIM—as overall complexity of "tying it all up" requires considerable amount of time and effort, while most often being out of project's scope and/or deliverables. This highly affects general data reusability on the output. Ongoing project's aims may be reached, but its overall value will be higher if you made results more reusable.

1 Introduction

The basis of the 3D models forming is data acquisition using LIDAR and orthophoto techniques. The main source of the data used to develop the model and 5D Building Information Modeling is a regulation plan of the central area of the city Banja Luka.

It was used existing urban plans and spatial documentation and regulation plans for the creating of the model. The main purpose of this work is the creation of 3D models of the central area of the city Banja Luka utilizing different CAD and GIS tools.

Software tools that are used for modeling are:

N. Mijic (✉) · M. Sestic · M. Koljancic
INOVA Informaticki Inzenjering, d.o.o, 78 000 Banja Luka, Bosnia and Herzegovina
e-mail: nikolina@geoinova.com

M. Hadžikadić and S. Avdaković (eds.), *Advanced Technologies, Systems, and Applications*, Lecture Notes in Networks and Systems 3,
DOI 10.1007/978-3-319-47295-9_22

Autodesk, AutoCAD Map 3D, Ecotect, Vasari, Autodesk Revit, INOVA AreaCAD-GIS and Unity.

Popular Autodesk tools are used for modeling and creating 3D models from classified objects. Ecotect and Vasari are now implemented in new software solution Autodesk Revit and they are used for analysis of such an automated process raise 3D of analytical model from paper documentation [1]. The final product of this research is a 3D model of Banja Luka city central area, which is created from paper documentation [2].

2 Methodology of the Data Collection for Creating 3D Model

LIDAR is today one of the most modern technology that is used in the survey and development of topographic maps for different purposes. The technology is based on collection of three different sets of data. Position sensors are determined using Global Positioning System (GPS), using phase measurements in the relative kinematics, use of Inertial Measurement Unit (IMU).

The last component is a laser scanner. The laser sends infrared light to the ground and is reflected to the sensor. The time between the broadcast signal reception to the knowledge of the position and orientation sensor, allows the three-dimensional coordinates to calculate the Earth. At cruising speed of about 250 km/h and an altitude of about 1000 m with standard the characteristics of the sensor (130,000 emission/s), collecting data on the position of points on the ground with a density of up to 100 points/m^2.

The usual relative accuracy of the model to include the error GPS and inertial system is 5–7 cm. Absolute error is always better than 15 cm and can be significantly reduced by using control points to the country. Almost all modern LIDAR systems, in addition to GPS, IMU and laser scanner, integrated RGB/NIR (Red-Green-Blue, Near Infra Red) camera high resolutions that allow the creation of high-quality orthophoto plans of resolution and up to 2 cm (depending on the level flyover) [3].

LIDAR has a very simple principle of measurement. The scanner emits pulses with a high frequency and is reflected from the surface back to the instrument. Mirror inside the laser transmitter is moved by rotating perpendicular to the tack allowing measurement in a wider band. Time elapsed from the emission to return every impulse and inclination angle from the vertical axis the instrument used to determine the relative position of each measured point. The absolute position sensor is determined by GPS every second, while the IMU provides or station. Data laser scanning combined with modern scanners and orientation to obtain three-dimensional coordinates of the laser footprint on the surface of the field [4].

3 Urban Planning for the Creating a 3D Model of the City

The workflow for the land development design is: land planning, surveying, site layout, grading, street design and documentation. Land planning is important for import and visualisation geospatial data. Creating a model is work through land planning scenarios. Work through planning and early designs for site layout, parcel layout, and street design. Surveying are used for import and analyze geospatial data to build a basemap, help plan fields surveys, and complement field survey data. Import process of the survey data, then build terrain models, and produce surveying documentation and deliverables [5].

Online 3D modeling has made great strides in recent years by showing its power to aid in the research and decision-making of urban planners. While it still doesn't have quite the buy-in many would hope, web technologies have made great improvements thanks in part to demands in both the gaming and architecture industries. Some companies have been combining efforts of the two fields to create useful civic engagement tools.

Civic analytics has been utilizing Autodesk, Inova and Unity software tools to show how the modeling of future landscapes and cities can play an iterative role in generating better public feedback and improved data analysis. For the city modeling it was used software support GREEN to BLUE design [6, 7]. The way of modeling was presented on Fig. 1.

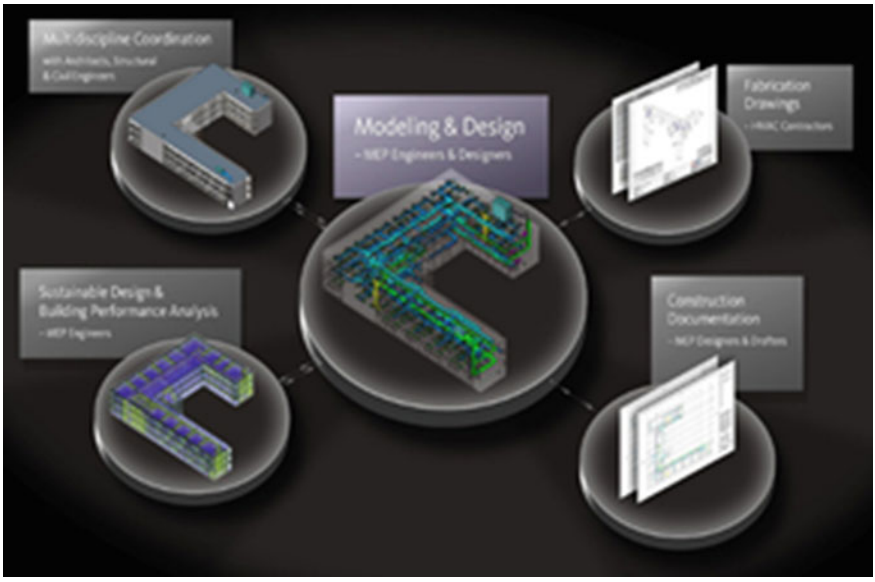

Fig. 1 2D CAD—GIS visualisation and 5D BIM, software support "GREEN TO BLUE DESIGN"

3.1 Urban GREEN—BLUE Grids

One attractive and efficient way to guide this necessary transformation is by developing green blue urban grids which will mitigate the effects of climate change and the energy and food shortages in urban areas. Our cities need to become more resilient to be able to tackle these challenges, as a lack of resilience will not only lead to a deficiency in technical infrastructural functioning but will also have consequences for a city's social and economic well-being. An important task for architects and urban planners is therefore to find attractive ways to integrate these measures in our cities and to assume directive roles in their implementation. In recent years there has been growing interest in more sustainable architecture and urban planning. Green roofs and facades are in fashion; rainwater increasingly remains above ground (Fig. 2).

There is an urban agriculture movement, and the first energy-neutral residential areas are already being realised. This shows that support already exists for new green-blue urban planning. What is still lacking is an overview of the possibilities and a critical and constructive assessment of these measures to ensure that the various possible measures are not counter productive.

This scientific knowledge is translated into practicable measures and their effects offering explanations of how they affect the various challenges, cost indications and spatial implications [8].

What is important now is to afford architects, urban developers, water managers, urban ecologists and everyone else involved in designing towns and cities a greater understanding of the effects, possibilities and interrelations between the various measures for green-blue urban grids, to ensure that those grids are integrated into the urban designs in a manner that is both aesthetic and acceptable to the citizens. The buffering and purification capacity of green roofs, wetlands, surface water with green banks, and more green urban areas in general, help to improve the urban water system in both quantitative and qualitative terms.

Fig. 2 The role of architects and urban planners—think global, act local

More urban water and green urban areas help to increase biodiversity in towns and cities and bind particulate matter; green surfaces and water surfaces have lower temperatures and by this reduce the risk of heat. Having more green areas substantially improves the sponge effect of towns and cities. The greater the proportion of green areas, the stronger the buffering capacity: clusters of trees and shrubbery buffer more than lawns alone [9].

The large leaf area means that more water evaporates in wooded parks and presents a greater cooling effect than do grassy areas. Initial studies already show the effectiveness of more green and more water in urban areas in terms of appeal, biodiversity, heat stress, water retention and improved water quality. Green-blue urban development provides biomass for energy production and presents opportunities for food production within towns and cities. We have only just started to identify and support these possibilities: the integral nature of and synergy between the possible measures and effects has barely been studied [9, 10].

3.2 Intelligent 3D Maps

The Autodesk AutoCAD platform provides more than simple, realistic 3D maps. Realize the full potential of 3D data with the AutoCAD tools. No need to change established processes, data, or technology—bring your existing 2D data to life in 3D with AutoCAD. The height of 2D objects can be readily populated using information from many different types of sensors.

For the forming 3D intelligent maps, are necessary data, which are collected with 2D GIS mapping and LIDAR technology. Intelligent 2D maps are formed for central area of the city Banja Luka (Bosnia and Herzegovina). They are very good, but not enough intelligent models [11]. The one of these maps for the central area of the city Banja Luka is shown in Fig. 3.

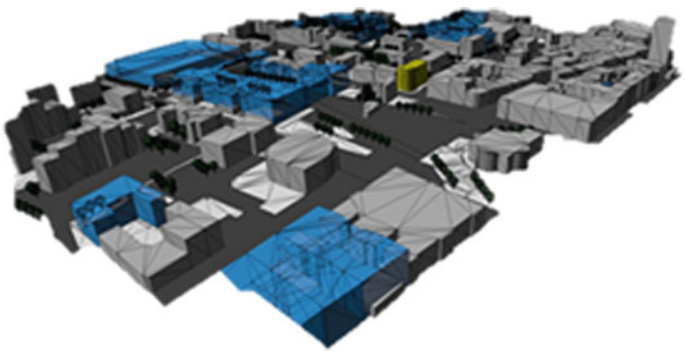

Fig. 3 GIS of the central area of the city Banja Luka, 2D intelligent maps

3.3 3D Visualisation

The use of visualization to present information is not a new phenomenon. It has been used in maps, scientific drawings, and data plots for over a thousand years. Major industries and most top companies use Autodesk 3D software for design visualisation, 3D architectural visualisation, and design animation. From abstract to photorealistic, our visualization and animation software helps ensure that you design vision is fully realized—creatively and technically before work begins. Featured design animation software are used:

Professional—grade creation, animation, texturing and modeling software. Integrates with a wide variety of building and creation software. Flexible subscription pricing to meet your company's needs. 3D visualisation have a high standard, but it's a problem all our architects draw and not modeling [12]. One of the example is shown on Fig. 4.

In Fig. 5, is shown a classic green building.

4 Building Information Modeling

Building Information Modeling (BIM) is changing how buildings, infrastructure, and utilities are planned, designed, built and managed. Autodesk BIM solutions help turn information into insight and deliver business value at every step in the

Fig. 4 Sample of 3D visualisation

Fig. 5 Classic green building

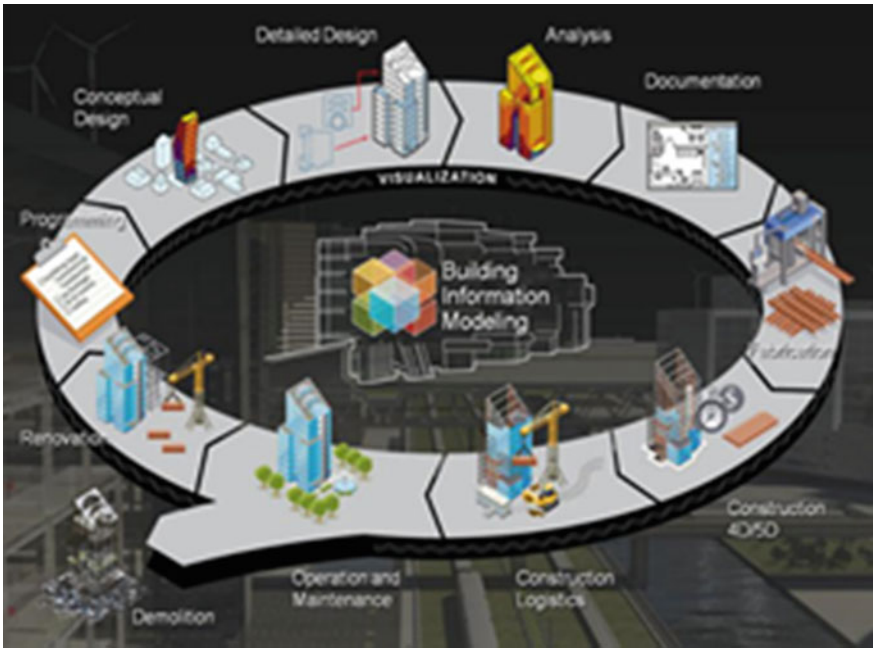

Fig. 6 Everything that is included in building information modeling

process. What is actually Building Information Modeling that is explained on Fig. 6. All the things that involves Building Information Modeling are shown on Fig. 7.

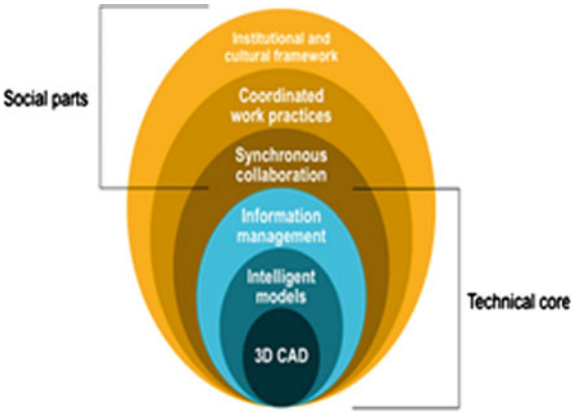

Fig. 7 Building information modeling technology

Building Information Modeling is primarily technology for sustainable and energy-efficient design. Building Information Modeling is a socio-technical system, and therefore completely new urban and architectural paradigm.

Building Information Modeling (BIM) is an approach to design that uses intelligent 3D computer models to create, modify, share and coordinate information throughout the design process. When used well, using BIM for building performance analysis can help you design sustainably.

High-performance buildings use far less energy, water, and money to run them. Learn or teach sustainable design and building performance analysis [13, 14].

5 Experimental Research—Case Study Banja Luka City Center

Experimental research of this paper is based on the creating a 3D model from the paper documentation. Source of data that was used is regulatory plan of the central area of the city Banja Luka. It was actually described a process of the automatic "lifting" of such a 3D analytical models from paper documentation. Steps that have been implemented when it was created a 3D model from the paper documentation are shown on Fig. 8.

The first step is a use a analog base geodetic maps digitizing. These maps are make in the cadastre for land planning. One of the analog base geodetic maps is shown on Fig. 9.

The next step is the creating, or using spatial planning in paper documentation for the creating a 3D model of the central area of the city Banja Luka (Fig. 10) [15].

Regulatory plan of the city is shown on Fig. 10.

After we used the existing spatial planning documentation, the existing regulatory plan of the city of Banja Luka in analog form, it was imported in AutoCAD. This step is shown on Fig. 11.

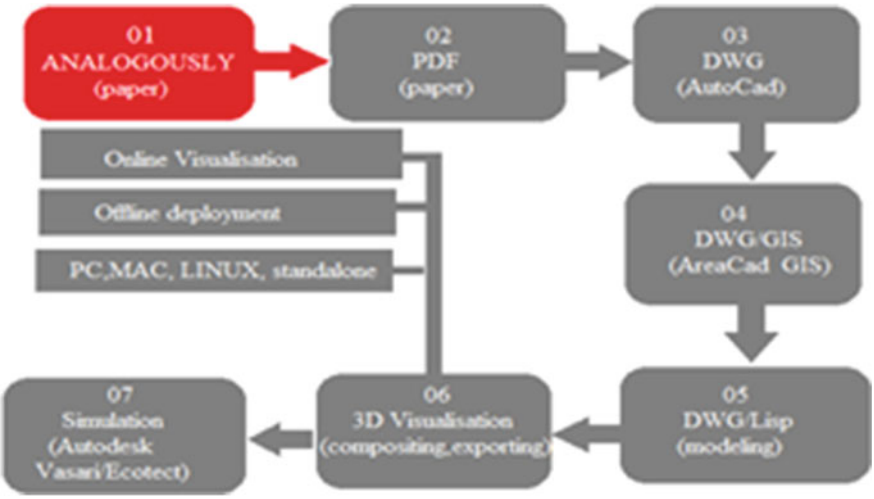

Fig. 8 Steps which are used for implementation of the 3D models

Fig. 9 Analog base/geodetic maps digitizing

Fig. 10 Spatial planing zoning and design

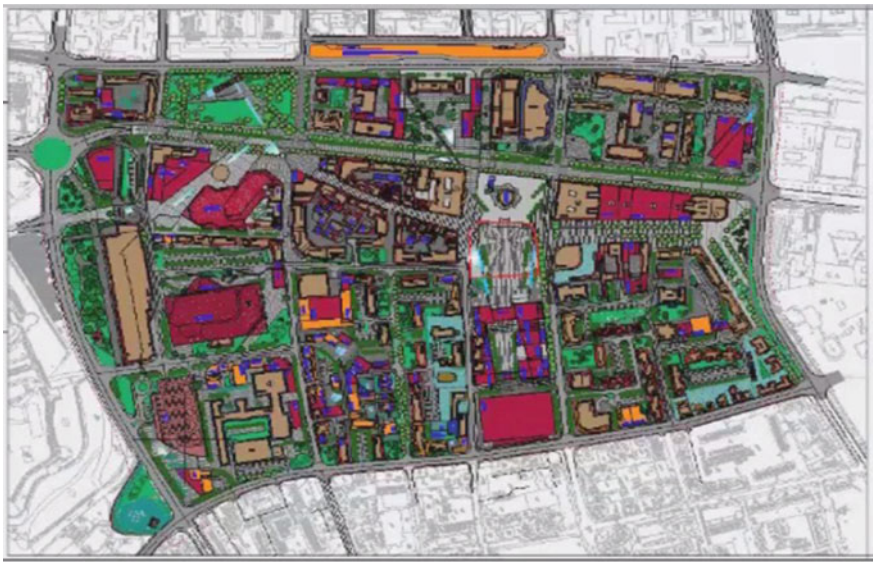

Fig. 11 Porting analog spatial plan to AutoCAD

When it was imported a spatial plan to AutoCAD then it was used AutoCAD Map 3D and INOVA AreaCAD-GIS software platforms for attaching GIS data [16]. These software platforms are shown on Fig. 12.

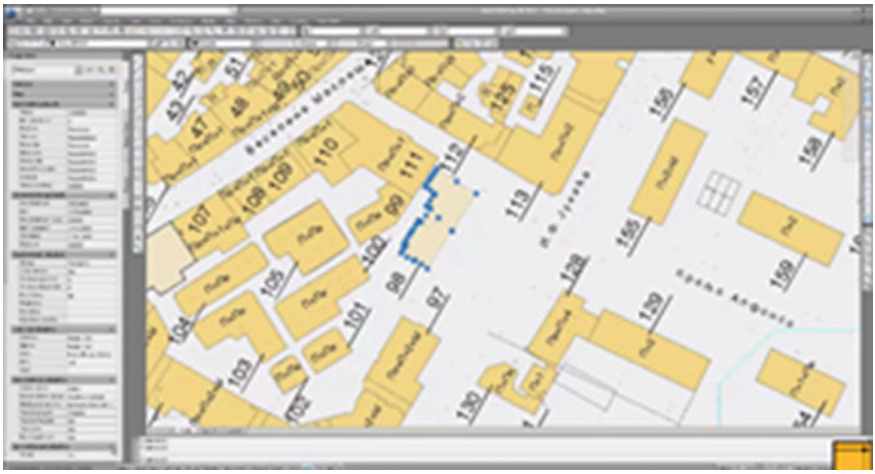

Fig. 12 Attaching GIS data using AutoCAD Map 3D and Inova AreaCAD GIS software platforms

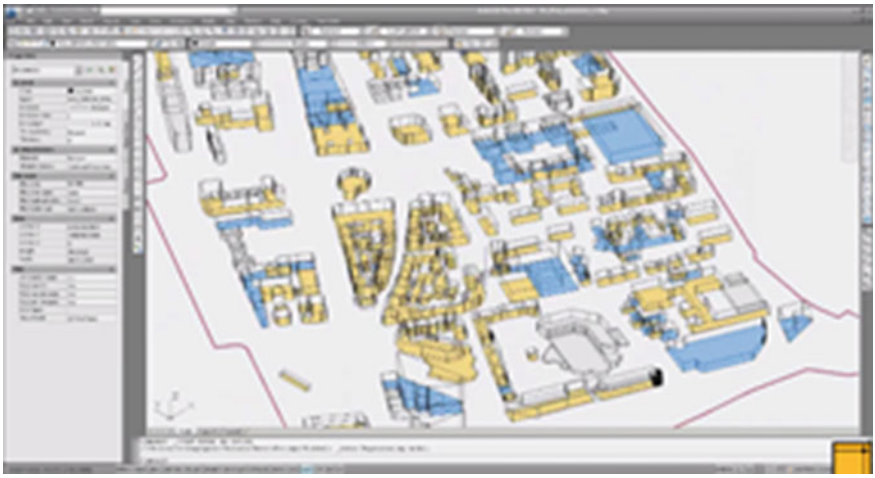

Fig. 13 Automated 3D model generation using GIS data and Inova AreaCAD GIS tools

Generation of the 3D model using GIS data and INOVA AreaCAD-GIS tools is now automated, after it was attached GIS data (Fig. 13).

3D model which was created using GIS data and INOVA AreaCAD-GIS tools was exported to new platform and that is a Autodesk Revit platform (Fig. 14).

Autodesk Revit platform is used to provide materials and shaders of the buildings in the central area of the Banja Luka (Fig. 15).

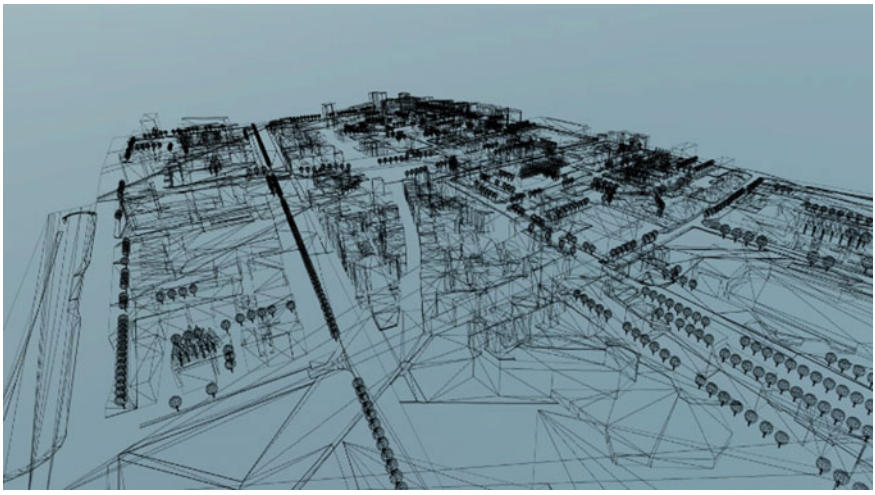

Fig. 14 Exporting 3D model to Autodesk Revit platform

Fig. 15 Autodesk Revit providing materials and shaders

After it was import the data in Autodesk Revit platform and provide the materials and shaders, the 3D model was exported to Unity platform (Fig. 16) [17, 18].

At the Unity platform we could saw a compositing and walkthroughs. After that was seen the 3D model of the city was imported in Autodesk Vasari and Ecotect platforms (Fig. 17).

Fig. 16 Exporting model to Unity platform compositing and walkthroughs

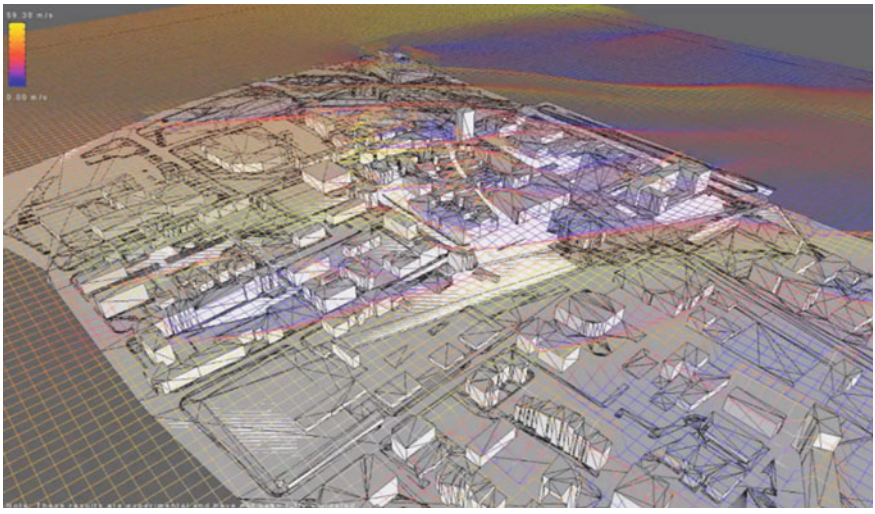

Fig. 17 Importing city model to Autodesk Vasari and Ecotect platforms

Autodesk Vasari and Ecotect platforms are used for climate analysis in BIM (Fig. 18).

BIM tools can be used to access, visualize and analyze weather data to help you understand your building site's climate. Autodesk Ecotect, Revit, Vasari and Green Building Studio each of these platforms have tools for climate analysis [19, 20].

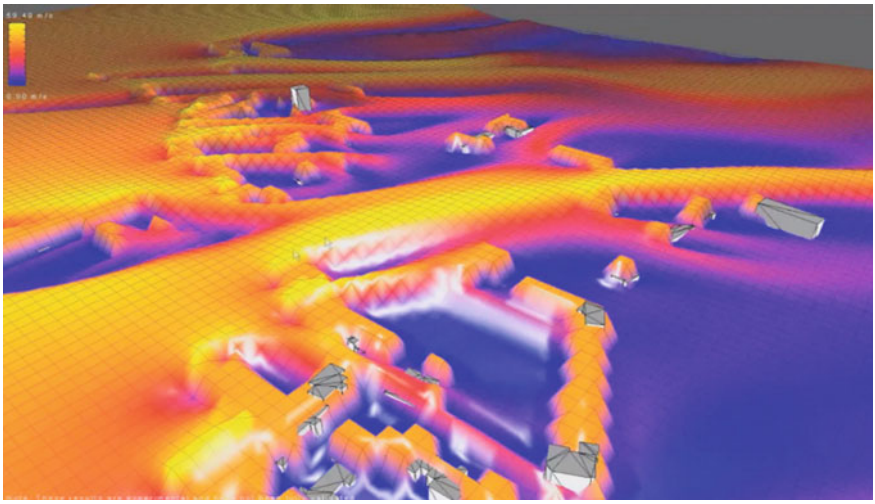

Fig. 18 Performing real-time wind simulation and analysis over imported model

6 Conclusion

For the creating 3D models of the city we can use very different platforms. In this paper it was shown how to convert paper documentation in 3D models. It was used a specific case of the central area of the city Banja Luka. There are a lot of Autodesk platforms, for creating 3D models. In this case study of the central area of the city Banja Luka, used a few different Autodesk platforms. It was used these software tools:

- Autodesk
- Autodesk AutoCAD Map 3D
- Autodesk Ecotect (now Revit)
- Autodesk Vasari (now Revit)
- Autodesk Revit
- INOVA AreaCAD-GIS
- Unity.

On the each of these platforms was imported a paper documentation of the regulatory plan of the central area of the city Banja Luka. It was started with AutoCAD in which was imported a paper documentation of the regulatory plan, spatial planning and zoning plan. Other Autodesk platforms are used for modeling and visualisation of the central area of the city. Autodesk Ecotect and Autodesk Vasari are used for real-time wind simulation and analysis over imported model. These all Autodesk platforms are very interesting, and can be used in many different ways.

References

1. http://autodeskvasari.com/photo
2. Upadhyay G, Kämpf JH, Scartezzini JL (2014) Ground temperature modelling: the case study of Rue des Maraîchers in Geneva. In: Eurographics workshop on urban data modelling and visualisation
3. Rajat Acharya (2014) Understanding satellite navigation. Academic Press, USA
4. Anil Maini, Agrawal Varsha (2014) Satellite technology: principles and applications, 3rd edn. Wiley, New York
5. Roure Ferran, Besuievsky Gonzalo, Patow Gustavo (2014) Hierarchical radiosity for procedural urban environments. Eurographics Workshop on Urban Data Modelling and Visualisation,
6. http://www.urbangreenbluegrids.com/about/introduction-to-green-blue-urban-grids/
7. http://www.urbangreenbluegrids.com/projects/plan-tide-dordrecht-the-netherlands/
8. http://hdl.handle.net/10.2312/udmv.20141071.007-012. doi:10.2312/udmv.20141071
9. http://www.autodesk.com/products/dynamo-studio/overview
10. http://sustainabilityworkshop.autodesk.com/building-design
11. https://www.google.com/search?q=autodesk+ecotect&biw=1920&bih=943&source=lnms&tbm=isch&sa=X&ved=0CAcQ_AUoAmoVChMI7ZrP-5fixgIVy1sUCh1Anwmn#imgrc=_
12. http://www.autodesk.com/solutions/building-information-modeling/overview
13. http://sustainabilityworkshop.autodesk.com/building-design/software
14. http://sustainabilityworkshop.autodesk.com/building-design/examples
15. Voiculescu Ishka, Davenport Cyndy (2015) Mastering: AutoCAD civil 3D. Autodesk Official Press, Sybex
16. https://www.youtube.com/view_play_list?p=F8ACB9BED56DE576
17. Whitbread Simon (2015) Mastering autodesk revit. Autodesk Official Press, Sybex
18. Bruy A, Anita G, Victor OF, Mandel A (2016) QGIS 2 coobook. Packt Publishing, UK
19. Nikolina M (2015) Maksim Sestic: CAD GIS 3D visualisation 5D BIM. In: Workshop on urban data modelling and visualisation. TU Delft, Netherlands
20. Information Resources Management Association (2016) Geospatial research: concepts, methodologies, tools and applications. IGI Global

Some Unconventional Profitability Determinants on the Banking Sector in Bosnia and Herzegovina

Deni Memic and Selma Skaljic-Memic

Abstract We examine factors that differentiate more profitable from less profitable banks in Bosnia and Herzegovina. We utilize some of the profitability measures as well as some independent variables that are not vastly explored in the existing literature. The study utilizes panel data linear regression with GLS random effects to observe the relationship between four bank profitability measures on one side and bank specific, macroeconomic and additional unexplored categorical variables on the other side. Our results suggest that lower bank profitability seems to be associated with higher operating expenses as share of total assets, higher bank concentrations, lower inflation rates, higher GDP growth rates and GDP per capita levels. We also find strong evidence that banks having foreign CEOs are more likely to be less profitable than banks with local CEOs, and some evidence that foreign owned banks seem to be less profitable than the locally owned ones, as well as that logo color choice seem to make profitability difference among banks. Bank profitability determinants on this banking market is a fairly unexplored area and should be explored more in the future research.

1 Introduction

What determines bank profitability on the banking market of Bosnia and Herzegovina? What differentiates more from less profitable banks? What are the key factors that can explain why some banks perform better than others? We seek for key profitability determinants of the banking market of Bosnia and Herzegovina. Bank managers have been in search for an optimal strategies in order to improve their banks' financial performance. Many of them tend to put strong focus on the internal factors in order to improve their financial performance, most of

D. Memic (✉)
Sarajevo School of Science and Technology, Sarajevo, Bosnia and Herzegovina
e-mail: deni.memic@ssst.edu.ba

S. Skaljic-Memic
Centralna Banka Bosne i Hercegovine, Sarajevo, Bosnia and Herzegovina

M. Hadžikadić and S. Avdaković (eds.), *Advanced Technologies, Systems, and Applications*, Lecture Notes in Networks and Systems 3,
DOI 10.1007/978-3-319-47295-9_23

them closely follow the key macroeconomic trends to predict the future events and create as accurate as possible financial plans.

For most of them, working in banks based in Bosnia and Herzegovina it is unclear which indicators can be the major determinants of different profitability measures. This study tries to answer these questions and pose some proposals for the bank managers in terms of profitability management and indicate which indicators managers should put more focus in the strive for enhanced financial performance.

Banking market, even though considered as one of the most highly regulated and best developed sectors in Bosnia and Herzegovina, it is still scientifically unexplored area. Lack of more extensive research of the banking sector in Bosnia and Herzegovina can be partially contributed to inexistence of central databases and unwillingness of regulatory authorities to dispose such databases to scientists that would be foundation for such research. Bosnian banking market has a few unique specifics which differentiate it to most of the banking markets in the region and wider. Unlike in many modern European countries, banking market in Bosnia and Herzegovina has very complex legal and inefficient and ineffective structure. Even though the banking market in Bosnia and Herzegovina is considered as one of the most developed, its complex and inefficient structure leaves a large space for further improvements. Undeveloped structure of the financial market in Bosnia and Herzegovina leaves the banking sector as the main source of financing the economy. The Constitution of Bosnia and Herzegovina (Ustav Bosne i Hercegovine) defines that the country structure consists of two separate entities: Federation of Bosnia and Herzegovina and Republic of Srpska and one district. Likewise, each entity has its own banking market. Another difference between Bosnian banking market and other developed European markets is in the regulator authority. Central banks around the world are in charge of managing monetary policy, as well as being a bank regulator.

Central Bank of Bosnia and Herzegovina is the authority in charge of the monetary policy, however the authority of regulating the banking sector is granted to each entity. Each entity has its own Law on banks (Zakon o bankama Federacije Bosne i Hercegovine and Zakon o bankama Republike Srpske) as well as its own banking agency. Agencija za bankarstvo Federacije Bosine i Hercegovine (Banking Agency of Federation of Bosnia and Herzegovina) or FBA is the banking regulator in one entity while Agencija za bankarstvo Republike Srpske (Banking Agency of Republic of Srpska) or ABRS is the banking authority in other entity. Banks registered in each entity are subject to periodical supervision of the respectful agency. Laws on the banking agencies (Zakon o Agenciji za bankarstvo Federacije Bosine i Hercegovine and Zakon o Agenciji za bankarstvo Republike Srpske) define the operations of each agency [9].

One of the few published studies examines the performance efficiency of banks in Bosnia and Herzegovina using data envelopment analysis (DEA) methodology [8]. The results show that efficiency of individual banks varied throughout the

observed period and not all of the banks were a part of the negative banking sector trend induced by the crisis. The study found no significant difference between performances of banks in different entities of Bosnia and Herzegovina, and between smaller and larger banks. The study provided useful feasible bank performance targets for the three observed years.

Another study of the banking market of Bosnia and Herzegovina examined competition and efficiency among banks using the most frequently applied measures of concentration k-bank concentration ratio (CRk) and Herfindahl-Hirschman Index (HHI) as well as evaluating the monopoly power of banks by employing Panzar-Rosse "H-statistic" [7].

The results of this study showed that Bosnia and Herzegovina banking market has a moderately concentrated market with a concentration decreasing trend. The Panzar-Rosse model suggested that banks in Bosnia and Herzegovina operate under monopoly or monopolistic competition depending on the market segment and that they earn their total and interest revenues under monopoly or perfectly collusive oligopoly. Scientists have studied bank profitability determinants of other counties. Some studies test bank-specific variables, other observe macroeconomic variables, while most of the studies observe the combination of the two groups of variables. One of the easiest studies conducted by Bourke [3] studies the performance of banks in twelve countries or territories in Europe, North America and Australia and examines the internal and external determination of profitability. Results parallel those in domestic US studies and provide some support for the Edwards-Heggestad-Mingo hypothesis of risk avoidance by banks with a high degree of market power. Molyneux and Thornton [11] replicated the methodology used by Bourke [3] in their note, as they examined the bank profitability determinants across eighteen European countries from the period between 1986 and 1989. They find evidence that the results do conform to the traditional US concentration and bank profitability studies, as long term bond rates and bank concentration ratios show significant relationship to bank profitability measures. Support is found for the expense preference expenditure theories, yet no support is found for the Edwards-Heggestad-Mingo risk avoidance hypothesis. One of the studies attempts to identify the determinants of successful commercial banks in order to provide practical guides for improved profitability performance of banks on the Malaysian banking market [5].

The authors use six different dependent variables including: return on assets, return on equity, net income before tax as percentage of total assets, net income after tax as percentage of total assets, net income before tax as percentage of shareholders capital and reserves and net income after tax as percentage of shareholders capital and reserves. The dependent variables used are internal (such as asset composition, deposit composition, capital, liquidity and expense management) and external (such as firm size, inflation, market growth, regulation, market share). Efficiency in expense management was shown to be one of the most significant determinants of bank profitability.

Vong and Chan [13] analysed determinants of bank profitability in Macao. The interest was at observing the impact of bank characteristics as well as macroeconomic and financial structure variables on the performance of the Macao banking industry. As expected the results show that the capital strength of a bank is of paramount importance in affecting its profitability. A well-capitalized bank is perceived to be of lower risk and such an advantage will be translated into higher profitability. On the other hand, the asset quality, as measured by the loan-loss provisions, affects the performance of banks adversely. No macroeconomic factors showed significant relationship with bank performance except the inflation rate. The aim of this study done by Athanasoglou et al. [2] was to examine the effect of bank-specific, industry-specific and macroeconomic determinants of bank profitability, using the traditional structure-conduct-performance (SCP) hypothesis. They used a GMM technique to a panel of Greek banks that covers the period 1985–2001. The study results showed that profitability persists to a moderate extent, indicating that departures from perfectly competitive market structures may not be that large. All bank-specific determinants, with the exception of size, affect bank profitability significantly in the anticipated way. The study however found no evidence in support of the SCP hypothesis.

Greek banking sector and its profitability determinants were studied by other authors [6] with results indicating that the introduction of the Euro has enhanced the competitiveness of the banking sector, with the management decision related variables exhibiting high impact on banks' profitability. Turkish banking sector profitability study from the period between from 2002 to 2010 shows that asset size and non-interest income have a positive and significant effect on bank profitability. However, size of credit portfolio and loans under follow-up have a negative and significant impact on bank profitability. On the other side among the tested macroeconomic variables, only the real interest rate affects the performance of banks positively [1]. Jordan banking sector study shows that variables such as higher capital, higher lending activity, lower credit risk and efficient cost management [12] are significantly related to bank profitability. According to the evidence provided by Miller and Noulas [10] USA banking sector large banks experienced poor performance because of a declining quality of the loan portfolio. Real estate loans proved to have a negative effect on large bank profitability, with lower levels of significance while construction and land development loans, have a strong positive profitability effect. One of the more recent research conducted by Dumicic and Ridzak [4] analyses the main determinants of the net interest margin of banks operating in several CEE countries in the period from 1999 to 2010. The results of this research showed that prior to 2008 the net interest margins declined primarily due to strong capital inflows and stable macroeconomic environment. The authors also showed that in the crisis period, significant rise in government debt accompanied by the increase in macroeconomic risks and abating capital inflows were significantly related to higher margin.

2 Methodology

The study uses data from the period between 2007 and 2012 from published audited bank financial statements. As banking market centralized database does not exist the financial data was drawn from each individual bank financial statement published on their respective web sites. In order to ensure the accuracy of the used financial data, audited financial statements were used. Manual data collection raised number of issues for the authors. Some of the banks did not publish their financial data in some of the years or published limited financial data and they are not included in the dataset. The bank-years also not included in the analysis banks that faced bankruptcy procedures in the observed periods and one banks operating under principles of Islamic banking, due to incomparable key financial indicators to traditional commercial banking. The study also excludes development banks due to their different technology, structure and goals compared to the commercial banks. The included data relevance is insured as in all observed years the included share of total assets does not drop below 85 % of total bank industry assets. The total bank asset value included in the study never drops below 80 % and in total covers more than 91 % of total assets. The final dataset includes total of 137 bank-year observations. The data is obtained from both constitutional entities Federation of Bosnia and Herzegovina and Republika Srpska. An overview of the data and variables used are given in Tables 1, 2 and 3).

Macroeconomic data are obtained from several sources including World Bank database and Agencija za statistiku Bosne i Hercegovine (Agency for Statistics of Bosnia and Herzegovina) (Table 2).

The two dependent profitability variables used in the study are: return on assets (ROA), and net interest margin (NIM). The independent variables used in the study are divided in three groups (a) bank-specific variables, (b) macroeconomic variables and (c) additional categorical variables additional indicating size, entity of origin, ownership origin, headquarters location, logo color and CEO origin. Bank-specific variables include capital to assets ratio (Capital/Assets), total revenue per employee, operating expenses to assets, natural logarithm of assets (ln Assets) and number of employees and number of branches. We exclude loan loss provisions as a variable from our study as it has proven to be one of the most important profitability determinant in existing literature and die to the lack of quality and consistent data on loan loss provisions on banks operating in Bosnia and Herzegovina.

Table 1 Number of bank-years used

Bank-years	2007	2008	2009	2010	2011	2012	Total
# of banks	17	22	24	24	25	25	137
Total # of banks	30	30	30	29	29	28	176
% of # included	56.7	73.3	80.0	82.8	86.2	89.3	77.8
% of assets included	80.3	95.1	95.3	92.7	92.7	92.5	91.6

Source Author's calculations

Table 2 Descriptive statistics full period 2007–2012

Var. type	Variable	Mean	Std. Dev.	Min	Max
Dep	ROA	0.003	0.022	−0.174	0.058
	NIM	0.631	0.101	0.270	0.860
Bank specific	Capital/assets	0.174	0.111	0.058	0.633
	Total revenue per employee	129,856	55,494	25,971	296,240
	Operating expenses to assets	0.044	0.020	0.018	0.174
	ln assets	19.932	1.158	17.026	22.175
	No of employees	411.569	373.493	29.000	1752.000
	No of branches	32.620	25.568	1.000	98.000
Macro	HHI	0.077	0.011	0.062	0.096
	CPI	2.676	2.418	−0.400	7.400
	GDPgr	1.274	3.128,052	−2.700	6.00
	GDPpc	3312.911	52.547	3197.91	3377.753
	M2GDP	54.251	2.623	49.800	57.900
	SASX10	1287.449	917.026	760.700	3676.950
	n = 137				

Source Author's calculations

Table 3 Overview of categorical explanatory variables used

Var. type	Variable	Description
Categorical	Dummy size	0 if bank is small (assets > BAM 1 million) 1 if the bank is large (assets < BAM 1 million)
	Dummy entity	0 if bank is from RS 1 if the bank is from FB&H
	Dummy ownership	0 if bank is locally owned 1 if the bank is foreign owned
	HQ in capital	0 if the headquarters are located in capital city 1 if the headquarters are not located in capital city
	Logo color	Red Green Blue Yellow Other
	CEO origin	0 if CEO is a of Bosnia and Herzegovina nationality 1 if CEO if a national of another country

Source Author's work

Macroeconomic variables include Herfindahl- Herschman Index (HHI), Consumer Price Index (CPI), Gross Domestic Product growth (GDPgr), Gross Domestic Product per capita (GDPpc), monetary aggregate M2 per GDP (M2GDP) and Sarajevo Stock Exchange index (SASX10).

The third group of independent variables include six categorical indicators showing bank size (Dummy size), constitutional entity origin (Dummy entity), ownership origin (Dummy ownership), headquarters location (HQ in capital), logo color (Logo color) and CEO origin (CEO origin). Banks are divided in two size groups; the bank is considered to be small if its total assets amount up to BAM 1 million, while the banks with assets larger than BAM 1 million are considered as large. Banks are divided into two groups according to the constitutional entity (Federation of Bosnia and Herzegovina and Republika Srpska) where they are licensed. Banks are divided in two groups (locally owned and foreign owned) according to their equity origin. Banks with headquarters in capital city Sarajevo are considered as one group while the banks having their headquarters in other cities are considered as other group. Five bank groups are also created in accordance with the dominant color on their respective logos. Bank CEO in an observed year, who is not of a Bosnian nationality is considered as foreign and those of a Bosnian nationality are considered local. The selected categorical explanatory variables can be regarded as unusual and novel. They were chosen in this study in order to assess potential new unexplored patterns in the used dataset as well as to asses if there is any evidence that such variables are significantly related to the bank profitability measures. Reviewing the existing literature that focuses on the determinants of bank performance it was not found that other authors utilised such variables which adds to our interest in exploring their potential relationship to bank performance. If the results are to show significant relationship patterns between these and profitability variables, this study can be a strong foundations to further research that would not be limited to financial sector in Bosnia and Herzegovina and wider.

Having in mind the historical dataset, we employ panel data linear regression with GLS random effects. The general linear model has the following form:

$$\mathbf{\Pi}_{it} = \boldsymbol{c} + \sum\nolimits_{k=1}^{K} \boldsymbol{\beta}_k \boldsymbol{X}_n^k \; + \; \boldsymbol{\varepsilon}_{it} \tag{1}$$

$$\boldsymbol{\varepsilon}_{it} = \boldsymbol{v}_i + \boldsymbol{u}_{it} \tag{2}$$

where $\mathbf{\Pi}_{it}$ is the profitability of a bank i at time t, with i = 1, …, N; t = 1, …, T, c is a constant term, $\boldsymbol{X}_{it}$ are k explanatory variables and $\boldsymbol{\varepsilon}_{it}$ is the disturbance with $\boldsymbol{v}_i$ the unobserved bank-specific effect and $\boldsymbol{u}_{it}$ idiosyncratic error. $\mathbf{\Pi}_{it}$ represents the chosen dependent variables including return on assets (ROA) and net interest margin (NIM). The final model form can be presented in the following way:

$$\mathbf{\Pi}_{it} = \boldsymbol{\alpha}_i + \sum\nolimits_{j=1}^{J} \boldsymbol{\beta}_j \boldsymbol{X}_{it}^j + \sum\nolimits_{k=1}^{K} \boldsymbol{\beta}_k \boldsymbol{X}_{it}^k + \sum\nolimits_{l=1}^{L} \boldsymbol{\beta}_l \boldsymbol{X}_{it}^l + \boldsymbol{\varepsilon}_{it} \tag{3}$$

where $\mathbf{\Pi}_{it}$ represents dependent profitability variables including on assets (ROA) and net interest margin (NIM), $\boldsymbol{X}_{it}^j$ represents bank specific variables, $\boldsymbol{X}_{it}^k$ macroeconomic variables and $\boldsymbol{X}_{it}^l$ additional categorical variables indicating size, entity of origin, ownership origin, headquarters location, logo color and CEO origin.

We utilize panel data linear regression with GLS random effects to observe the relationship between six bank profitability measures and bank specific and macroeconomic data. For each of the two dependent variables we utilize unified step-by-step approach towards constructing the full model. The initial step includes satisfying the key logistic regression assumptions. Such procedure eliminated some of the independent variables as being highly correlated with other variables which are retained in the models. The stepwise procedure towards constructing the full model is the following. In the first model we test the magnitude and significance of the relationship between individual banks' profitability measures and bank-specific ratios. We call this mode a Bank specific model. In second model we test the relationship between individual banks' profitability measures and chosen macroeconomic variables and we call this a Macro model. The third model combines the first two models and is called a Combined model. In the fourth model we test the relationship between individual banks' profitability measures and additional categorical explanatory variables and we call this model a Categorical model. The fifth and last model combines models (3) and (4) as it tries to explain different bank profitability measures by (a) bank-specific variables, (b) macroeconomic variables and (c) additional categorical explanatory variables and is referred to as a Full model. Such procedure is repeated for each profitability measure. All of the models are created with random effects.

3 Results

The first tested variable is ROA. Bank specific model explains 8 % of the ROA variability (overall R2) with Operating expenses to assets ratio being the only variable with a statistically significant impact (coefficient −0.209, p-value <0.10). As expected its negative sign shows that the higher the ratio of operating expenses in total assets, banks tend to have lower profitability measured by ROA. Other bank specific variables including the Capital/Assets ratio and ln Assets do not seem to have significant relationship to ROA.

Macro model including macroeconomic variables explains 6 % of the ROA variability which is surprisingly just slightly less than the Bank specific model. Out of the four retained macroeconomic variables, HHI being the only variable with a statistically significant impact (coefficient −0. 382, p-value <0.05). With its negative coefficient sign, it shows that with the higher concentration Herfindahl-Herschman Index, banks tend to have lower profitability measured by ROA. Other macroeconomic variables including CPI, GDPgr and GDPpc do not seem to have significant relationship to ROA. Combined model that includes all Bank specific and Macro model variables explains 14 % of the ROA variability. Unlike for the first two models Capital/Assets and GDPgr have significant relationship to bank

profitability measured by ROA. The model shows that banks with higher capital ratios tend to have lower ROA (coefficient −0. 367, p-value <0.05), as well as that banks' ROA seem to decrease when there is a GDP growth recorded (coefficient −0. 207, p-value <0.10).

Unexpectedly the Categorical model exceeds the variability explanation power compared to both Bank specific and Macro models individually as it explains 12 %, but has no statistically significant variables.

Full model constructed with the use of three groups of variables explains 23 % of ROA variability. The model does not have significant bank-specific variables. The model includes HHI as the only macroeconomic variable with a statistically significant impact (coefficient −0. 361, p-value <0.05). Next we tested profitability determinants of NIM. Bank specific model explains 15 % of the NIM variability, with Capital/Assets ratio being the only variable with a high statistically significant impact (coefficient 0.336, p-value <0.01). The model shows that banks with higher capital ratios benefit from higher net interest margins.

Macro model seem to have substantially lower explanatory ability as has an R2 of 4 % of NIM variability. The model includes HHI as the only variable with a high statistically significant impact (coefficient −2.124, p-value <0.01). With its negative coefficient sign, shows that with the higher concentration Herfindahl-Herschman Index, banks tend to have lower profitability measured by NIM. Combined model explains 22 % of the NIM variability, and is substantially higher than for ROA and ROE models. Capital/Assets ratio following the pattern exhibited in the Bank specific model (coefficient −0.354, p-value <0.01), with HHI from the Macro model (coefficient −2.180, p-value <0.01). Table 4 gives and overview of the ROA models.

Categorical model substantially exceeds the variability explanation power of both Bank specific and Macro models and the Combined model as it explains 44 % of NIM variability. Dummy ownership variable has a negative and statistically significant relationship to NIM (coefficient −0. 0831, p-value <0.05) and indicates foreign owned banks seem to be less profitable than the locally owns ones measured by net interest margin. Banks having blue or other color logos seem to be earning lower returns on equity the ones having red logo colors (coefficients −0.185 and −0.121 with p-values <0.01, <0.05 respectively).

Full model explains 51 % of NIM variability. The model includes Capital/Assets ratio (coefficient −0.372, p-value <0.01), HHI (coefficient −2.126, p-value <0.01) and the same variables included in Categorical model (Dummy ownership, Blue and other logo colors) with almost same effects, same relationship direction and statistical significance. These variables indicate that foreign owned banks seem to be less profitable than the locally owns ones and that banks having blue or other color logos seem to be earning lower net interest margins than the ones having red logo colors. Table 5 gives and overview of the NIM models. Table 6 gives a comparative overview of the two full models.

Table 4 ROA models

Independent variable: ROA	Bank specific model	Macro model	Combined model	Categorical model	Full model
	(1)	(2)	(3)	(4)	(5)
Capital/assets	−0.00831 (0.0286)		−0.367** (0.166)		0.0125 (0.0363)
Operating expenses to assets	−0.209* (0.111)		0.00799 (0.00650)		−0.150 (0.119)
ln assets	0.00201 (0.00314)		−0.00271 (0.00365)		0.00795 (0.00651)
HHI		−0.382** (0.167)	−0.000245 (0.000219)		−0.361** (0.166)
CPI		0.00730 (0.00650)	−0.00371 (0.0290)		0.00750 (0.00646)
GDPgr		−0.00225 (0.00365)	−0.207* (0.110)		−0.00239 (0.00363)
GDPpc		−0.000225 (0.000219)	0.00213 (0.00319)		−0.000236 (0.000217)
Dummy size (large)				0.00148 (0.00775)	−0.00730 (0.00955)
Dummy entity (FB&H)				−0.00300 (0.00840)	−0.00273 (0.00914)
Dummy ownership (foreign)				−0.00140 (0.00840)	−0.0103 (0.0109)
HQ in capital (yes)				−0.00849 (0.00889)	−0.00581 (0.00969)
Logo color (green)				−0.000317 (0.00978)	−0.00257 (0.0105)
Logo color (blue)				−0.0115 (0.0103)	−0.0118 (0.0111)
Logo color (yellow)				0.0121 (0.0177)	−0.00112 (0.0203)
Logo color (other)				−0.0210 (0.0136)	−0.0174 (0.0146)
CEO origin (foreign)				−0.0117 (0.00825)	−0.00888 (0.00854)
Constant	−0.0269 (0.0672)	0.759 (0.712)	0.790 (0.716)	0.0155 (0.0121)	0.662 (0.718)
R2 overall	0.08	0.06	0.14	0.12	0.23
Fixed effects	No	No	No	No	No
# of bank-years	137	137	137	137	137
# of years	6	6	6	6	6

Standard errors in parentheses
Source Author's calculations
*$p < 0.10$, **$p < 0.05$, ***$p < 0.01$

Table 5 NIM models

Independent variable: NIM	Bank specific model	Macro model	Combined model	Categorical model	Full model
	(1)	(2)	(3)	(4)	(5)
Capital/assets	0.336*** (0.124)		0.354*** (0.121)		0.372*** (0.128)
Operating expenses to assets	−0.110 (0.447)		−0.134 (0.432)		0.0107 (0.419)
ln assets	0.0107 (0.0157)		0.00696 (0.0152)		0.0370 (0.0229)
HHI		−2.124*** (0.595)	−2.180*** (0.593)		−2.126*** (0.586)
CPI		0.0208 (0.0231)	0.0279 (0.0232)		0.0263 (0.0228)
GDPgr		−0.00753 (0.0130)	−0.0110 (0.0130)		−0.0101 (0.0128)
GDPpc		−0.000674 (0.000779)	−0.000957 (0.000781)		−0.000912 (0.000766)
Dummy size (large)				−0.00817 (0.0301)	−0.0415 (0.0336)
Dummy entity (FB&H)				−0.00749 (0.0343)	0.00819 (0.0321)
Dummy ownership (foreign)				−0.0831** (0.0339)	−0.0856** (0.0382)
HQ in capital (yes)				−0.0563 (0.0362)	−0.0398 (0.0341)
Logo color (green vs. red)				−0.0468 (0.0398)	−0.0428 (0.0371)
Logo color (blue vs. red)				−0.185*** (0.0419)	−0.163*** (0.0392)
Logo color (yellow vs. red)				−0.0948 (0.0717)	−0.108 (0.0713)
Logo color (other vs. red)				−0.121** (0.0554)	−0.125** (0.0513)
CEO origin (foreign)				0.0263 (0.0312)	0.0148 (0.0301)
Constant	0.365 (0.330)	2.983 (2.537)	3.714 (2.557)	0.798*** (0.0493)	3.116 (2.530)
R2 overall	0.15	0.04	0.22	0.44	0.51
Fixed effects	No	No	No	No	No
# of bank-years	137	137	137	137	137
# of years	6	6	6	6	6

Standard errors in parentheses
Source Author's calculations
*$p < 0.10$, **$p < 0.05$, ***$p < 0.01$

Table 6 Models comparison

Dependent variable	ROA	NIM
Capital/assets	0.0125 (0.0363)	0.372*** (0.128)
Operating expenses to assets	−0.150 (0.119)	0.0107 (0.419)
ln assets	0.00795 (0.00651)	0.0370 (0.0229)
HHI	−0.361** (0.166)	−2.126*** (0.586)
CPI	0.00750 (0.00646)	0.0263 (0.0228)
GDPgr	−0.00239 (0.00363)	−0.0101 (0.0128)
GDPpc	−0.000236 (0.000217)	−0.000912 (0.000766)
Dummy size (large)	−0.00730 (0.00955)	−0.0415 (0.0336)
Dummy entity (FB&H)	−0.00273 (0.00914)	0.00819 (0.0321)
Dummy ownership (foreign)	−0.0103 (0.0109)	−0.0856** (0.0382)
HQ in capital (yes)	−0.00581 (0.00969)	−0.0398 (0.0341)
Logo color (green vs. red)	−0.00257 (0.0105)	−0.0428 (0.0371)
Logo color (blue vs. red)	−0.0118 (0.0111)	−0.163*** (0.0392)
Logo color (yellow vs. red)	−0.00112 (0.0203)	−0.108 (0.0713)
Logo color (other vs. red)	−0.0174 (0.0146)	−0.125** (0.0513)
CEO origin (foreign)	−0.00888 (0.00854)	0.0148 (0.0301)
Constant	0.662 (0.718)	3.116 (2.530)
R2 overall	0.23	0.51

Standard errors in parentheses
Source Author's calculations
*$p < 0.10$, **$p < 0.05$, ***$p < 0.01$

4 Discussion

In this paper we aimed at answering the following questions: What differentiates more from less profitable banks? What are the key factors that can explain why some banks perform better than others? We were in search for the key profitability determinants of the banking market of Bosnia and Herzegovina. The study is based

on the existing literature and findings but files two major gaps in the literature: (a) gives the first scientific insight to the bank market of Bosnia and Herzegovina and its profitability determinants, (b) introduces some new unexplored profitability determinants not only for the Bosnian banking market, but for the banking markets in general, such as logo color or equity origin. Return on assets seems to be determined by operating expenses to assets ratio and Herfindahl-Herschman Index, when observed in individual models and as expected suggesting that the higher the ratio of operating expenses in total assets, banks tend to have lower profitability measured by ROA indicating that operating expenses tend to have a significant negative relationship to banks' profitability. On the other side Herfindahl-Herschman Index shows that with the higher concentration Herfindahl-Herschman Index, banks tend to have lower profitability measured by ROA. Unexpectedly such results indicates that the higher the concentration or large banks is the lower their profitability is. One of the reasons for such an outcome could be that even though there is a higher concentration of larger banks taking a higher market share, they still act as competitors among themselves, driving the loan prices downwards and decreasing the profit margins. Such result is confirmed in the NIM models showing an even stronger relationship represented in the lower negative regression coefficient.

Our Combined model results shows that banks with higher capital ratios tend to have lower ROA, as well as that banks' ROA seem to decrease when there is a GDP growth recorded. Lower ROA associated with higher capital ratios can be explained with an effect of a lower leverage and higher cost of funds. In the Full model, no variables seem to have significant relationship to profitability measured with return on assets. We find that other tested bank-specific variables do not seem to have determining impact on returns on bank assets. We also find that find that other macroeconomic variables such as inflation rates and GDP per capita do not seem to affect bank returns on assets. We find no evidence that additional factor variables such as ownership origin and logo colors included in the study play an important role in determining banks' returns on assets. Net interest margins are the best explained profitability measure in this study, and seem to be lower with higher bank capital levels.

Some of the reasons behind such a finding could be that banks with higher capital ratios are regarded by customers as more stable and secure and accordingly have more profitable customers, or that the more capitalized banks (which tend to be smaller in size) attract more premium customers that prefer close bank relationship to lower price level. We find evidence that with the higher concentration on the market, banks tend to have lower net interest margins. Such results confirm similar findings from ROA models. Our results show that foreign owned banks seem to be less profitable (NIM measured) than the locally owns ones and that banks having blue or other color logos seem to be earning lower net interest margins than the ones having red logo colors. Having in mind that most of the Bosnian banks have been privatized by large foreign banking institutions, one would expect that banks in foreign ownership would be more efficient and profitable than the banks with major local ownership.

The results indicate at a somewhat different scenario where locally owned banks on average have higher net interest margins than the foreign owned ones. Similar reason may apply, as locally owned banks tend to be smaller in size and accordingly focus on relationship banking attracting premium customers willing to be charged higher interest premiums in exchange to closer and more personal relationship with the bank. Interesting enough, capital to asset ratio shows to be relevant in the NIM model, which is a before-loan loss-provision-based-model, but the effect disappears in the ROA models, which are after-loan loss-provision-based-models. One of the reasons for such a result could be that different bank provisioning policies among different banks in the observed period, cancel the significant effects visible prior to loan loss provision booking.

5 Conclusions

This study has expanded the existing literature twofold. First, we tested the main bank profitability determinants proposed in the existing literature (bank specific and macroeconomic variables) on the unexplored banking market of Bosnia and Herzegovina. The chosen dependent variables are also literature-grounded. The list of bank specific variables we used was limited by the lack of centralized bank financial data. Second, we utilized and tested some unconventional explanatory variables such as bank size, capital origin, CEO origin and logo color and their relationship to bank profitability. Based on this study results we can generally conclude that lower bank profitability seems to be associated with higher operating expenses as share of total assets, higher bank concentrations, lower inflation rates, higher GDP growth rates and GDP per capita levels. We also find strong evidence that banks having foreign CEOs are more likely to be less profitable than banks with local CEOs, and evidence that (for certain profitability measures) foreign owned banks seem to be less profitable than the locally owned ones, as well as that banks having blue or other color logos seem to be less profitable than the ones having red logo colors.

Comparing the obtained results to the results from the existing research we can conclude that we found evidence of similar relationship direction in which cost management efficiency [5, 12] and higher capital levels [13], are associated with higher bank profitability. Unexpectedly and unlike in the existing literature reviewed, we found evidence that lower bank profitably is associated with higher bank concentration, higher GDP growth rates and GDP per capita levels, foreign CEOs, major foreign capital. Our results also suggest that banks of different size, banks located in different entities as well as banks located having headquarters in the capital city versus other cities are not likely to have different profitability levels.

These results are may be used efficiently not only by bank top managers and owners in but also stakeholder groups in different industries in a way that they should focus on factors that they can impact in order to improve their profitability such as operating costs management, CEO choice as well as logo colors choice.

These results may be further explored on different datasets from similar and not so similar countries in order to compare the key profitability determinants.

We propose that further research is conducted on the basis of these results in order to gain additional insight into the bank profitability determinants. More detailed observation of unexplored and unconventional determinants is recommended for future research. The future interest can be aimed at can be aimed on the Bosnian banking market and extended to the other banking markets in the area and wider in order to observe potential similarities and differences between the markets.

Appendix

See Table 7.

Table 7 Descriptive statistics per observed year-groups

Variable	Mean	Std. Dev.	Min	Max
Group 1—year 2007; n = 17				
ROA	0.0090428	0.0089347	0.000783	0.0369884
NIM	0.6356207	0.0982577	0.4301132	0.834275
Capital/assets	0.1219324	0.0747478	0.058144	0.3225325
Total revenue per employee	123293.2	66778.23	25971.37	290869.1
Operating expenses to assets	0.0385852	0.0144808	0.0189638	0.0790731
ln assets	20.14149	1.079934	18.36366	22.05809
No of employees	446.1765	342.041	99	1548
No of branches	35.58824	22.87209	6	91
Group 2—year 2008; n = 22				
ROA	0.0053868	0.018984	−0.0558091	0.0576865
NIM	0.6152948	0.124768	0.369876	0.8597982
Capital/assets	0.1816675	0.1467761	0.0625389	0.58003
Total revenue per employee	133666.4	63983.93	45355.93	293028.8
Operating expenses to assets	0.0443558	0.018175	0.0198322	0.08279
ln assets	19.9346	1.272549	17.23899	22.17498
No of employees	454.9091	427.8537	30	1752
No of branches	34.72727	27.49231	1	98
Group 3—year 2009; n = 24				
ROA	−0.001281	0.0226998	−0.075157	0.0263779
NIM	0.6183333	0.085202	0.4506259	0.8253461
Capital/assets	0.1890106	0.1305344	0.0683205	0.6333499
Total revenue per employee	132999.7	53830.5	37444.44	255170.8
Operating expenses to assets	0.0428316	0.0148192	0.0236775	0.079227
ln assets	19.86587	1.220743	17.28704	22.03759

(continued)

Table 7 (continued)

Variable	Mean	Std. Dev.	Min	Max
No of employees	394.625	381.2143	36	1634
No of branches	31	26.3917	1	93
Group 4—year 2010; n = 24				
ROA	−0.001281	0.0226998	−0.075157	0.0263779
NIM	0.6183333	0.085202	0.4506259	0.8253461
Capital/assets	0.1890106	0.1305344	0.0683205	0.6333499
Total revenue per employee	132999.7	53830.5	37444.44	255170.8
Operating expenses to assets	0.0428316	0.0148192	0.0236775	0.079227
ln assets	19.86587	1.220743	17.28704	22.03759
No of employees	394.625	381.2143	36	1634
No of branches	31	26.3917	1	93
Group 5—year 2011; n = 25				
ROA	0.0056639	0.0090134	−0.0262773	0.0180217
NIM	0.6554911	0.086205	0.496952	0.8142396
Capital/assets	0.1830597	0.0909696	0.0789482	0.4383098
Total revenue per employee	129082.7	50424.13	45161.76	226577.6
Operating expenses to assets	0.0427649	0.0153886	0.0178906	0.0930781
ln assets	19.90453	1.143879	17.85182	22.11347
No of employees	389.76	365.2428	57	1576
No of branches	31.28	25.37801	1	92
Group 6—year 2012; n = 25				
ROA	0.0057828	0.0083875	−0.0173978	0.0194928
NIM	0.6577033	0.0845158	0.5020645	0.8561758
Capital/assets	0.1722354	0.0683763	0.0708549	0.3468149
Total revenue per employee	132020.3	47348.4	68404.17	241661.3
Operating expenses to assets	0.0468788	0.0304002	0.0176706	0.174257
ln assets	19.96975	1.063431	17.99145	22.04347
No of employees	389.92	356.5448	62	1552
No of branches	32.72	25.26777	1	92

Source Author's calculations

References

1. Anbar A, Alper D (2011) Bank specific and macroeconomic determinants of commercial bank profitability: empirical evidence from Turkey (SSRN scholarly paper no. ID 1831345). Social Science Research Network: Rochester, NY
2. Athanasoglou PP, Brissimis SN, Delis MD (2008) Bank-specific, industry-specific and macroeconomic determinants of bank profitability. J Int Financ Markets Inst Money 18 (2):121–136
3. Bourke P (1989) Concentration and other determinants of bank profitability in Europe, North America and Australia. J Bank Finan 13(1):65–79

4. Dumicic M, Ridzak T (2013) Determinants of banks' net interest margins in Central and Eastern Europe. Finan Theor Prac 37(1), 1
5. Guru BK, Staunton J, Balashanmugam B (2002) Determinants of commercial bank profitability in Malaysia. J Money Credit Banking 17:69–82
6. Mamatzakis EC, Remoundos PC (2003) Determinants of Greek commercial banks profitability, 1989–2000. Spoudai 53(1):84–94
7. Memić D (2015) Banking competition and efficiency: empirical analysis on the Bosnia and Herzegovina using panzar-rosse model. Bus Syst Res J 6(1):72–92
8. Memić D, Skaljić-Memić S (2013) Performance analysis and benchmarking of commercial banks operating in Bosnia and Herzegovina: a DEA approach. Bus Syst Res 4(2):17–37
9. Memić D (2013) Predicting credit default in Bosnia and Herzegovina using traditional statistical and artificial intelligence methods (Doctoral dissertation). Retrieved from COBISS. (COBISS.BH-ID 514184130)
10. Miller SM, Noulas AG (1997) Portfolio mix and large-bank profitability in the USA. Appl Econ 29(4):505–512
11. Molyneux P, Thornton J (1992) Determinants of European bank profitability: a note. J Bank Finan 16(6):1173–1178
12. Ramadan IZ, Kilani QA, Kaddumi TA (2011) Determinants of bank profitability: evidence from Jordan. Int J Acad Res 3(4):180–191
13. Vong PI, Chan HS (2009) Determinants of bank profitability in Macao. Macau Monetary Res Bull 12(6):93–113; Chen W-K (1993) Linear networks and systems. Wadsworth: Belmont, CA, pp 123–135

Closed-Loop Temperature Control Using MATLAB@Simulink, Real-Time Toolbox and PIC18F452 Microcontroller

Edin Mujčić, Una Drakulić and Merisa Škrgić

Abstract Today's way of life is closely linked with technology and it would be impossible without a microcontrollers. They are represented in all spheres of life: in the automotive industry, robotics, computer systems, home appliances, etc. Also, today's life is unthinkable without computers. The combination of computer and microcontroller provides a very great possibilities, which uses the good features of both. This chapter describes the use of a computer in combination with MATLAB@Simulink, Real-time Toolbox and PIC18F452 microcontroller for closed-loop temperature control. Control and settings for temperature are in MATLAB@Simulink and they can be very easily adjusted. Also, all the information: the refrence temperature, information from controller and the measured temperature are available at any time in MATLAB@Simulink and can be processed and stored. For real-time operation is used Real-time Toolbox. The information is sent from computer over serial port to PIC18F452 microcontroller. The PIC18F452 microcontroller receives information and processes them. Information from PIC18F452 microcontroller is amplified using a transistor that works as the switch and the thyristor which is used to turn on the heater. Turning off thyristor is automatically passing supply voltage through zero. Temperature measurement is performed using the temperature sensor LM335. Output signal from the sensor is amplified by using operational amplifier LM324 and after that sent in PIC18F452 microcontroller. The microcontroller processes information and after that send it over serial port to computer. In this way the loop of temperature control is closed using a computer and PIC18F452 microcontroller.

E. Mujčić (✉) · U. Drakulić · M. Škrgić
University of Bihać, Bihać, Bosnia and Herzegovina
e-mail: edin.mujcic@gmail.com

M. Hadžikadić and S. Avdaković (eds.), *Advanced Technologies, Systems, and Applications*, Lecture Notes in Networks and Systems 3,
DOI 10.1007/978-3-319-47295-9_24

1 Introduction

Temperature is a fundamental and quantitative physical science size of heat. As such, it had to first of all get independent, objective measure for accurate quantitative comparisons of the degree heat of object, system or process. Temperature is a measure of the internal energy of the system, while heat is measure of how energy transferred from one system to another. MATLAB is a very developed language of technology that combines low cost, visualization and programming in simple development environment MATLAB [1, 2]. It contains a collection of predefined functions that are grouped in tool groups (Toolboxes) intended to solve various problems from scientific field. MATLAB contains different Toolboxes: Optimization Toolbox, Neural Network Toolbox, Fuzzy Logic Toolbox, Control System Toolbox, Signal Processing Toolbox, Statistics Toolbox, Real-time Toolbox, etc. There are many applications of these tools, but we are focused on the Real-time Toolbox [3, 4]. Real-time simulation represent the simulation speed of execution as in the real time, there is no faster or slower than reality. It is based on the integration of fixed step time, which is specified in microseconds or milliseconds. Simulation time represents simulation real-time display and measured simulation time in real time which performs simulation. The use of real-time simulation include [5]:

- Setting up and development of prototype
  - Validation algorithm
  - Easy and fast implementation
- Testing of industrial equipment
  - Interaction generate disorders
  - Normal and critical situations
  - Analysis of equipment from different manufacturers.

Here is described one practically implemented system for closed-loop temperature control. The described system is realized using the PIC18F452 microcontroller from familly 18F Microchip manufacturers. The PIC18F452 microcontroller has many number of components. PIC microcontroller owns 40 or 44 I/O pins, which makes it a good choice for the realization of these simple devices.

Main features are: collection of 35 instructions, 1024 × 14 bits of program memory flash type, 68 × 8 bit memory RAM type of data, 64 × 8 bit memory EEPROM type of information, 13 I/O lines, 8-bit timer, 4 interrupt sources, possibility of programming protective bits, using energy saving sleep mode. Practical realization use standard quartz crystal operating frequency of 4 MHz [6–8].

In this paper is described use of PIC18F452 microcontroller in combination with software package MATLAB@Simulink and Real-time Toolbox for closed-loop temperature control.

2 Closed-Loop Temperature Control

Temperature is one of the most important and the most common measurement size in the technique. People are constantly related with temperature: air temperature, daily temperature changes, seasonal temperature changes, temperature of human body, temperature coolant in the car, etc. Temperature is a physical value which is used for expressing the thermal state of a substance. It depends on how much of internal energy has a certain object with certain weight and pressure. For precise temperature control is used closed-loop system. It is shown in Fig. 1.

Temperature reference value, desired temperature, is compared with measured temperature value. Deviation between reference and measured temperature value is sent in controller. Based on error, controller affects on executive element in order to reduce this error to zero. Executive element effects on heater, which heats the object. Temperature is measured with temperature sensor. This size is very small and need additional amplifier, which is then compared to reference value. Two most used types of temperature controllers are:

- The controller with direct ON/OFF temperature control
- Proportional controller with width modulated temperature control

2.1 The Controller with Direct ON/OFF Temperature Control

An ON/OFF controller is the simplest form of temperature control device (see Fig. 2). Output from the device is either "on" or "off", with no middle state. ON/OFF temperature controller switch output only when temperature crosses the setpoint. For heating control, output is "on" when temperature is below the setpoint, and "off" above the setpoint. On/off control is usually used where precise control is not necessary, in systems which can not handle energy's being turned "on"and "off"frequently, where mass of system is so great that temperatures change extremely slowly or for a temperature alarm [9].

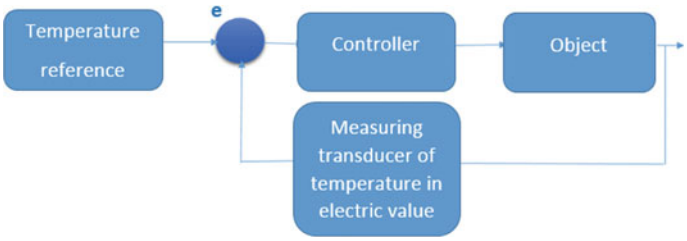

Fig. 1 Closed-loop temperature control

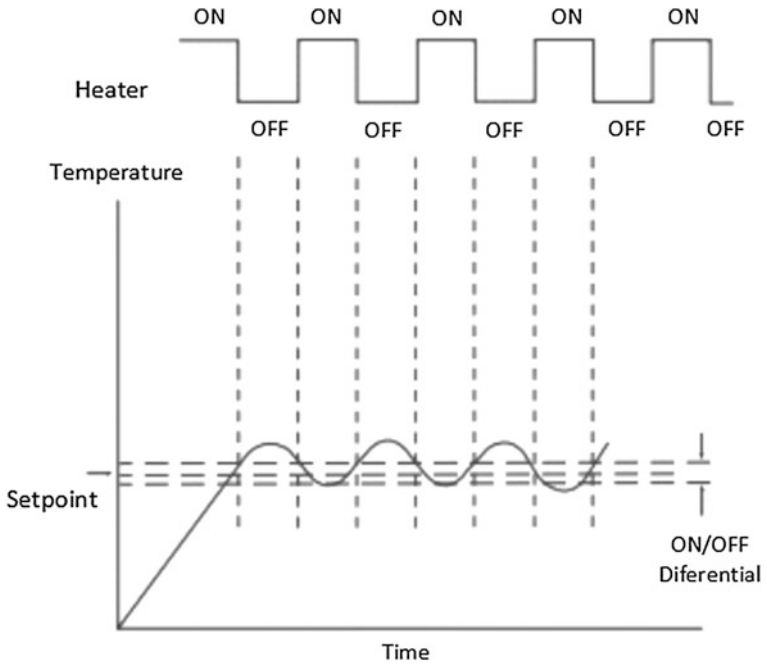

Fig. 2 On/off temperature control

2.2 *Proportional Controllers with Width-Modulated ON/OFF Temperature Control*

Proportional controls are designed to eliminate cycling associated with on/off control. Proportional controller decreases average power being supplied to heater as temperature approaches setpoint (see Fig. 3). This has effect of slowing down heater, so that it will not overshoot setpoint but will approach setpoint and maintain stable temperature. This proportioning action can be accomplished by turning output "on" and "off" for short intervals [9]. Proportioning action occurs within a "proportional band" around the setpoint temperature. Outside this band, the controller functions as an on/off unit, with the output either fully on (below the band) or fully off (above the band). Proportional controller decreases the average power being supplied to heater as temperature approaches setpoint. This has effect of slowing down heater so that it will not overshoot the setpoint, but will approach setpoint and maintain a stable temperature. This proportioning action can be accomplished by turning the output "on" and "off" for short intervals. Time period between two successive turnons is known as the "cycle time" or "duty cycle".

Proportioning action occurs within a "proportional band" around the setpoint temperature. Within the band, the output is turned "on" and "off" in the ratio of the measurement difference from the setpoint. At the setpoint (the midpoint of the

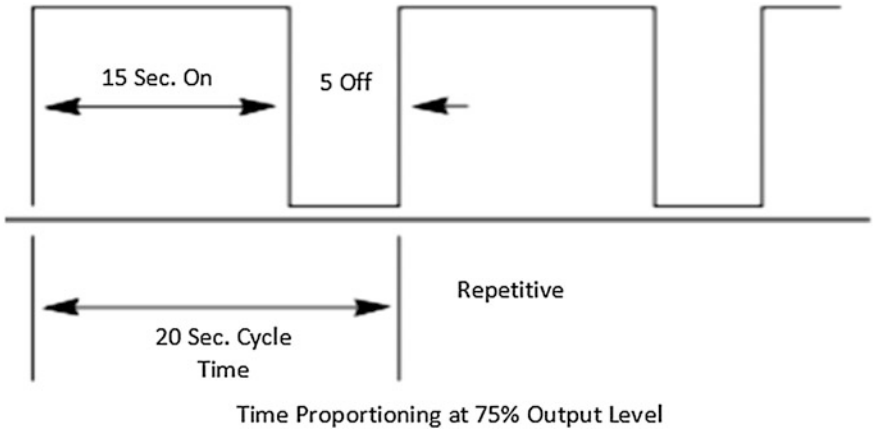

Fig. 3 Proportional controllers with width-modulated ON/OFF temperature control

proportional band), the output on/off ratio is 1:1 [9]. If temperature is below set-point, output will be "on" longer. If the temperature is too high, output will be "off" longer. One of the advantages of proportional control is simplicity of operation. It may require an operator to make a small adjustment (manual reset) to bring the temperature to setpoint on initial startup, or if process conditions change significantly. This proportional controller varies the ratio of "on" to "off" to control temperature in closed-loop.

3 Closed-Loop Temperature Control Using MATLAB@Simulink, Real-Time Toolbox and PIC18F452 Microcontroller

In this section of the chapter is suggested use of programming language MATLAB@Simulink and PIC18F452 microcontroller for closedloop temperature control. For real-time operation is used Real-time Toolbox. In Fig. 4 is shown functional block diagram for closed-loop temperature control.

Datas from computer over serial port and integrated circuit MAX232 are sent in the PIC18F452 microcontroller. The PIC18F452 microcontroller processes received data and forward them to output port RB7.

After amplification in power amplifier, which is realized by using transistor and thyristor, turns on heater that heats the object in which there is the heater. Turning off the thyristor is automatically when passing the supply voltage heaters through zero. With the temperature sensor LM335 is measured temperature inside object. Information of measured temperature is sent to amplifier implemented with the operational amplifier LM324. The sensor LM335 on its output provides change of

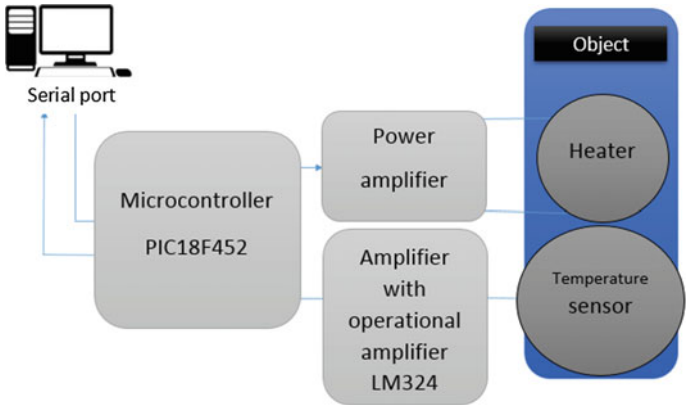

Fig. 4 Block diagram for temperature control using PIC18F452 microcontroller

10 mV when temperature change for 1 K. It is small signal and for that reason it must be amplified using the operational ampfier LM324. That amplified signal is sent in the PIC18F452 microcontroller, i.e. pin RA1. From pin RA1 analog signal is forwarded in A/D convertor.

In A/D convertor analog voltage value is converted to digital. Digital information of measured temperature value, using serial port, is forwarded to computer.

In Fig. 5 is shown appearance of the finished system for closed-loop temperature control using MATLAB@Simulink, Real-time Toolbox and PIC18F452 microcontroller.

Fig. 5 Appearance of the finished system for closed-loop temperature control

In the black box is located heater and temperature sensor, and it is environment in which temperature is controled. As the box is made of metal, there are also a large heat loss, which requires more frequent involvement of the heater.

For communication (sending and receiving data) with the PIC18F452 microcontroller are used the simulink blocks "Packet Input" and "Packet Output" which are previously set for the serial communication. That is shown in Fig. 6.

Of course, the same set is in the PIC18F452 microcontroller. In Fig. 7 is shown simulink scheme that is used for temperature control using the PIC18F452 microcontroller. Using Real-time Toolbox is allowed to work in real time. For that is used Real-Time Windows Target rtwin.tlc. Measured temperature is processed in PIC18F452 microcontroller and than over serial port is forwarded to block "Packet Input". After that, receiving, measured temperature is sent to block "Processing the measured temperature". In this block information of temperature is processed and adjusted for the range in which there is reference temperature value. However, for room temperature output value from this block is zero and with increasing

Fig. 6 Block "Packet Input" for receiving data using serial port

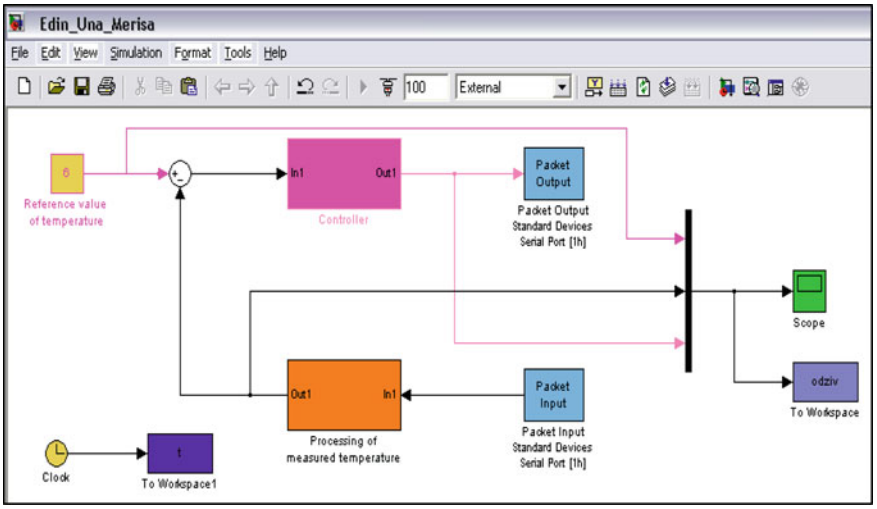

Fig. 7 Simulink scheme for closed-loop temperature control using MATLAB@Simulink and real-time toolbox

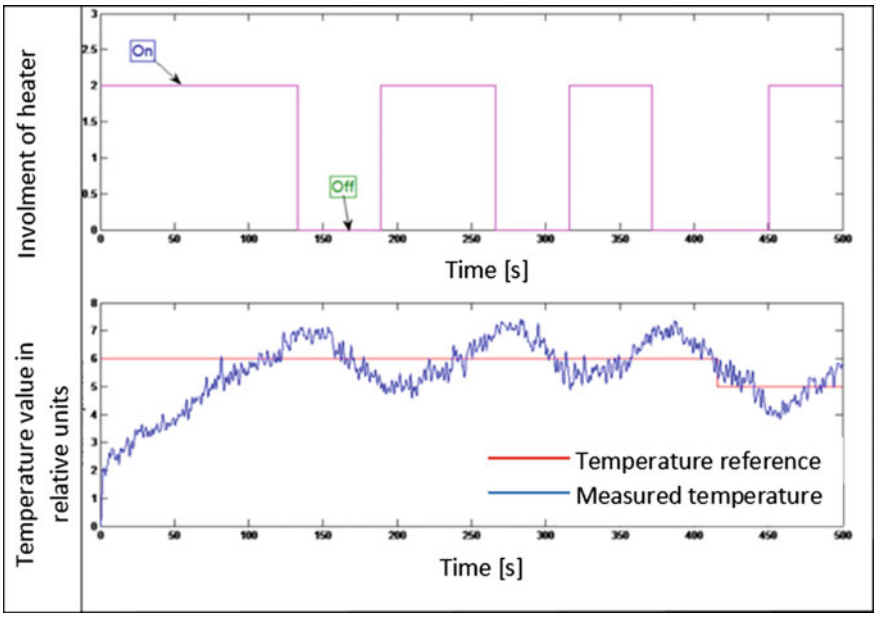

Fig. 8 Experimental results obtained using closed-loop temperature control for designed system

temperature at the same time that value is also increasing. Than, processed value of measured temperature in adder is compared with the reference temperature value.

Using, in this case, ON/OFF temperature controller, this value is processed and sent to block "Packet Output", and than over serial port is forwarded to PIC18F452 microcontroller and power amplifiers on heater.

4 Experimental Results

In this section of paper are presented experimental results for closed-loop temperature control using MATLAB@Simulink, Real-time Toolbox and the PIC18F452 microcontroller. It is used ON/OFF temperature controller. Because of great features of simulink, we can quickly and easily replace ON/OFF temperature controller with another temperature controller, e.g. the PID controller. Values of reference temperature is in relative units for easy and precise results presentation. After experiment analysis we got experimental results as shown in Fig. 8. Based on Fig. 8, we can conclude that closed-loop temperature control is working properly. When temperature exceeds set limit heater is turning off, and inversely. Maximum and minimum temperature value is adjusted within ON/OFF temperature controller. Error that occur when reading measured temperature occur because of to 8-bit resolution A/D converter. Taking average temperature value is obtained nearly ideal value of measured temperature. Temperature reference value can be optionally seted during work by simply entering another value in block "Reference value of temperature". To show temperature value we can use different temperature scales.

5 Conclusion

Based on the experimental result, we can conclude that designed system is working properly and that can be used to measure temperature in closed loop. If generalize, we can conclude that combination of MATLAB@Simulink, Real-time Toolbox and microcontroller can be used on different systems. In this way are used good features of MATLAB@Simulink for easy adjustment parameters of system as well as good features of PIC18F microcontroller series. All-important information's can be stored and displayed using wide spectrum of tools for graphical processing information.

References

1. Matlab R (2009) Documentation. The Mathworks
2. Gilat A (2011) MATLAB an introduction with applications, 4th edn. Wiley, New York

3. Ban Ž, Matuško J, Petrović I (2010) Primjena programskog sustava Matlab za rješavanje tehničkih problema, Graphis, Zagreb
4. Lent CS (2013) Learning to program with MATLAB. Wiley, New York
5. Real-Time Windows Target User's guide: for use with real-time workshop, The Mathworks, version 2, pp 3–33
6. Dogan I (2008) Advanced PIC microcontroller projects in C. Elsevier, Burlington
7. PIC18F42X, Data Sheet, FLASH-Based 8-Bit CMOS Microcontroller, 2003
8. Chartrand L, Huang HW (2005) PIC microconteroller: an introduction to software & hardware interfacing, Mankato
9. http://www.omega.com/temperature/Z/pdf/z110–114.pdf. 16 Mar 2016

Advertising LED System Using PIC18F4550 Microcontroller and LED Lighting

Edin Mujčić, Una Drakulić and Merisa Škrgić

Abstract In recent years, interest of the LED lighting is increased drastically in different applications. The reason for that are great advantages LED lighting. Advantages are: small dimensions, low power consumption, long life (up to 50,000 h), top colorful solution (RGB lighting) and ability to adjust the brightness. System enriched microcontroller can in many cases replace the man. Such system reduces dimensions of device and power consumption. Reason for that are very good features of microcontrollers: small size, can be programmed, minimum number of external components are required for normal operation, very long life, etc. In this chapter of the book, we described method of designing advertising LED system using PIC18F4550 microcontroller. LED strips are used for making letters and light-emitting diodes are used for additional effects. The PIC18F4550 microcontroller is used to control advertising LED system (on/off letters and additional effects). We conducted analysis of electricity consumption creation of advertising LED system. For additional savings of electricity consumption is integrated infrared motion sensor. In this way is enabled long-term operation advertising LED system especially in rural areas in conditions where LED advertising system is powered by battery or powered by combination of batteries and photovoltaic cells.

1 Introduction

The occurence of microcontrollers and microprocessors are regarded as one of the greatest technical achievements that characterized twentieth century. Main difference between microcontrollers and microprocessors is that they are the first optimized for speed and performance with computer programs, while microcontrollers are optimized towards integration of a large number of circuits real-time control, mass production, low cost and low power consumption [1]. Microcontrollers are also more resistant on variation of voltage, temperature, humidity, vibration, etc.

E. Mujčić (✉) · U. Drakulić · M. Škrgić
University of Bihać, Bihać, Bosnia and Herzegovina
e-mail: edin.mujcic@gmail.com

M. Hadžikadić and S. Avdaković (eds.), *Advanced Technologies, Systems, and Applications*, Lecture Notes in Networks and Systems 3,
DOI 10.1007/978-3-319-47295-9_25

Huge advantage is reflected in the fact that can be programmed, beside Assembler, and in high-level programming languages: C, Pascal, Basic, etc. [2]. This increases number of users who can write programs and thus also apply [1, 3]. They are used in a wide variety of modern devices such as: robots, telecommunication devices, satellites, cars, measuring instruments, mobile phones, cameras, etc. Also they are widely used in many home devices such as washing machines, microwave ovens, breadmakers, etc. [3]. Today on market there are few major manufacturers microcontroller which in its production program have different microcontroller families. The most popular of them are Intel, Motorola, Atmel and Microchip. In this chapter of the book is used PIC18F4550 microcontroller [4–6].

LED lighting is based on light-emitting diodes (LED) which emitting light when electric current through them. Color of light emitted by such LEDs depends on a few factors of which the most important are semiconductor and additional admixtures. LED light can variate from infrared to ultraviolet part of spectrum [7]. The first commercial use of LED lighting is focused on various indicators in electrical technology. Initially they were applied only to expensive equipment in laboratories. Later, LED lighting has found its usage in many electrical devices such as TVs, telephones, watches, calculators, lighting, etc. With development of LED technology is increasingly being directed towards to lighting. LED lighting consumes up to 60 % less energy so that a lightly higher price can compensate with saving through few years [8].

In this chapter is designed advertising LED system using PIC18F4550 microcontroller and LED technology. ON/OFF control of letters and additional effects is completely controlled by PIC18F4550 microcontroller, which is programmed in programming language Assembler. For additional savings of electricity consumption is embedded infrared motion sensor. Also, it's performed analysis of electricity consumption created advertising LED system.

2 The PIC18F4550 Microcontroller

The PIC18F4550 microcontroller belongs 18F series of microcontrollers from Microchip company [4, 5]. Microcontrollers of this manufacturer are characterized by low cost and more importantly free technical support (compilers, development systems) [5].

Considering to own harvard structure, memory map is divided in program memory, data memory and EEPROM. Processor in microcontroller (CPU) uses a technique of overlapping. Purpose of that is all instructions are executed (except branching) in one cycle. For these reason the basic tact is divided by 4, because the phase of execution of commands are overlapping. All commands have fixed length 2 bytes which means that memory addressing is limited. Memory is divided in 16 pages, and selection of pages is performed in appropriate control registers. This feature significantly slows microcontroller. However, advanced compilers preform

intelligent planning allocation of memory how would variables, that are commonly used, be located in the same memory bank.

Program memory is 32 KB and the RAM size 2 KB. There is also 256 BEEPROM memory [4, 5]. Processor has extended instruction set compared to the earlier series (16 and 17) as well as new ways of addressing. That way commands are added on hardware multiplication and division, incrementing and decrementing with conditional leap, etc. Program counter has width 21 bits and it can be accessed only indirectly through certain registers [9, 10]. Microcontroller also has buffer (stack), but unfortunately can only be used indirectly writing desired content in the special register and then with special instruction contents of the register puts in buffer. Datas are also located in that register. Peripherals tact depends by frequency of oscillator. Frequency of oscillator is maximum 48 MHz, which gives processor of microcontroller 12 MHz. For this purpose is used PPL circuit and frequency dividers. The most important thing is that for work of USB module microcontroller must be provided external tact of 24 MHz.

PIC18F4550 microcontroller has advantage over competing microcontrollers because tact can be independent of tact for CPU [4]. Mechanism of interruption is organized as a single interrupted vector. It contain address of interrupt routine in which is need to examine source of interruption and define desired action. There is no interrupted vector for each group or interrupted sources, which is one of the disadvantages of microcontroller. Because of that it loses its speed and transparency.

The PIC18F4550 microcontroller has numerous collection of hardware peripherals that enable implementation in many applications. Microcontroller owns 35 I/O lines that are multiplexed with parts of data register and signals of other modules [4]. In Fig. 1 is shown package of microcontroller in 44-pin and 40-pin package [4, 5].

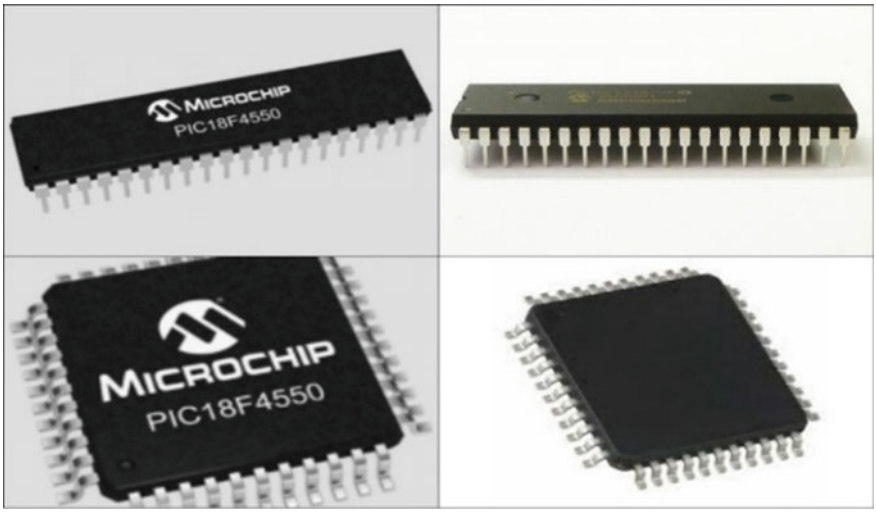

Fig. 1 The PIC18F4550 microcontroller in 44-pin and 40-pin package

Operating modes PIC18F4550 microcontrollers are [4]:

- Run mode: CPU and peripherals are turned on.
- Idle mode: CPU is turned off, peripheral is turned on and current is up to 5.8 μA.
- Sleep mode: CPU and peripherals are turned off and current is up to 0.1 μA.

Memory of PIC18F4550 microcontroller is organised in three different memory [5]:

- Program memory
- Data memory (RAM)
- EEPROM data memory.

Data memory and program memory are separated, which enables access for both memory in the same time. EEPROM data memory for practical implementation can be considered as peripheral device. Also, EEPROM data memory access over control memory [5]. Microcontroller series PIC18 are integrated such as 21-bit program counter. Address of program memory (2 MB) is enabled using program counter. If access memory location in between 2 MB, access is regular. If access memory location over 2 MB than result is logic "0" (NOP instruction). The PIC18F4550 microcontroller has Flash memory capacity 32 MB and can write 16 384 instruction [5].

Microcontroller serves PIC18 are using two interrupt vectors:

- Reset vector whose address is 0000 h
- Interrupt vector whose address is 0008 and 0018 h.

In Fig. 2 is shown PIC18F4550 microcontroller in DIP-40 package.

Each of 40 pins has its own label and generally more purpose. That is used to reduce number of pins. While programming, purpose of pins can be defined.

3 Led Lighting

LED (Light Emitting Diode) lighting is growing very quickly and showing as the "lighting of the future". Currently, LED lighting is used in traffic signals, automobile industry, backlights of televisions and monitors, phones with camera and also in many applications for decorative lighting, internal and external both [11].

In Fig. 3 is shown various implementations of LED lighting. LED lighting is based on semiconductor LEDs that are emitting light when electric current flows trough them. Color of light emitted by LEDs, depends of several factors. The most important factors are semiconductor and added impurities. Range of light is from infrared to ultraviolet part of spectrum.

Public interest for LED lighting in various applications has increased drastically in recent years. Popularity of LED lights is growing mainly because it following all

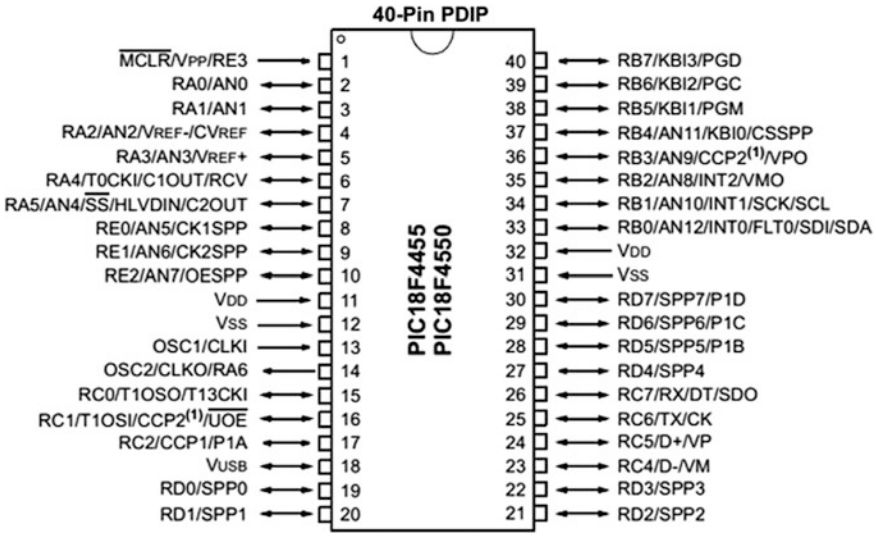

Fig. 2 The PIC18F4550 microcontroller in DIP-40 package [4, 5]

Fig. 3 Various implementations of LED lighting

basic trends. Lighting objects can be small, sophisticated and enabled extra multicolored solution (RGB lighting).

LED lighting provides whole new perception of lighting and switching from "era bulb" to "era of digital and creative lighting". LED lighting is no longer pure, static need for light, but now it presents constitutive part of design for interior and

exterior. Permanent drastic progress in development of LED lighting, which includes much improved performance of diodes, also appropriate optics, opens up endless possibilities for lighting solutions. It enables modern architectural solution and has become constitutive part of modern design [12].

Advantages of LED lighting over conventional light sources are [12]:

- Incomparably improved uniformity of light in comparison with other conventional light sources
- Lower power consumption
- Average duration is 10–15 years
- Resistance to mechanical damage and vibration
- No UV or IR radiation
- With instantly turning on there is no strobe effects
- Very small dimensions.

Such as all new technology that drastically progresses, LED technology has also a few disadvantages [12]:

- Start price
- Heat sensitivity (reduce the efficiency at higher temperatures)
- Weak horizontal dispersion
- New technology (lack of consultation, advice and implementation).

LED light sources also provide possibility of light direction of light (narrow beam of light), reducing unnecessary spending light. LED lighting produces less pollution of light, but at the same time possibility of much more efficient and precise deployment lamps.

4 Advertising LED System Using PIC18F4550 Microcontroller and LED Lighting

In this chapter of the book is designed advertising LED system using PIC18F4550 microcontroller and LED lighting. For creation advertising LED system are used: PIC18F4550 microcontroller, LED strips, LED lamps, adapter, infrared motion sensor, 24 transistors working as switches and plexiglass size 70 × 70, etc. On plexiglass is glued photofoil with desired motive in which are carved letters and desired shapes.

In Fig. 4 is shown LED stripes which are shaped on appropriate size and placed on appropriate place on plexiglass.

Each letter has two connectors (for positive and negative pole) which are connected on circuit board with transistors which are working as switches. Power

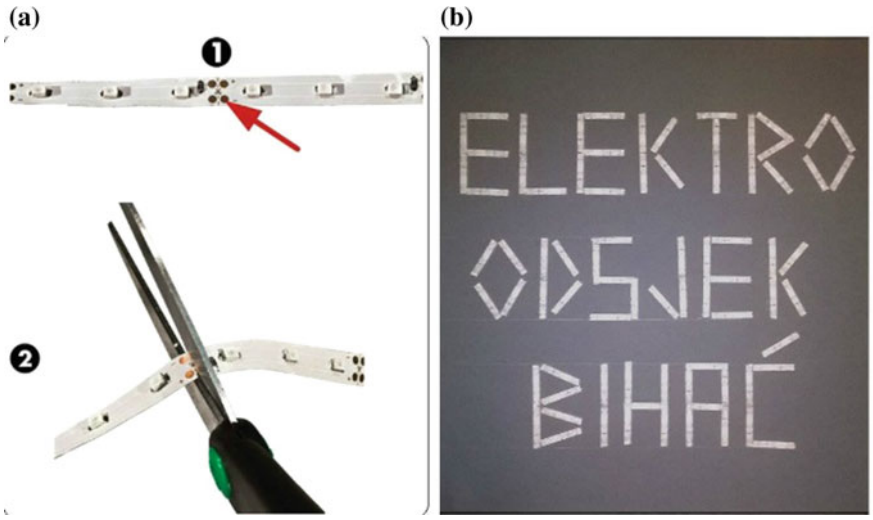

Fig. 4 **a** Cutting LED stripes, **b** placing LED stripes on appropriate place on plexiglass

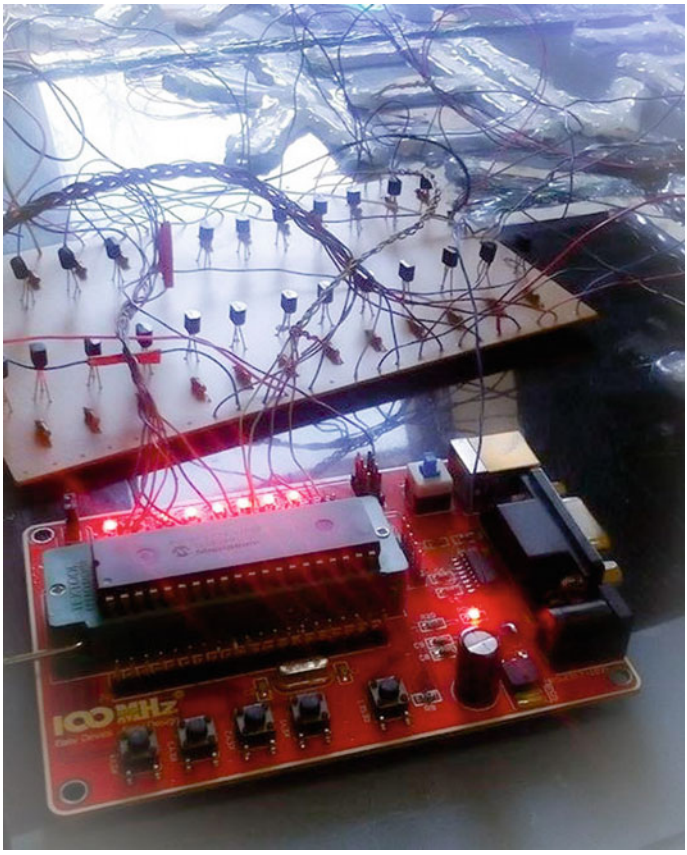

Fig. 5 Energy part of circuit, development environment and PIC18F4550 microcontroller

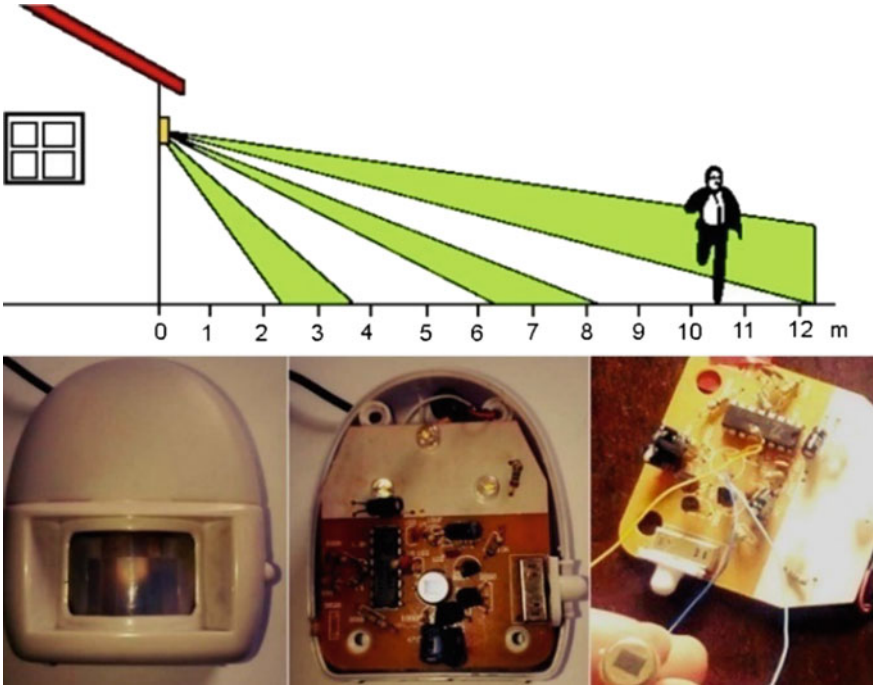

Fig. 6 Infrared motion sensor

supply for advertising LED system has two voltage levels. First voltage level (12 V) is used for power part and LED stripes. The second voltage level (5 V) is used for PIC18F4550 microcontroller and its development environment. For this purpose is used integrated circuit LM7805 on whose output is obtained stable voltage of 5 V which is required to operate PIC18F4550 microcontroller. Energy part of circuit is necessary because PIC18F4550 microcontroller on output pins provides voltage of 0 or about 5 V, and LED stripes works at 12 V with much higher consumption.

For programming PIC18F4550 microcontroller is used development environment MPLAB. Program is written in programming language Assembler. Using ICD2 programmer, hexadecimal code is transferred in PIC18F4550 microcontroller.

In Fig. 5 is shown energy part of circuit, development environment and PIC18F4550 microcontroller.

As the output ports are used PORT A, PORT B, part of PORT C and PORT D, and as input port is used PORT E (pin RE0) on which is connected infrared motion

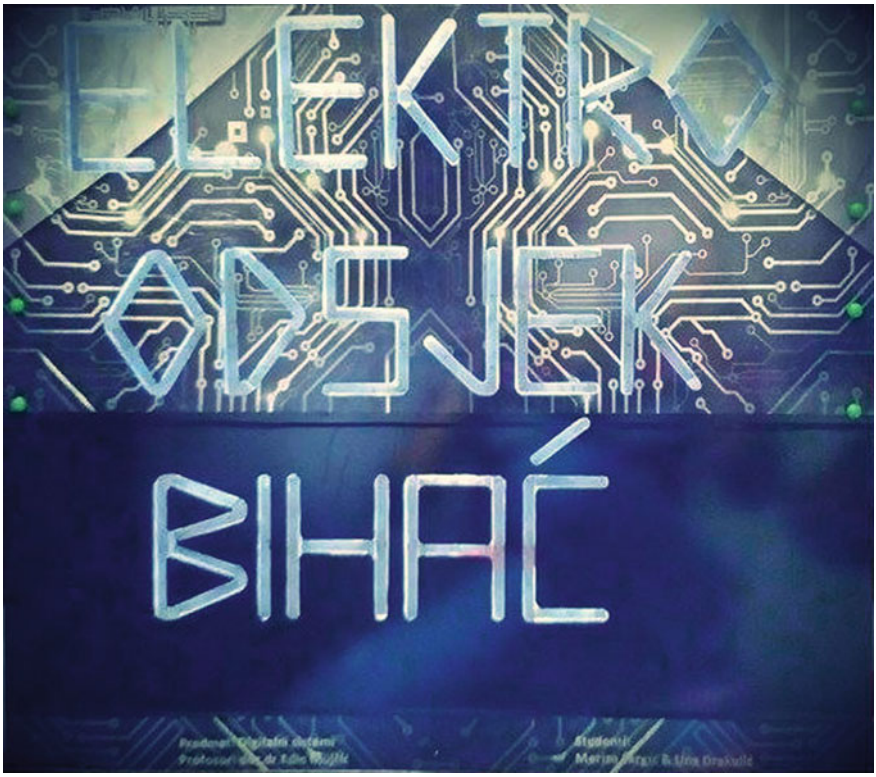

Fig. 7 Appearance of advertising LED system

sensor [13]. This sensor enables that advertising LED system is turning on only in someone's presence. Otherwise advertising LED system is turned off. In Fig. 6 is shown infrared motion sensor and the way it works.

This enable reducing power consumption when there is no presence of motion infront of advertising LED system. It is important when advertising LED system is powered by battery or powered by combination of batteries and photovoltaic cells. In Fig. 7 is shown appearance of advertising LED system when power is turned off. In Fig. 8 is shown final appearance of advertising LED system (power is turned on). On advertising LED system, letters "ELEKTRO ODSJEK" are blue color, and letters "BIHAĆ" are white color. LED diodes which are placed on sides are green color.

Maximum consumption electrical current when all letters and LED diodes are turned on is 15.24 Wh. Average consumption advertising LED system is 6 Wh, while minimum consumption (when is only one letter turned on) is 1.8 Wh.

In case when advertising LED system is powered by battery 100 Ah, advertising LED system can work constantly about 8 days. Using infrared motion sensor that time period is significantly prolonged.

Fig. 8 Final appearance of advertising LED system

5 Conclusion

In this chapter is described way to design light advertising LED system using PIC18F4550 microcontroller and LED technology. LED strips are used for making letters and LED diodes for additional effects. Control of advertising LED system, turning on and off letters and diodes, is controlled by PIC18F4550 microcontroller.

Based on analysis of average power consumption. We can conclude that consumption is very low compared to any other technology for lighting. Using motion sensors consumption is significantly reduced.

References

1. http://sh.wikipedia.org/wiki/Mikrokontroler. 02 Feb 2016
2. http://mikrokontroleri.weebly.com/uvodni-pojmovi—programiranje.html. 02 Feb 2016
3. Đorđević D, Đorđević Ž (2007) Komunikacija mikrokontrolera PIC16F877 preko SPI modula. Elektronski fakultet, Niš
4. http://ww1.microchip.com/downloads/en/devicedoc/39632c.pdf. 15 Mar 2016

5. http://www.microchip.com/wwwproducts/en/PIC18F4550. 01 Mar 2016
6. Mane-Deshmukh PV, Ladgaonkar BP, Pathan SC, Shaikh SS (2013) Microcontroller PIC18f4550 based wireless sensor node to monitor industrial environmental parameters. Int J Adv Res Comput Sci Software Eng 3(10)
7. Hong E, Narendran N (2004) A method for projecting useful life of LED lighting systems. Lightening Research Center, Rensselaer Polytechnic Institute, Troy
8. Akasaki I, Amano H, Nakamura S (2016) Filling the world with new light and saving energy and resources. Nobel Prize in Physics 2014 (18 Mar 2016)
9. Živanović D (2011) RS232komunikacijamikrokontrolerasa PC microcontroller serial communication with PC, vol 10, Ref. F-18, INFOTEH-JAHORINA, pp 980–983
10. Dogan I (2008) Advanced PIC microcontroller projects in C (from USB to ZIGBEE with the PIC 18F series). Newnes
11. Moreno I (2012) New use of LED light. In: Conference paper, Nov 2012
12. Mala škola LED tehnologije i rasvjete, Izvor: soled.hr + pro-laser.hr (18.03.2016)
13. Xie D, Liu H, Li B, Zhou Q, Yuan X (2013) Target classification using pyroelectric infrared sensors in unattended wild ground environment. Int J Smart Sens Intell Syst 6(5)

Compact Modelling of Non-linear Components in Verilog-A

Mujo Hodzic and Aljo Mujcic

Abstract This paper describes process of development compact models in the case of nonlinear overvoltage protection components. Verilog-A is a language that is widely used for development compact models of nonlinear components. An implementation of MOV and GDT compact models in Verilog-A hardware description language is presented. The Verilog-A codes of modeled components are sufficiently simple and based on mathematical description of voltage-current characteristics of selected overvoltage protection components. The proposed models are added into TINA circuit simulation environment and simulations are conducted for surge pulse 8/20 μs. The aim of the paper is to describe the process of model development using Verilog-A language and conduct the simulations in TINA software tool for simulation of electronic circuits.

1 Introduction

The design of complex electronic circuits includes simulation as an unavoidable step. The simulations, reflecting the actual behavior of the system, are directly dependent on the models of the particular components. The correct simulation results can be achieved with numerical simulations only if the valid models are used. The components are presented by a mathematical model including equations that describes the relationship between input and output values. Each model is based on parameters that define it. The parameters of a particular component are obtained by measurements and represent the basis for mathematical description of

M. Hodzic (✉)
BH Telecom d.d, Sarajevo, Bosnia and Herzegovina
e-mail: mujo.hodzic@bhtelecom.ba

A. Mujcic
Faculty of Electrical Engineering Tuzla, University of Tuzla, Tuzla,
Bosnia and Herzegovina
e-mail: aljo.mujcic@gmail.com

M. Hadžikadić and S. Avdaković (eds.), *Advanced Technologies, Systems, and Applications*, Lecture Notes in Networks and Systems 3,
DOI 10.1007/978-3-319-47295-9_26

the model. Electronic circuit simulation tools use mathematical models to describe the behavior of the electronic components or sub-circuits.

The most widely used hardware description language for electronic circuits and device models is SPICE. The circuit modelling and simulations are based on a text-file description of the circuit's components and connections. There are numerous simulation tools based on SPICE concept. They take a netlist as input and translate textually based description into equations to be solved.

In order to provide users of SPICE class simulators to create models of new components for their simulations in a more flexible manner the Verilog-A Hardware Description Language (HDL) language is introduced [1]. Verilog-A is intended to describe analog hardware and defines a behavioral language for analog systems.

Verilog-A HDL is derived from the IEEE 1364 Verilog HDL specification [1]. The language provides high level behavioral descriptions of components and sub-systems. Many systems are multidisciplinary and include electrical and non electrical components. Verilog-A cover simulations of both electrical and non electrical systems.

Verilog-A is a subset of Verilog-AMS language used for modelling and simulation of the mixed analog and digital circuits. Verilog-A as a standard is not available as stand-alone and it is part of the Verilog-AMS standard. The language reference manual is available at the Accellera website [2]. Verilog-AMS as an industry standard is appropriate for the simulation of both continuous time and event driven modeling semantics [1]. Therefore, this language provides simulation of analog, digital, and mixed analog/digital circuits. In this paper, we presented that Verilog-AMS and Verilog-A as its subset is well suited for the simulation of nonlinear overvoltage protection components.

Appliances in households, equipment in business buildings or factories are vulnerable to over-voltages that may originate due to atmospheric discharges or energy release present in the power supply system. Continuous and reliable operation of overvoltage sensitive systems (telecom centers, base stations, data centers) requires installation of two or more stages of surge protective devices [3].

Metal-Oxide Varistors (MOVs) and Gas Discharge Tubes (GDTs) are key components in surge protection systems. Voltage-Current (V-I) characteristics of the surge protection elements are highly nonlinear [3]. These components can be installed as a single protective elements or may be combined and installed as a complex protection circuit.

This paper presents the compact modelling of surge protection nonlinear components in Verilog-A and the simulations using TINA electronic circuit simulator. In the second section, we present a brief introduction to Verilog-A. The basis of the compact modelling in Verilog-A is also described in this section. Verilog-A code of MOV and GDT models are described in third section. Simulation results and discussion are also described in this section. Conclusion remarks are provided in the last section.

2 Compact Modelling in Verilog-A

Verilog-A is primarily designed to allow users of SPICE simulators to create as simple as possible mathematically defined models for their simulations. Verilog-A is intended to describe analog hardware and it is different from Verilog aimed for digital circuits.

The model in Verilog-A is also based on a text-file description of the model. In order to be a part of the simulation environment like SPICE models, the Verilog-A code must be converted into low-level C language by a code generator. The generated C code is then directly compiled into the simulator resulting in an equivalent SPICE model. Compact models written in Verilog-A should run reasonably fast, and simulator developers must follow rules to make this happen [4].

Comparing with C and other programming languages, the Verilog-A includes many mathematical built-in functions. These functions provide easier mathematical descriptions of component and modelling process is straightforward [3]. New models are then added automatically into simulation environment.

MATLAB as a high-performance language for technical computing is often used for compact model development. It provides programming in an easy-to-use environment, powerful data manipulation and advanced visualization routines. However, the models developed in MATLAB cannot be used in circuit simulators. With built in functions Verilog-A becomes practically as easy to use as MATLAB, and it can be used directly in circuit simulators.

SPICE is based on Kirchhoff's laws to formulate the circuit equations. SPICE simulators, in the process of solving circuits, build a system of nonlinear differential equations. SPICE combines the equations of the individual components with equations representing Kirchhoff's laws to formulate the system of equations that it solves when simulating the circuit. The result of simulation is obtained by solving the formed system of equations. On the other side, the equations in Verilog cannot be solved one at a time. These equations represent a simultaneous system of equations that must be solved all at once. Thus, the SPICE simulator should include Verilog module compiling and dynamically linking to the body of the SPICE code and solve the integrated system.

The Verilog code is based on a unit called module that is used to describe a component. The components are constructed using nodes where the endpoints of branches may connect and branches as a single path between two nodes. Any arbitrary component can be described with a collection of nodes and branches [1].

In Verilog-A, as in Verilog, a circuit can be described through a hierarchical composition of basic modules. The Verilog-A allow usage of built-in simulator primitives for the circuit description. Those built-in primitives define basic circuit components including resistors, capacitors, diodes, transistors, and some integrated circuits.

The module that uses equations to describe a component is referred to as a behavioral model. In that case, the simulation model is based on a desired external circuit behavior. With structural modelling, on the other side, different elements are

connected together to get the final design. The different circuit elements are connected to implement functions we are looking for. The module also may contain both equations (behavior) and connections of other modules (structure). The description incorporates two facts: how the nodes and branches are connected (topology), and relation between potential and flow on each branch (the branch relations).

The key feature required in the language is the ability to implement derivatives for some components. Verilog-A simulator compute partial derivatives of the currents and charges in a compact model making the modelling a much straighter forward process.

The modeling and simulation of the nonlinear components that include these principles are shown in the next section.

3 Verilog-A Models of Overvoltage Components

The two overvoltage circuit protection components are described and modelled in this paper: MOV and GDT. The MOVs allow voltages up to a designed clamping level to pass through to the load during operation while the GDTs operate as shunt components in response to a surge that exceeds the striking voltage.

3.1 Modeling of Metal Oxide Varistor

Metal-oxide varistor is voltage-dependent resistor with a highly nonlinear voltage-current relation. MOVs are made of a ceramic material obtained by mixing ZnO with a small amount of additives such as B_2O_3, CoO and MnO.

The static voltage-current characteristics can be described with the following equation [3]:

$$i = kV^{\alpha} \tag{1}$$

where coefficients k and α are to be determined for a given MOV (α is between 25 and 60, k is usually less than 10^{-100}) [3, 5, 6].

The static V-I characteristic should incorporate some additional time delay in the conduction mechanism of the varistor in order to achieve a good match between the model behavior and actual varistor. The MOV's residual voltage depends on the current surge wavefront shape. From the measurement results can be observed that the residual voltage increases when the current front time decreases. The rise time of the current surge pulse (10/350 and 8/20 μs) is less than fall time [3]. The different rise and fall time causes two different V-I characteristics. The residual voltage changes according to one V-I characteristic when current rises and according to another one when current surge falls. The another dynamic property is

that the residual voltage reaches its maximum before the current maximum. Therefore, the varistor numerical model must provide dynamic V-I characteristic.

The model of the varistor suggested by the IEEE Working Group [4] is shown in Fig. 1. The proposed model is frequently dependent describing different delays in the conduction mechanism at different wavefronts of surge current. Non-linear characteristics of the varistor consists of two branches separated by R-L filter, which consists of resistance R2 and inductance L2. For fast surge wavefronts, most of the current flows through the first nonlinear branch A0, while at the impulse tail, the voltage drop across R2-L2 filter becomes lower and nonlinear element in second stage with lower voltage takes over majority of the surge current [5].

The non-linear elements A0 and A1 are defined with V-I curves given in the IEEE document [5]. These curves can be fitted with the following expression [7]:

$$U = kb^{I}I^{c} \tag{2}$$

where U is voltage across the varistor and I is current through varistor. The coefficients k, b, and c are obtained from fitting of the curves proposed by the IEEE Working Group [5].

Verilog-A code of IEEE MOV model containing the first RL filter, varistor capacitance and first nonlinear branch is listed in Fig. 2. The second nonlinear branch and RL filter are not presented in the Fig. 2.

The IEEE MOV model is composed of two nonlinear branches divided by RL filters (Fig. 1). The inductance L1 (line 2) represents the inductance of the current path through the arrester. The resistance R1 in line 4 provides convergence in the numerical simulations [6].

The nonlinear elements A0 and A1 are modeled with Eq. (2). The first nonlinear element A0 is listed in lines from 8 to 23 (Fig. 2). The nonlinear VI characteristic is also divided into three regions. The second nonlinear branch A1 can be modeled using the same code as for the nonlinear element A0. The nonlinear elements A0

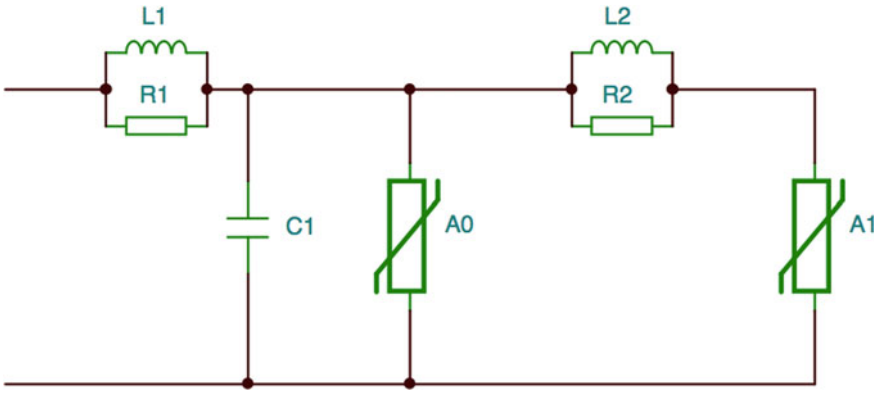

Fig. 1 Electrical scheme of IEEE model [4]

Fig. 2 Verilog-A code of IEEE varistor model

```
1.// The first RL filter
2.    V(br_ug1) <+ L1 * ddt(I(br_ug1));
3.    V(br_ugp1) <+ I(br_ugp1) * 1e-6;
4.    V(br_ur1) <+ I(br_ur1) * R1;
5. // Varistor capacity
6.        I(br_c) <+ C * ddt(V(br_c));
7.// The first nonlinear branch
8.    ibr1 = I(br_nonlin1);
9.    if (ibr1 > Imin) begin
10.        pom1 = pow(b1, ibr1);
11.        pom2 = pow(ibr1 , c1);
12.        pv1=pn * k1* pom1 * pom2;
13.    end else if (ibr1 < -Imin) begin
14.        pom1 = pow(b1, -ibr1);
15.        pom2 = pow(-ibr1 , c1);
16.        pv1= -pn * k1* pom1 * pom2;
17.    end else begin
18.        pom1 = pow(b1, Imin);
19.        pom2 = pow(Imin , c1);
20.        rlinearno=pn*k1*pom1*pom2/Imin;
21.        pv1 = rlinearno * ibr1;
22.    end
23.    V(br_nonlin1) <+ pv1;
```

and A1 are separated by the R-L filter (Fig. 1). The varistor capacitance C is presented in line 6 (Fig. 2).

The presented MOV model were implemented in TINA circuit simulation software as the Verilog-A model. Simulations are conducted for surge current pulse 8/20 μs [3]. The waveform of current pulse is presented in Fig. 3. The amplitude of the pulse used in simulations is 10 kA.

The residual voltage on MOV is also presented in Fig. 3. By comparing the waveforms of current and residual voltage can be seen that the voltage peak across the MOV occurs before the current peak.

Experimental investigations on the metal-oxide varistors provided an observation that MOVs behave differently for different surge wavefronts. Therefore, static frequency-independent model can't be used since MOV's response depends on rate of rise and magnitude of surge pulses. Influence of the rate of rise of the current pulse and its decay at the back edge of pulse can be clearly shown with the V-I

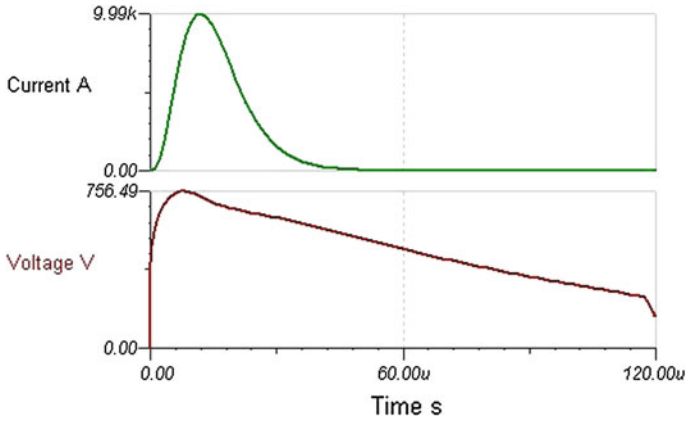

Fig. 3 The waveform of surge current pulse 8/20 μs and residual voltage on MOV

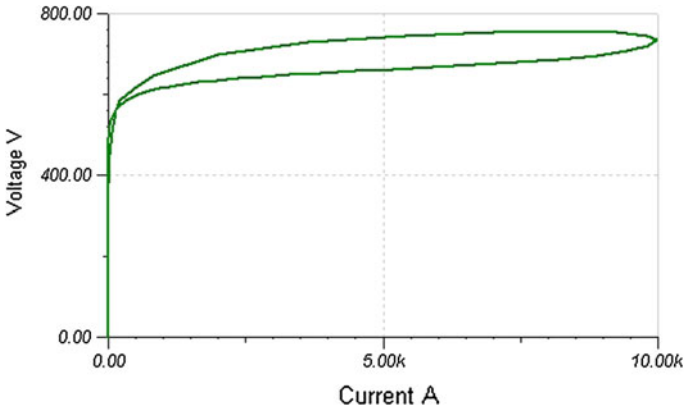

Fig. 4 Dynamical V-I characteristic of IEEE varistor model

characteristic obtained using the waveforms from Fig. 3. In this case the current is shown on the x-axis and the residual voltage on the y-axis. On that way, the dynamic *V-I* characteristic of MOV is obtained. The simulated MOV dynamic *V-I* characteristics is given in Fig. 4. The area of the V-I curve indicates dynamic characteristic of the varistor.

3.2 Modelling of Gas Discharge Tube

GDT usually consist of two or three electrodes that face each other across a short distance. The electrodes are placed in a glass or ceramic package and aligned with

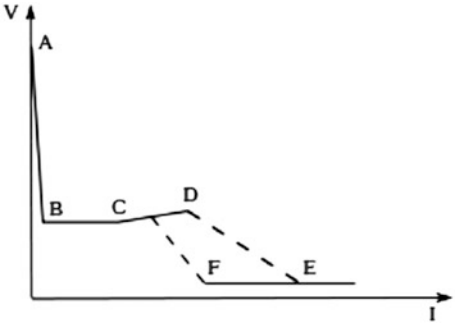

Fig. 5 GDT V versus I characteristic

the small gap between. The gap between electrodes is filled with air or an inert gas (neon or argon) [3].

A typical V-I curve for GDT is shown in Fig. 5. GDT has symmetrical V-I characteristics [3, 8, 9].

When a voltage applied to the GDT electrodes is below its striking voltage (DC firing voltage of the gap), the current through the arrester is close to zero. At the point A, GDT switches from an insulating to conducting state. Once a potential reaches the striking voltage, the voltage across GDT suddenly collapses causing negative incremental resistance dV/dI [3].

The segment of the curve between points B and D is known as glow region. This region can be divided into two subregions. In the first subregion (BC) the voltage across GDT is approximately independent of the current and it is called normal glow region. The second subregion is characterized by positive incremental resistance dV/dI [3].

When the current increases (DE), the GDT voltage decreases to the level called arc voltage, where it stays until the surge passes. The arrestor stays conductive until its current falls below a sustaining value.

After the surge disappears, the current will be reduced to the arc extinguishing current. At this value (point F) the arc is stopped and replaced by glow discharge [3].

GDT voltage versus current characteristic is segmented on three parts. The first part of the characteristic is region when the GDT is in the OFF state. In the OFF state, only a leakage current flows between GDT terminals. This segment is modeled with high ohm resistor.

The segment of the curve between points A and E is described with the following equation:

$$U_1 = U_p \tau^{\frac{I}{c}} \tag{3}$$

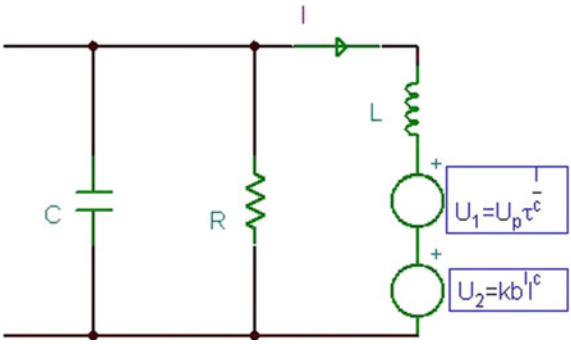

Fig. 6 Electrical scheme of GDT model

where U_1 is voltage across the current controlled voltage source and I is current through in the branch with nonlinear elements. The voltage U_p and coefficients τ and c are obtained from fitting of the curve.

At the level called arc voltage, where it stays until the surge passes, the arrestor is modelled with Eq. (2).

The GDT model is composed of two current controlled voltage sources modelling (Fig. 6). The inductance L takes into account this dynamic response. The parallel capacitance C shows the behavior at nonconductive state. The resistance *R* includes leakage current also at nonconductive state (Fig. 6).

The Verilog-A code of GDT model is given in Fig. 7. The segment of the curve between points A and E is described with Eq. (3) and Verilog code is listed in lines from 6 to 13 (Fig. 7). At the arc voltage level, the arrestor is modelled with Eq. (2) and Verilog code is listed in lines from 14 to 35. The varistor capacitance C is presented in line 1, resistance R in line 2 and inductance *L* in line 3 (Fig. 7).

Simulations are conducted in TINA circuit simulation software for surge current pulse 8/20 μs [3]. The waveform of surge current pulse 8/20 μs and residual voltage on GDT is presented in Fig. 8. V-I characteristic of GDT models is given in Fig. 9.

```
1.    I(bac)<+C*ddt(V(bac));
2.    I(bac)<+V(bac)/R;
3.    V(ban1)<+L*ddt(I(ban1));
4.    ibr2 = I(bn1n2);
5.    Up=pn1/Imin;
6.    if (ibr2 > Imin) begin
7.        pv2 = Up*pow(tau, ibr2/15);
8.        end else if (ibr2 < -Imin) begin
9.        pv2 = Up*pow(tau, -ibr2);
10.        end else begin
11.        pv2 = Up * ibr2;
12.        end
13.    V(bn1n2) <+ pv2;
14.    ibr1 = I(bn2c);
15.    if (ibr1 >= Imin) begin
16.        pom1 = pow(b1, ibr1/2);
17.        pom2 = pow(ibr1 , c1);
18.        pv1=pn * k1* pom1 * pom2;
19.    end else if (ibr1 <= -Imin) begin
20.        pom1 = pow(b1, -ibr1/2);
21.        pom2 = pow(-ibr1 , c1);
22.        pv1= -pn * k1* pom1 * pom2;
23.    end else if(ibr1 >= 0 & ibr1 < Imin)
begin
24.        pom1 = pow(b1, Imin);
25.        pom2 = pow(Imin , c1);
26.        rlinearno = pn * k1* pom1 * pom2 / Imin;
27.        pv1 = rlinearno * ibr1;
29.    end    else begin
30.        pom1 = pow(b1, -Imin);
31.        pom2 = pow(-Imin , c1);
32.        rlinearno = -pn * k1* pom1 * pom2 / Imin;
33.        pv1 = rlinearno * ibr1;
34.    end
35.    V(bn2c) <+ pv1;
```

Fig. 7 Verilog-A code of GDT model

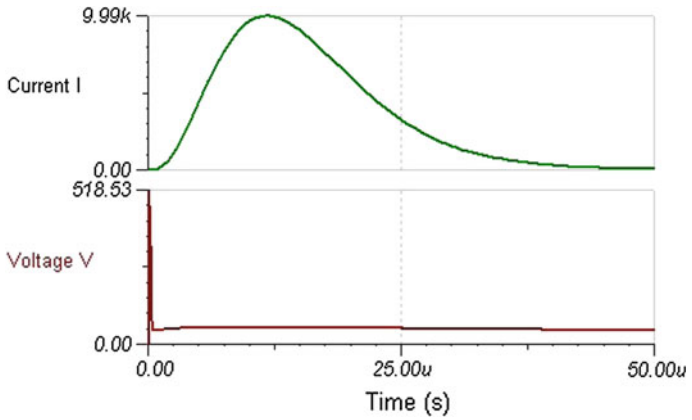

Fig. 8 The waveform of surge current pulse 8/20 μs and residual voltage on GDT

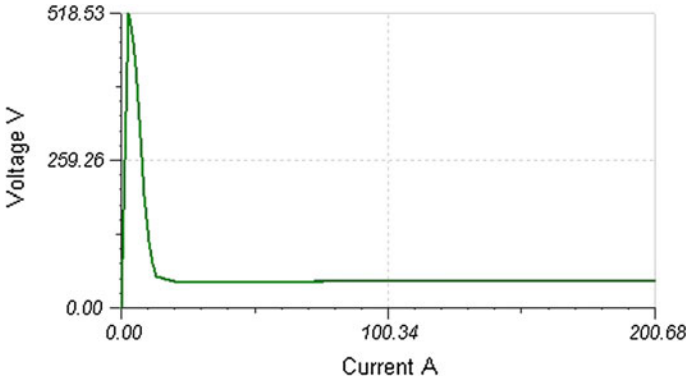

Fig. 9 V-I characteristic of GDT model

4 Conclusion

The paper presents an implementation of MOV and GDT compact model in Verilog-A hardware description language. These models are sufficiently simple and incorporated in circuit simulator. The Verilog-A code modeled components that are simulated in TINA circuit simulator. In the first case, the modeling of the MOV is focused on obtaining the dynamic characteristics with two nonlinear branches. In the second case, GDT is modelled using a serial connection of two non-linear characteristics. The models of highly nonlinear V-I characteristics of overvoltage components presented in the paper runs fast and converges without difficulties.

References

1. Kenneth S, Kundert OZ (2004) The designer's guide to VERILOG-AMS. Kluwer Academic Publishers, New York, Boston, Dordrecht, London, Moscow
2. Accellera (2010) Verilog-AMS language reference manual, version 2.2. http://www.accellera.org
3. Standler RB (1989) Protection of electronic circuits from overvoltages. Dover Publications, Inc., New York
4. Mcandrew C et al (2015) Best practices for compact modeling in Verilog-A. J Electron Devices Soc 3(5)
5. IEEE Working Group 3. 4. 11 (1992) Modeling of metal oxide surge arresters. IEEE Trans Power Deliv 7(1)
6. Suljanovic N, Mujcic A, Murko V (2006) Practical issues of metal-oxide varistor modeling for numerical simulations. In: International conference on lightning protection ICLP, Kanazawa
7. Zitnik B, Babuder M, Muhr M, Zitnik M, Thottappillil R (2005) Numerical modelling of metal oxide varistors. In: Proceedings of the XIVth international symposium on high voltage engineering, Tsinghua University, Beijing, China, 25–29 Aug 2005
8. Basso T, Sinard T, France T (1997) Spice model simulates spark-gap arrestor—EDN access. [Online]
9. Julio GZ (2008) Gas discharge tube modeling with PSpice. IEEE Trans Electromagn Compat 50(4)

Adaptive Tool for Teaching Programming Using Conceptual Maps

Tomislav Volarić, Daniel Vasić and Emil Brajković

Abstract The crucial information about learner in an E learning system is in fact the information about learner's level of knowledge. In everyday practice teacher must know what the student knows to adapt to learner's individual needs, and his features. In adaptive e learning system, the system has to have information about student's knowledge to implement learning strategies to achieve maximum effect. Many researches show that learning using e learning system shows best learning effects. This article shows how to use semi-automatic tool for teaching main concepts of programming using concept map. Concept map is used as an ontology that teachers use to construct domain knowledge that is used to asses' student's knowledge and construct student model. Based on student model system decides which concepts to include in teaching process. We utilize CM Tutor (Content Modeling Tutor) (Volaric in Oblikovanje modela nastavnih lekcija u inteligentnom sustavu e-učenja. Split, 2014) module to evaluate student's performance through qualitative and quantitative means. Experiments are made on 2 generations on students of University of Mostar to evaluate the systems effectiveness and improve systems performance based on student's feedback.

1 Introduction

Students learn by doing and experiencing, content in Learning Management Systems (LMS) should simulate active construction of knowledge, for that LMS systems should be more then content delivery systems. Building such courses in

T. Volarić (✉) · D. Vasić · E. Brajković
Faculty of Science and Education, University of Mostar, Matice hrvatske b.b,
88 000 Mostar, Bosnia and Herzegovina
e-mail: tvolaric@fpmoz.ba

D. Vasić
e-mail: daniel@fpmoz.ba

E. Brajković
e-mail: emilbrajko@fpmoz.ba

M. Hadžikadić and S. Avdaković (eds.), *Advanced Technologies, Systems, and Applications*, Lecture Notes in Networks and Systems 3,
DOI 10.1007/978-3-319-47295-9_27

LMS systems can be a difficult and exhausting task for instructional designers. LMSs, such as Moodle aim at supporting teachers in creating, administering, and holding online courses by providing them with a variety of features. Such features assist them in administrative issues. However, LMSs typically do not consider individual differences of learners and treat all learners equally regardless of their needs and characteristics. Most of the time for building interactive learning material is spent for adapting content material to be more interesting for individual students. Adaptive e learning systems automatically detect user level of knowledge and/or level of interest and adapt course material according to student's needs. Knowing how to adapt to students is lesser problem than knowing whom to adapt. One of the major challenges of web-based instruction has, and continues to be, accommodating students with differing profiles, expectations, prior experiences, and learning abilities [1]. The question how to adapt is answered in teacher module where set of rules predefine how to adapt course material according to student type and/or student level of knowledge.

2 Student Modelling

Student model construction is a basic and core issue of adaptive learning system. Conceptually, the student model is a proper subset of the expert model. Such student models are called overlay models because the student model can be visualized as a piece of paper with holes punched in it that is laid over the expert model, permitting only some knowledge to be accessible [2]. This way of modeling student has been implemented in Tutoring Expert System (TExSys) [3]. Modeling student's actions in e learning system can be done based on many different parameters. Vast amount of data is exchanged between the learner and the system that adaptive module can use to build the model of student's behavior. Vagale and Niedrite [4] proposes that we divide all data included model based on some categories (personal data, personality data, pedagogical data, cognitive data, history data, etc.). In which the main components used for modeling described in this article are pedagogical data—data that characterizes anything that a learner must learn, and cognitive data—data that represents which concepts user knows and the more important data user doesn't know. The model proposed in this article uses the data as shown in Fig. 1. To classify student into 4 different categories, the assumption is that student has no lack of knowledge, only that has knowledge at the level of recall. The last category synthesizes the last 3 levels into one category.

This approach of student modeling is based on conceptual maps, concept maps are often used for structuring knowledge, and the development of logical thinking and learning skills. CM Tutor is a plug-in for Moodle LMS that is trying to make solve problem of adaptability in LMS systems. Through traditional cycle of testing and teaching CM Tutor is trying to adapt course material to student's individual level of knowledge.

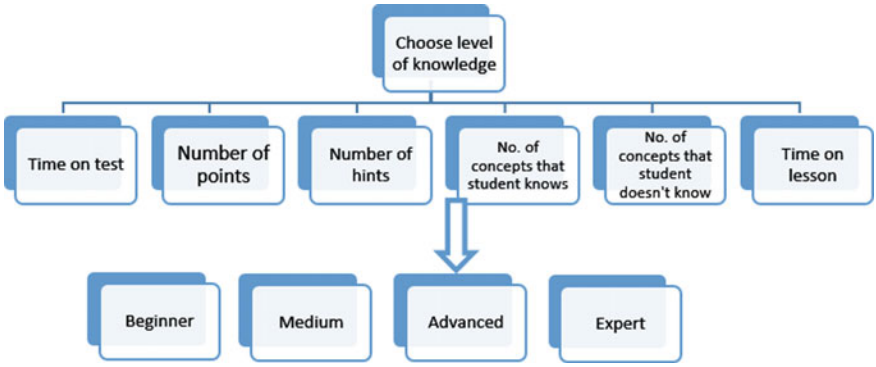

Fig. 1 Classification of student based on different criterion

Testing knowledge of each relations boils down to the principle hiding information that a student should be able to supplement, so teaching is essentially reduced to a student that individually is trying reproduce experts conceptual map.

Student is trying to get the idea of how certain relations constitute the entire conceptual map. The process of teaching and learning based on the approach of sequencing implemented in SCORM 2004 specifications [5], and that is that concepts that the system considers that a student has been mastered are exempted from the teaching and learning process.

The goal of CM Tutor is to make the classification of students and the class to which the student belongs to and then deploy a follow-up needed to the same student to move on to the next category.

According to the classes we decided to follow Bloom's taxonomy [6] of classifying students in four different categories. The method of testing the level of knowledge is with the questions of objective type. At different levels, we can examine the student's knowledge with objective type assignments that relay on Bloom's taxonomy. The question types that are delivered to student via test are:

- Recall assignments (required short answer)—this question, a student responds with one or a few words, and even shorter sentence (Recall).
- Supplementing assignments—supplement the sentence that is missing the student needs to record the sentence (Recall).
- Assignments of alternative choice—usually the default statement, the student needs to recognize that it is true or false (analysis, recognition).
- The tasks of multiple choices—contain the statement or question, and 4–5 of the proposed responses, including student should choose one right. Such tasks can be examined knowledge of the facts, an understanding of principles and even the application of knowledge.
- Connectivity assignments—complex concepts in the two series are to be mutually linked (analysis).

- The tasks of definition of ordering—students need to take care of the order by some principle in the assignment (synthesis).
- The tasks of the two criteria of choice—a task contains a variety of data, and the students are asked to classify them according to two criteria of choice.

The process of student classification is executed after every test. At first level "Beginner" student is being asked questions that examine student recall level on whole domain knowledge. If student successfully after that is classified into next category the questions that are adjusted to category that student belongs to. The system adapts in the way that after testing of student's knowledge system delivers only the lesson material for the concepts that student doesn't know. An adaptive model incorporates the adaptive theory of an adaptive e-Learning system by combining the domain model with the student model. The process of adaptive modeling starts with selecting representative nodes by analyzing the student needs from the student model [7] which is fully implemented in CM Tutor.

3 Student Classification

The way of classifying students into categories according to some criterion(s) is called a stereotyping. The assumption of stereotyping is that students at the same level of knowledge can be classified in the same category [8]. The classification student's knowledge into some category has been proposed by B. Bloom in renowned Bloom's taxonomy of Educational Objective in cognitive domain [9, 10]. This way of student classification has been used for decades in educational system. According to this we have defined 5 categories that student can belong to. According to this taxonomy there are 6 mayor outcomes—Knowledge, Comprehension, Application, Analysis, Synthesis, and Evaluation. The classification criteria used in this paper are consistent with Bloom's taxonomy of knowledge. In a way that sufficient grade (2) describe the knowledge level reproduction, good (3) understanding, very good (4) application, excellent (5) analysis, synthesis and evaluation, while inadequate (1) describes the lack of knowledge. As defined in previous section user can be a member of one of four categories (beginner, medium, advanced and expert) the process of teaching and testing in this model is ended when user reaches the expert category. The process of classification is implemented using Fuzzy Analytic Hierarchy Process (FAHP) [11] and The Technique for Order of Preference by Similarity to Ideal Solution (TOPSIS) [12] based on criterion(s) that are predefined by experts. FAHP method is first used to determine the weight criteria for decision-making using triangular fuzzy numbers. Then with TOPSIS method order of stereotypes of student was defined.

The AHP is based on the subdivision of the problem in a hierarchical form. The traditional AHP method is problematic in that it uses an exact value to express the decision-makers opinion in a pair-wise comparison of alternatives. Chang introduced a new approach for handling FAHP, with the use of triangular fuzzy numbers

for pair-wise comparison scale of FAHP, and the use of the extent analysis method for the synthetic extent values of the pair-wise comparisons, as shown in Fig. 2.

Let

$$X = \{x_1, x_2, \ldots, x_n\} \tag{1}$$

be an object set, and

$$U = \{u_1, u_2, \ldots, u_n\} \tag{2}$$

be a goal set. According to the Chang's extent analysis method [11], each object is taken and extent analysis for each goal is performed respectively:

$$M_{gi}^1, M_{gi}^2, \ldots, M_{gi}^m, \quad i = 1, 2, \ldots, n \tag{3}$$

where all the M_{gi}^j $(j = 1, 2, \ldots, m)$ are triangular fuzzy numbers. The value of fuzzy synthetic extent with respect to the object is defined as.

To obtain $\sum_{j=1}^{m} M_{gi}^j$, perform the fuzzy addition operation of m extent analysis values for a particular matrix such that:

$$\sum_{j=1}^{m} M_{gi}^j = \left(\sum_{j=1}^{m} l_j, \sum_{j=1}^{m} m_j, \sum_{j=1}^{m} u_j \right) \tag{4}$$

And to obtain $\left[\sum_{j=1}^{n} \sum_{j=1}^{m} M_{gi}^j\right]^1$, perform the fuzzy addition operation of $\sum_{j=1}^{m} M_{gi}^j$, $(J = 1, 2, \ldots, m)$ values such that:

$$\sum_{i}^{n} \sum_{j=1}^{m} M_{gi}^j = \left(\sum_{j=1}^{m} l_j, \sum_{j=1}^{m} m_j, \sum_{j=1}^{m} u_j \right) \tag{5}$$

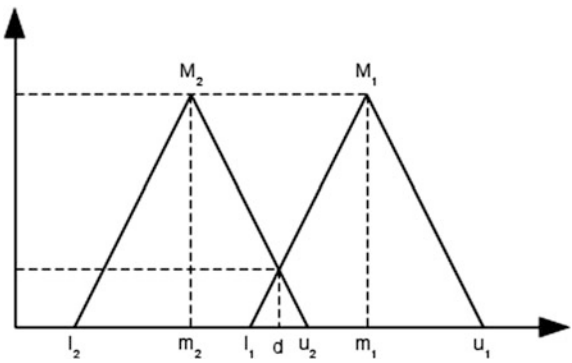

Fig. 2 The intersection between two triangular fuzzy numbers M_1 and M_2

As M_1 and M_2 are two triangular fuzzy numbers, the degree of possibility of $M_1 > M_2$ is defined as:

$$V(M_1 \geq M_2) = \underset{x \geq y}{SUP}[\min(\mu M_1(x), \mu M_2(y))] \tag{6}$$

When a pair (x, y) exists such that $x \geq y$ and $\mu M_1(x) = \mu M_2(y)$, then we have $V(M_1 \geq M_2) = 1$. Since M_1 and M_2 are convex fuzzy numbers we have that: $V(M_1 \geq M_2)$ is 1 if $m_1 \geq m_2$, 0 if $l_2 \geq u_1$ and $\frac{l_2 - u_1}{(m_1 - u_1) - (m_2 - l_2)}$, otherwise.

$$V(M_1 \geq M_2) = hgt(M_1 \cap M_2) = \mu M_1(d) \tag{7}$$

where d is the ordinate of the highest intersection point D between $\mu(M_1)$ and $\mu(M_1)$ like shown on Fig. 4. The degree possibility for a convex fuzzy number to be greater than k convex fuzzy numbers M_1 $(i = 1, 2, \ldots, k)$ can be defined by:

$$\min V(M \geq M_i), \quad i = 1, 2, 3, \ldots, k \tag{8}$$

Assume that $d(A_i) = \min V(S_i \geq S_k)$, $k = 1, 2, \ldots, n; k \neq i$, then the weight vector is given by:

$$W' = (d'(A_1), d'(A_2), \ldots, d'(A_n))^T \tag{9}$$

where A_i are n elements. Via normalization, the normalized weight vectors are

$$W = (d(A_1), d(A_2), \ldots, d(A_n))^T \tag{10}$$

where W is a non-fuzzy number. FAHP method is used to determine the weight criteria for decision-making process. In the FAHP procedure, the pair-wise comparisons in the judgment matrix are fuzzy numbers. The TOPSIS method requires only a minimal number of inputs from the user and its output is easy to understand. The only subjective parameters are the weights associated with criteria. The fundamental idea of TOPSIS method is that the best solution is the one which has the shortest distance to the ideal solution and the furthest distance from the anti-ideal solution. TOPSIS method was firstly proposed by Hwang and Yoon. According to this technique, the best alternative would be the one that is nearest to the ideal positive solution and farthest from the ideal negative solution. The positive ideal solution is a solution that maximizes the benefit criteria and minimizes the cost criteria, whereas the negative ideal solution maximizes the cost criteria and minimizes the benefit criteria. The method is calculated as follows [13].

Establish a decision matrix for the ranking. The structure of the matrix can be expressed as follows:

$$D = \begin{matrix} A_1 \\ A_2 \\ \dots \\ A_n \end{matrix} \begin{bmatrix} c_{11} & c_{12} & \dots & c_{1n} \\ c_{21} & c_{22} & \dots & c_{2n} \\ \dots & \dots & \dots & \dots \\ c_{m1} & c_{m2} & \dots & c_{mn} \end{bmatrix} \tag{11}$$

where A_i denotes the alternatives i, $i = 1, 2, \ldots, m$. F_j represents jth criteria, related to ith alternative; and c_{ij} is a crisp value indicating the performance rating of each alternative A_i with respect to each criterion c_{ij}. Calculate the normalized decision matrix. The normalized value r_{ij} is calculated as:

$$r_{ij} = \frac{w_{ij}}{\sqrt{\sum_{j=1}^{J} w_{ij}^2}} \tag{12}$$

where $j = 1, 2, \ldots, J;\ i = 1, 2, \ldots, n$. The weighted normalized decision matrix is calculated by multiplying the normalized decision matrix by its associated weights. The weighted normalized value v_{ij} is calculated as:$v_{ij} = w_{ij} * r_{ij}, \quad j = 1, 2, \ldots, J, \quad i = 1, 2, \ldots, n$where w_j represents the weight of the jth criteria. Positive ideal solution (PIS) and negative ideal solution (NIS) are calculated as follows:

$$A^* = \left\{ v_1^*, v_2^*, \ldots, v_n^* \right\}, \quad \text{maximum values} \tag{13}$$

$$A^- = \left\{ v_1^-, v_2^-, \ldots, v_n^- \right\}, \quad \text{maximum values} \tag{14}$$

Calculate the separation measures, using the m-dimensional Euclidean distance [12]. The distance of each alternative from PIS and NIS are calculated:

$$d_i^* = \sqrt{\sum_{j=1}^{n} \left(v_{ij} - v_j^* \right)^2}, \quad j = 1, 2, \ldots, J \tag{15}$$

$$d_i^- = \sqrt{\sum_{j=1}^{n} \left(v_{ij} - v_j^- \right)^2}, \quad j = 1, 2, \ldots, J \tag{16}$$

Calculate the relative closeness to the ideal solution and rank the alternatives in descending order. The closeness coefficient of each alternative is calculated, Table 1.

$$CC_i = \frac{d_i^-}{d_i^* + d_i^-}, \quad i = 1, 2, \ldots, J \tag{17}$$

Table 1 The linguistic scale and corresponding triangulary fuzzy numbers

Linguistic scale	Explanation	TFN	Inverse TFN
EQUAL	States that this criterions are equal (are the same)	$(1\ \ 1\ \ 1)$	$(1\ \ 1\ \ 1)$
EQUALLY IMPORTANT	States that this criterions are equally important	$\left(\frac{1}{2}\ \ 1\ \ \frac{3}{2}\right)$	$\left(\frac{2}{3}\ \ 1\ \ 2\right)$
LESS IMPORTANT	States that one criterion is less important than other	$\left(1\ \ \frac{3}{2}\ \ 2\right)$	$\left(\frac{1}{2}\ \ \frac{2}{3}\ \ 1\right)$
IMPORTANT	States that one criterion is more important than other	$\left(\frac{3}{2}\ \ 2\ \ \frac{5}{2}\right)$	$\left(\frac{2}{5}\ \ \frac{1}{2}\ \ \frac{2}{3}\right)$
VERY IMPORTANT	States that one criterion is very important than other	$\left(2\ \ \frac{5}{2}\ \ 3\right)$	$\left(\frac{1}{3}\ \ \frac{2}{5}\ \ \frac{1}{2}\right)$
EXTREAMLY IMPORTANT	States that one criterion is extremely more important than other	$\left(\frac{5}{2}\ \ 3\ \ \frac{7}{2}\right)$	$\left(\frac{2}{7}\ \ \frac{1}{3}\ \ \frac{2}{5}\right)$

where the index value of CC_i lies between 0 and 1. The larger the index value, the better performance of the alternatives. By comparing CC_i values, the ranking of alternatives is determined. The fuzzy evaluation matrix shown in Table 2 was defined by experts for definition criterions hierarchy. The fuzzy evaluation matrix has been defined with fuzzy triangular members using Saaty scale [14]. Table of mutual comparison of criteria are made by consensus of three experts. This comparison can also be made in such a way that every expert gives his assessment and then take the arithmetic mean of the expert's grade. After this calculation is performed according to the procedure described above and obtained by the vector of the relative importance of the criteria.

The result is a vector from Eq. 18

$$W = \begin{pmatrix} 0.1745 & 0.0284 & 0.2189 \\ 0.1677 & 0.2048 & 0.2055 \end{pmatrix} \tag{18}$$

Feature vector W is end result of FAHP method and is calculated only once that we mentioned above. This result keeps showing up as one of the input parameters for TOPSIS method by which we make classification of students into one of the

Table 2 Fuzzy evaluation matrix

	C1	C2	C3	C4	C5	C6
C1	$(1\ \ 1\ \ 1)$	$\left(\frac{2}{3}\ \ 1\ \ 2\right)$	$\left(\frac{1}{3}\ \ \frac{2}{5}\ \ \frac{1}{2}\right)$	$\left(\frac{2}{7}\ \ \frac{1}{3}\ \ \frac{2}{5}\right)$	$\left(\frac{2}{7}\ \ \frac{1}{3}\ \ \frac{2}{5}\right)$	$\left(\frac{1}{3}\ \ \frac{2}{5}\ \ \frac{1}{2}\right)$
C2	$\left(\frac{1}{2}\ \ 1\ \ \frac{3}{2}\right)$	$(1\ \ 1\ \ 1)$	$\left(\frac{2}{5}\ \ \frac{1}{2}\ \ \frac{2}{3}\right)$	$\left(\frac{2}{7}\ \ \frac{1}{3}\ \ \frac{2}{5}\right)$	$\left(\frac{1}{3}\ \ \frac{2}{5}\ \ \frac{1}{2}\right)$	$\left(\frac{2}{3}\ \ 1\ \ 2\right)$
C3	$\left(2\ \ \frac{5}{2}\ \ 3\right)$	$\left(\frac{3}{2}\ \ 2\ \ \frac{5}{2}\right)$	$(1\ \ 1\ \ 1)$	$\left(2\ \ \frac{5}{2}\ \ 3\right)$	$\left(\frac{2}{3}\ \ 1\ \ 2\right)$	$\left(\frac{2}{3}\ \ 1\ \ 2\right)$
C4	$\left(\frac{5}{2}\ \ 3\ \ \frac{7}{2}\right)$	$\left(\frac{5}{2}\ \ 3\ \ \frac{7}{2}\right)$	$\left(\frac{1}{3}\ \ \frac{2}{5}\ \ \frac{1}{2}\right)$	$(1\ \ 1\ \ 1)$	$\left(\frac{1}{2}\ \ \frac{2}{3}\ \ 1\right)$	$\left(\frac{2}{5}\ \ \frac{1}{2}\ \ \frac{2}{3}\right)$
C5	$\left(\frac{5}{2}\ \ 3\ \ \frac{7}{2}\right)$	$\left(\frac{5}{2}\ \ 3\ \ \frac{7}{2}\right)$	$\left(\frac{1}{2}\ \ 1\ \ \frac{3}{2}\right)$	$\left(1\ \ \frac{3}{2}\ \ 2\right)$	$(1\ \ 1\ \ 1)$	$\left(\frac{2}{5}\ \ \frac{1}{2}\ \ \frac{2}{3}\right)$
C6	$\left(2\ \ \frac{5}{2}\ \ 3\right)$	$\left(\frac{1}{2}\ \ 1\ \ \frac{3}{2}\right)$	$\left(\frac{1}{2}\ \ 1\ \ \frac{3}{2}\right)$	$\left(\frac{2}{7}\ \ \frac{1}{3}\ \ \frac{2}{5}\right)$	$\left(\frac{2}{7}\ \ \frac{1}{3}\ \ \frac{2}{5}\right)$	$(1\ \ 1\ \ 1)$

Table 3 Student result's on exam

	C1	C2	C3	C4	C5	C6
GradeBeg	2	3	4	5	6	4
GradeMed	2	2	3	5	2	4
GradeAdv	0	1	0	2	0	0
GradeEx	1	0	0	2	1	0

Table 4 Result of students classificaiton

Rank	Category
1	Beginner
0.878764908	Medium
0.007471244	Advanced
0.062575942	Expert

categories. At the start of testing delivered questions that test all levels of knowledge according to the classification of the questions according to Bloom's Taxonomy [15].

If the student knows certain concept according to TOPSIS classification then we test and deliver teaching material for only the concepts that student doesn't know on certain level of knowledge. Table 3 are shown the test ratings. By this is meant the result of the test, which covers all levels of knowledge. For the other criteria necessary to define what is the level required for a certain level of knowledge and consequently make assessments. For example, if an expert should take one minute for C1 or C2 then the student can get the highest score only if he/she is inside or close to that time. Otherwise student gets smaller grade for that criterion.

Table 4 shows the results of classification with TOPSIS method. The result shows that with the results on test shown in Table 3. we get classification that student belongs to category Beginner. So the next step is to adjust the teaching process based on the concepts that student is shown not to know.

4 Methodology

In the experiment we determine to what extent the second variable (consequences) depends of the first (impact). In our approach, the dependent variable is the knowledge of students and the independent variable is the system CM Tutor whose effects we want to investigate. The main goal of the experiment is to determine if there is, what is and the impact of certain independent variables on a given dependent variable. The experiment we did three times, the second and third time we repeated the test after an upgrade on CM Tutor, the first iteration (Fig. 3) had no visualization of concepts. In CM Tutor version 2—after the survey of satisfaction students were dissatisfied with the clarity issue of questions; a good suggestion is to visually see what they are asked (within the CM Tutor raised the graphical environment that visually examine student knowledge as shown in Fig. 4).

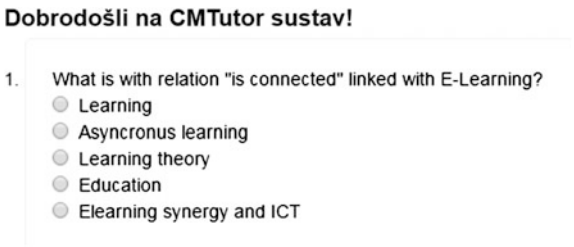

Fig. 3 Example of question with CM Tutor version 1

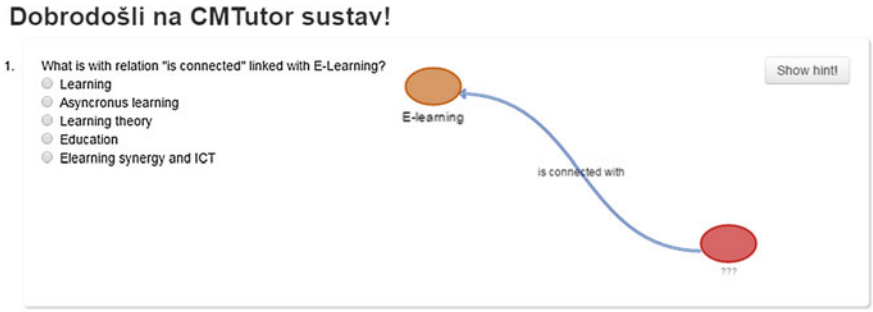

Fig. 4 Example questions with visualization

4.1 Experiment Methodology

The third update is the hints integration where the student can ask the system to help him with the question. The experimental research was conducted at the Faculty of Natural Science and Education of the University of Mostar, in the computer lab. The first phase of the experiment was 09/05/2014. Then made the upgrade CM Tutor with the help of a satisfaction survey, introduced the visual part of the system because the biggest criticism was as incomprehensible questions. The second phase of the experiment was 02/07/2014, and the third phase was made 27/05/2015.

4.2 Experiment Population

The study was conducted on 20 students, after equalizing groups (some students are not doing both experiments) we got 8 students, and after that in year 2015 after third update study was conducted on 5 students where we tried calculated the effect size of teaching with CM Tutor after final updates. Participants are students of 1st year student of computer science and information technology combinations while listening to the course "Programming in Java". Students get extra points for the course on the basis of test results. Students had the domain knowledge of programming in

Java. Students are examined the basic concepts of programming in Java. The students are taught and examined with the help of CM Tutor.

4.3 Experiment Results

Results of testing were processed in Microsoft Office Excel 2007 program, in Fig. 2 the results of testing before and after visualization are shown. For the effect size we used Cohen's d effect size. Cohen's d is defined as the difference between two means divided by a standard deviation for the data. The research results show that there are significant differences between teaching and non-visualization of the CM Tutor. This shows that there is statistical significant difference between CM Tutor with and without visualization. Effect size according to Cohen is 0.91, which is statistically large impact. This result can be attributed to the fact that the first versions of CM Tutor students were not clear questions and upgrading the CM Tutor (visualization) we got much better results. The second part of experiment we measure effect-size of CM Tutor itself as shown in Fig. 5 100 % of students show better results after the usage of CM Tutor. The replication of the experiment is planned on larger population to check the consistency of this experimental evaluation. The Cohen d between pretest and post test data is 1.6714. With a Cohen's d of 1.6714, 95 % of the treatment group will be above the mean before the treatment, 42 % of the two groups will overlap, and there is a 87 % chance that a person picked at random from the treatment group will have a higher score than a person picked at random from the group after treatment with CM Tutor, Fig. 6.

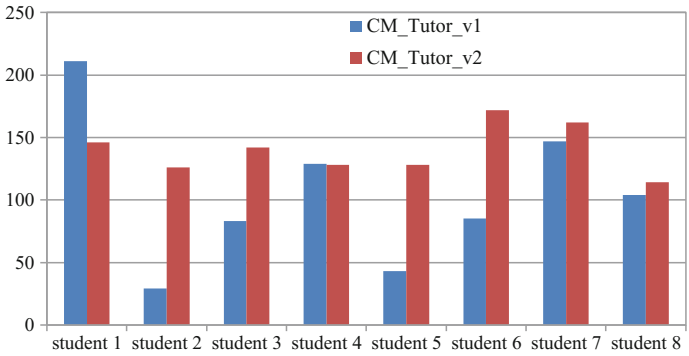

Fig. 5 The final number of points on both versions of the CM Tutor

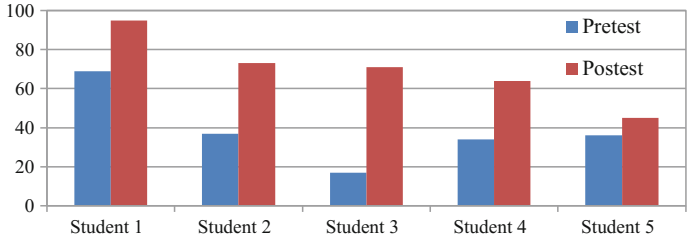

Fig. 6 The final results of the CM Tutor evaluation on "java programming" course

5 Conclusions

In this article the qualitative and quantitative experiment was made to check the effect size of CM Tutor, Moodle LMS plugin that introduces the concept of adaptability in modern LMS systems. Teacher must know what the student knows to adapt to learner's individual needs, and his features. In this adaptive e learning system, the system tries to model the student's knowledge using FAHP and TOPSIS. After the classification the system implements learning strategies to achieve maximum effect. This system uses simple concept map that is uploaded into LMS system, and the system itself caries out the learning strategies needed to achieve maximum effect to achieve certain learning outcomes. The qualitative and quantitative 2-years-old research show very good results, and shows area for advances in research. For future research the experiment will be conducted to test effect size and efficiency of this system.

References

1. Abidi R, Sibte S (2015) Intelligent information personalization. In: Intelligent user interfaces. IGI Global, pp 118–146. Available at http://services.igi-global.com/resolvedoi/resolve.aspx?doi=10.4018/978-1-60566-032-5.ch006. Accessed 15 July 2016
2. VanLehn K (1988) Student modelling. In: Polson MC, Richardson JJ (eds) Foundations of intelligent tutoring systems. Lawrence Erlbaum Associates, Pittsburgh, pp 55–79
3. Stankov S et al (2008) TEx-Sys model for building intelligent tutoring systems. Comput Educ 51:1017–1036
4. Vagale V, Niedrite L (2014) Learner model's utilization in the e-learning environments. In: Kalja A, Haav HM, Robal T (eds) Databases and information systems VIII. IOS Press, Amsterdam, pp 162–173
5. ADL Technical Team Contributors (2004) Sharable content object reference model (SCORM). In: Advanced distributed learning, p 180. Available at http://www.adlnet.org/
6. Bloom BS (1956) Taxonomy of educational objectives, the classification of educational goals. McKay, New York
7. Esichaikul V, Lamnoi S, Bechter C (2011) Student modelling in adaptive E-learning systems. Knowl Manage E-Learn Int J 3(3):342–355. Available at http://www.kmel-journal.org/ojs/index.php/online-publication/article/view/124

8. Grubišić A, Stankov S, Žitko B (2013) Stereotype student model for an adaptive e-learning system. Int J Comput Electr Autom Control Inf Eng 7(4):440–447
9. Volarić T, Brajković E, Sjekavica T (2014a) Integration of FAHP and TOPSIS methods for the selection of appropriate multimedia application for learning and teaching. Int J Math Models Methods Appl Sci 8:224–232. Available at http://www.naun.org/main/NAUN/ijmmas/2014/a482001-305.pdf
10. Volarić T, Brajković E, Vasić D (2014b) Utjecaj mobilnih uređaja u nastavi. Suvremena pitanja 17:50–67. Available at http://www.maticahrvatska-mostar.ba/images/pdf/suvremena_pitanja/SP_17.pdf
11. Chang D-Y (1996) Applications of the extent analysis method on fuzzy AHP. Eur J Oper Res 95(3):649–655. Available at http://linkinghub.elsevier.com/retrieve/pii/0377221795003002. Accessed 15 July 2016
12. Ishizaka A, Nemery P (2013) Multi-criteria decision analysis: methods and software. Wiley, New Jersey
13. Klir GJ, Yuan B (1995) Fuzzy sets and fuzzy logic: theory and applications. Prentice Hall PTR, Upper Saddle River
14. Saaty T (1980) The analytic hierarchy process. McGraw Hill International, New York
15. Scott T (2003) Bloom's taxonomy applied to testing in computer science classes. J Comput Sci Coll 19(1):267–274. Available at http://dl.acm.org/citation.cfm?id=948775&CFID=380881129&CFTOKEN=42051081
16. Volaric T (2014) Oblikovanje modela nastavnih lekcija u inteligentnom sustavu e-učenja. Split

Kockica: Developing a Serious Game for Alphabet Learning and Practising Vocabulary

Sena Bajraktarević and Belma Ramić-Brkić

Abstract Serious games have had a great impact on education of children and especially, children with disabilities. Kockica is a first 3D serious game developed in native (Bosnian) language and as such, is culturally appropriate for B&H children. The game is intended to help children learn alphabet and improve their verbal skills in a fun and joyful way. The idea of the game is to encourage parents to participate in children's play and learning time, and to offer teachers a new interactive tool that could potentially speed up the learning process and at the same time make it more interesting and fun. The game presented in this paper is developed in collaboration with professionals working at an NGO "EDUS—Education for All", program devoted to evidence-based work with children with disabilities. In this paper we present a pilot study conducted with neuro-typical children, including correction feedback received from the teachers.

1 Introduction

Gaming has the great potential of deeply engaging children in a given task. Today's young generations are labelled as Generation N or the Net Generation since from the early days they seem to be surrounded by technology [1]. No longer it is considered as novelty, but rather as a normal surrounding. Education represents an area that could significantly gain from increased use of technology in early learning and education of children. On the other hand, it seems least predominant in this field, especially in Bosnia and Herzegovina. However, this trend is changing. We have a number of parents, preschool teachers, young individuals, that are willing to invest time in educating themselves regarding the use of technology in education

S. Bajraktarević (✉) · B. Ramić-Brkić
University Sarajevo School of Science and Technology, Hrasnicka cesta 3A, Sarajevo, Bosnia and Herzegovina
e-mail: sena.bajraktarevic@stu.ssst.edu.ba

B. Ramić-Brkić
e-mail: belma.ramic@ssst.edu.ba

M. Hadžikadić and S. Avdaković (eds.), *Advanced Technologies, Systems, and Applications*, Lecture Notes in Networks and Systems 3,
DOI 10.1007/978-3-319-47295-9_28

purpose. Preschool and elementary school teachers are recording presentations on specific topics (e.g. Chinese stick multiplication), and posting it on-line using a number of currently available educational platforms such as Osnovna.ba, Bookvar and Eduvizija. Further on, teachers are on their own initiative giving students on-line homework and assignments to improve their knowledge and skills on the use of technology.

The work presented in this paper shows the novel game idea and its logic developed in collaboration with Dr. Nirvana Pištoljević, education specialist, game development process as well as initial output and corrective suggestions received from the trained EDUS (edusbih.org) staff and children attending their programs.

2 Related Work

Regardless of a child's abilities, research has shown that computer-assisted interventions do indeed enhance and advance children's skills at a quicker pace, compared to traditional teaching and educational methods [1, 2]. Further on, an increased number of parents and teachers are looking for different ways and approaches to teaching which could be used and applied at homes and in classrooms, especially when talking about children with developmental delays and disabilities [3–6].

A number of companies developing 3D educational games worldwide are increasing. One of the famous companies is "Toca Boca" from San Francisco founded in 2010 [7]. They are developing educational games for tablets and smart-phones with the focus on user-friendliness. The philosophy behind the game is to stimulate learning of children through the fun way of play. They call their own games "digital toys".

As mentioned earlier, the trend of using technology for educational purposes is slowly but steadily reaching the region of Bosnia and Herzegovina. One such project is "LeFCA", a learning framework for children with autism developed in collaboration with SSST and EDUS [8]. Within the framework, Shapes game(s) were developed though which students were taught the matching concept ("Find the same" task), Pointing out/Selecting ("Which shape does not belong" task; or "Select the shape heard" task) and Labelling ("What is the shape called" task). Using similar technology, they went further on to create an interactive 2D e-learning book for children available through their website [9].

Even though there exists a number of educational games, even games specifically developed for children with autism (e.g. Autism Speech Assistant AAC; Touch Emotions), their main disadvantage is the language in which they are developed, limiting it only to, in majority of cases, an English speaking region [10, 11]. Due to technology development and constant decrease in sizes of various communication devices, these games are almost by default developed for smart-phones and tablets, which is yet another additional limiting circumstance.

Kockica is unique for so many reasons; firstly, it is written in a native (Bosnian) language with the possibility of easy transition to any language; Secondly, it is a 3D educational game and thirdly, it can be played on a Desktop monitor using mouse as well as on touch screen based technology.

3 Kockica

Even though the main target were children with disabilities, the game can be used by other children with or without disabilities since it is based on basic learning interaction. The main goal of this game is to teach children alphabet and naming of colors and objects. The flowchart shown in Fig. 1, shows the general interactive logic and structure of the game.

As can be seen from the Fig. 1, Kockica encompasses two pillars: one being an alphabet and another, virtual room for stimulation of language, learning different colors and matching games. The first pillar consists of four levels, starting with three letters and the numbers of letters in the next levels are increasing by two (see Figs. 2, 3, 4 and 5). Virtual room offers a child an option of learning about colors and objects. If child chooses through a menu bar button "Colors/Boje", when in the room, then they will be given a possibility to click on the object and learn the name of its color. The same principle is applied for objects but instead of hearing its color, a child will hear the name of the object (see Figs. 6, 7 and 8).

Within the game we also created a test that can be used to check if a child has learned the color of an object or a name of an object. It is activated by clicking the button in the right corner of the screen. Prompted voice guides a child to find a specific object inside the virtual room. A child can navigate through the room by moving mouse right or left. In the case of correct answer voice provides reinforcement (e.g. Bravo, applause) to a child on successfully completing the given task. In the case of an incorrect answer, child is being given another instruction with the same order, meaning a child is given another option to try his/her knowledge.

3.1 Game Development

The aim of the created game was to stimulate early child development and support learning. The game encompassed different tasks and assignments such as learning ABC's, color matching and interactive search for different objects in the virtual child room filled with appropriate toys and furniture that can be found in almost all children's rooms. The target audience are children with and without disabilities. A variety of methods is used to teach particular concepts—examples include matching, sorting and searching. The game can also be easily customized to fit the child's individual needs. Randomization of a task is only implemented within the

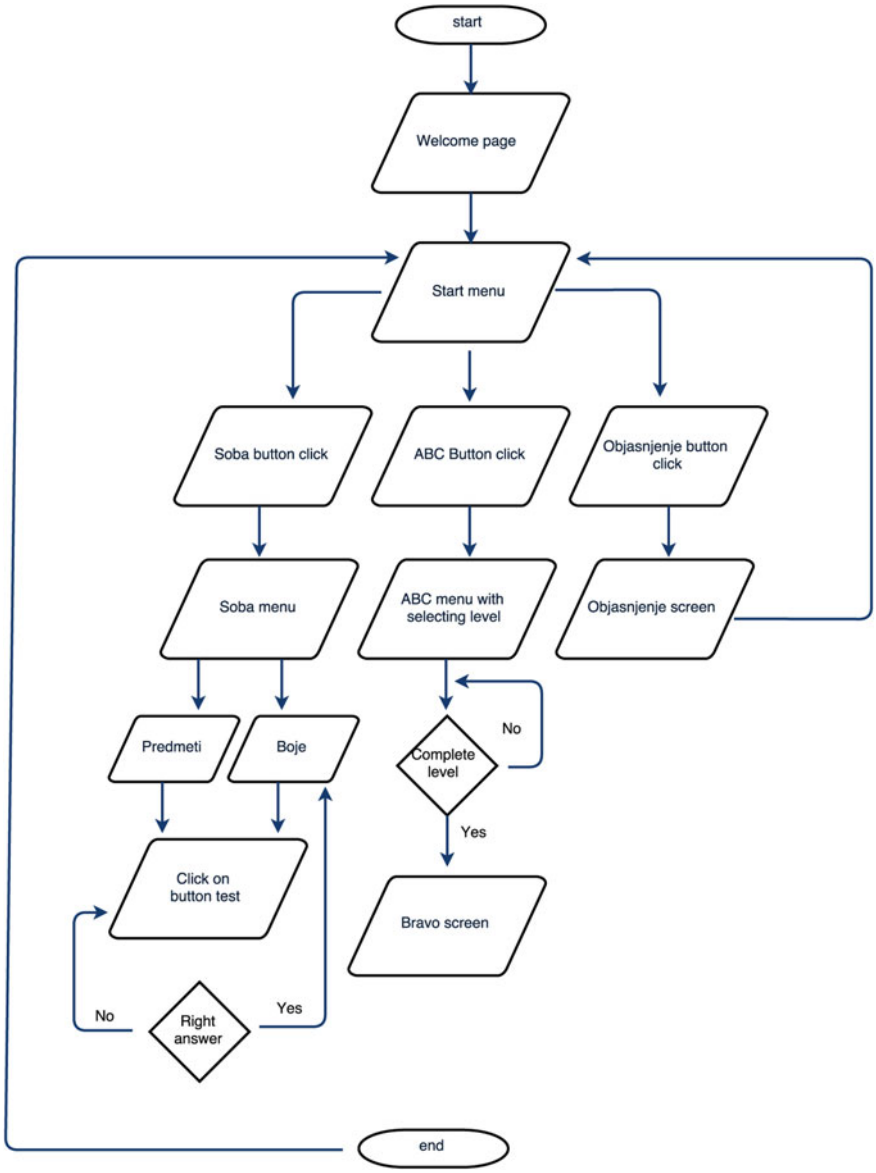

Fig. 1 Game logic and structure

test component of a game, where every time the icon in the right corner is clicked, a different question is prompted.

Each task within the game has clear written on screen task requiring child's response (e.g. "Match given letters with the boxes"). A child needs to perform an

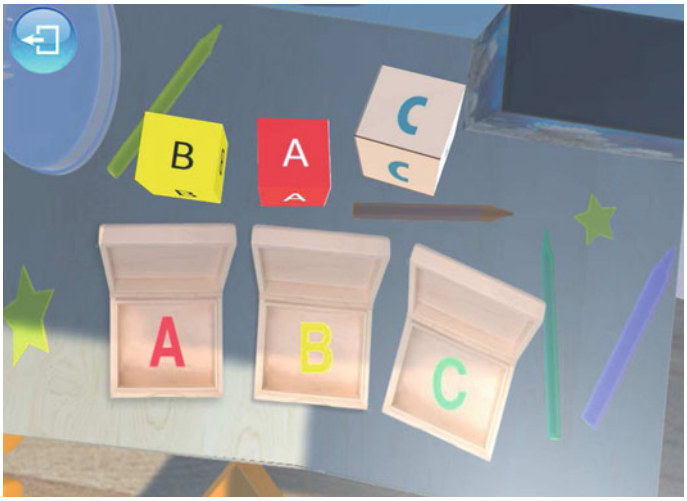

Fig. 2 ABC game—level 1

Fig. 3 ABC game—level 2

action to complete the given task (e.g. drag-and-drop the matching letter). After each correct matching, a child receives a verbal feedback (e.g. a child's voice saying "hurray") and after a completion of a level, smiley face is shown followed by a child's voice saying "Bravo (Well done)".

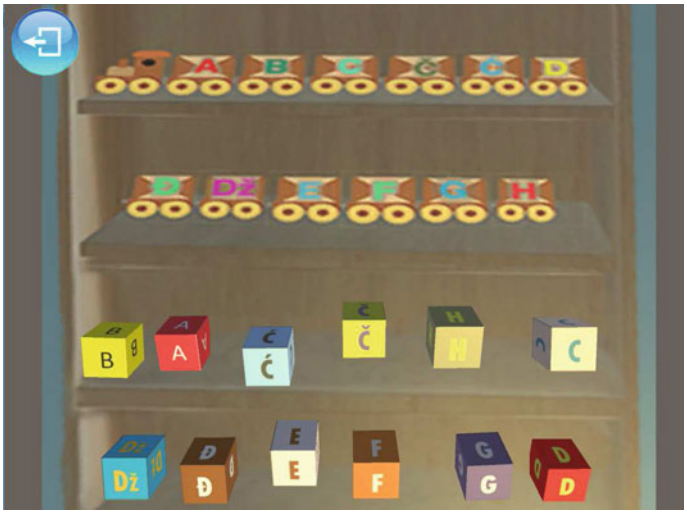

Fig. 4 ABC game—level 3

Fig. 5 ABC game—level 4

3.2 Game Production

The game was produced on a MacBook Pro computer. The 3D objects were modelled using Cinema 4D while the game logic was added through Unity. All objects had to be exported from Cinema 4D using .c4d format. The work in Unity

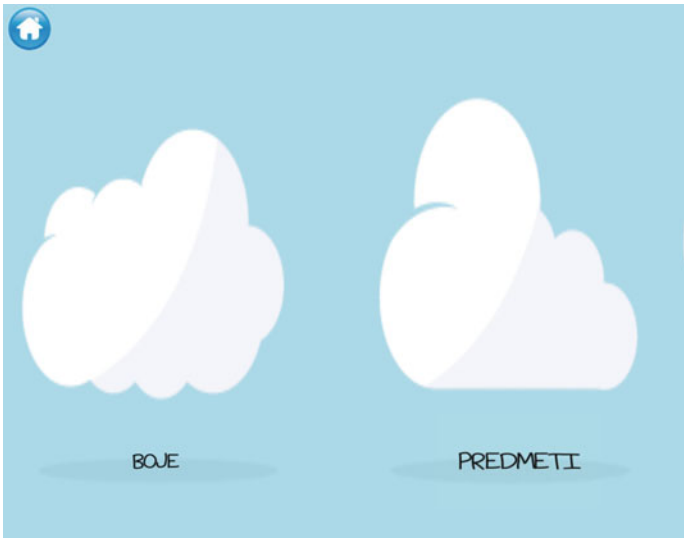

Fig. 6 Menu screen for choosing a different task: colors or objects

Fig. 7 Virtual children's room on computer

consisted of several parts: scripts for menu buttons, voice, and alphabet blocks along with their right positions. The problems were more challenges faced during the modelling faze, such as unstable virtual room with limited controlled movement and pivot points on models. Both issues were overcome through application of

Fig. 8 Virtual children's room for mobile platforms

creative method and approaches such as reducing resolution and adding the hidden objects.

The voice was given by a seven old years old Adna Grobovic. iPhone 6 plus was used for voice recording while editing was done in GarageBand program.

The game was exported and could be played as a stand-alone application, without the need of internet connection and using different devices such as the tablet, computer and smart-phone.

The game was tested on two devices:

1. "Sony VPCL111FX/B—VAIO L Series All-in-One 24" Touch Screen Desktop PC, running at 2.7 GHz with 4 GB of RAM, and NVIDIA GeForce G210M GPU with 512 MB of dedicated video RAM;
2. "Lenovo ThinkPad 2 10.1", running at 1.80 GHz with 2 GB RAM.

4 Primary Feedback

Preliminary evaluation was done with two typically developing children ages 7 and 4, after they played the game several times. Children were then asked general questions such as: "How do you like the game?", "What did you like the most?", "Would you like to play it again?", etc. The purpose of this evaluation was to check the child's level of immersion, curiosity and likeness of the game itself. We were interested in their psychological reactions to the game such as enjoyment and motivation to engage in game-play. The feedback received has been positive and we plan to run an extensive evaluation of the game with a larger participant population (with and without disabilities). We are very interested in evaluation the pace at which children adapt knowledge presented through different game levels within the Kockica game and the level of enjoyment with which they do so.

From the received feedback we found that:

- Children were fond of the game outline and design;
- Would prefer more objects such as dolls in the virtual room;
- Wanted to play the game again.

In this preliminary stage, we have also asked EDUS teachers to evaluate the created game before the main evaluation that will be performed with children with disabilities. Their feedback was most valuable since the game was not intended to substitute human interaction but rather serve as a tool for a different approach in learning a particular skill. The comments received indicate:

- A strong value of created game as no other game exists in a native language, and there are children which need it and could significantly benefit from it.
- Game manual was evaluated as a positive game addition as it reduces the time needed for transferring the knowledge onto new staff members and parents.

Lastly, we identified additional features that need to be implemented in the game prior to running the main study on a large sample of children with disabilities:

- randomizing the order of letters;
- adding more colors and objects;
- learning object names and colors and then evaluating the knowledge by asking questions such as "Where is the bear?" and "What is the color of a bear?" (currently implemented on a limited number of objects within the virtual room).

5 Conclusions and Future Work

We strongly believe that giving children additional tools for learning and stimulation, such as here explained serious game, may significantly speed up the learning process. Children already spend a significant portion of their free time using various technology devices. Through the use of this educational game, parents can make sure that that time is not ineffective but rather vary productive.

The advantage of using games in education lies in its transferability. The game can be played at home, with parents, siblings as well, and in the classroom with the teachers.

The level of engagement depends greatly on the quality of the game design and the creativity of the designer. Therefore, we plan to work more closely on the design, as well as on the expansion of given tasks and learning assignments such as numbers, additional objects and colors. The aim of this project is to create a fully functional game that will cover one complete teaching task and bring to achieving

learning outcome specified in the teaching program. The preliminary results have revealed us the hidden potential of the created game as well as further steps that need to be implemented in order for the game to be used as a teaching tool in the schools.

References

1. Annetta LA, Murray MR, Laird SG, Bohr SC, Park JC (2006) Serious games: incorporating video games in the classroom. Educause Q 3:16–22
2. Tanaka JW, Wolf JM, Klaiman C, Koeing K, Cockburn J, Heirlihy L, Brown C, Stahl S, Kaiser MD, Schultz RT (2010) Using computerized games to teach face recognition skills to children with autism spectrum disorder: the Let's face It! Program. J Child Psychol Psychiatry 51(8):944–952
3. Moore D, Taylor J (2000) Interactive multimedia systems for students with autism. J Educ Media 25(3):169–177
4. Bosseler A, Massaro DW (2003) Development and evaluation of a computer-animated tutor for vocabulary and language learning in children with autism. J Autism Dev Disord 33 (6):653–672
5. Putman C, Chong L (2008) Software and technologies designed for people with autism: what do users want? In: Assets'08: proceedings of the 10th international ACM SIGACCESS conference on computers and accessibility, NY, USA, pp 3–10
6. Grynszpan O, Weiss PLT, Perez-Diaz F, Gal E (2014) Innovative technology-based interventions for autism spectrum disorders: a meta-analysis. Autism 18(4):346–361
7. Toca Boca: A new way to play! (2016) Available via https://tocaboca.com. Cited May 2016
8. Hulusuic V, Pistoljevic N (2012) "LeFCA": learning framework for children with autism. In: VS-GAMES'12: virtual worlds for serious applications, pp 4–16
9. Hulusic V, Pistoljevic N (2012) Zaljubljeni Vuk/The Wolf in Love. Available via http://edusbih.org/book. Cited May 2016
10. Speech Assistant (2016) Available via https://www.autismspeaks.org/autism-apps/speech-assistant. Cited May 2016
11. Teach-Emotions (2016) Available via https://play.google.com/store/apps/details?id=com.specialiapps.touchemotions&hl=en. Cited May 2016

Aviončíći: Developing a Serious Game for Counting and Color-Matching

Adna Kolaković and Belma Ramić-Brkić

Abstract Increasing body of research is being focused on developing tools and applications that could improve a variety of skills of children with disabilities. Gaming industry is the fastest growing industry and as such is as of recently being enriched with a number of educational games specifically designed for children with disabilities. Their main disadvantage is the inability to be used in Bosnia and Herzegovina, where exists an increasing number of children that could significantly benefit from them. Therefore, we here present an original educational game *Aviončíći* developed in a native (Bosnian) language with a focus on special interest area: air-planes. The main purpose of the game is to teach children basic counting, color matching and color sorting by taking them through the airport. Preliminary results show the positive feedback on the game design and logic. This represents the first stage of the project, where in the further studies we plan to run a more extensive evaluation on children performance and learning pace.

1 Introduction

Children with disabilities experience a range of difficulties in social interaction, verbal and non-verbal communication, and therefore require a special set of tools and methods to accept and learn new material. With the increased use of technology across all fields and spheres of life, we consider the use of technology for the educational purposes as a next big step in Bosnia and Herzegovina.

Gaming is the fastest growing industry and quite naturally, educational games are as well gaining on the popularity. It has been shown that individuals with disabilities have specifically strong interests in video games [1, 4–8, 10]. Zakari

A. Kolaković · B. Ramić-Brkić (✉)
University Sarajevo School of Science and Technology, Hrasnicka cesta 3A, Sarajevo, Bosnia and Herzegovina
e-mail: belma.ramic@ssst.edu.ba

A. Kolaković
e-mail: adna.kolakovic@stu.ssst.edu.ba

M. Hadžikadić and S. Avdaković (eds.), *Advanced Technologies, Systems, and Applications*, Lecture Notes in Networks and Systems 3,
DOI 10.1007/978-3-319-47295-9_29

et al. [9] did a thorough review of 40 serious games developed for children with Autism Spectrum Disorder (ASD) and concluded that playing games does indeed help children in certain areas, such as expressing their feelings, but also poses a limiting factor for children with sensory processing disorder, lacks the possibility of improving imaginative play and teaching first aid. Even with the increase number of developed serious games, none of them are written in Bosnian language.

Children with disabilities often also have a strong focus on things of interest. These special interest areas are important and might be considered as a form of intense hobby [10]. In a research done by Winter-Messier [3], it was reported that there exists a strong positive relationship between special interests and improvements in children's social, communication, emotional, sensory, and fine motor skills. Identified special interests were grouped in the following themes: transportation, music, animals, sports, video games, motion, pictures, woodworking, and art. In particular, air-planes and role-playing games were identified as special interest areas.

In this paper we present a novel game, developed for children in Bosnia and Herzegovina. Having in mind that children tend to be easily distracted by outside stimuli, it is important to ensure that the child is not bored or too distracted, to offer unambiguous feedback, and clear goals [2]. Therefore, the created game is focused on an identified special interest area (air-planes) and is developed in collaboration with Dr. Nirvana Pištoljević, educational specialist, and a number of professionals working at an NGO "EDUS—Education for All" (edusbih.orgedusbih.org). In following sections, we will present the idea behind the game, the development process and stages that we have successfully completed.

2 Aviončíći—Game Design

The main purpose of this game is to teach children counting, color recognition and color matching through the use of an interesting and visually appealing objects such as airport, air-plane, passports and luggage.

The general game interactive logic is presented through a flowchart, shown in Fig. 1. The game is composed of several levels of varying difficulty though which a child will be taught a number of different skills.

Color-selecting skill is taught through a number of tasks where a child is asked to click on an object of randomly specified color. The color will be both written and pronounced to a child once the level starts. The purpose of this task and its sub-levels is not only to teach a child a color but also to help them identify objects they will continue to see throughout the airport. The following tasks are created:

- Selecting a gate of required color (Fig. 2);
- Selecting a bag of required color (Fig. 3);
- Selecting an air-plane of required color (Fig. 4);

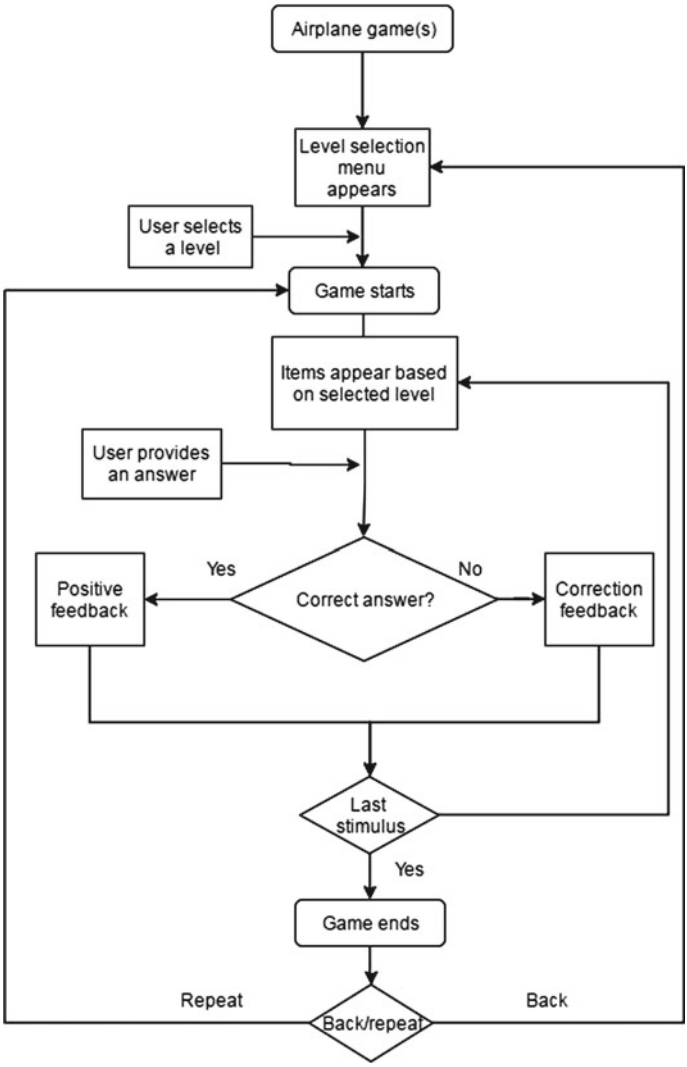

Fig. 1 Game logic and structure

Color-matching skill is taught through two game levels where in first, a child is asked to match the color of a passport with the color of provided basket. The second level consists of two baskets and a child is asked to sort the passports in both (Figs. 5 and 6).

Another segment of the game is intended to teach children to count and therefore we have modelled a 3D scene where a child counts how many planes have landed in a particular animated sequence. This is the basic counting skill since the numbers are in the range from 1 to 10 (see Fig. 7).

Fig. 2 Selecting adequate airport gate

Fig. 3 Selecting adequate bag

2.1 Game Development

The aim of the created game was to advance children achievement in particular tasks such as color matching and counting, by integrating interactive, virtual component in the classroom curriculum. Special attention was paid to the game theme, colors, complexity of scenes, tasks and visual/audio feedback.

Fig. 4 Selecting particular plane

Fig. 5 Matching passports—level I

Fig. 6 Matching passports—level II

Fig. 7 Counting the planes that have landed

At the beginning of each task, a computer generates a random:

- color that needs to be identified;
- the number of planes that are landing and need to be counted;
- and the position of passports that need to be sorted.

The concept of color is therefore being thought using multiple exemplars (e.g. planes, passports, gates) and a variety of methods (e.g. identification and sorting) eliminating the possibility of memorizing.

The assignment is always written in the top left corner of the screen in white letters, distinguishing them from the task's color that needs to be identified or matched.

A child should:

- click on the plane/bag of requested color;
- drag-and-drop when playing a task requiring passport matching;
- or select one of three randomly given numbers when done counting the planes that have landed.

In the case of a correct answer, a child is given an audio and visual feedback (e.g. "hurray"). For an incorrect answer, there is an audio feedback (e.g. a sound indicating the wrong answer) and visual (e.g. the correct answer is highlighted).

2.2 Game Production

Avionči ći was developed on a personal computer using a Gigabyte motherboard, model P43-ES3G. It runs a 64-bit Windows 7 Ultimate operating system, version 6.1.7601 (Service pack 1), with 4 GB of random access memory and Intel Core 2 Quad central processing unit, each core running on 2.83 GHz. I recently installed AMD/ATI Radeon HD 5700 [2] graphics card, which has 1 GB of extra random access memory, with 1280 × 1024 × 60 Hz resolution.

We used Autodesk 3ds Max 2008 software package for modelling the 3D object. All of the models were created using box-modelling technique and were exported into FBX format to be used in Unity.

Following the import of all the models, separate scenes were made for each level of the game, including all the menus. To complete the back-end of the game, scripts were written in C# programming language using MonoDevelop—a built-in programming environment for Unity. During this process several challenges were faced: alignment in drag and drop levels and color matching but were successfully overcome.

The game was tested on a Sony VPCL111FX/B—VAIO L Series All-in-One 24" Touch Screen Desktop PC, running at 2.7 GHz with 4 GB of RAM, and NVIDIA GeForce G210M GPU with 512 MB of dedicated video RAM.

3 Preliminary Feedback

We collaborated with a number of EDUS teachers in order to evaluate the work that has been implemented so far. We were interested in the effectiveness of our game and whether they would find the design, tasks, difficulties, appropriate for children with disabilities and if they would use this game as part of their curriculum, therefore in their classrooms. The preliminary playtesting has been positive. The teachers found the game engaging and fun and as a result following features will be added to the game:

- A segment where a combination of skills could be taught/tested. For example: counting of the air-planes of the same color or size; counting of the bags of the same color or type; finding item location or finding an item based on location;
- In a level where planes are parked, add additional sub-levels where a child will be prompted to identify the plane of the same color and size and therefore they will be introduced a concept of bigger/smaller;
- Apply similar concept on a task where a child is asked to identify a bag color; Introduce different types of bags and excel matching skills;
- Within the airport, model a 3D scene where a child will be asked to identify the location of a random object (e.g. passport, bag, air-plane toy). This way a child will learn: on top, inside, in front, behind, underneath, near, above and below other items. Children will be given a random location and will be asked to find an object based on the given location.

Once the changes are implemented, we plan to perform an extensive evaluation of the game on a large sample of children.

4 Conclusions and Future Work

The created game, Aviončići, shows promise of an effective tool that could be used for educational purposes. It is free, can be played at home, classroom or during a field trip, and can be run on multiple operating systems (i.e., MAC OSX, Windows). The game is not intended to substitute human interaction but rather to be used in conjunction with teachers, parents, siblings. Unquestionably, incorporating educational games and technology per se in the classroom, requires significant effort on the part of educators as well as parents.

We plan to continue working on adding all suggested features so the game covers one complete learning topic. The next step involves creating a story plot that will be used as a tool for helping teachers, but more specifically parents, prepare their children for travelling (e.g. holidays, vacations, etc.).

Lastly, we are interested in the importance of the game theme in child's adoption of new skills, i.e., whether the children with a special interest area in planes will adopt new skills faster using Avionči ći than using a different game teaching the same skills.

References

1. Moore D, Taylor J (2000) Interactive multimedia systems for students with autism. J Educ Media 25(3):169–177
2. Sinclair J, Hingston P, Masek M (2007) Considerations for the design of exergames. In: GRAPHITE'07: proceedings of the 5th international conference on computer graphics and interactive techniques in Australia and Southeast Asia, ACM, NY, USA, pp 289–295
3. Winter-Messiers MA (2007) From tarantulas to toilet brushes, understanding the special interest areas of children youth with Asperger syndrome. J Remedial Spec Educ 28(3):140–152
4. Putman C, Chong L (2008) Software and technologies designed for people with autism: what do users want? In: Assets'08: proceedings of the 10th international ACM SIGACCESS conference on computers and accessibility, NY, USA, pp 3–10
5. Durkin K (2010) Videogames and young people with developmental disorders. Rev Gen Psychol 14(2):122
6. Tanaka JW, Wolf JM, Klaiman C, Koeing K, Cockburn J, Heirlihy L, Brown C, Stahl S, Kaiser MD, Schultz RT (2010) Using computerized games to teach face recognition skills to children with autism spectrum disorder: the Let's face It! Program. J Child Psychol Psychiatry 51(8):944–952
7. Ferguson B, Anderson-Hanley C, Mazurek MO, Parsons S, Warren Z (2012) Game interventions for autism spectrum disorders. Games Health Res Dev Clin Appl 1(4):248–253
8. Grynszpan O, Weiss PLT, Perez-Diaz F, Gal E (2014) Innovative technology-based interventions for autism spectrum disorders: a meta-analysis. Autism 18(4):346–361
9. Zakari HM, Ma M, Simmons D (2014) Review of serious games for children with autism spectrum disorder (ASD). In: SGDA 2014: proceedings of 5th international conference on serious games development and applications 2014, Berlin, Germany, pp 93–106
10. Mazurek MO, Engelhardt CR, Clark KE (2015) Video games from the perspective of adults with autism spectrum disorder. J Comput Hum Behav 51:122–130